

Department of
Biotechnology and Biosciences

PhD program in Chemical, Geological and Environmental Sciences Cycle XXXV

Curriculum in Chemistry

Synthesis and Biological Characterization of Toll-like Receptor 4 Agonists as Innovative Vaccine Adjuvants

Surname ROMERIO

Name Alessio

Registration number 794964

Tutor:

Supervisor: Dr. Francesco PERI

Coordinator: Dr. Marco MALUSÀ

ACADEMIC YEAR 2021/2022

Index

Index	I
Abbreviations	IV
INTRODUCTION	1
Vaccines	2
History of Vaccination	2
Inoculation, variolation and the smallpox vaccine	2
Jenner's vaccine shortcomings and nineteenth century advances	3
Vaccine classes	5
Attenuated vaccines	6
Inactivated vaccines	7
Subunit vaccines	7
Toxoid vaccines	8
Protein vaccines	8
Virus-like particle vaccines	10
Polysaccharide and glyconjugated vaccines	11
Nucleic Acid Vaccines	12
DNA vaccines	13
mRNA vaccines	13
Vaccine Adjuvancy	15
Current Adjuvants	17
Aluminium-based adjuvants	17
Emulsion-based adjuvants	18
PRRs targeting adjuvants	20
Immunity	22
Innate Immunity	23
Adaptive Immunity	24
The interface: how innate immunity primes adaptive immunity	24
Pattern Recognition Receptors (PRRs)	26
Toll-like Receptors (TLRs)	27
TLR4 and its ancillary proteins: a peculiar case	29
Lipid Binding Protein (LBP)	29
Cluster of Differentiation 14 (CD14)	30
Myeloid Differentiation protein 2 (MD-2)	31
Toll-like Receptor 4 (TLR4)	33
Downstream Signaling	34
MyD88-dependent Pathway	35
TRIF-dependent Pathway	35
Lipopolysaccharide (LPS)	36
Aggregation Properties	38
LPS-TLR4 Interaction	40
TLR Modulators: Increasing the chemical variety of small molecule-based TLR4 modulators: an overview	43
Abstract	43
Introduction	44
Glycolipid-Based TLR4 Modulators	50
Agonists	50

MPLA	50
Enzymatically Modified Lipid A	51
Glucopyranosyl Lipid Adjuvant (GLA)	52
Trehalose Derivatives (LAM)	53
Antagonists	55
Anionic monosaccharide-based TLR4 Antagonists	55
Cationic monosaccharide-based TLR4 antagonists	58
Non-Glycolipid TLR4 Modulators	59
Agonists	59
Linear lipid A analogues (E6020)	59
Pyrimidoindoles	60
New rationally designed TLR4 agonists	60
TLR4 Antagonists	61
TAK-242	61
Calixarene Amphiphiles	62
Opioid Derivatives	63
Peptide Antagonists PIP2 and cPIP2	63
Cardiolipin	64
Alpinetin	65
Ferulic Acid	65
Conclusions	66

AIM OF THE WORK 68

RESULTS AND DISCUSSION 73

Chapter I: Synthetic Glycolipids as Molecular Vaccine Adjuvants: Mechanism of Action in Human Cells and

In Vivo Activity 74

ABSTRACT	74
Introduction	75
Results And Discussion	77
Synthesis of FP molecules	77
In vitro binding tests: FP11 and FP18 bind to human MD-2	78
TLR4 Binding of FP11, FP18, and FP111. Computational studies	79
TLR4 activation by synthetic agonists	80
Activation of MyD88 and TRIF pathways in human macrophages	81
Adjuvant activity of FP11 and FP18 and in vivo toxicity: OVA immunization experiments	86
Conclusions	87
Experimental section	88

Chapter II: "NEW SYNTHETIC AGONISTS OF TLR4 RECEPTOR" 94

DESCRIPTION	94
PRIOR ART	94
SUMMARY OF THE INVENTION	99
DETAILED DESCRIPTION OF THE FIGURES	105
GLOSSARY	111
DETAILED DESCRIPTION OF THE INVENTION	112
EXAMPLES	137
Chemistry	137
Biology	154
CLAIMS	158
ABSTRACT	166

Chapter III: Unpublished Chemical and Biological Work 167

FP20 <i>ex vivo</i> and <i>in vivo</i> Biological Data	167
FP20 Glycosylation	169

First Attempts and Modified Koenigs-Knorr Protocol	169
Bismuth Triflate Protocol	171
NIS and HOFox Protocol	174
FP20Rha and FP207 Biological Assessments	176
<i>In Vitro</i> Activity	176
Mechanism of Action Assessment	176
<i>In Vivo</i> Studies	178
CONCLUSION	179
AUTHOR'S CONTRIBUTION	185
Patents and Publications	186
Communications	186
ANNEXES	187
<i>Supplementary Information of Synthetic Glycolipids as Molecular Vaccine Adjuvants: Mechanism of Action in Human Cells and In Vivo Activity</i>	188
Molecular Formula Strings	188
Computational Methods	189
Docking calculations of the binding of FP11, FP18, and FP111 to TLR4/MD-2	190
MD simulations of (TLR4/MD-2) ₂ complex with FP11 and FP18	192
Chemical synthesis procedures	197
NMR spectra	204
In vitro evaluation of the cytotoxicity of compounds FP11 and FP18	217
BIBLIOGRAPHY	219

Abbreviations

AcOEt. Ethyl Acetate

AcOH: Acetic acid

APC: Antigen Presenting Cells

BCR: B Cell Receptor

CD14: Cluster of Differentiation 14

CMC: Critical Micellar Concentration

CTL: Cytotoxic T Lymphocyte

DAMP: Damage Associated Molecular Pattern

DC: Dendritic Cells

DCC: dicyclohexylcarbodiimide

DCM: Dichloromethane

DMAP: N, N-Dimethylaminopyridine

DMSO: Dimethylsulfoxide

dsRNA: double strand RNA

EDC: 1-ethyl-3-(3-dimethylaminopropyl) carbodiimide

EtPet: Petroleum Ether

HMGB1: High Mobility Group Box 1

HOFox: 3,3-difluoroxindole

IFNAR: IFN- α/β receptor

Ig: immunoglobulin

IRF: Interferon Regulator Factor

Kdo: 3-deoxy-D-manno-oct-2-ulosonic acid; 2-Keto-3-deoxyoctonic acid

LBP: Lipid Binding Protein

LPS: Lipolysaccharide

LRR: Leucin-Rich Repeat

LTA: Lipoteichoic Acid

MD-2: Myeloid Differentiation protein 2

MeOH: Methanol

MOA: Mechanism of Action

MPLA: Monophosphate Lipid A

MyD88: Myeloid Differentiation primary response gene 88

MHC: Major Histocompatibility Complex

NLRP3: NLR family pyrin domain containing 3

NK: Natural Killer cell

OMV: Outer Membrane Vesicle

PAMP: Pathogen Associated Molecular Pattern

PRR: Pathogen Recognition Receptor

SOI: Site Of Injection

STAT: Signal Transducer and Activator of Transcription

TBAF: tetrabutylammonium fluoride

TBDMS: *tert*-Butyldimethylsilane

TCR: T Cell Receptor

THF: Tetrahydrofuran

TIRAP: Toll-Interleukin 1 Receptor (TIR) domain containing Adaptor Protein

TLR: Toll-Like Receptor

Tol: Toluene

TRAM: TRIF-Related Adaptor Molecule

TRIF: TIR-domain protein inducing Interferon

INTRODUCTION

Vaccines

Vaccines have been one of the greatest breakthroughs in the history of medicine and they contributed to save several tens of millions of lives over two and a half centuries.¹

The principle behind them is easy: they work exposing the body to an attenuated infection from a pathogen to build up a long lasting adaptive immunity with relative safety.²

History of Vaccination

Inoculation, variolation and the smallpox vaccine

Some kind of proto-vaccinations practices have been diffused for centuries in various parts of the world: inoculation or variolation were known in China, Middle-East, India and Africa, and were brought to Europe by Lady Montague in 1721.^{1,3}

Variolation, the practice of inoculating a non-immune patient with a small dose of pustule fluids from a smallpox infected person, helped reducing smallpox mortality rate from 17.5% to 2% in variolated patients in XVIII century London.³ It even changed the tides of the American Revolution, when George Washington started a variolation campaign in the smallpox-struck Continental Army.⁴ However, variolation was far from perfect: many patients died from the practice, as physicians inoculated them with too large a dose of fluids containing the smallpox virus in its full strength, without any kind of attenuation or inactivation.^{1,3}

The first real, attenuated vaccine was developed by Edward Jenner in 1796. Aware of the variolation practice, he observed that the milkmaids who caught cowpox from their cows never got infected with smallpox. He then proceeded to inoculate cowpox to his gardener's son and subsequently exposed him to smallpox: the boy demonstrated immunity from smallpox, proving the viability of this new method.^{3,5}

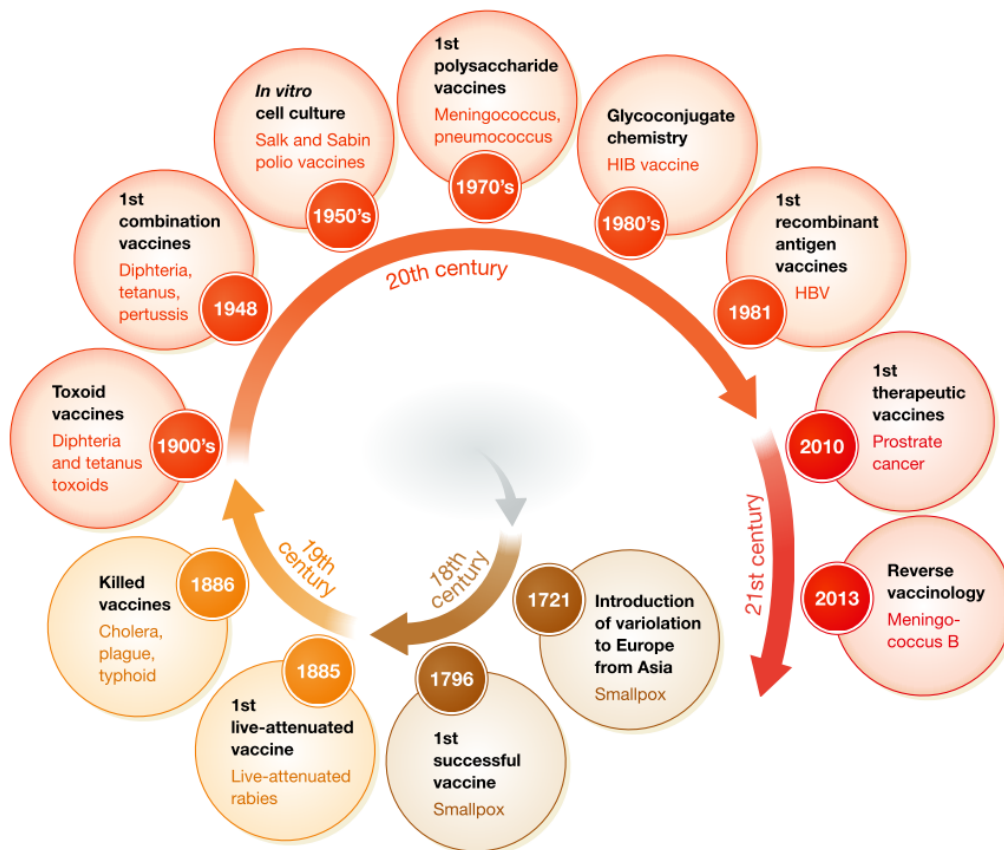


Figure 1 Development and advancements of vaccinology. Since its inception, variolation was commonly used in Asia and Africa; it was later introduced in Europe in 1721. This technique prompted a series of studies eventually leading to the first real vaccination in 1796. Since then, many researchers contributed to make vaccination always safer and more efficient through technological breakthroughs such as inactivated vaccines, subunit vaccines (such as toxoid or polysaccharide), recombinant vaccines and more recently through reverse vaccinology and nucleic acid vaccines. ⁶

After this first experiment, vaccination (from *vacca*, cow in latin) efficacy was proved in the UK, where a prodigious decline in smallpox mortality was observed. The practice of vaccination was indeed so successful that smallpox was declared eradicated by the World Health Organization after a massive, decade-long and world-spanning effort, while today several vaccines against a plethora of different diseases are mandatory in most countries around the world.^{1,3}

Jenner's vaccine shortcomings and nineteenth century advances

This huge success, however, is not entirely ascribable to Jenner, as his original vaccine had many shortcomings: it possessed a low safety profile, various collateral effects (including fever and the eruption of pustules) and the practically non-existent shelf life, as cowpox pustule fluid could only

be conserved for few hours to few days. The really short shelf life in particular hampered the ability of carrying the vaccine outside Europe: indeed, in an effort to immunize the people in the colonies, the Spanish crown, resorted to use 22 orphan children as “live vectors” for the vaccines, in an extremely unethical but exceptionally successful vaccination campaign that spread the vaccine in the Americas, the Philippines and China. ^{1,7}

These shortcomings were dealt with through the work of Pasteur, Koch, von Behring and Ehrlich in the end of the nineteenth century as they focused their work in the medical field and on bacteria.

Vaccinology — 1875 through World War I and 1930

Great awakening 1875 — discovery and rational empiricism. Focus on bacteria and antibodies (rabies virus exception).

Giants were

Louis Pasteur — immunoprophylaxis, attenuation.

Robert Koch — methodology, etiology, hypersensitivity, postulates.

Emil von Behring — antibodies and immunotherapy.

Paul Ehrlich — specific receptor—ligand binding, specific chemotherapy, antibody quantification.

By 1929:

Humoral immunologic phenomena described

Immunotherapy dominates the field

Credible and useful vaccines

Smallpox and rabies

Killed and/or attenuated typhoid, shigella, cholera

Plague, diphtheria, tetanus, pertussis, and tuberculosis

Table 1 Advances of vaccinology in the end of the XIX century and contributions of Pasteur, Koch, von Behring and Ehrlich to the field.⁸

Pasteur noted the attenuation of fowl plague bacteria in laboratory cultivation. He observed that these attenuated strains still maintained the ability to induce resistance against subsequent infection while causing milder collateral effects, opening the gate for attenuated live vaccines.⁸

Koch mastered the technology of pure culture, which brought to the discovery of many bacteria and to the definition of specific disease aetiology.⁸

Von Behring has been the recipient of the first Nobel Prize for his studies on passive immunity (i.e. antibody transfer from immune to infected patients) and opened the way to toxoid vaccines with his work on bacterial toxins and their detoxification for immunization purposes.^{8,9}

Finally, many important advances in the medical field of the era were made by Ehrlich: not only he developed the first synthetic drug, Salvarsan, for the treatment of syphilis, but he also studied the

specific complementarity between chemicals and proteins, developing the concept of specific ligand-protein binding which dominates our understanding of biology in general and immunity in particular.^{8,10}

Vaccine classes

All these advances allowed the development of several vaccines for a variety of diseases with different manufacture and mechanism of action – which also affects the efficacy and safety profile of the vaccine itself.

These can be classified as follows: attenuated vaccine, inactivated vaccine, subunit vaccines (a broad category ranging from toxoid to polysaccharide) and modern nucleic acid vaccines.

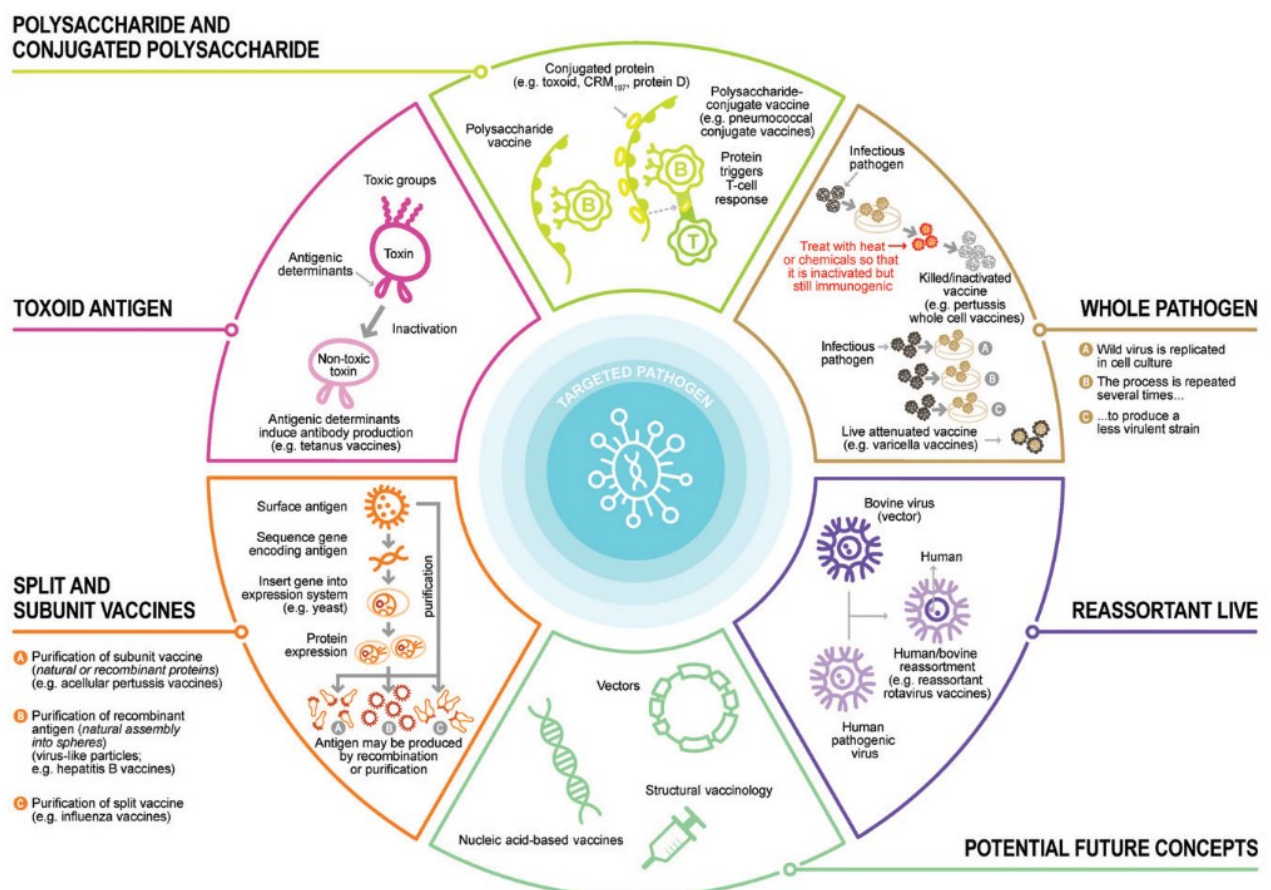


Figure 2 Different classes of vaccines. Based on the production method, vaccines may contain whole pathogens, alive or killed, smaller bits of pathogen cells, such as proteins, or polysaccharide, deactivated toxins or nucleic acid able to replicate pathogen parts. The amount of antigens, and therefore efficacy and safety, contained vary with the methodology: safer vaccines, containing less antigens, may require vaccine adjuvants for a proper immunization.¹¹

Attenuated vaccines

Attenuated vaccines were the first kind of vaccines and have been developed through Pasteur efforts. They contain alive pathogens that have been weakened by repeated passages through a series of *in vitro* cultures (typically chick embryo cells). This way, the infective agent becomes better at infecting culture cells but progressively lose toxicity in the original host. This process can be enhanced and sped up by cold temperature, so that the pathogen loses the ability to replicate physiological temperature.¹¹

These kinds of vaccines have the highest efficacy, as the patient's immune system is presented with the whole pathogen and its set of antigens, building up a strong and long-lasting immunity; furthermore, they help immunizing non-vaccinated people by "viral shedding", i.e., the excretion of viral particles.¹¹

Nonetheless, it is also the least safe approach as immunocompromised individuals may lack the ability to fight the attenuated virus, leading to severe infection; moreover, there is the (extremely rare) possibility that the pathogen reverts to its infectious form, kickstarting the clinical disease in its full swing.

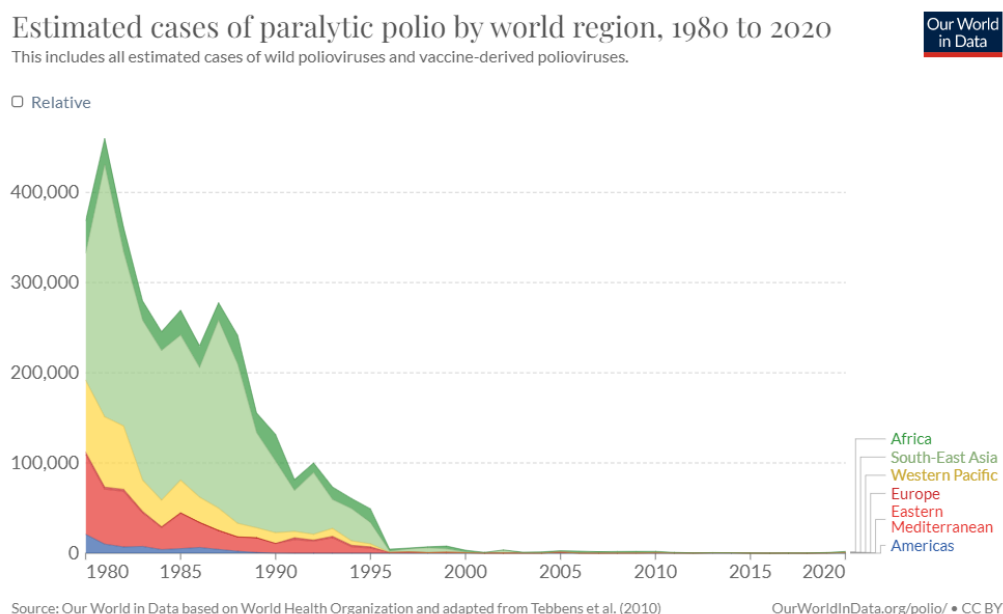


Figure 3 Numbers of polio induced paralysis in the world since 1980, comprising cases due to vaccine reversion. In 1985, the Global Polio Eradication Initiative (GPEI) was launched with the aim of eradicating polio by distributing the OPV vaccines worldwide. Since then, polio cases have steadily decreased to the point where polio is almost eradicated today.^{12,13}

Many widespread and mandatory vaccines are part of this class, as for example the trivalent MMR (measles, mumps and rubella) vaccines or the tetravalent MMR+varicella, which prevent countless child infections and deaths every year. Another successful example is the OPV (oral poliovirus vaccine) developed by Jonas Salk: it was pivotal in contrasting poliomyelitis, a devastating disease which can cause life-lasting paralysis. Thanks to the OPV, from being a common and diffused disease, polio is now on its way as the second eradicated human virus: there are only 22 wild cases reported in the mountains between Afghanistan and Pakistan and in Mozambique today.^{13,14}

Inactivated vaccines

Differently from attenuated vaccines, in which the pathogen is alive, inactivated vaccines only contain pathogens that have been killed or otherwise made unable to replicate by treatment with heat, radiation or chemical agents such as formalin. This way, the pathogen cannot by any mean cause an infection and a disease, however the immune system is still challenged with the whole cell and its array of antigens, inducing a robust immunity.

While the advantage in safety over attenuated vaccines is evident (pathogen reversion is totally impossible as replication is completely shut down), for the same reason inactivated vaccines are less efficient, because less pathogenic cells are present.

This small drop in efficacy doesn't affect inactivated vaccines successes. Many important vaccines are in this class: some examples are cholera, pertussis and hepatitis A vaccines; but also IPV (inactivated polio vaccine), a safer OPV counterpart used in countries in which polio is under control and where the efficacy/risk ratio has to be lower than in places in which polio is still circulating.^{1,13}

Subunit vaccines

Subunit based vaccines, as the name goes, don't contain the whole pathogenic cell but only a part of it: this way, safety profile is increased, but efficacy may be reduced, as the immune system is challenged with only portions of the pathogen. For this reason, a large amount of such vaccines required adjuvants in their formulation to retain immunogenicity. Subunit vaccines can be divided into toxoid, protein, virus-like particles, polysaccharide and polysaccharide conjugates.¹¹

Toxoid vaccines

Toxoid vaccines emerged in the 1920s as a safe and effective mean to protect the population against nasty diseases like diphtheria and tetanus, which used to cause death in large numbers of children. They are based on the detoxification of purified bacterial toxins by treatment with chemicals and/or heat. The detoxified toxins, called toxoids, are then injected in a healthy individual in order to induce toxin-directed antibodies.¹⁵

As toxoid vaccines don't challenge the patient with pathogen cells, they are considered much safer than whole cell vaccines, to the point that the World Health Organization recommends their use also in immunocompromised patients.^{16,17}

However, this safety comes with a price: the immunity they induce is only directed toward the bacterial toxins, which means they only prevent pathogenesis, but can't protect against infection or transmission. For the same reason, these vaccines are less efficient in building a strong immunity, so that they require multiple primary doses and booster throughout an individual's life.^{11,16,17}

Protein vaccines

Protein vaccines are widely used today. They are prepared using purified antigenic protein, which can be obtained either by whole pathogen split or by genetic engineering through recombinant organisms.

The common influenza vaccine is a widespread example of a protein vaccine derived by viral splitting: starting by the 1970s, split vaccines began substituting the attenuated vaccines, as the latter required a long preparation process. Influenza vaccine is now prepared by chemical disruption of the viral membrane, obtaining the antigens and killing the virus: immunogenicity is retained, while the number of adverse reactions is minimized. This translates to a great advantage, as the influenza virus is to be repeated yearly and prevents millions of flu cases each year, which could be fatal to elder or very young population.

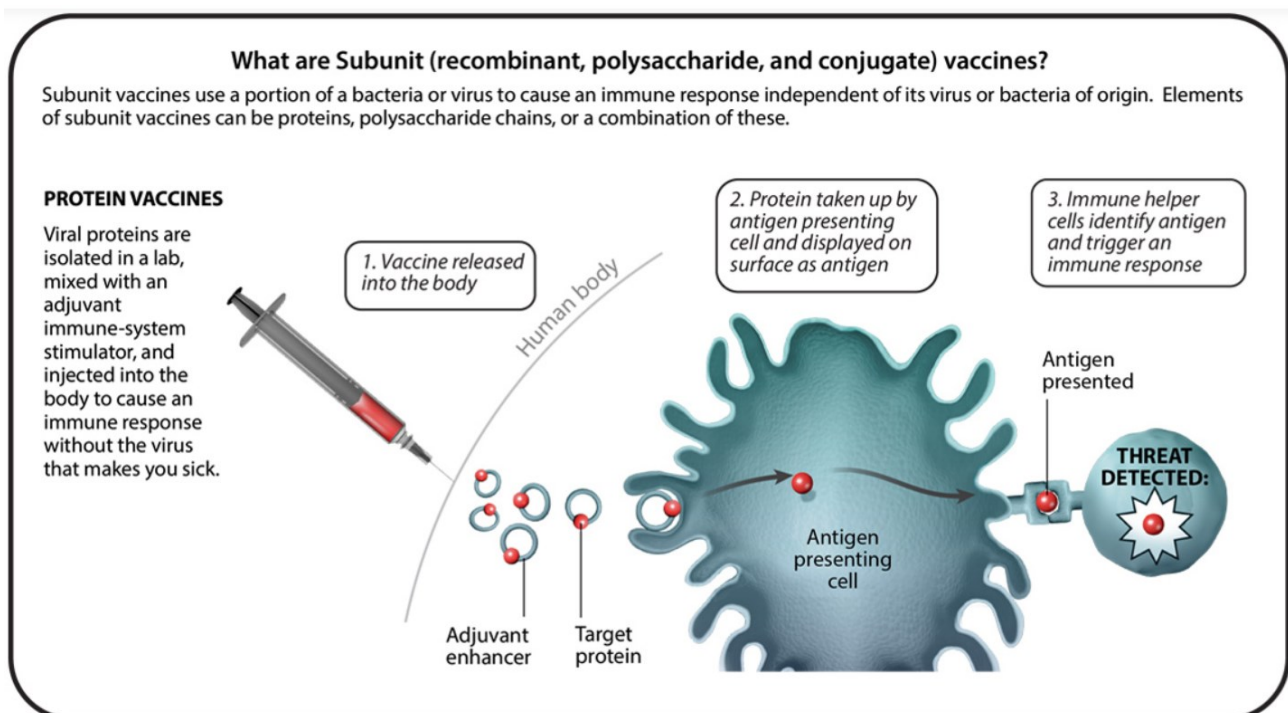


Figure 4 Strategy underlying protein vaccines. A target antigen protein, enhanced by an adjuvant, is injected in the body; patient's immune system recognizes it as foreign and start the adaptive immune response.¹⁸

An important example of the recombinant genetic engineering vaccine is instead the one against hepatitis B, the antigen of which is produced by yeast (Engerix[®], Recombivax-HB[®]) or mammalian (GenHevac-B[®]) cells transfected with the HBsAg gene and then purified.¹⁹

A more modern approach of this same strategy is reverse vaccinology, in which the genome of a pathogen is screened to find genes encoding for potential antigens. These genes are then expressed, and the resulting proteins tested for their activity as antigens to induce antibodies. This strategy proved indispensable in developing a vaccine against *Neisseria meningitidis* B: this strain possesses a capsular polysaccharide similar to human polysaccharides, which hampered the development of polysaccharide vaccines used against different strains of the same bacteria. Reverse vaccinology allowed to identify four new proteins as antigens that have been included in a tetravalent meningococcal B vaccine (Bexsero[®]).

Virus-like particle vaccines

Virus-like particles are a subset of protein vaccines in which the protein antigens self-assemble in a particle resembling the natural virion structure. This conformation allows for a better recognition by the immune system and thus a higher efficacy than in normal protein vaccines, while still being unable to replicate as genetic code is missing. Another advantage over protein vaccines is that in many cases inactivation or splitting is not required, so eventual damages to antigen's epitopes are avoided.^{11,20}

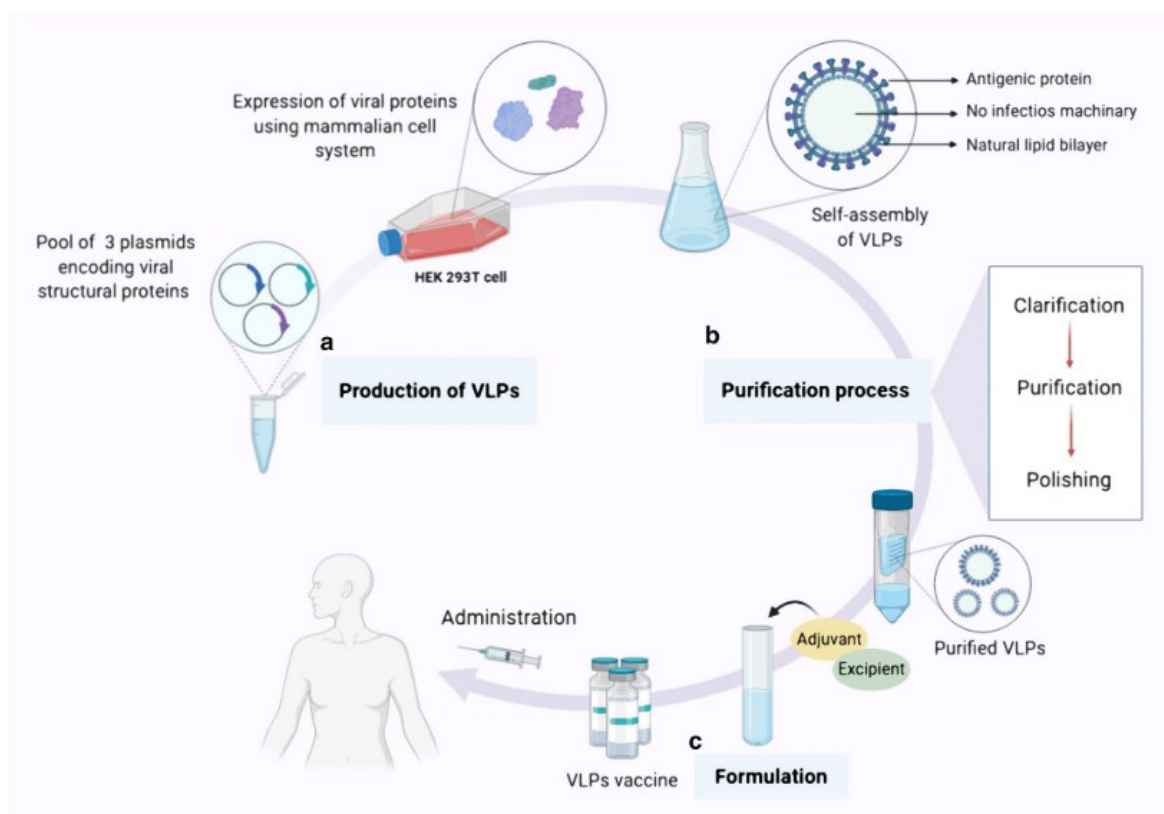


Figure 5 Process of production of VLPs vaccines. **A)** Cloning and expression of viral proteins needed for VLPs; said proteins will self-assemble in non-infectious particles. **B)** Purification of VLPs from unwanted contaminant through clarification and polishing. **C)** Formulation of purified VLPs into a vaccine, comprising the addition of adjuvants needed for good level of efficacy.²¹

Human papillomavirus (HPV) vaccines currently in use in many countries in the world are based on VLP technology. Gardasil[®], developed by Merck and Co Inc. and approved in 2006 is a quadrivalent HPV vaccine that uses Alum as an adjuvant, while Cervarix[®] developed by GSK and commercialized in 2009 is a bivalent HPV vaccine using an MPLA based adjuvant system. Taken together, these vaccines contribute to suppress the number of cervical carcinoma in female population, with efficacy rates as high as 95%.^{20,22}

Many other VLP vaccines are currently in development, like Norwalk, parvovirus and influenza vaccines, but probably the most interesting VLP candidates are chimeric VLPs, where a foreign protein is fused onto a VLP in order to elicit an immunization against it. Chimeric VLPs are currently being studied for interesting application such as nicotine addiction suppression, Alzheimer Disease prevention or type II diabetes treatment²⁰

Polysaccharide and glycoconjugate vaccines

The idea for polysaccharide vaccines emerged in the 1920-30s after Avery and Heidelberger observation that *Streptococcus pneumoniae* capsular polysaccharides (CPS) elicit an immune response and Francis and Tillet observation that infected patients produced CPS targeted antibodies.^{23,24}

CPS are present on most bacterial strains' membrane, where they have both a structural and a defensive function, as they mask other antigens present on cell surface. As they are for the most part different from human-expressed oligosaccharide, they are a prime target for immunization: indeed, various CPS-based vaccines have been developed, comprising *S. pneumoniae*, *Haemophilus influenzae* and *Neisseria meningitidis*.²⁵

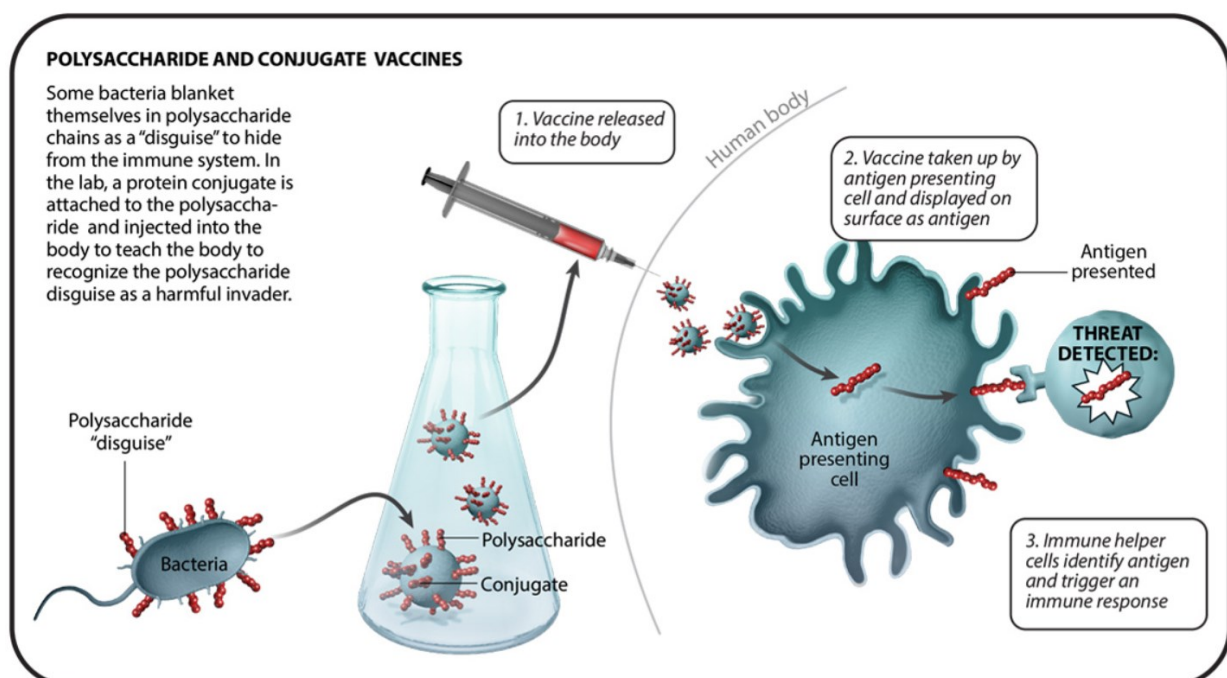


Figure 6 Mechanism of action of polysaccharide vaccines. As is the case for protein vaccines, bacterial polysaccharides are purified and injected in the body, so that the immune system can recognize them and build up an immune memory.¹⁸

Though successful and safe, CPS vaccines have the major drawbacks of only eliciting T_H1 immune response, independent from T_H2 cells, which is weaker than T_H2 immune response; consequently, they are completely unactive on children below 2 years old, the ones who would need them the most.¹¹ In order to address these two drawbacks, development refocused on conjugating glycans on the surface of immunogenic proteins, so to elicit a stronger and T_H2 immune response involving T cell and proliferation of B cell, with the formation of immunological memory. The most used proteins for glycoconjugate vaccines are inactivated toxins, such as diphtheria toxoid, which is proved to be nontoxic by years of use in toxoid vaccines. Following this strategy, CPS vaccines have been repurposed and today they protect countless people against severe diseases such a meningitis or pneumonia.²⁵

Nucleic Acid Vaccines

Recent years advances in nucleic acid manipulation and in immune system understanding allowed for development of nucleic acid-based vaccines, particularly the seminal studies of Karikò on the ablation of RNA recognition by Toll-Like Receptors (TLRs).²⁶

The general principle behind them is to inject DNA or mRNA in a patient in order to haywire cellular machinery into expressing a desired protein (i.e., an antigen) for the immune system to recognize: the genetic material would be uptaken into cells, translated into proteins which would be secreted or exposed on the membrane where APC could engulf and digest them and subsequently T and B cell would be activated.

This approach has the potential to revolutionize vaccine field, as nucleic acids are nowadays easily and readily available, but there are still many challenges left to overcome, for example the requirements for cold chain transportation system due to low thermostability of DNA or mRNA formulations. This technology is indeed still new and no nucleic acid-based vaccine was approved for human use until the recent COVID-19 pandemic.²⁷

DNA vaccines

DNA vaccines can be divided in two categories: pure DNA vaccines and DNA vector vaccines.

Pure DNA vaccines are based on the delivery of a recombinant plasmid with the aim of expressing an antigen upon transfection and integration of plasmid DNA into host genome. While there have been some successful example of this strategy in experimental settings, transfer of this technology from animals to human have proven difficult, mainly for concerns regarding the disruption of host genome.²⁸

A safer approach to DNA vaccines is vector-based DNA delivery. In this strategy, a vector is chosen (commonly, a silenced chimpanzee adenovirus) to bring DNA into a cell nucleus, where the genetic material is translated and expressed without being incorporated into the host genome, a clear safety advantage. Two prominent examples of this technology are Oxford/Astrazeneca and Janssen COVID-19 vaccines, which were quickly developed during 2020 pandemic and given emergency use approval by several regulatory agencies across the world.²⁷

mRNA vaccines

mRNA vaccines are a safer approach than DNA vaccines, even though they use the same basic idea. Indeed, in mRNA case, the nucleic acid remains into the cytosol, without entering cell nucleus for their action.²⁷

However, they come with their own challenges, mRNA is much more unstable than DNA and it is also easily targeted and degraded by immune system upon recognition by TLR3, TLR8 and TLR9. Thus, mRNA has to be carefully prepared and modified, for example using pseudouridine in spite of uridine or adding post-translational modifications.²⁶

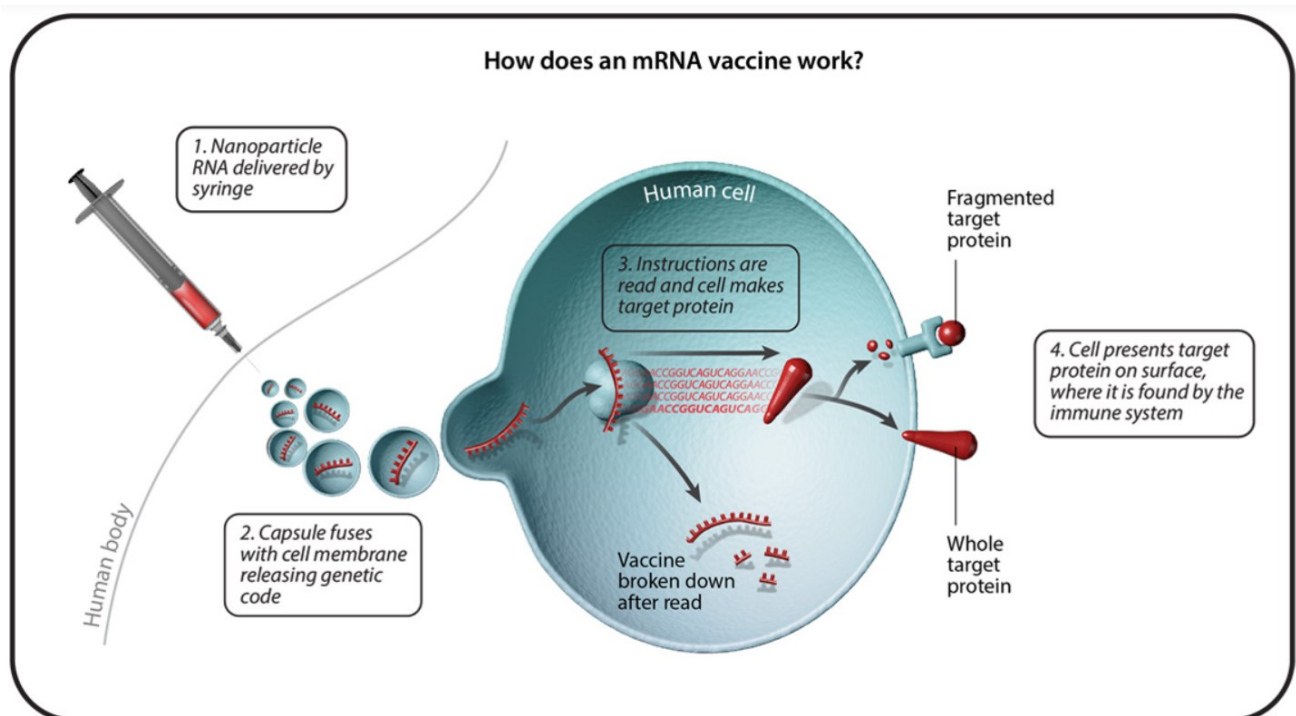


Figure 7 Mechanism of mRNA vaccines. In this kind of vaccines, nanoparticle containing mRNA of a target antigen are injected in the body and internalized into cells. mRNA is translated by the cell, which then expose or release the antigen protein: the latter is then recognised by the immune system, initiating the immune response.¹⁸

Whilst mRNA vaccines were limited to animal vaccines and experimental cancer immunotherapy, 2020 COVID-19 pandemic pushed development in this field at a neck breaking pace, and two mRNA COVID-19 vaccines, developed by Pfizer/BioNTech and Moderna, were approved in the fall of 2020 for the use on the population. These vaccines have the advantages of being easily developed, as mRNA is readily produced in bioreactors, and of possessing high efficacy in preventing severe form of the disease. However, the technology is still new, which means that the cost of the single dose is still quite high (12-20 \$), and also the problem of the thermostability of the formulations is not yet solved, which requires a cold chain at -70°C for transportation, hampering the access in tropical and poor countries.²⁷

Vaccine Adjuvancy

As previously described, most modern vaccines don't rely anymore on challenging a patient's immune system with a whole pathogen, be it attenuated or inactivated; rather, the preferred approach is using a subunit or even more recently a nucleic acid-based vaccine.

While the latter types of vaccines are inherently safer and less severe adverse events are observed following their administration, they are also less potent and efficient in stimulating a strong and long-lasting immunity, as they lack the variety and the quantity of antigens naturally expressed by a pathogen.²⁹

The first solution put in practice to overcome this problem was simply to increase both the dosing of the antigen and the number of primary and booster shots. However, there are two great disadvantages with this solution: the possibility of missing one or more booster shots, as in some cases they are years apart (compounded by natural avoidance for needle in part of the population), which lower protection coverage and raises the risk of outbreaks; and the requirement for large amount of precious antigens, which are not always easily available.^{2,17}

A different, more efficient solution is to include adjuvants in vaccine formulations. Vaccine adjuvants are materials that are able to enhance the immune response to antigens contained in a vaccine, thus increasing vaccine efficacy in building a strong immune memory.² A further advantage is that, using adjuvants, less amount of antigen is required to elicit a good response, so dosage in a single vaccines can be lowered: therefore, more vaccines can be produced with the same amount of materials.²⁹

Adjuvant	Description	Disease target (Vaccine)	Stage of Advancement/Key elements
Adjuvants in Licensed Vaccines			
Alum (aluminum salts)	Stable suspension of hydroxide and phosphate salts or amorphous aluminum hydroxide-sulfate (AAHS)	Included in several routine vaccines for children such as DTaP	Several decades of safety and immunogenicity data in humans. Novel formulations of Alum [6] or Alum used as particulate delivery system for immune potentiators is on-going [7]
Oil-in-water emulsions (MF59, AS03, AF03)	Squalene oil in water emulsions stabilized with non-ionic surfactant(s); could include other oils and stabilizers	Products for seasonal Flu (such as MF59 in Fludac) or Pandemic Flu (such as AS03 in Pandemrix)	Huge database of safety and immunogenicity with influenza antigens. Effective pandemic adjuvant for higher antibody response as seen in H1N1 2009 pandemic and on-going covid-19 pandemic
MPL	A naturally derived TLR4 ligand adsorbed onto L-tyrosine depot along with chemically modified allergens in an allergy vaccine	For pollen allergies on named patient basis in Europe (Pollinex)	As TLR4a adsorbed onto Alum or L-tyrosine, or delivered in a liposome, MPL is one of the first widely evaluated TLR agonist as a vaccine adjuvant
AS04	TLR4 agonist MPL adsorbed onto Alum	HPV (Cervarix) and HBV (Fendrix)	AS04 was first combination adjuvant licensed that paved path to developing similar synergistically acting adjuvants
RC-529	Synthetic glycolipid TLR4a adsorbed to Alum	Was licensed in Argentina in Hepatitis B vaccine Supervax. In clinical development for influenza vaccine	This Lipid A mimetic was one of the early synthetic immune potentiator tested in clinic for its adjuvant action
AS01	Liposome co-delivering MPL and QS21 (Saponin)	Malaria (RTS,S) vaccine, Herpes Zoster vaccine (HZ/su) and Shingles vaccine (Shingrix)	AS01 is the first adjuvant exemplifying synergy between three different adjuvants
CpG ODN (1018 ISS)	A soluble oligonucleotide serving as a ligand to TLR9	HBV vaccine (Hepilisav-B) in adults 18 or older	Its approval in the HBV vaccine has enabled the use of CpG in on-going Covid19 collaborations (Table 3)
Virosomes	Unilamellar liposomes associated with viral proteins and phospholipids from a strain of influenza virus	Was licensed in Flu vaccine (Inflexal) and HAV vaccine (Epxal), both of which are now off-market	Developed around 1980s and over 50 million doses distributed worldwide; Virosomes are well-tolerated and immunogenic

Table 2 A list of vaccine adjuvants currently approved for commercial use. For decades, alum was the only licensed adjuvants, but in the last 20 years several new compounds and formulations emerged as adjuvants.²⁹

Even though vaccine adjuvants advantages are evident, our poor understanding of the cellular mechanism behind immunity hampered research and development of this field, which really started to gain traction in the last 20-30 years.²⁹ Indeed, for more than 70 years, from its inception in the 1920s, Alum was the only vaccine adjuvant licensed for human use, and whilst it has been widely used for decades, its mechanism of action was only characterized in recent years.³⁰

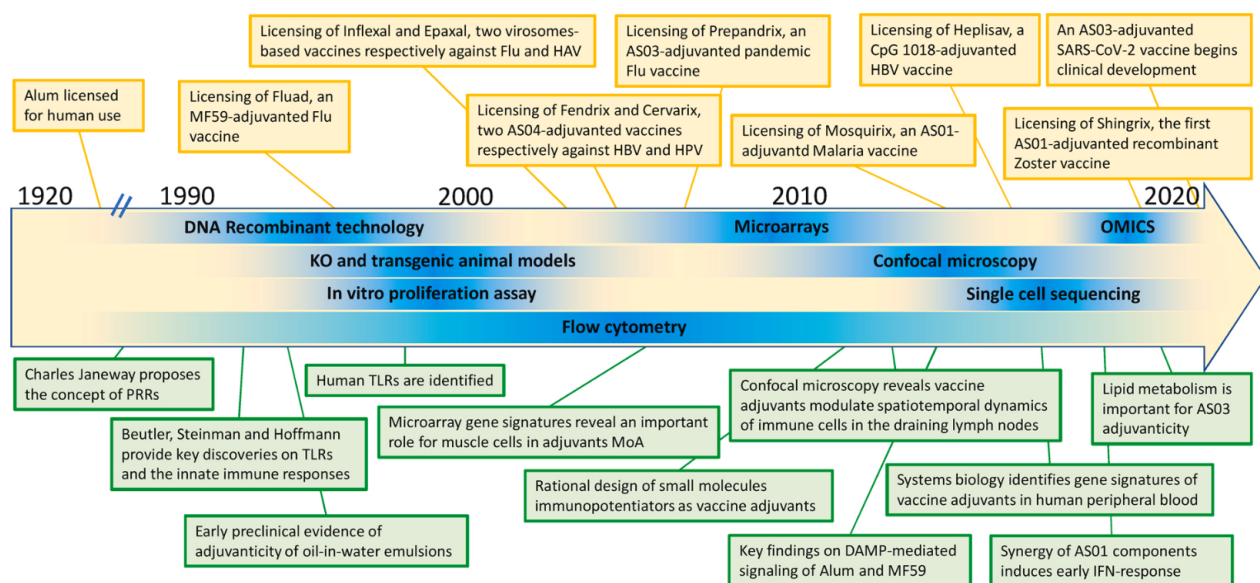


Figure 8 A schematic representation of the advancements in the field of vaccine adjuvants and of the technology breakthrough that allowed them. Most of the advancements have been made in the last 30 years, after Charles Janeway's discovery of Pattern Recognition Receptors (PRR).²⁹

Following several key technological advances, comprising systems biology approaches, as well as a renewed interest in vaccine adjuvancy, many progresses have been made and since the early 2000s a dozen of new adjuvants were licensed for use in human, with many more currently undergoing clinical trials, often based on oil-in-water emulsion or on molecules recognized by Pattern Recognition Receptors (PRRs) like protein of the TLR family.²⁹

Current Adjuvants

Aluminium-based adjuvants

For many decades, Alum was the only human approved vaccine adjuvant, and it is still prominent today, both alone and in coformulations such as Adjuvant System 04 (AS04).²

Chemically speaking, Alum refers to water-soluble $AlK(SO_4)_2$ to which a phosphate buffer solution containing an antigen is added, followed by basic precipitation in presence of NaOH. Thus, the real adjuvant results to be a mixture of aluminium hydroxide and aluminium phosphate, in the form of amorphous $Al(OH)_x(PO_4)_y$.^{2,30}

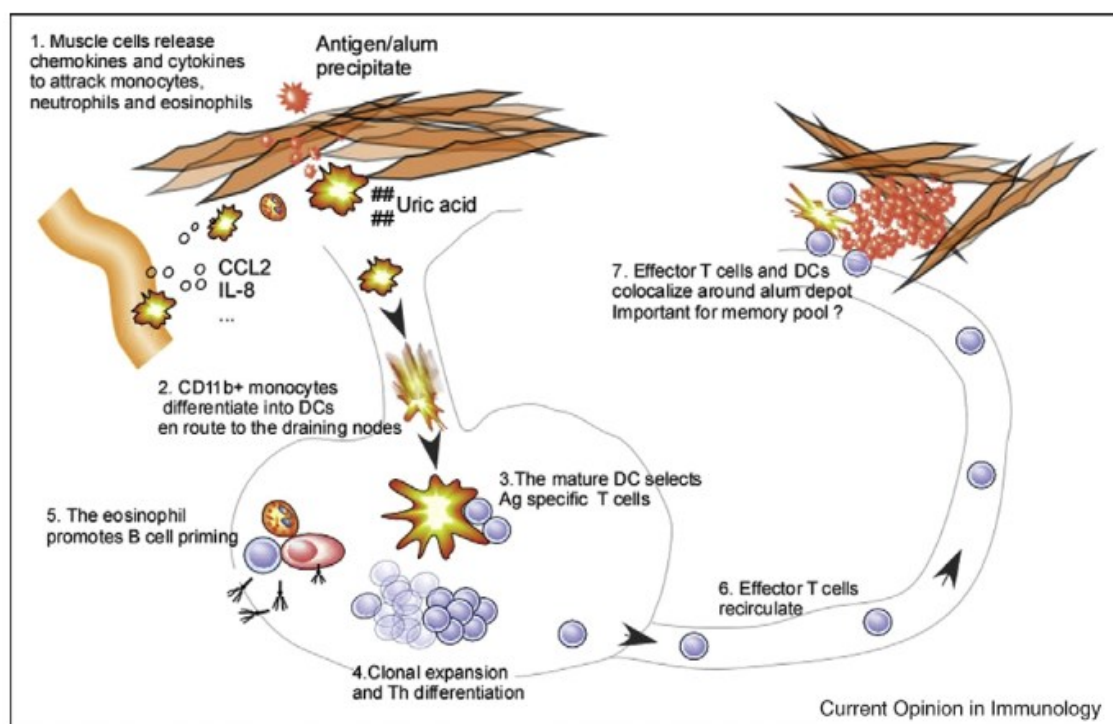


Figure 9 Mechanism of action of alum. Following injection, alum precipitates damage surrounding tissues, causing the release of uric acid. Uric acid acts as a DAMP, recruiting macrophages and dendritic cells that internalize the antigen and present it to naïve T and B cells. Alum is known to induce a T_H2 skewed immune response and a long-lasting B cell memory.³⁰

Until recently, its mechanism of action was unclear, with many speculations ranging from electrostatic exchange to a depot effect.² However recent studies proved that alum elicit immune response by causing endosomal damages upon internalization; this causes uric acid release, which is sensed as a stress signal which provokes immune cells recruitment on the injection site.³⁰ Eventually, this recruitment leads to the build-up of a strong immune response skewed towards T_H2 activity, suitable to a fight extracellular pathogens.^{19,30}

Even though the mechanism underlying its activity was unclear, Alum has been widely used for decades in many important vaccines, such as those against hepatitis A and B, encephalitis, polio and many others. Furthermore, Alum is also used as a platform to develop combination adjuvants and as a reference for new adjuvants activity.³¹

Emulsion-based adjuvants

Emulsion-based adjuvants were firstly established after 1937 Freund's observation that guinea pigs challenged with *Mycobacterium tuberculosis* killed using a water-in-oil paraffin emulsion developed higher antibodies titres than usual.³²

Despite these promising beginnings and many years of development, the so-called Freund's adjuvant was deemed too reactogenic for the use in humans by the WHO after failed trials in the 1960s; therefore it was never approved for use in human, though it remains in use in some veterinary vaccine formulations.³³

Toxicity was probably due to high levels of oil in the emulsion and their non-biodegradable nature (mineral oils, paraffins). Therefore, as interest for emulsion adjuvants remained high, and efforts were refocused towards the development of oil-in-water emulsions using natural oils such as squalene or tocopherol, which were firstly developed in the 1980s.²

They were firstly believed to form a slow-releasing antigen depot in the site of injection, allowing for prolonged immune system challenge, but this idea was recently disproven: the leading theory is that the emulsion creates an "immunocompetent" environment at the SOI, leading to the recruitment of immune cells and enhancing antigen uptake by directly increasing pinocytosis and phagocytosis, mostly eliciting a T_H2 response.³⁴

Emulsion Adjuvant	Composition (mgs per 0.25 mL) or in 0.5 ml Human dose			Buffer	Mean size by DLS (nm)	Method of Manufacturing	Clinical Development Stage
	Oil(s)	Surfactant(s)	Other components				
MF59	Squalene - 10.75	PS80–1.25; Span85–1.25	N/A	Citrate buffer; pH 6.0–6.5	160 ± 10	High -Shear homogenization followed by Microfluidization	Licensed
AS03	Squalene - 10.75; α -Tocopherol (immunostimulant) - 11.87	PS80–4.825	N/A	Modified Phosphate buffered Saline; pH ~ 6.8	155 ± 10	High -Shear homogenization followed by Microfluidization	Licensed
Squalene-in-Water Emulsion (SWE)	Squalene - 9.75	PS80–1.175; Span85–1.175	N/A	Citrate buffer; pH ~6.5	142 ± 5	High -Shear mixing followed by Microfluidization	Pre-clinical
SE in GLA-SE or SLA-SE	Squalene - 8.6	synthetic PCs - 2.73; Poloxamer 188–0.125	Glycerol (aqueous buffer component); May contain α -Tocopherol - 0.05 (antioxidant)	Ammonium Phosphate buffer; pH ~ 5.7	120 ± 40	High -Shear mixing followed by Microfluidization	Ph I - Ph III
AF03	Squalene - 12.5	Span80–1.85; Eumulgin B1–2.38	Mannitol - 2.3	Phosphate buffered Saline; pH ~ 7.2	100 ± 20	Phase inversion Temperature (PIT)	Licensed

Table 3 Properties of emulsion-based adjuvants²⁹

Today, oil-in-water emulsion formulations are used as adjuvants in several human vaccines, either by themselves or in combination with other adjuvants (i.e., PRRs targeting adjuvants). The most prominent, emulsion-only approved formulations are MF59 and AS03.²⁹

MF59 is composed by an emulsion of squalene in water with the addition of surfactants such as Span 85 and Tween 10 and is the second adjuvant ever approved for human use in influenza vaccines (Fluad[®], approved in Europe in 1997) and has been used in flu vaccines ever since.³⁵

AS03 (Adjuvant System 03, GSK) instead is a mixture of squalene and α -tocopherol in presence of Tween 80, which was approved in 2009 and used in Pandemrix[®] vaccine against the H1N1 swine flu pandemic that swept the world in 2009-2010, which makes it the first adjuvant used to fight a pandemic.³⁶

These successes increased the interest in emulsion based adjuvants, stimulating research to the point that many new such adjuvants are currently in development or undergoing clinical trial, such as Montanide ISA 51 or SWE.²⁹

PRRs targeting adjuvants

A more modern approach to adjuvants aims to enhance the immune response to an antigen by targeting Pattern Recognition Receptors (PRRs). PRRs are a large protein superfamily involved having the specific job to recognize Pathogens or Damages Associated Molecular Patterns (PAMPs or DAMPs) and triggering cytokines release: this event causes immune cells recruitment and maturation, allowing for a stronger and longer-lasting immunity, normally skewed towards a T_H1 response.²⁹

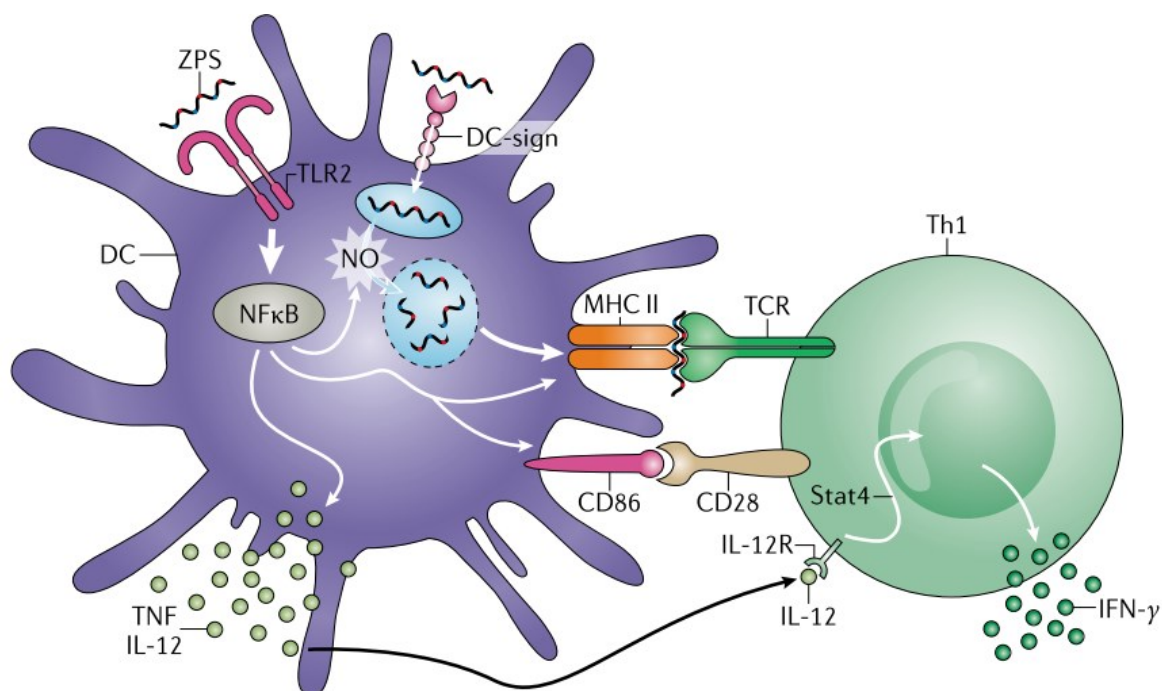


Figure 10 General mechanism of action of PRRs targeting adjuvants. Adjuvant binds to a PRR (here, TLR2), inducing immune activity and causing immune cells recruitment on the SOI. Immune cells uptake antigens, process them in lysosomes and expose them on their surface for T and B cells priming.³⁷

The most interesting family of PRRs are Toll-Like Receptors (TLRs), expressed on most immune cells as well as on epithelial and endothelial cells.³⁸ Their widespread presence in the body and deep involvement in immune system made them prime candidates as adjuvant targets, with the development of several pure and combination adjuvants, such as 1018 ISS, MPL[®], AS01 and AS04.²⁹ 1018 ISS is a water soluble CpG oligonucleotide which acts as an agonist TLR9, leading to production of proinflammatory cytokines such as IL-1 α , IL-1 β and TNF- α . 1018 ISS was recently approved for the use in a novel hepatitis B vaccine (Hepelisav-B[®]) by Dinavax, which only requires two doses and covers against all known subtypes of the virus.^{29,39}

MPL[®] is the trade name of Monophosphoryl lipid A (MPLA), a chemically detoxified derivative of *Salmonella minnesota* lipopolysaccharide (LPS). It retains LPS ability to bind and act as an agonist for TLR4, but without the toxic effects of its parent molecule. This makes MPL[®] an optimal immune system elicitor, able to induce several cytokines, comprising IFN- γ .⁴⁰

While It is used as itself in Pollinex Quattro[®], a vaccine against allergic rhinitis, it is more common to find it formulated in combinations with other adjuvants, in formulations such as AS01 and AS04.⁴¹ AS04 comprises MPL[®] adsorbed onto Alum and was licensed for human use in 2009, making it the first PRRs targeting adjuvant ever approved in human: it is currently in use in vaccines against HPV (Cervarix[®]) and HBV (Fendrix[®]).^{2,22}

AS01 is a combination of three adjuvants: MPL, QS-21 (a saponin from *Quillaja saponaria* acting by destabilization and consequent immune cell recruitment) and a liposome as delivery system. This adjuvant system exploits the synergistic effects between the three components to deliver an immune response stronger than the one obtainable by the single components. It was recently licensed in vaccines against malaria (Mosquirix[®]) and herpes zoster (Shingrix[®]).³⁷

The great success, both medical and economical, of these vaccines prompted advances in their research: several PRRs targeting adjuvants are currently being developed, with many already in clinical trial, as GLA-SE (TLR4), flagellin (TLR5) and Imiquimod (TLR7), which will hopefully help in producing safer and more effective vaccines in the future.⁴²⁻⁴⁴

Immunity

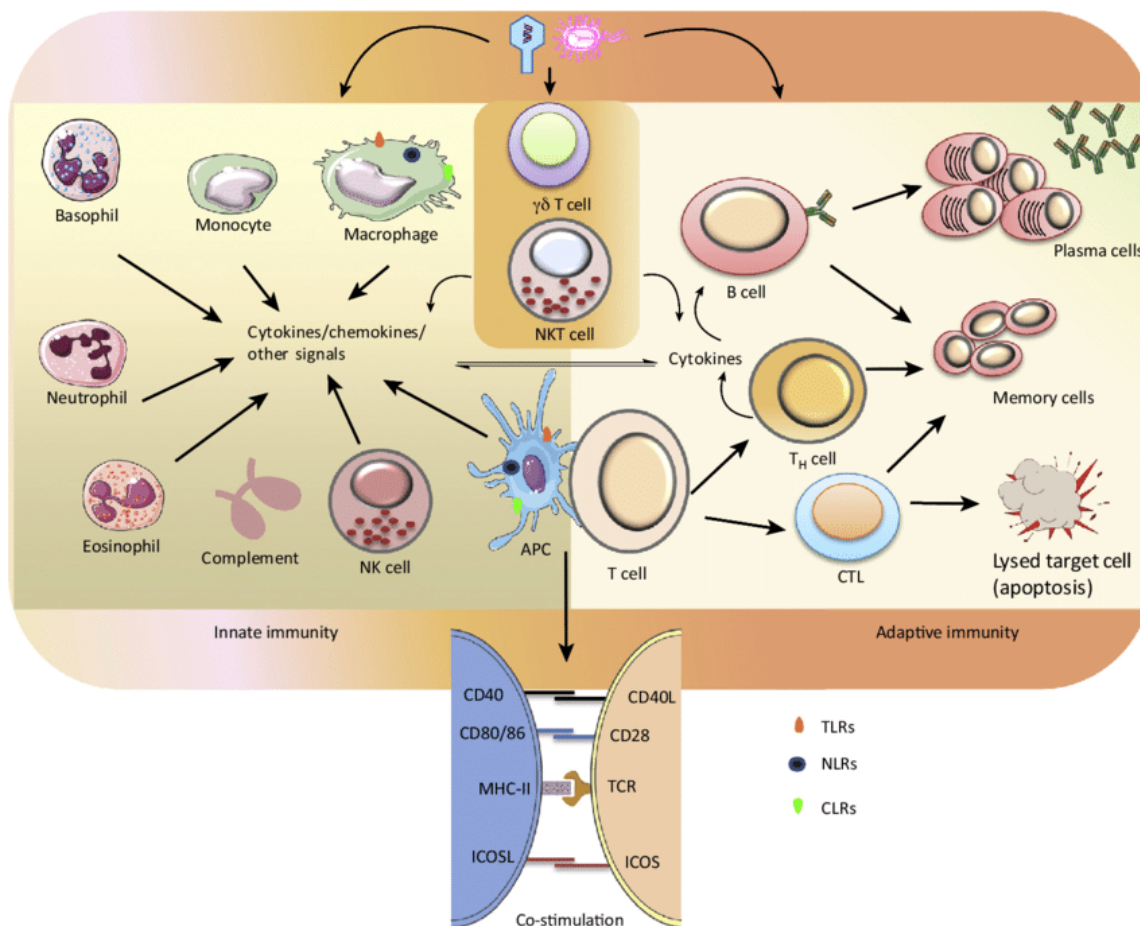


Figure 11 The immune system is composed by a variety of different cells and is commonly divided in two compartments: innate and adaptive immunity. Innate immune cells, such as macrophages, dendritic cells or neutrophils compose the innate immunity, who fight immediately and aspecifically against threats. Cytokines released by innate immune cells elicit activation of adaptive immune cells such as B cells, TH cells or CTLs that are able to fight specific menaces with high efficacy. At the interface between the two, APCs prima naïve T and B cells, while NKTs attack non-self entities.⁴⁵

Vaccines work by challenging the immune system with a non-infectious version of a possible menace: this way, the immune system itself has the possibility to learn to recognize and fight a pathogen, producing specific antibodies and memory cells with relative safety.

To achieve this result, vaccines exert their activity on both the innate and adaptive immune subsystems, the two “branches” the immune system is commonly divided: the cross-talk between cells of the two subsystem in the lymph nodes is what allows vaccine protective effect.⁴⁶

Innate Immunity

Innate immunity is the first line of defence of multicellular organisms, as it acts immediately (minutes to hours) against any internal or external threats; however, as its response is not specific against a particular menace, it is also less efficient than adaptive immunity.

It is based on the recognition of DAMPs and PAMPs, which happens through the binding to specific Pattern Recognition Receptors (PRRs, as TLRs) expressed on cellular or endosomal membrane in an array of specialized cells, such as monocytes, macrophages, DCs, glial cells, depending on the interested tissue.

DAMPs are small molecules or peptides (such as uric acid or HGMB1) released by damaged cells as a stress signal: it may be triggered by the presence of a tumor (i.e., HGMB1), viral infection (i.e., annexin) or cell tissue damage (i.e., uric acid, released upon Alum-induced cell damages). Their release alerts nearby cells of the presence of a problem, in order to recruit immune cells to deal with it.⁴⁷

PAMPs, on the other hand, are compounds or proteins (such LPS or Spike) produced by pathogens as part of their housekeeping metabolism: often they have a structural role for the cell (i.e., LPS or LTA) or are involved in their infective and reproductive cycle (i.e., Spike or dsRNA). As their presence and structure is indispensable for pathogen survival, and as such they're highly conserved over evolution, which makes them prime targets for recognition by the immune system.^{48,49}

Upon binding to PRRs, these molecules kickstart a series of events in the cell, mediated by kinases cascades, which brings to the release of nuclear effectors (i.e., NF- κ B, IRF3). These effectors cause the transcription of genes encoding for cytokines production, which after translation are released in the extracellular medium, triggering the inflammatory response, the first and more immediate way through which our body reacts to a threat.⁵⁰

More and different immune cells are thereupon recruited on site, while monocytes start maturing into macrophages and DCs: these two types of immune cells clear the site through phagocytosis and pinocytosis, eliminating the menace and digesting it in their lysosomes.

Of interest is the case of DCs, as they become APC: upon lysosomal digestion, peptides and proteins uptaken by phagocytosis are subsequently treated and exposed for recognition by T cells.⁵¹

Adaptive Immunity

Contrarily to innate immunity, adaptive immunity is highly specific and efficient toward a definite challenge, but it is also very slow to build up for the first time (several days to few weeks): the cells composing adaptive immunity have to be primed and need time to mature before fighting an unknown infection, as this requires genetic and epigenetic changes.⁴⁶

Adaptive immunity is based on the recognition of antigens (foreign molecular structure expressed by pathogens) by antibodies produced by B cells and by MHC I receptor on CD8⁺ T cells.

Antibodies can be either present as surface protein on B cells (IgD) or in solution as free protein (IgA, IgE, IgG, IgM). In both cases, when an antibody binds to its antigen epitope, the latter is marked for destruction by either the B cell itself or by other immune cells, such as macrophages.⁵¹

CD8⁺ T cells, also called Cytotoxic T Lymphocytes (CTLs), are a specialized T cell population whose job is to recognize and destroy infected cells. Through their MHC I receptor, CTLs bind foreign antigens exposed by cells infected by smaller microorganisms and kill them by cell lysis.⁵²

Interestingly, after the first infection, primed and mature adaptive immune cells do not disappear completely from the organism: a small fraction of them undergoes epigenetic variations so they become long-lived “memory cells”. Memory cells retain all the genetic information that made them able to successfully fight the infection, so that if the body is challenged a second time with the same pathogen, they can quickly replicate and eliminate the threat – memory cells induction is the main goal of vaccination.⁵³

The interface: how innate immunity primes adaptive immunity

Even if the immune system is classically divided in the two sections of innate and adaptive, and immunology is therefore similarly compartmentalized, in reality these two bodies work as a whole to protect the host organism: this is evident by looking at the interface between innate and adaptive immune system, where innate immune cells kickstart adaptive cells maturation – who in turn regulates innate cells activity.⁴⁶

Communications between the two branches happen mostly through cytokines and chemokines released in the extracellular milieu, which influence the behaviour of surrounding cells, shaping the

immune activity towards a type 1 or type 2 response: type 1 response involves cell/pathogen lysis and IgG production, and it is more suited to fight microbial infections (virus, bacteria, fungi, protozoa); type 2 response is instead more suited to fight parasites or venom, through IgE release, mucus secretion and invader expulsion.⁵⁴

When a threat is perceived by innate immune cells through the PRRs on their surface, they start fighting the infection by cell lysis (granulocytes, eosinophils, basophils, NK) or phagocytosis (macrophages, microglia, DCs) and releasing cytokines based on the PRR that was activated. However, some specialized cells -mostly DCs-, upon phagocytosis and lysosomal destruction, digest pathogen proteins in the endoplasmic reticulum and expose them on the cell membrane through their MHC I and II receptor, becoming APC.⁵¹

APC migrates in the lymph nodes, where they present the antigens exposed on their surface to naïve CD4⁺ and CD8⁺ T cells T Cell Receptor (TCR), to prime their maturation and differentiation in T helper cells (T_H) or CTLs respectively. While CTLs role is to kill pathogen-infected cells, as described above, T_H have an important regulatory role in shaping the overall answer of the immune system to the infection through the cytokine they release and the priming of B lymphocytes.

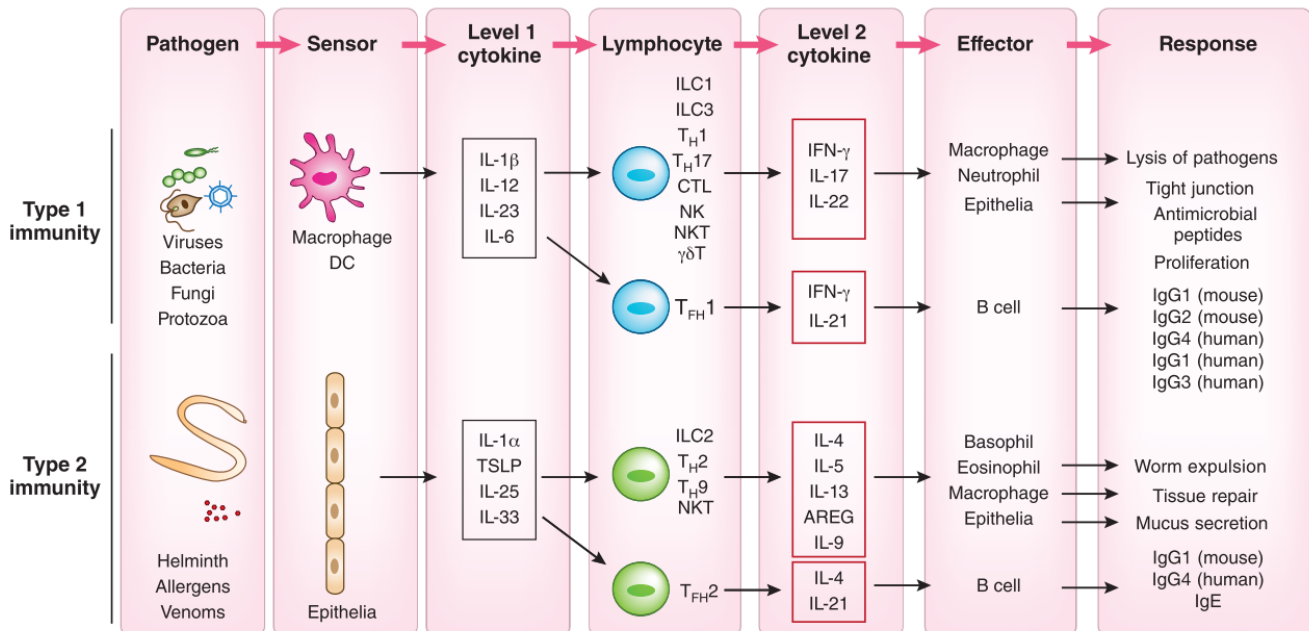


Figure 12 Adaptive immunity response strongly depends on the priming received by the innate immune system. Type 1 immunity, more suited to fight small organisms as viruses, bacteria, fungi and protozoa, is characterized by T_H1, T_H17, T_{FH}1 presence and it is induced by release of IL-1 β , IL-6, IL-12 and IL-23 by macrophages and DCs. On the other hand, Type 2 immunity, apt to defend against large parasites, allergens or venoms, is characterized by T_H2, T_{FH}2 and T_H9 and is induced by epithelial cells release of IL-1 α , IL-25, IL-33 and TSLP. In both cases, the mechanism is the same: following a challenge, a set of innate immune cells release a first level of cytokines, priming lymphocytes; lymphocytes then release a second set of cytokines that influence immune cells behaviour and response.⁵⁴

There are several T_H subtypes, involved in type 1 (mainly T_{H1} , T_{H17} , T_{FH1}) or type 2 (mainly T_{H2} , T_{H9} , T_{FH2}) immunity, and their maturation is influenced by APC-released cytokines: IL-1 β , IL-6, IL-12 and IL-23 causes type 1 T_H maturation, while IL-1 α , IL-25, IL-33 and TSLP are involved in type 2 T_H differentiation.⁵⁴

In both subsets, T_{HS} have the role of directing innate immune cell response to be more efficient, while T_{FHS} engage with the BCR on naïve B cells surface, which triggers their maturation.

B cell maturation is the final stage for an efficient adaptive response. After T_{FHS} stimulation in the lymphoid follicles, B cells undergo several genetic and epigenetic changes which result in V(D)J recombination and isotype switching. V(D)J recombination is the process in which the variable, diversity and joining segments of antibodies genes are recombined to try and produce antibodies a given antigen: high affinity mutants are selected for replication and further improvements. Isotype switching is the process through which cause the constant region of the heavy chain to change, switching the subtype of antibodies produced by the B cell.⁵¹

These two events produce a specific and efficient immune response for the ongoing infection, and are both influence by cytokines expressed by T_{FHS} , which in turn were shaped by innate immune cells cytokines.⁵⁴

Pattern Recognition Receptors (PRRs)

The immune system is a well-oiled machine able to shape its response in the most adequate way for fighting the menace it is challenged with. To achieve this result, immune cells use chemokines and cytokines to communicate vital information such as the site and extent of infection and more importantly its nature: viral, helminthic, tissue damage, etc. Production of the correct type of cytokines is induced and depends on the DAMPs and PAMPs sensed by cells through their PRRs.⁵⁴

PRRs are a broad range of proteins whose job is to recognize and bind to a given PAMP or DAMP and transmit the binding signal into the cell through a kinases cascade, so that the cell can appropriately respond, for example maturing into a macrophage or a DC or releasing the suitable set of cytokines.⁴⁹

PRRs are expressed by innate immune cells and some epithelial and endothelial cells. PRRs can be found either on the cell surface, localized mainly in specialized, lipid-rich compartments called lipid rafts, or in endosome, in order to recognize intracellular threats.⁵⁵

PRRs in human encompass several protein family, having different role: C-type Lectins Receptors (CLRs), specialized in recognising carbohydrate-based PAMPs, particularly fungi ones; NOD-Like Receptors (NLRs), whose role is to recognize bacterial peptidoglycan in cytoplasm; Rig-1-Like Receptors (RLRs), which senses viral presence by dsRNA binding; and Toll-like Receptors (TLRs).^{48,56} Differently from CLRs, NLRs and RLRs, that are more specialized, TLRs recognizes a wide variety of structurally unrelated PAMPs and DAMPs, ranging from viral dsRNA to nucleus stress signal HMGB1 to bacterial LPS: for this reason, TLRs are the most widely studied PRRs class and the most interesting targets for vaccine adjuvants development.⁵⁰

Toll-like Receptors (TLRs)

TLRs are a class of PRRs belonging to the Interleukin-1 Receptor/Toll-like Receptor superfamily, which shares the Toll-IL-1-Receptor (TIR) domain, a protein/protein interaction surface responsible for downstream signaling, bound either to TIRAP/MyD88 or TRAM/TRIF protein effector.

TLRs are characterized by their horseshoe shape given by a Leucine-Rich Repeat (LRR) domain: the LRR is the portion of the protein responsible for ligand binding and recognition. Upon binding, TLRs undergo homodimerization or heterodimerization (in the case of TLR1/TLR2 and TLR2/TLR6): dimerization causes conformational changes in the TIR domain, which is the event that triggers downstream signaling by kinases cascade amplification, eventually leading to inflammation and immune response.³⁸

Thirteen TLRs have been characterized so far in mammalian, ten of which are present in human, with different localizations, functions, and molecular target. TLR1, TLR2, TLR4, TLR5, TLR6, TLR10, TLR11, TLR12 and TLR13 are expressed on the cells surface and sense for external threats, while TLR3, TLR7, TLR8 and TLR9 are localized in endosomes and are responsible for recognizing internal infections.³⁸

While molecular targets of TLR10, TLR12 and TLR13 (and so their exact functions) remain unknown to date, the main ligands of the others are well characterized.

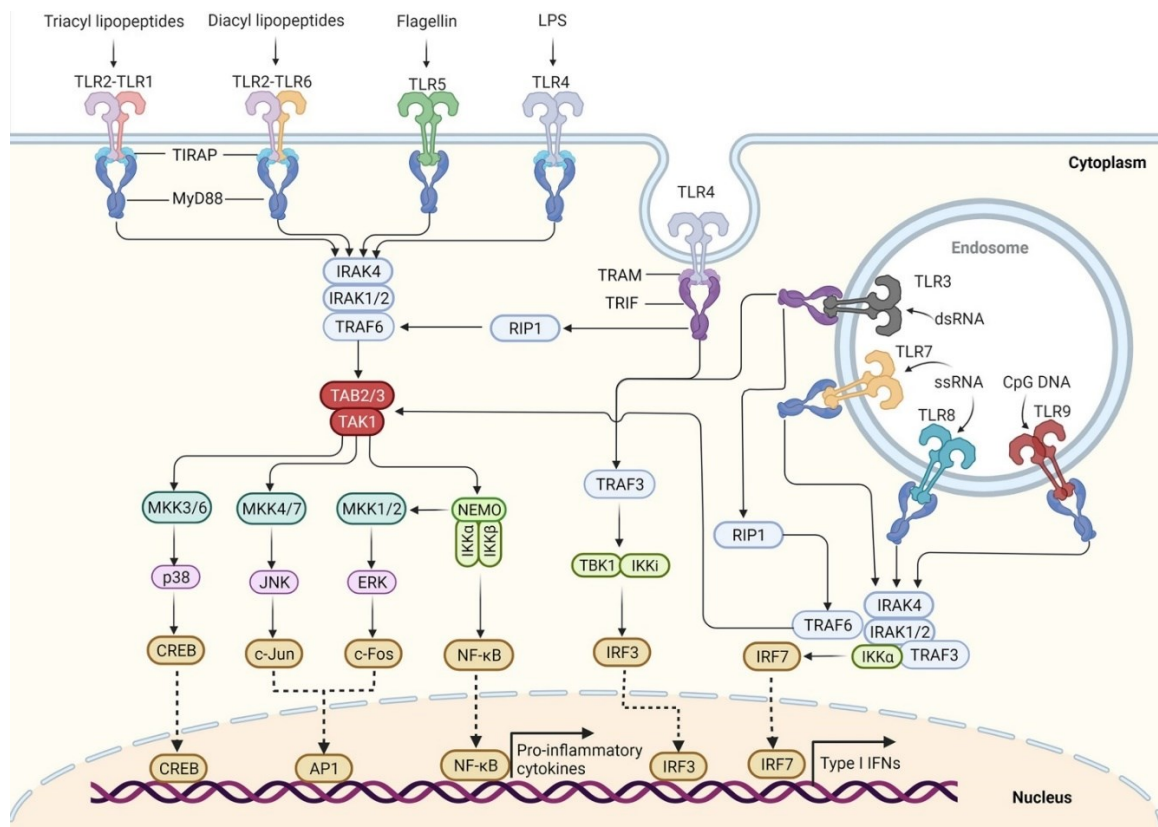


Figure 13 An overview of the TLR family and the PAMPs they recognize. It is possible to distinguish two sets of TLRs: cell membrane TLRs (TLR1, TLR2, TLR4, TLR5 and TLR6) and endosomal TLRs (TLR3, TLR7, TLR8 and TLR9). The first group recognizes PAMPs related to bacterial presence in the body, while the second binds to PAMPs present in case of intracellular infection. In both cases, upon PAMP binding, a kinase cascade kickstart inflammatory response.⁵⁷

All endosomal TLRs recognizes exogenous nucleic acid released in the cytoplasm as result of cellular invasion by microbes: TLR3 and TLR8 bind to viral dsRNA, TLR7 binds viral ssRNA, while TLR9 recognizes bacterial and viral CpG DNA.⁵⁸

Cell surface TLRs ligands are more diverse in structure, and the PAMPs recognized are related to bacteria, fungi and parasites like profilin (TLR11) or flagellin (TLR5).⁴⁴

Furthermore, some cell surface TLRs have interesting and peculiar characteristics. TLR2 is the only TLR receptor able to heterodimerize with two other receptors, and the ligands it recognizes differ depending on the second TLR involved: in combination with TLR1, TLR2 binds to Gram-positive bacterial triacylated lipoproteins and parasitic GPI-anchored proteins, while in combination with TLR6 it recognizes Gram-positive bacterial diacylated lipoproteins as well as fungal zymosan.⁴⁹

On the other hand, TLR4 is the only TLR having both downstream pathways. For this reason, it is a very interesting candidate as a vaccine adjuvant target, as being able to select for one pathway over the other can lead to different and targeted immune responses, more suitable to various kind of vaccines.⁴⁴

TLR4 and its ancillary proteins: a peculiar case

TLR4 main role is to sense the presence of Gram-negative bacteria, through its ability to bind and recognize LPS, a necessary component of Gram-negative bacterial outer membrane. However, TLR4 can also bind a variety of structurally different DAMPs, ranging from nuclear proteins such as HGMB1 and IFI16 to oxidised phospholipids, even though the exact mechanism of their recognition is not yet entirely clear.^{59,60}

On the other hand, since its discovery in 1997, TLR4 recognition of LPS have been widely studied and characterized, and today a clear picture of its mechanism is available. Due to the relatively small presence of free LPS in solution, as most of it remains on bacterial membrane, LPS recognition is a complex mechanism involving a series of auxiliary proteins, which make possible to detect even pM concentration of LPS in the organism: Lipid Binding Protein (LBP), Cluster of Differentiation 14 (CD14) and Myeloid Differentiation protein 2 (MD-2), who forms a stable complex with TLR4.⁶¹

Lipid Binding Protein (LBP)

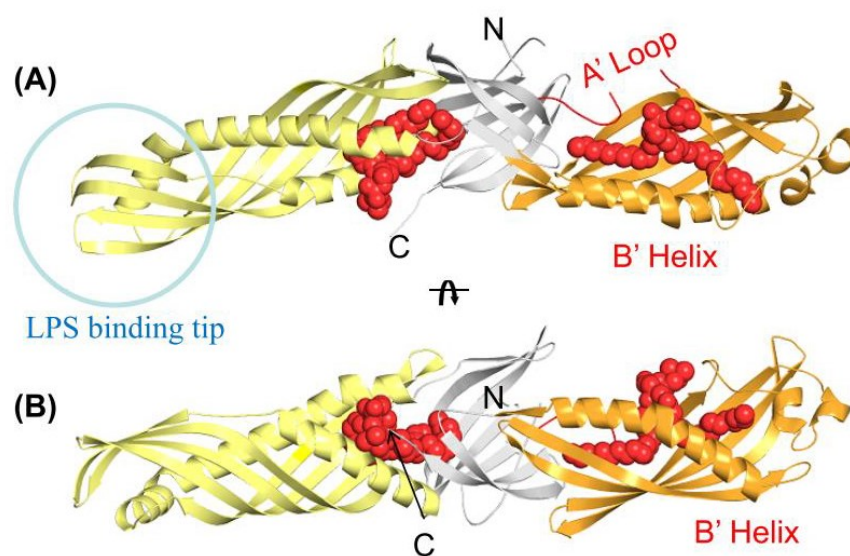


Figure 14 Structure of LBP. **A)** representation of the three domains: N-terminal (yellow), central (grey) and C-terminal (green); bound LPS is shown as red spheres. **B)** 90° rotated view of LBP.

LBP has the crucial role of extracting single molecules of LPS from bacterial membrane or from free floating aggregates or vesicles and present it to either CD14: without its action, LPS would be too tightly packed for TLR4 binding, thus the immunostimulatory activity would be too weak.⁶²

LBP is a 58-60 kDa boomerang shaped protein, composed of three domains: C-terminal, central and N-terminal, with this latter domain being responsible for LPS binding.⁶³

This domain is indeed rich in positively charged residues near the tip of the protein, which can interact with the several negatively charged phosphates present on LPS; furthermore, it also presents a hydrophobic pocket pointing toward the central domain to accommodate LPS lipidic chains.⁶²

Cluster of Differentiation 14 (CD14)

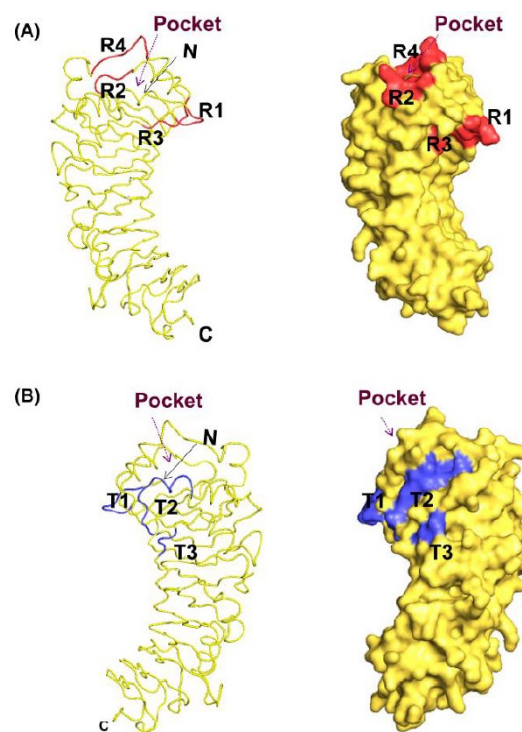


Figure 15 Representation of CD14. **A)** LPS binding pocket, on the tip of the protein, is colored in red. **B)** 180° rotated view, with LPS binding pocket colored in blue.

CD14 can be expressed in two forms: either as a soluble protein (sCD14) in the extracellular milieu or as a membrane bound protein (mCD14) anchored to the immune cell membrane by a glycosylphosphatidylinositol moiety.⁶⁴

It contains a LRR domain, and it shows the characteristic solenoid shape of such proteins; contrarily to most LRR proteins, though, its binding pocket appears to be on the tip instead that in the concave region. The binding only happens through a hydrophobic pocket, lacking any positively charged residue: this suggests that CD14 is not meant to retain its ligand for long times, but just to carry it to the next protein in the pathway.⁶⁵

Indeed, recent studies show that CD14 forms a ternary complex with LBP and LPS, where LBP catalyses multiple LPS transfers to sCD14 or mCD14, and then CD14 quickly pass LPS to the TLR4/MD-2.^{65,66}

CD14 role appears to be to enhance local LPS concentration to increase TLR4 sensitivity: indeed it is demonstrated that TLR4 requires CD14 presence to detect LPS when concentration is lower than 100 ng/mL, while CD14-mediated activation is not needed above this concentration.⁶⁷

Furthermore, the involvement of CD14 appears to be fundamental for TLR4-mediated LPS endocytosis, which triggers the TRAM/TRIF signaling pathway.⁶⁸

Myeloid Differentiation protein 2 (MD-2)

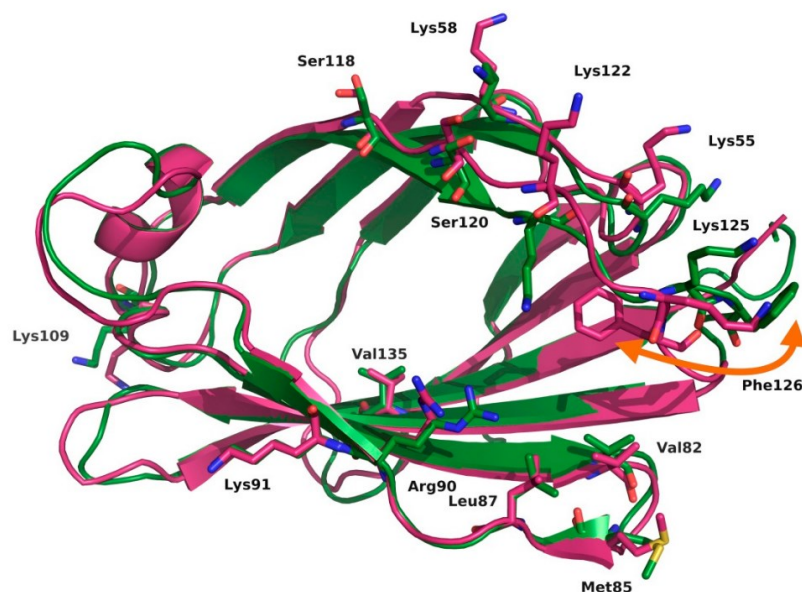


Figure 16 Top view representation of MD-2. In the figure, agonist (magenta) and antagonist (green) conformations obtained by X-ray crystallography are superimposed. Phe126 position switch is marked.⁶⁹

MD-2 is the final protein involved in LPS recognition. It is a small protein of c.a. 20 kDa belonging to the Cup family, characterized by the presence of a large hydrophobic pocket used to carry or store lipid molecules. The “cup fold” in cup proteins consists of two antiparallel β sheets that can be separated to accommodate the lipid ligand in the hydrophobic core.⁷⁰

In MD-2, the cup fold is peculiarly large, consistently with the need of binding such a large molecule; furthermore, the external rim is characterized by the presence of several lysines and arginines, to strengthen the interaction with the negatively charged hydrophilic core portion of LPS, while the larger O-antigen portion interacts with TLR4 LRR moiety. Interestingly, on the rim is located Phe126, a residue that undergoes conformational change upon ligand binding and it is therefore thought to be part of the signaling process.⁷¹

MD-2 is always found complexed to TLR4, in a stable heterodimer formed as early as in the endoplasmic reticulum. Their interaction is mediated by charge enhanced hydrogen bonding happening MD-2 and two distinct portions of TLR4 LRR called A and B patches. TLR4 A patch is predominantly rich in negatively charged residues, while the B Patch is mainly composed by positively charged residues: those charged patches interact with oppositely charged surfaces on MD-2.⁷¹

MD-2 acts as a high affinity binding unit for LPS, and TLR4-mediated LPS recognition is completely abolished in MD-2 absence.⁷²

Toll-like Receptor 4 (TLR4)

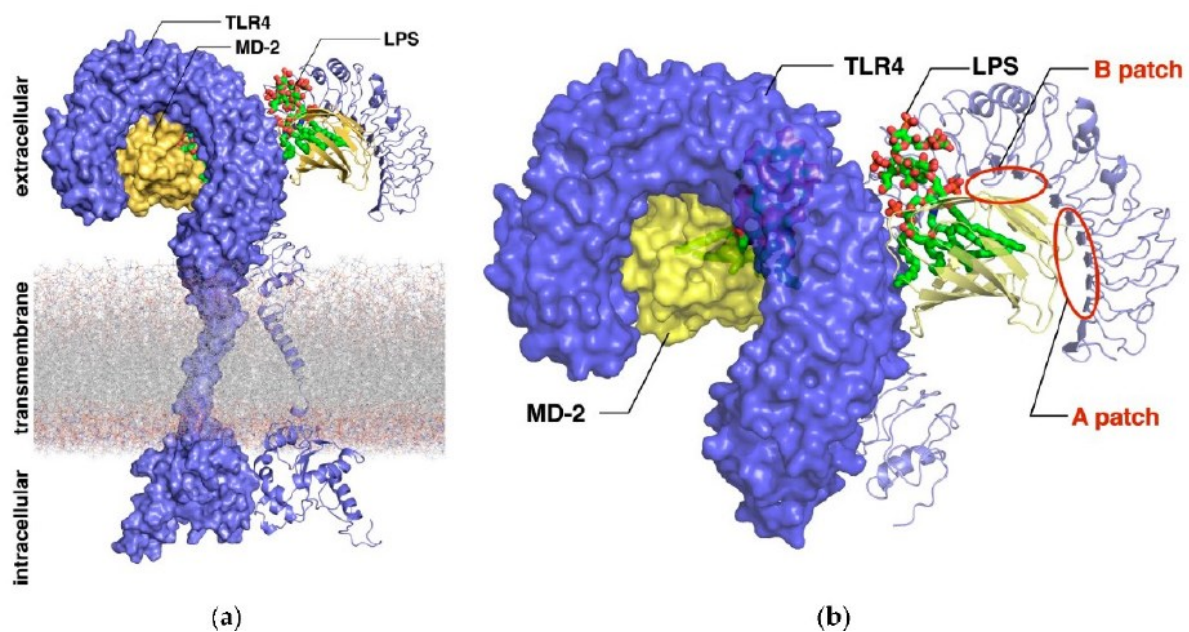


Figure 17 3D structure of (TLR4/MD-2/LPS)₂ complex. A) Complete representation, showing the three domains of TLR4: ectodomain, transmembrane helix and cytosolic tail. B) Close-up of the ectodomain; the A and B patch, needed for TLR4/MD-2 heterodimerization are marked.⁶⁹

TLR4 itself is the final LPS receptor, and with the help of LBP, CD14 and MD-2 can detect LPS down to pM concentration: TLR4 is thus one of the most sensitive receptors and can effectively spot the presence of even the smallest bacterial infection.^{38,73}

TLR4 is a rather large type I transmembrane molecule of c.a. 95 kDa composed by 800-850 residues (depending on the host organism), divided in three domains: an extracellular domain (ectodomain), a transmembrane helix and an intracellular cytosolic tail.³⁸

The ectodomain is the largest of the protein, with more than 600 residues, and is the region where LPS binding and MD-2 interaction happen. The ectodomain is a conserved LRR region: it is composed of many LRR modules, each 20-30 residues long showing a LxxLxLxxN residues pattern. In a single module, leucines point inward the protein, forming a core stabilised by hydrophobic interactions, while the variable aminoacids point outwards to the solvent, forming an interactive surface for ligand/other protein binding. LRR modules form strands stacking parallels to each other in larger sheets, giving the protein the typical horseshoe shape.^{71,74}

The cytosolic tail is shorter, 175-200 residues. It is responsible for the transmission of the binding signal downstream: upon ligand binding and receptor dimerization, the TIR domain present in the

cytosolic tail undergoes conformational changes that cause activation either of the MyD88-dependent or independent pathway, depending mainly on the involvement of CD14.⁴⁶

Downstream Signaling

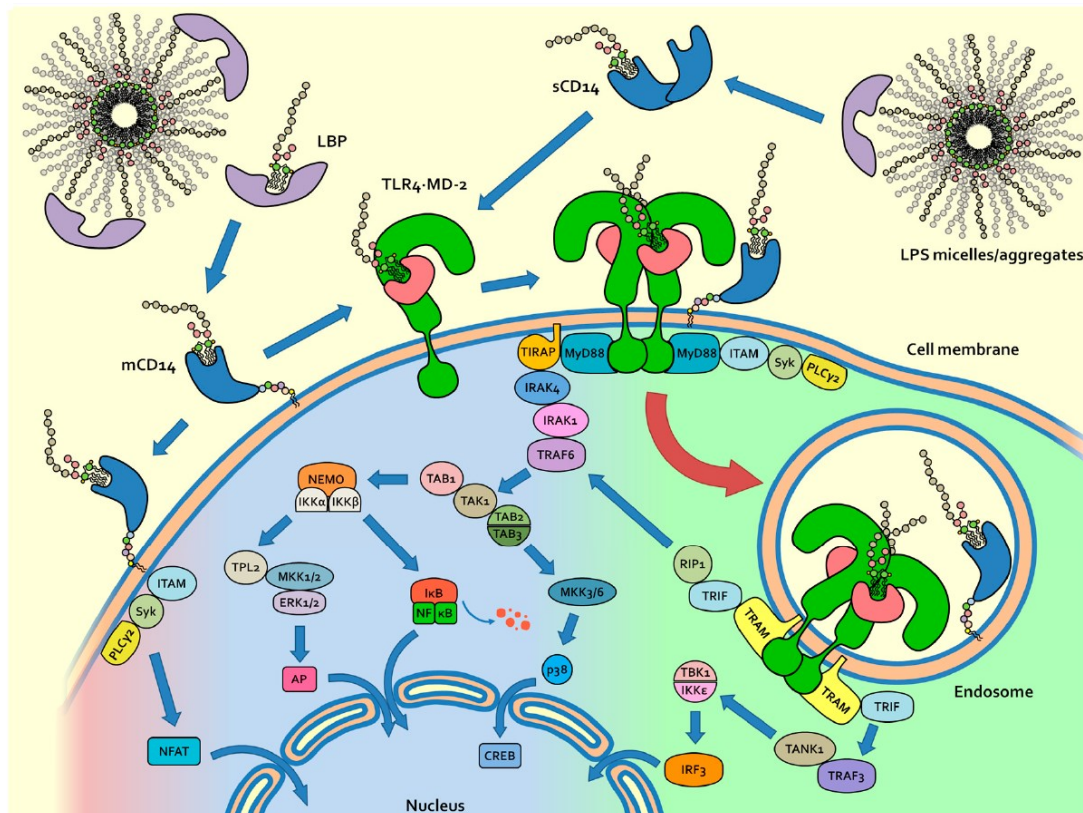


Figure 18 The complete signaling pathway of TLR4. Upon LPS binding, favoured by LBP and CD14, TLR4 dimerizes. This event changes the conformation of the TIR domain, recruiting the Myddosome, which triggers various kinases, such as IRAK4 and IRAK1. A subsequent cascade leads to NEMO activation and nuclear localization of various DNA effector such as NF- κ B and AP-1. However, if mCD14 is involved in the process, TLR4 is internalized in an endosome and the TRIF-dependent pathway is triggered leading to IRF3 localization in the nucleus.⁶¹

A peculiarity of TLR4 is its ability to trigger both possible downstream pathways for TLRs: the MyD88-dependent and the TRIF-dependent pathway. The two pathways induce the production and release of different sets of cytokines which in turn shape the immune response in slightly different ways, depending on the conditions of TLR4 activation. This makes TLR4 unique in its role as a link between innate and adaptive immune systems: a role that would be interesting to exploit for vaccine adjuvancy.⁴⁶

MyD88-dependent Pathway

The MyD88-dependent pathway is the most common in the TLRs family, as it is present in all TLRs except for TLR3. TLR4 dimerization and conformational changes in the TIR domain recruit the proteins necessary for building the so-called myddosome: The first protein in the myddosome is TIRAP (TIR domain containing Adaptor Protein, also known as MAL), which then recruits MyD88 through interactions in its Death Domain.³⁵

MyD88 then starts an intracellular kinases cascade by activation of IRAK4 and IRAK1. Through TRAF6 activation and IKK kinases, the cascade eventually leads to I κ B α phosphorylation and NF- κ B translocation to the nucleus, where it induces proinflammatory cytokines translation, such as IL-1 α , IL-1 β , IL-6, IL-12 and TNF- α , leading to a robust T_H1 skewed immune response.⁴⁶

TRIF-dependent Pathway

Only used by TLR3 and TLR4, in TLR4 the TRIF-dependent pathway is mediated by the participation of mCD14 to LPS recognition process. Upon internalization, TRAM (TRIF-Related Adaptor Molecule, also known as TICAM-2) is recruited on TLR4 TIR domain. TRAM works as an adaptor for the binding of TRIF (TIR-domain protein inducing Interferon, also known as TICAM-1), which can then interact both with TRAF6 and RIP1, on the N-terminal and C-terminal domain respectively. Both can induce to NF- κ B translocation as in the MyD88-dependent pathway, giving a similar immune response but at a delayed rate.⁷⁵

However, TRIF also recruits TRAF3, an effector activating TANK1 and I κ B ϵ kinases which in turn phosphorylate and activate IRF3, a crucial regulator of type I interferons transcription. Type I interferons, such as IFN- α and IFN- β play a key role in immune response against viruses: once produced and released by immune cells, they bind the IFN- α/β receptor (IFNAR) on target cells, which in turn kickstarts the production of proteins (i.e., STAT, IRF9) able to interfere (hence the name) with replication of viral RNA and DNA, preparing host cells to resist viral infections.⁴⁹

Lipopolysaccharide (LPS)

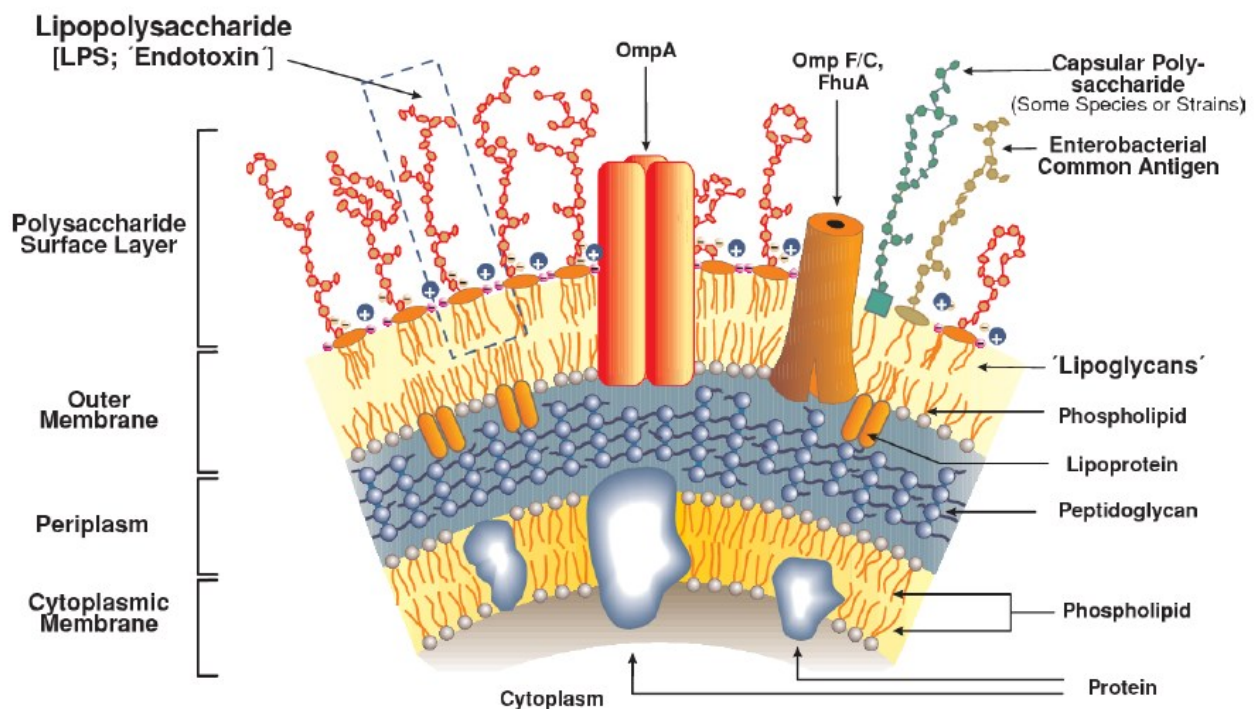


Figure 19 Gram-negative bacteria cell membrane. Gram-negative bacteria possess two membranes separated by the periplasm and a thin layer of peptidoglycan. The innermost membrane, the cytoplasmic membrane, is mainly composed by common phospholipid. The outer membrane outer leaflet, on the other hand, is constituted by LPS. LPS has a fundamental structural role in the membrane, it is involved in strain-strain recognition and creates a permeability barrier against foreign agents (e.g., antibiotics).^{76,77}

LPS, also called endotoxin, is the main component of the outer leaflet of Gram-negative bacteria outer membrane and is the most potent immunostimulatory known to date.⁷⁷

It plays a fundamental role in maintaining the shape and organization of the membrane and in protecting the cell from foreign agents (biological or chemical), and its low fluidity provides the bacterium with a resistant wall impermeable to an array of antibiotics or detergents wall; furthermore, it helps masking other antigens present on the membrane, so to go unnoticed to host's immune system.⁷⁷

As LPS has such a critical role for cell viability, its overall structure is conserved over evolution in all Gram-negative bacteria, even though with differences between different species, and sometimes even within the same strain. For this reason, our innate immune system evolved to recognize it as a preferential target ligand.⁷⁷

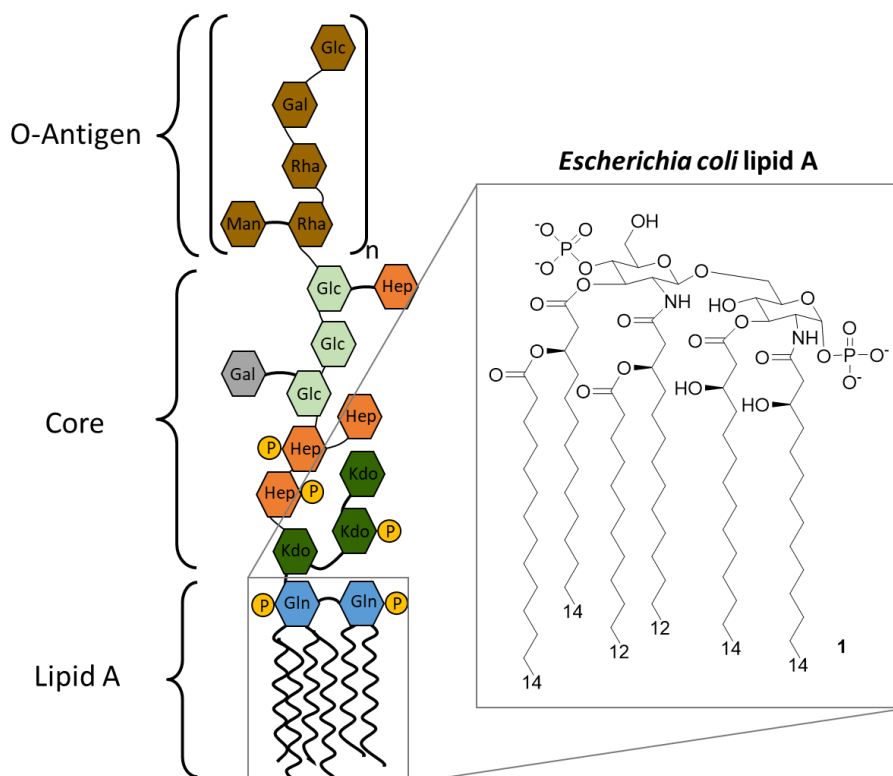


Figure 20 LPS structure. LPS can be divided in three sections: a long polysaccharide called O-antigen, a shorter core oligosaccharide and the lipophilic lipid A. Lipid A is the immunogenic portion of LPS, the pharmacophore of the entire molecule, and in most instances is composed by a diglucosamine scaffold bound to two phosphates and a variable number of lipidic chains.

LPS structure can be divided in three portions: O-antigen, core and lipid A, with the latter being the most conserved. The O-antigen is the region of LPS with the highest variability, but, in most bacteria, it is commonly composed by a polysaccharide formed c.a. 50 repeating units of smaller, 2-8 membered oligosaccharide.⁶¹

The core is a shorter, more conserved oligosaccharide, commonly divided in two subsections: outer core and inner core. While the outer core has still a good degree of variability and is composed mainly by common hexose sugars (like glucose, galactose, N-acetyl glucosamine), the inner core is commonly composed by rare sugars: one to three heptoses bound to one to three 3-deoxy-D-manno-oct-2-ulosonic acid (Kdo). Kdo presence is highly conserved, being observed in most bacteria to date, as it is the case for the $\alpha(2\rightarrow6)$ linkage between the last Kdo unit in the core and lipid A.⁶¹

Lipid A is the most conserved region of LPS; therefore, it is the region our immune system binds through the TLR4/MD2 hydrophobic pocket and can be considered the pharmacophore of the entire molecule, which makes it the most interesting starting point for TLR4 modulation. Lipid A is almost always built around a $\beta(1\rightarrow6)$ linked disaccharide scaffold composed by two D-glucosamines, bearing two phosphates and several lipidic chains. The phosphates are on the extremities of the

backbone, in position 1 and 4', and in some case can be substituted with small polar groups like ethanolamine, further phosphates or further sugars. Position 2, 3, 2' and 3' can be esterified with up to four lipidic chains, either linear or branched with further esters.⁷⁸

The number and nature of the lipidic chains are pivotal for host's immune response, as it is shown by the emblematic case of *Yersinia pestis*: if grown at 27 °C, it produces an highly immunogenic lipid A bearing 6 chains, one of which unsaturated; however, if grown at 37 °C (physiological temperature of most of his hosts, comprising humans), its lipid A only presents 4 fully saturated lipidic chains, which have a reduced impact on immune response and allow the pathogen to be more virulent.⁷⁹

Aggregation Properties

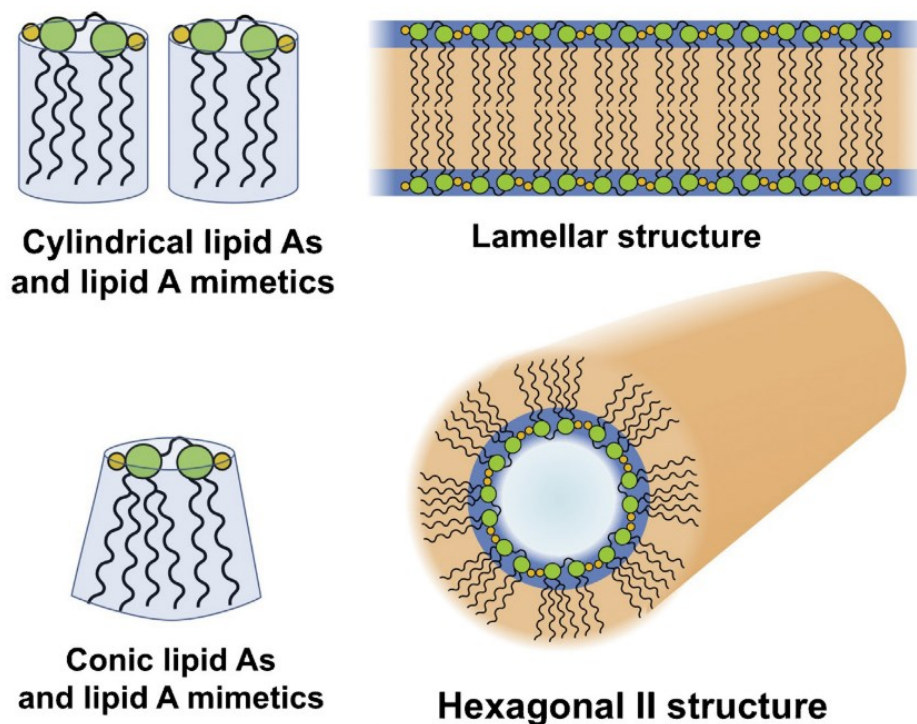


Figure 21 Relation between shape and aggregation of LPS. LPS having a cylindrical three-dimensional shape aggregate in a lamellar structure, while conical LPS assume an inverted hexagonal structure.⁸⁰

Bearing a large hydrophilic portion (O-antigen and core) as well as a highly hydrophobic one (lipid A), LPS is an amphiphilic molecule. This means it naturally aggregates in an aqueous environment, such as bodily fluids, and it does so with a very low Critical Micellar Concentration (CMC), which can be roughly estimated to be 10^{-8} M for most strains.⁷⁶

Indeed, when excreted by the outer membrane, they are always in the form of aggregates due to the low CMC. Furthermore, in many instances LPS is released by bacteria in the form of Outer Membrane Vesicles (OMVs) for cell-cell communication purposes or in some cases for carrying toxic compounds into other bacterial strains to lessen competition over resources.⁸¹

While there is still some debate, it seems like the aggregates, and not the single molecules, are the biologically active unit of LPS, as demonstrated by Mueller et al., which means that aggregation properties play a key role in eliciting an immune response.⁸²

It has been shown, indeed, that LPS aggregating in a lamellar pattern, forming a lipidic bilayer structure, exhibit in general a low immunogenicity, as is the case for *Rhodobacter sphaeroides*. On the other hand, LPS whose aggregates take an inverted hexagonal structure (that is, with the lipidic chain pointing towards the solvent) exhibit strong immunostimulatory properties: this is the case, for example, of *Escherichia coli*, whose LPS is the most biologically active one.⁸⁰

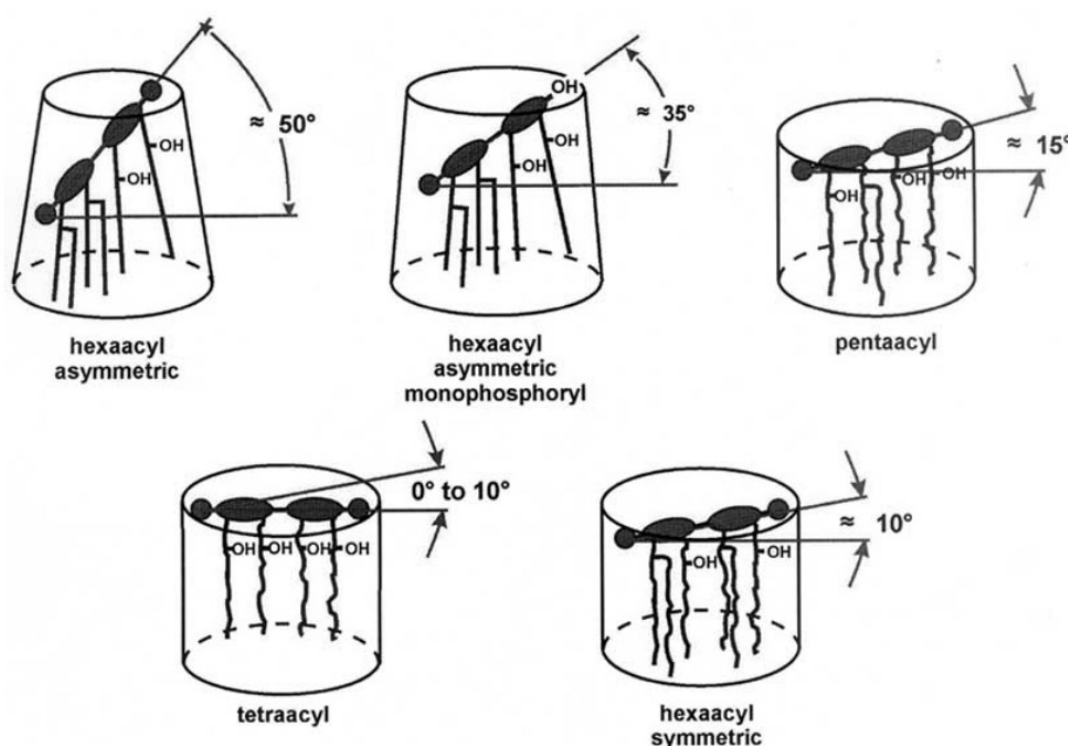


Figure 22 Relation between chemical formula of lipid A and the angle between sugar scaffold and lipid chains. The number of phosphates and the distribution of lipid chains are the main contributor to the angle, with an even distribution leading to a small angle and an uneven distribution leading to a large angle. Larger angles are correlated to higher immunogenicity.⁸³

Most of the aggregation properties are given by the structure of the lipid A, particularly by its three-dimensional shape and by the fluidity of the lipidic chains it bears. The shape of lipid A varies between conical and cylindrical, with conical favouring an inverted hexagonal aggregation pattern and cylindrical a lamellar ordered structure. Lipid A shape depends on the tilt angle between the disaccharide backbone and the lipidic chains: uneven acylation patterns lead to conical shapes, as in the case of *E. coli* lipid A, whose six acyl chains in a 4+2 pattern leads to a tilt angle of about 50°; while even an even distribution of lipidic chains, as in *R. sphaeroides* 2+2 pattern, leads to a tilt angle of 0° and to a cylindrical shape. Tilt angles in the middle range (25°-45°), like in the case of MPLA, lead to mixed aggregates and to moderate biological activity.⁸³

Chains fluidity is the ability of the various atoms to freely rotate around their bonds, changing the conformation of the molecule: it is influenced by the nature of the lipidic chains themselves (their length and eventually the presence of unsaturation) and by the temperature. The nature of the lipidic chain is an intrinsic parameter: shorter and more unsaturated chains require less energy to have high fluidity, and *vice versa*. Therefore, every hydrophobic molecule possesses a critical temperature T_c (or melting temperature T_m): when $T < T_c$, most lipidic chains are in a trans (zig-zag) conformations, so the molecule behaves as a gel and forms highly ordered structures (such as lamellar bilayers); when $T > T_c$, on the other hand, the lipids possess enough energy to go into gauche, staggered conformation, leading to a liquid crystal-like behaviour and to more disordered aggregates (such as inverted hexagonal).⁷⁶

LPS-TLR4 Interaction

LPS is mainly recognized by the immune system through the hydrophobic lipid A, as mentioned, because it is the most conserved region, as opposed to the hydrophilic O-antigen and core. Indeed, all the proteins involved in LPS binding are characterized by a hydrophobic pocket (LBP, CD14, MD-2), even though two of it (LBP and MD-2) also possess a positively charged rim to interact with phosphates both on lipid A and the core: the hydrophilic region is mainly bound by TLR4 LRR domain, with reduced specificity.⁷¹

The central event in LPS-TLR4 interaction is the binding of lipid A in MD-2 hydrophobic pocket, which causes several conformational changes leading to complex dimerization. Therefore, MD-2 binding has been studied both with agonists (LPS or lipid A) and antagonists, such the biosynthetic lipid A

precursor Lipid IVa and the synthetic drug candidate Eritoran – both which bear four lipidic chains and two phosphates. ^{84,85}

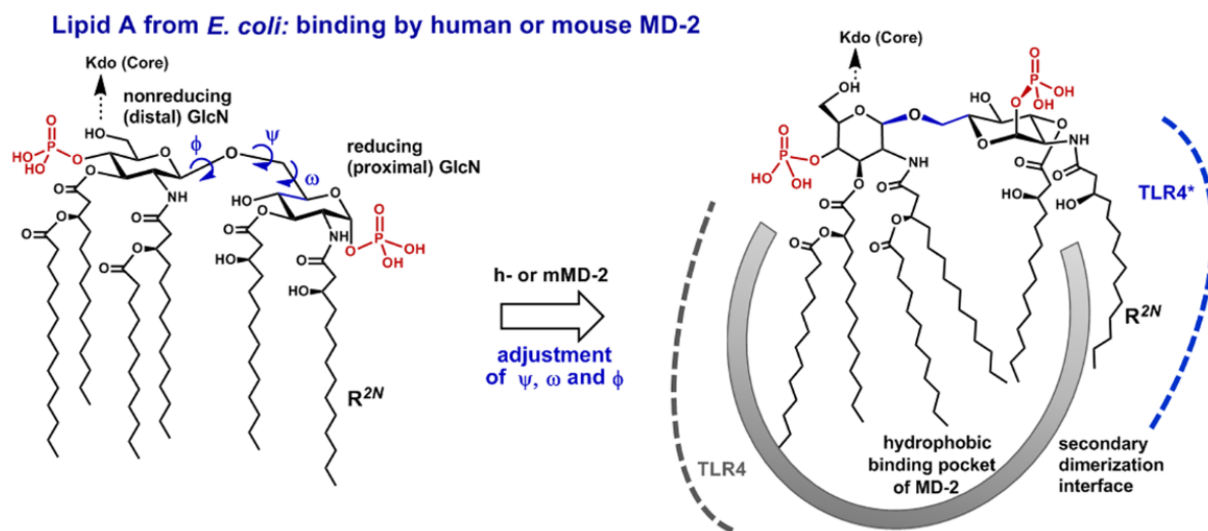


Figure 23 *E. coli* LPS binding with MD-2. Due to rotational freedom of lipid A backbone and the defined size of MD-2 hydrophobic pocket, one of the lipidic chains protrudes outside MD-2. This creates a hydrophobic surface that interacts with a second TLR4/MD-2/LPS*, favouring dimerization and triggering the immune response. ⁸⁶

Crystallography data show that specific residue-molecule interactions are not necessary for a strong binding, indicating that the most important parameter is not the chemical formula of the chains, but rather their total surface area: this is consistent with overwhelming experimental data on binding between different LPS and MD-2. Nonetheless, the number of the chains as well as their length seem to be pivotal in switching ligand activity between antagonist and agonist. Indeed, antagonist ligands are normally characterized by four or less acyl chains and are entirely and deeply buried into MD-2 hydrophobic pocket, with the glucosamine scaffold well anchored to the rim and c.a. 5 angstroms down in the pocket. On the other hands, agonist LPSs commonly more than four lipidic chains, which means that it cannot be completely accommodated by MD-2 hydrophobic pocket: this way, one of the lipid chains protrude on the exterior of MD-2, creating a hydrophobic surface indispensable for complex dimerization, as demonstrated by co-crystallization of MD-2 and *E. coli* LPS. ^{86,87}

This hydrophobic surface is completed by conformational changes of Phe126 present on MD-2 external rim, acting as a switch: when no ligand or an antagonist is bound, Phe126 points to the

interior of the protein; but, when engaged with an agonist, interactions with the protruding acyl chain force Phe126 to point out to the solvent, enhancing the hydrophobic surface.⁸⁶

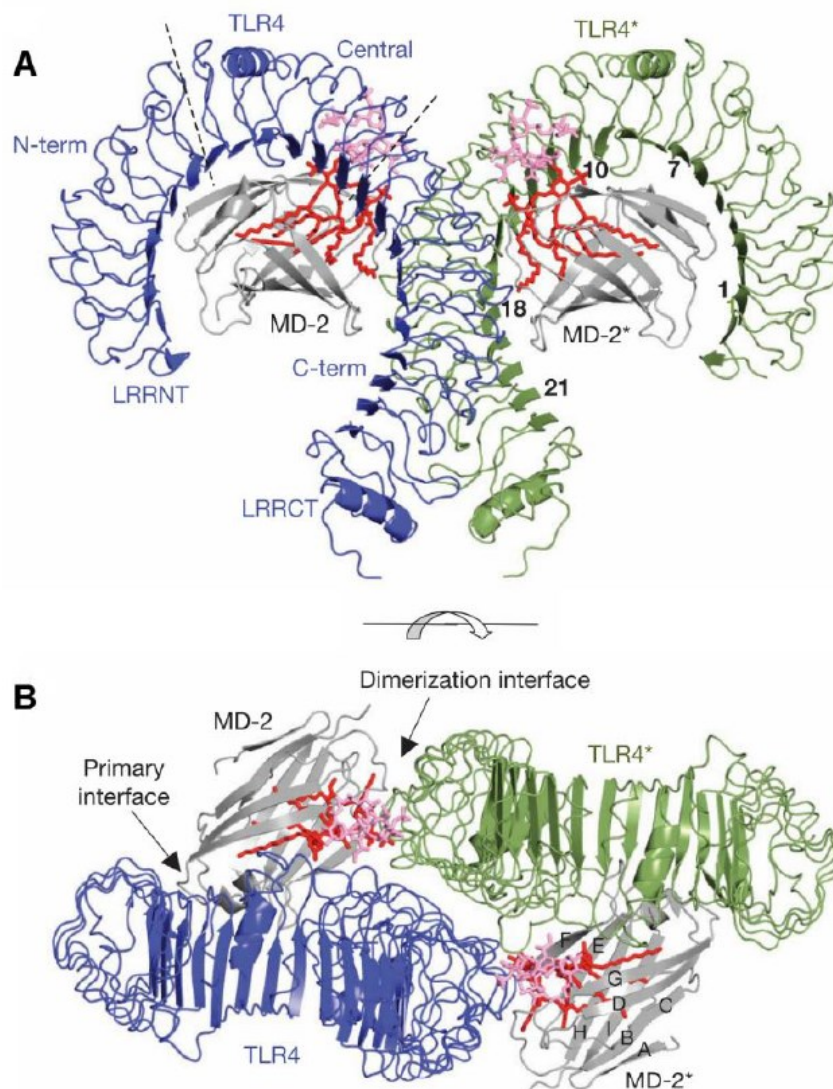


Figure 24 (TLR4/MD-2/LPS)₂ complex. **A**) Front view; the three sections of the LRR (N-Terminal, central and C-terminal) are marked. **B**) Top view; here are shown the two interaction surfaces: the primary interface, formed by A and B patches, binds TLR4 to MD-2; the dimerization interface, instead, is formed upon LPS binding by Phe126 and one LPS chain and allows for TLR4 dimerization.⁷¹

The hydrophobic surface thus created interacts with a similar region at edge of the central and the C-terminal region of the ectodomain of a second unit of TLR4/MD-2*: if TLR4/MD-2* too bound an agonist, the interaction between the two complexes is strong enough to induce receptor dimerization and the creation of a (TLR/MD-2/LPS)₂, which leads to downstream signaling through a kinase cascade induced by intracellular TIR domains conformational changes.⁸⁷



TLR Modulators: Increasing the chemical variety of small molecule-based TLR4 modulators: an overview

Alessio Romerio and Francesco Peri*

Adapted from Romerio, A.; Peri, F. Increasing the Chemical Variety of Modulators: An Overview.

Front. Immunol. 2020, 11 (July), 1–16.

Abstract

Toll-Like Receptor 4 (TLR4) is one of the receptors of innate immunity, it is activated by Pathogen- and Damage-Associated Molecular Patterns (PAMPs and DAMPs), and triggers pro-inflammatory responses which belong to the repertoire of innate immune responses, thus protecting against infectious challenges and boosting adaptive immunity. Mild TLR4 stimulation by non-toxic molecules resembling its natural agonist (lipid A), provided efficient vaccine adjuvants. The non-toxic TLR4 agonist Monophosphoryl lipid A (MPLA) has been approved for clinical use, thus suggesting the development of other TLR4 agonists as adjuvants or drugs for cancer immunotherapy.

TLR4 excessive activation by Gram-negative bacteria lipopolysaccharide (LPS) leads to sepsis, while TLR4 stimulation by DAMPs is a common mechanism in several inflammatory and autoimmune diseases. TLR4 inhibition by small molecules and antibodies could therefore provide access to innovative therapeutics targeting sepsis, acute and chronic inflammations.

The potential use of TLR4 antagonists as anti-inflammatory drugs with unique selectivity and a new mechanism of action compared to corticosteroids or other non-steroid anti-inflammatory drugs, fuelled the search for compounds of natural or synthetic origin able to block or inhibit TLR4 activation and signaling. The wide spectrum of clinical setting to which TLR4 inhibitors can be applied include autoimmune diseases (rheumatoid arthritis, inflammatory bowel diseases), vascular inflammation, neuroinflammations and neurodegenerative diseases.

The last advances (from 2017) in TLR4 activation or inhibition by small molecules (molecular weight <2 kDa) are reviewed here. Studies on pre-clinical validation of new chemical entities (drug hits) on cellular or animal models, as well as new clinical studies on previously developed TLR4 modulators are reported. Innovative TLR4 modulators discovered by computer-assisted drug design and artificial intelligence approach are described. Some “old” TLR4 agonists or antagonists such as MPLA or Eritoran are under study for repositioning in different pharmacological contexts. The mechanism of action of the molecules and the level of TLR4 involvement in their biological activity are critically discussed.

Introduction

The immune system is a complex molecular and cellular machinery evolved to defend a multicellular organism from external pathogens and internal damages. It consists of innate immunity, based on the recognition of microbial pathogen-associated molecular patterns, PAMPs and endogenous danger-associated molecular patterns, DAMPs, and adaptive immunity, mediated by the generation of a wide collection of antigenic sensors – the antibodies, produced by B cells.⁴⁶

Innate immunity is the first line of defence of a multicellular organism against internal or external threats. The molecular sensors of innate immunity are pattern recognition receptors (PRR), a large protein category comprising C-type Lectin Receptors, NOD-like receptors, RIG-I-Like Receptors and, most importantly, Toll-like Receptors. Toll-like Receptors (TLRs) are a family of proteins, in humans 10 TLRs have been identified that recognize different molecular determinants or patterns from bacteria, viruses and fungi.⁴⁸

TLR4, found in the plasma membrane of neutrophils, macrophages, dendritic and endothelial cells, selectively recognizes and responds to Gram-negative bacteria lipopolysaccharide (LPS) and lipooligosaccharide (LOS).^{38,50}

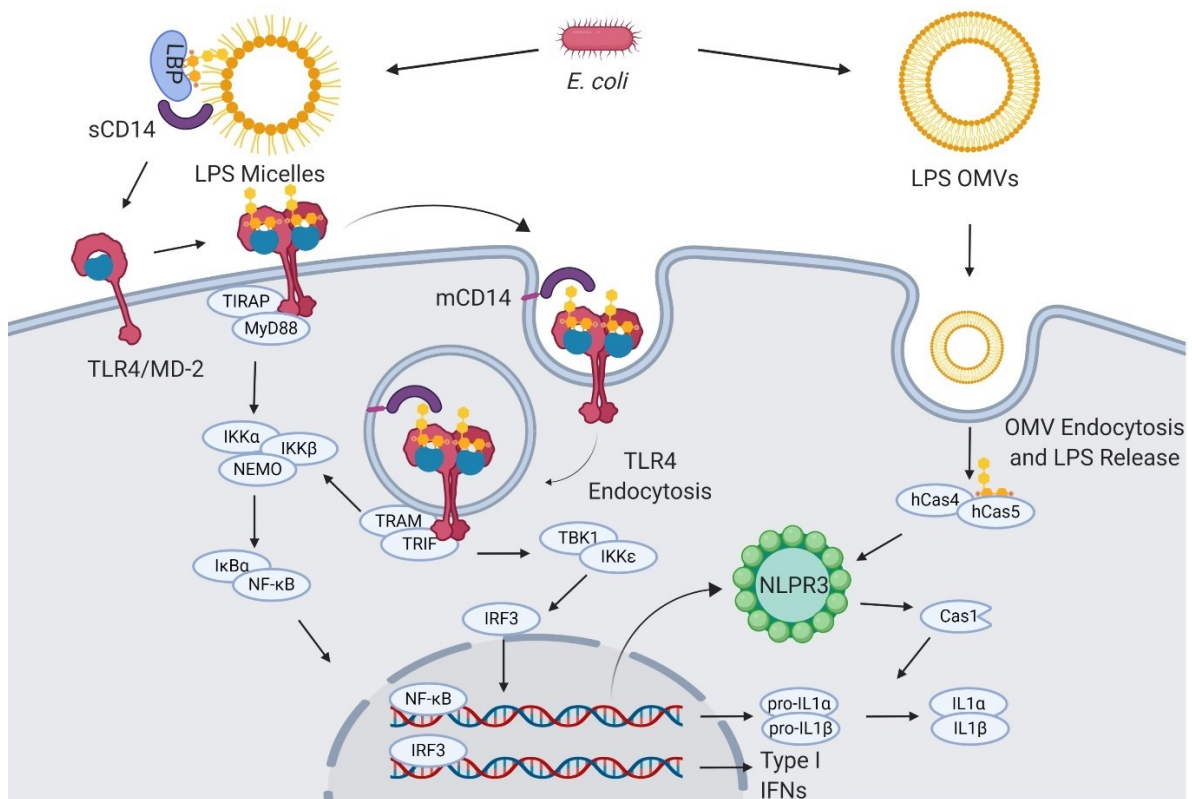


Figure 25 LPS signaling. Extracellular gram-negative bacteria release LPS in the form of micelles or OMVs. OMVs and micelles containing LPS can be delivered intracellularly where LPS activates caspase-dependent responses (right). Soluble LPS-binding protein (LBP) allows CD14 to capture LPS monomers. CD14 increases the sensitivity of TLR4-MD2 for LPS and favors the re-location of the complex formed by LPS, CD14, and TLR4-MD2 in the plasma membrane lipid rafts. Once in the lipid rafts, TLR4-MD2 starts TIRAP-MyD88-dependent responses. CD14 also induces the endocytosis of LPS and TLR4-MD2. From endosomes TLR4-MD2 triggers the TRAM-TRIF pathway and thereby sustains the activation of NF- κ B and the production of type I IFNs.^{65,68,81,83}

LPS is the main chemical component of the Gram-negative bacteria outer membrane, its chemical structure is characterized by a polysaccharide, the O-antigen, and a shorter oligosaccharide, the core region, bound to a glycolipid moiety called lipid A. Lipid A is the minimal LPS portion required to trigger immune activity, through binding of CD14 and subsequently to the TLR4/MD-2 dimer on the plasma membrane.^{77,78}

LPS is released from bacterial membrane as micelles, or it can be actively secreted via the formation of outer membrane vesicles (OMVs).⁸⁸ OMVs can directly deliver LPS in the cytosol of immune cells, where inflammatory caspases (caspase-4/5) serve as a specialized LPS receptor to induce the activation of the inflammasome and the production of bioactive interleukin-1 β (IL-1 β) and IL-18.⁸¹

In contrast to OMVs, the LPS contained in micelles requires the presence of accessory soluble proteins, such as LPS binding protein (LBP), and subsequently CD14 and MD-2 to be recognized by TLR4.

LBP is required for transferring LPS monomers from micelles to TLR4-MD2, via the interaction with both soluble and membrane-anchored CD14.^{65,66,89} The interactions between LBP and CD14 form a “capture and concentration module” upstream of TLR4-MD2 that regulates the ligand availability. The process starts with the contact of LPS micelles with a soluble LPS-binding protein (LBP). CD14 is then recruited and a transient ternary complex (LPS micelle-LBP-CD14) is formed. LPS transfer happens during this phase, in which, via electrostatic interactions, LBP catalyses multiple rounds of LPS monomer transfer to either soluble or membrane-bound CD14 (sCD14 and mCD14, respectively). Subsequently, s/mCD14 dissociates from the complex and the single LPS molecule bound to the CD14 is then transferred to MD2 with the assistance of LRR13-LRR15 domains of TLR4 that trigger the dimerization of TLR4-MD2 and its activation. (Ryu et al., 2017; Huber et al., 2018). Concomitantly with LPS presentation, mCD14 also facilitates the relocation of TLR4-MD2 in lipid rafts, where multiple signaling molecules are recruited to contribute to cell activation. (Triantafilou et al., 2002). Lipid rafts also favor the action of TLR4-independent effectors, such as specialized proteins for the internalization of the complex formed by LPS, mCD14, and TLR4-MD2.^{68,90} Once engaged by CD14, TLR4-MD2 undergoes an internalization process and moves in the endosomal compartment, where it triggers the TRIF Related Adaptor Molecule (TRAM) and TIR-Domain-Containing Adapter-Inducing Interferon- β (TRIF)-dependent pathway, which sustains the activation of NF- κ B and also induces the production of type I interferons (IFNs).

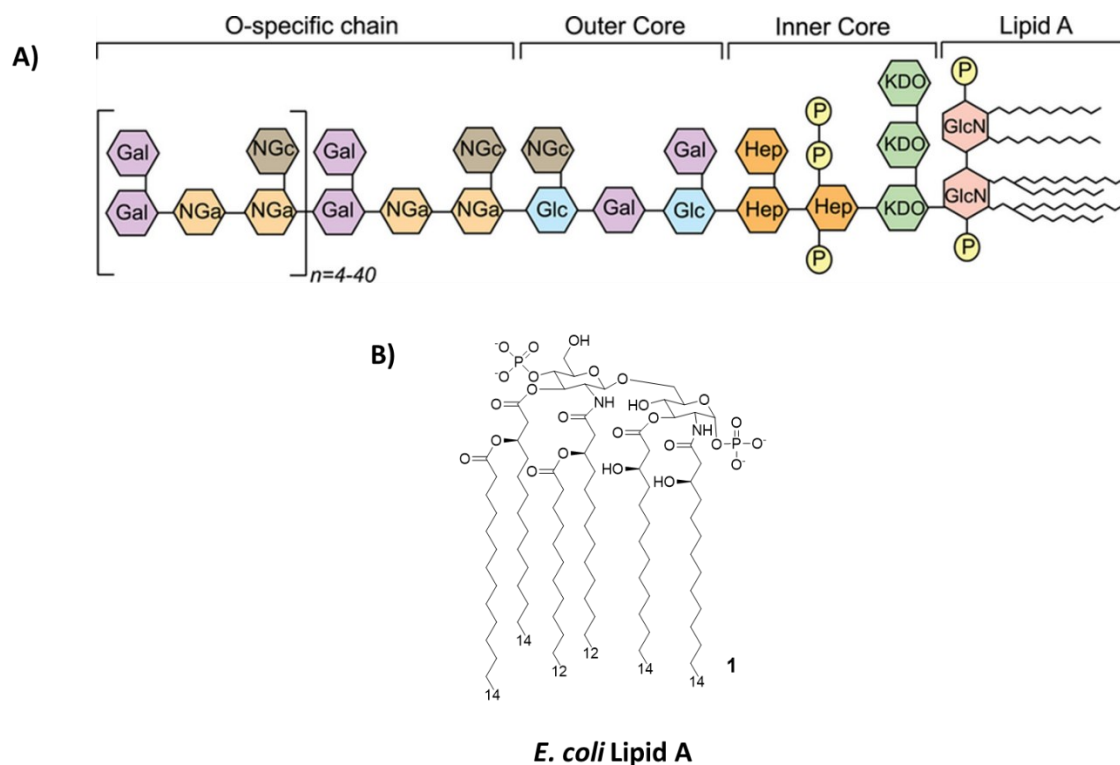


Figure 26 LPS Structure. **A)** General structure, highlighting the different regions of LPS (O-antigen, core, and lipid A) and the various sugars composing it. **B)** The molecular structure of *Escherichia coli*'s lipid A.

TLR4 excessive activation by LPS can lead to pathologies such as sepsis and septic shock, one of the leading death causes in western world, with a mortality rate between 20-50%; furthermore it can induce the immune system to attack cells from its own organism, causing an array of autoimmune diseases.^{91,92}

Modulating TLR4 activation and signaling is therefore of fundamental importance from a pharmacological and clinical point of view. On one hand, innate immunity stimulation is useful for the development of vaccine adjuvants or cancer immunotherapeutic drugs^{46,93}. On the other hand, TLR4 inhibition is a therapeutic approach to Gram-negative and sterile sepsis, as well as autoimmune inflammatory pathologies such as atherosclerosis, rheumatoid arthritis, or haemorrhagic shock^{44,90,94,95}. Indeed, two compounds, Eritoran and Tak-242, reached phase III clinical trials as antisepsis agents and both failed to meet their endpoints.^{44,96}

In the perspective of developing new TLR4-directed drugs, the recent achievements (last 3 years, from 2017) on the discovery of synthetic and natural molecules that modulate TLR4 activity as agonists or antagonists are reviewed, as a follow-up of our recent review on this topic.⁹⁷ We focus on small molecules with drug-like properties, dividing them in two main categories according to

their chemical structure, namely glycolipid- and non-glycolipid-based TLR4 modulators. (Tables 1 and 2)

Compound	Class	Drug Development Stage
MPLA (24)	Glycolipid based	Approved by FDA as vaccine adjuvant
BECC438 (25)	Glycolipid based	<i>In vitro</i>
GLA (26)	Glycolipid based	Clinical
LAM (27)	Glycolipid based	<i>In vitro</i>
E6020 (28)	Non-glycolipid	<i>In vivo</i>
1Z105 (29)	Non-glycolipid	<i>In vivo</i>
PTC (30)	Non-glycolipid	<i>In vitro</i>
LS-like (31)	Non-glycolipid	<i>In vitro</i>
VS1-like (32)	Non-glycolipid	<i>In vitro</i>
Saturated cardiolipins (33)	Non-glycolipid	<i>In vitro</i>

All agonists are validated according to the three postulates described in the text (34).

Table 4 TLR4 agonists presented in this review, ranked by chemical structure (glycolipid or non-glycolipid) and stage of drug development.

The validation of a new chemical entity as a selective TLR4 agonist or antagonist is a crucial step in the drug development process. While TLR4 antagonists (inhibitors) validation is straightforward, as the TLR4 selectivity can be assessed through competition experiments with LPS -the natural TLR4 agonist-, TLR4 agonism assessment requires more careful investigation because it could be affected by false positive results due to endotoxin contamination. Therefore, 3 postulates have been proposed in order to ascertain and validate TLR4 agonists activity: (I) the requirement of both TLR4 and MD-2 for the agonist effect; (II) the agonist or the active portion of it should be reproduced synthetically and the synthetic derivative should preserve TLR4 activity; and (III) a specific molecular interaction between the agonist and TLR4/MD-2 must be identified.⁹⁸

Glycolipid-based compounds are Lipid A mimetics that can be obtained by 1) chemical modification of natural LPS/Lipid A, 2) direct extraction of lipid A variants after bacterial engineering or 3) full chemical synthesis.^{40,99,100}

Some non-glycolipid compounds still reproduce the arrangement of lipid chains and phosphates found in the Lipid A but are devoid of the disaccharide scaffold (as in the case of Eisai's E6020). Others have a chemical structure totally unrelated to lipid A, and have been developed by computer-

assisted drug design (CADD), and machine learning approach or have been selected from libraries of compounds.^{101–103}

The clinical and pharmacological potential of newly discovered, low-molecular weight (<2 kDa) compounds together with the preclinical and clinical validation level of known lead compounds is reviewed, paying special attention to validation of TLR4 targeting. Table 1 and Table 2 give a general picture of the state of the art in the clinical development of, respectively, small molecule-based TLR4 agonists and antagonists.

Compound	Class	Drug Development Stage	MOA
FP7-like (35, 36)	Glycolipid based	<i>In vivo</i>	Competitive inhibition
LAM (37)	Glycolipid based	<i>In vitro</i>	Competitive inhibition
IAXO (38)	Glycolipid based	<i>In vivo</i>	Competitive inhibition; LPS sequestration
TAK-242 (39)	Non-glycolipid	Clinical	Non-competitive inhibition
Calixarenes (40)	Non-glycolipid	<i>In vitro</i>	Competitive inhibition
Opioid (41)	Non-glycolipid	<i>In vitro</i>	Competitive inhibition
Pip2 (42)	Non-glycolipid	<i>In vivo</i>	Competitive inhibition
Unsaturated cardiolipins (33)	Non-glycolipid	<i>In vitro</i>	Competitive inhibition
Alpinetin (43)	Non-glycolipid	<i>In vivo</i>	Down-regulation of TLR4 expression
Ferulic acid (44)	Non-glycolipid	<i>In vivo</i>	TLR4/MD-2 complex disruption

Table 5 TLR4 antagonists presented in this review, ranked by chemical structure (glycolipid or non-glycolipid), stage of drug development, and mechanism of action (MOA).

Glycolipid-Based TLR4 Modulators

Agonists

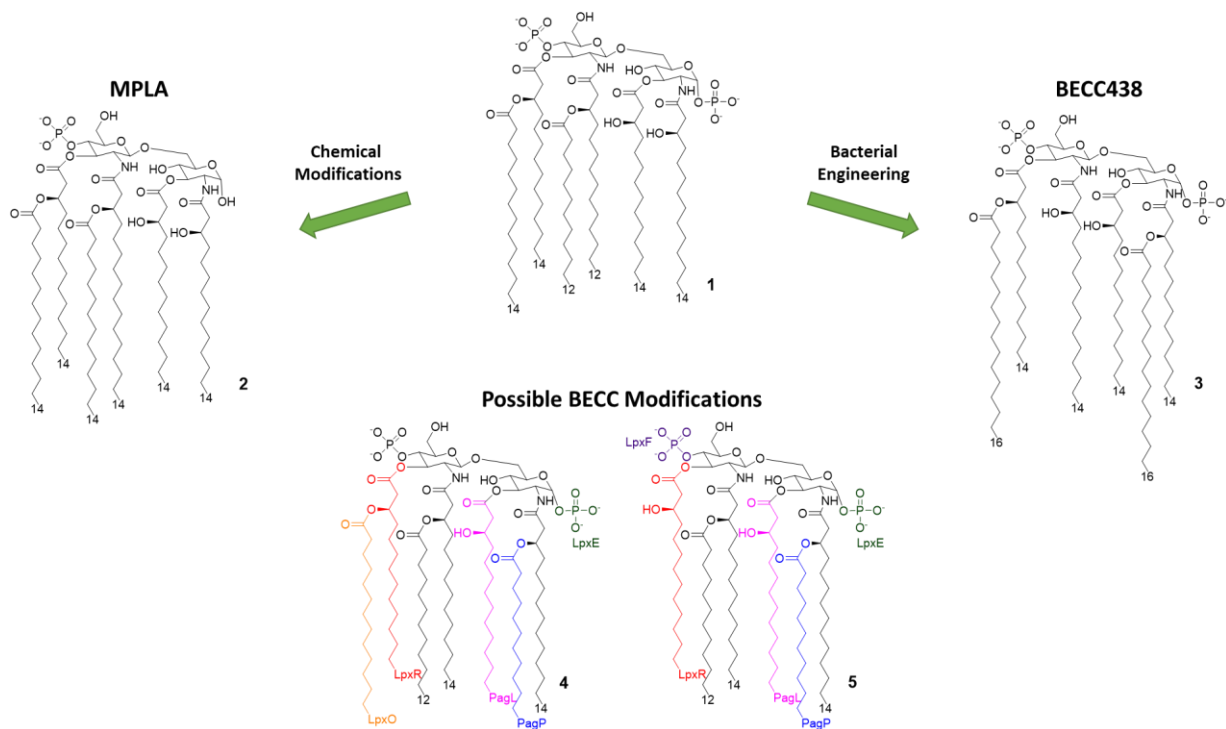


Figure 27 Lipid A variants obtained by chemical and enzymatic modification. MPLA is obtained by chemical hydrolysis of the C-1 phosphate of the *Salmonella Minnesota* LPS. BECC (Bacterial Enzymatic Combinatorial Chemistry) allows for the selective modification of single or multiple fatty acid chains or phosphates (depicted by colors associated to involved enzymes) in order to obtain compounds such as BECC438 with high purity.

MPLA

Monophosphoryl Lipid A (MPLA, compound 2, **Figure 27**) is a well characterized TLR4 agonist.⁴⁰ MPLA is chemically derived from *Salmonella minnesota* LPS by treatment by mild acidic conditions, thus achieving the cleavage of the lipid A portion from the oligosaccharide core and the hydrolysis of the 1-phosphate group. TLR4 requirement for MPLA action has been thoroughly validated by numerous studies involving TLR4^{-/-} mice.^{40,104}

MPLA is a potent TLR4 agonist, but weaker than LPS, as MPLA affinity to TLR4/MD-2 is weaker than LPS. It has been also suggested that MPLA-activated TLR4 signal goes only or preferentially through TRIF-dependent and not through MyD88-dependent cascade. TRIF bias has been proposed to be related to the weaker inflammatory power and the reduced toxicity compared to LPS. TRIF bias also switches T-cell immunity to T_H1 helper, better suited for long-lasting immunization.^{85,105}

MPLA is the only TLR4 agonist to be approved by FDA for the use as a vaccine adjuvant on human (Cervarix[®], Fendrix[®]).^{22,45}

Because of its immunostimulating activity and the lack of toxicity, the use of MPLA has been envisaged in a wide array of clinical settings. In a recent study it has been hypothesized that MPLA stimulatory activity on the innate immune system could mitigate the radiation injury provoked by ionizing radiation (IR) in cancer radiotherapy.¹⁰⁶ Pre-treatment with MPLA prevented IR-provoked cell apoptosis *in vitro* and effectively attenuated tissue damage *in vivo*. Authors used siRNAs to knock down TRIF and MyD88 in wild type RAW264.7 cells. It was found that MPLA significantly inhibited apoptosis in TRIF knock-down cells while in MyD88 knock-down cells, MPLA had no effect on cell apoptosis induced by irradiation. These data point out that MyD88 signaling pathway mainly accounts for the radioprotective effects of MPLA, contrarily to the TRIF-biased action of MPLA previously discussed.

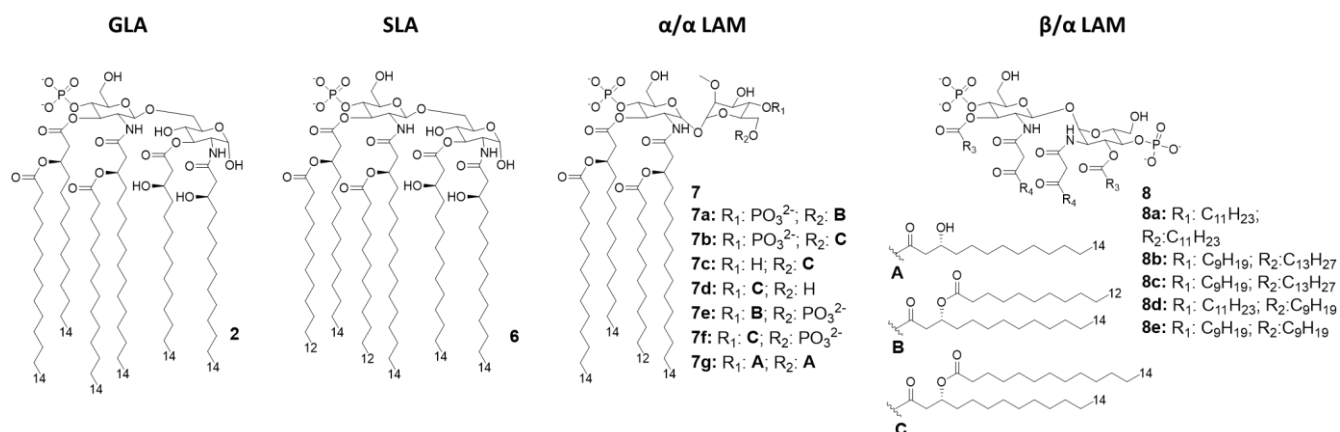


Figure 28 Disaccharide-based synthetic Lipid A analogues. **GLA** is a fully synthetic MPLA. **SLA** is a second generation GLA optimized to be more compatible with MD-2 (by introducing C12 acyl chains). **LAMs** are trehalose-derived compound: changing the absolute configuration of the glycoside bond LAM allow the switch from TLR4 agonism to antagonism.

Enzymatically Modified Lipid A

The approval of MPLA fostered the development of synthetic or semi-synthetic Lipid A variants as TLR4 modulator candidates for clinical use.

In 2013, Needham et al. developed a new technology to obtain naturally derived TLR4 agonist, by a technique which was lately named bacterial enzymatic combinatorial chemistry (BECC). BECC consists in bacterial gene engineering, removing or adding enzymes in LPS biosynthesis pathway, allowing the isolation of LPS/lipid A variants with non-natural modifications and their straightforward isolation from bacterial pellets without further purification.¹⁰⁷

In 2017, BECC was performed on an attenuated *Yersinia pestis* strain, thus obtaining lipid A variants which were then screened *in vitro* and *ex vivo*, showing TLR4 activation levels comparable to those obtained with previously described MPLA.⁹⁹

Particularly, a compound named BECC438 (compound 3, **Figure 27**) showed good *in vitro* activity, which suggested a follow-up study *in vivo*, to confirm its viability as a vaccine adjuvant and to compare its efficacy to other adjuvants (Alum and PHAD). All mice immunized using non-formulated BECC438 as adjuvant survived after being challenged with *Y. pestis*: indeed, BECC438 group's survival rate (100%) was better than both Alum and Glucopyranosyl Lipid Adjuvant (GLA, see next paragraph) groups (both scored 80% survival rate), suggesting that properly formulated BECC438 could exceed GLA efficacy and encouraging follow-up studies on its use as a vaccine adjuvant.¹⁰⁸

Glucopyranosyl Lipid Adjuvant (GLA)

The Glucopyranosyl Lipid Adjuvant (GLA, **Figure 28**) has been developed by Avanti Polar Lipids Inc. as a fully synthetic MPLA analogue having TLR4 agonistic activity (tradename: phosphorylated hexa-acyl disaccharide PHAD®). (Reed and Carter, 2014; Shaw *et al.*, 2016) Being fully synthetic, the main advantage of this compound is its chemical homogeneity, which improves activity and safety with respect to MPLA, a semi-synthetic molecule. Moreover, LPS contamination is avoided.¹⁰⁹

In recent years, GLA has been formulated as a vaccine adjuvant both as aqueous formulation (GLA-AF) and as an oil-in-water stable emulsion (GLA-SE), and then compared to MPLA for the activity, showing an overall better response.^{109,110}

GLA-AF was tested as a nasal vaccine adjuvant for HIV immunization *in vivo* on mice and rabbits, resulting in a good immunization profile with strong mucosal immune responses.^{111,112} In 2018, Anderson *et al.* tested HIV immunization in humans following nasal administration of a vaccine containing GLA-AF as adjuvant and the HIV-1 CN54gp140 antigen. Early transcriptional signatures were investigated to identify differentially expressed genes (DEG) and blood transcription modules (BTM) correlated with vaccination and successful immunization.¹¹³ Results were encouraging, indicating the activation of numerous vaccine related DEG and BTM, thus suggesting that immunization occurred. However, the small number of subjects involved and lack of analysis in the first 7 days suggest that additional studies are needed to validate data.

Recent advancement in cancer immunotherapy involving TLR to (re-)activate immune cell, suggested the use of a GLA-SE (named G100) as a stand-alone cancer immunotherapeutic.^{43,114}

Following a successful *in vivo* study on an A20 lymphoma murine tumour model in which half of mice got regression in a dose dependent manner,¹¹⁵ a first clinical trial was started on a small number (n=10) of patients affected by merkel cell carcinoma (MCC), based on intratumoral injection of a low dose of G100. Out of the 10 patients, 3 presented local disease and were then treated with surgery (cohors A), while 7 presented a metastatic disease (cohors B). All patients in cohors A successfully completed surgery and radiotherapy after administration of G100, and two of them remained recurrence free; patients in cohors B received only G100 and two of them went in full remission.¹¹⁶

The brilliant results obtained by GLA experimentations urged the development of even better TLR4 glycolipid agonist, having higher efficiency and lower toxicity. On this way, Carter et al. recently developed a second-generation lipid adjuvant (SLA), reducing from C14 to C12 the length of two lipid chains (compound 6, **Figure 28**). Computational docking studies show that the reduction of the Hydrophobic part make this lipid A derivative better accommodate into the MD-2 hydrophobic pocket, allowing for and stronger interaction with TLR4/MD2.⁴²

The activity of SLA and its TLR4 selectivity has been assessed both *in vitro*, *ex vivo* and *in vivo*⁴² SLA has been then formulated as an oil-in-water stable emulsion (SLA-SE) and tested *in vivo* as an adjuvant for nasal *Enterotoxigenic E. coli* vaccine in comparison with double-mutant LT (dmLT) adjuvant: results suggest that SLA-SE is at least as effective as dmLT, but it is able to further augment some of the specific immune responses.¹¹⁷

Trehalose Derivatives (LAM)

While TLR4 plays a pivotal role in innate immunity, particularly protecting against infectious challenges and boosting adaptive immunity, it is not the only factor causing inflammation neither the only LPS receptor. Indeed, caspase 4, 5/11 mediated NLRP3 inflammasome, activated by cytosolic LPS, is a crucial pathogenic factor in a variety of acute and chronic immune related diseases.¹¹⁸

In order to obtain new agonists with increased TLR4/inflammasome selectivity, Zamyatina and coworkers aimed to design molecules capable of activating only the TLR4 pathway, without activating NLRP3. To achieve this result, according to a computational structural analysis of the TLR4 dimerization process, two separate hydrophobic clusters are needed in the ligand to optimize the binding with the hydrophobic pocket of MD-2/TLR4, crosslinking the second MD-2*/TLR4* thus forming the activated (TLR4/MD-2/ligand)₂ complex. Seven novel trehalose-derived disaccharides

were projected and synthesized based on a α,α -(1-1')-linked diglucosamine scaffold (Lipid A Mimetics, α/α LAMs, **Figure 28**). The conformational rigidity of the α,α glycosidic bond was exploited by rational design to obtain the two separate hydrophobic clusters for MD-2 binding and TLR4 activation.^{119,120}

The activity of α/α LAM was tested on mononuclear cells (MNC), human airway epithelial cells (Calu-3) and human monocytic cell line THP-1 and observed that, while 4'-6-diphosphate compounds (compounds 7a-b and 7e-f, **Figure 28**) induced both TLR4 and caspase 4/11 activity, monophosphate compounds 7c and 7d (**Figure 28**) effectively decoupled TLR4 and NLRP3, exclusively activating TLR4 without triggering a NLRP3-dependent response: these results open the way for future synthesis of safer TLR4 agonists and for clarifying the role of caspase 4/11 activation in inflammasome.¹¹⁹

Interestingly, changing the stereochemistry of α/α glycosidic bond into β/α bond, a shift from TLR4 agonism to antagonism was observed¹²⁰. Indeed, five novel β (1-1') α linked diglucosamine LAMs, containing 2-N-, 2'-N-linked β -ketoacyl lipid chains were synthesized (α/β -LAMs, compounds 8, **Figure 28**). These new compounds were then tested for their antagonist activity *in vitro*, obtaining full inhibition of LPS-stimulated cytokine production at 1 $\mu\text{g}/\text{mL}$ concentration. Surprisingly, concentrations higher than 10 $\mu\text{g}/\text{mL}$ showed reduced antagonist activity, probably because the formation of aggregates. Finally, molecular dynamics simulations showed that MD-2 affinity of LAMs is higher than LPS. The keto-enolic tautomerism on acyl chains of LAMs very likely provides free hydroxyls that can be involved in additional interactions through hydrogen bonds with residues at the rim of MD-2 binding pocket.¹²⁰

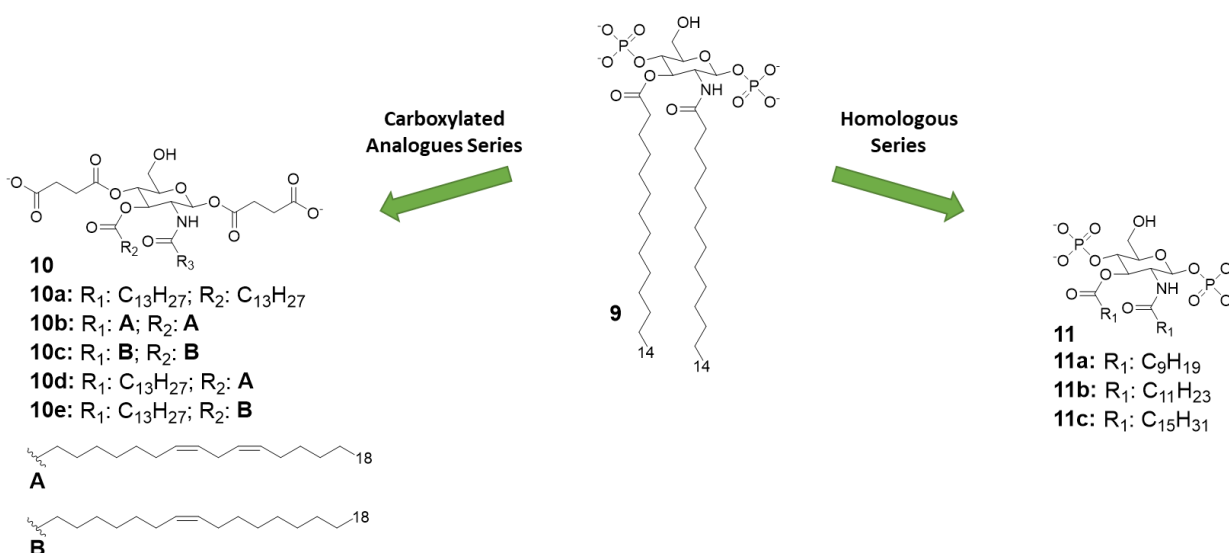


Figure 29 Monosaccharide TLR4 antagonist of the FP series and their carboxylate analogues

Antagonists

Anionic monosaccharide-based TLR4 Antagonists

Synthetic monosaccharide mimetics of Lipid X, a monosaccharide biosynthetic precursor of lipid A, showed TLR4 antagonist activity in murine macrophages.^{121,122}

A large panel of synthetic monosaccharide-based TLR4 modulators, named Gifu Lipid As, contain one or two phosphates groups and a variety of modifications in fatty chains length and nature, as well as in their binding mode to glucosamine: esters, amide, ethers and amines were used.^{123,124}

Following this trend, monosaccharide-based pure TLR4 antagonists, called FP compounds, were developed, active in inhibiting the LPS-stimulated TLR4-dependent cytokine production in human and murine macrophages in a dose-dependent manner (IC₅₀ from 0.46 to 3.2 μM).¹²⁵

FP compounds were tested as potential therapeutics in different clinical settings. The lead compound FP7, with two C-14 fatty acid chains, showed the ability to protect motoneurons from microglia activated by LPS in an *in vitro* motoneurons/microglia co-culture model of ALS.¹²⁶

The capacity of FP7 to protect mice from DAMP/TLR4 activation as a consequence of influenza virus pulmonary infection was evaluated.⁶⁰ FP7 turned out to protect mice from acute lung injury (ALI), one of the most prominent influenza-related damages, and increase survival after viral infection with an efficiency similar to Eritoran, a well-established TLR4 antagonist developed by Eisai.¹²⁷ In this model of infection, ALI would induce DAMP release from damaged tissues, likely HMGB1 and oxidized phospholipids, that in turn hyperactivate TLR4 with subsequent cytokine storm and acute

sepsis-like syndrome. Experiment on DCs activated by HMGB1 suggest that FP7 can block HMGB1-dependent TLR4 activation. Further data should be collected to assess the activity of this type of antagonist to block TLR4 activation by oxidized phospholipids (oxPL) and other DAMPs that highly likely are produced by ALI.

TLR4 gene deletion in haematopoietic and non-haematopoietic cells protects animals against cardiovascular diseases (CVD), thus suggesting a key role of the receptor in these pathologies.¹²⁸

The potential of FP molecules to impact on inflammatory CVD was investigated *in vivo* on Angiotensin II-infused apolipoprotein E-deficient mice. After validating the capacity of FP7 to inhibit cytokine production *in vitro* on human umbilical vein endothelial cells (HUVEC), THP-1 and RAW 264.7 cells, *in vivo* experimentation demonstrated that Angiotensin II and FP7 co-administration prevented the initiation of sterile inflammation, protecting mice from consequent CVD.¹²⁹

Interestingly, in addition to inhibition of LPS-induced TLR4 signaling, FP7 negatively regulated TLR4 activation in response to ligands of sterile inflammation, namely hydroperoxide-rich oxidised LDL (oxLDL), *in vitro* and Angiotensin II infusion *in vivo*.¹²⁹

Taken together, these studies suggest that FP molecules are able to contrast the action of structurally diverse DAMPs, from HMGB1, to oxLDL.^{60,129}

The synergistic action of FP monosaccharides with antibacterial peptides neutralizing LPS was recently investigated.¹³⁰ After LPS stimulation, FP7 was co-administrated to cells together with two anti-microbial peptides : cecropin A–melittin (CA–M) or LL-37, a human cathelicidin, which binds to and neutralize LPS.^{131,132} A synergy between TLR4 antagonists and cationic peptides was observed in inhibiting TLR4-dependent cytokine production and NF-κB activation. Interestingly, the synergy was observed also in the case TLR4 was activated with lectins. DOSY NMR experiments and TEM microscopy images suggest a change in supramolecular aggregation state of peptides caused by the interaction with FP7.¹³⁰

Two studies focused on the investigation of the structure-activity relationship (SAR) in FP monosaccharides (as depicted in **Figure 29**): one explored the effect of the length of saturated fatty on the TLR4 activity and the second investigated both the effect of unsaturated fatty chains and the suitability of succinate groups as bioisosteres of phosphate groups.^{133,134}

In both studies, molecules were firstly designed *in silico*, through docking with MD-2 receptor followed by and molecular dynamics simulation. Molecules were then synthesized and tested for their capacity to bind to MD-2 and to inhibit LPS-stimulated TLR4 activation in human and murine

macrophages. The first study pointed out a very precise trend of activity on cells and MD-2 binding potency, indicating the compounds with C12 and C14 carbon chains (**Figure 29**) are the most active in inhibiting TLR4 activation and cytokine production.¹³³ Interestingly, the compound with C16 was found to be totally inactive. The C12 and C14 compounds, respectively named FP12 and FP7 (respectively Compounds 11b and 9, **Figure 29**), showed to form less tight aggregates, with a higher fluidity of fatty acid chains, than the C16 compound. As in the case of lipid A derivatives it is very likely in this class of amphiphilic monosaccharides the supramolecular structure and the stability of aggregates influences the biological activity.^{82,83}

The carboxylate analogues (Compounds 10, **Figure 29**) with two succinate esters units instead of phosphates, retained TLR4 antagonist activity with an IC₅₀ in the same range of lead compound FP7. Furthermore, the structure of the fatty acid chains turned out to be essential to TLR4 activity. Paralleling the SAR results in the FP family, the series of saturated fatty chains presented a maximum activity again around C12 and C14, while shorter chains (C10) and longer (C16) were unable to interact with MD-2 to inhibit TLR4-dependent cytokine production. On the other hand, unsaturated lipids retained activity even with longer chains (C18). It is known that unsaturated fatty acids are present in TLR4 antagonists such as the LPS synthesized by *Rhodobacter sphaeroides* (RS-LPS) or *Rhodobacter capsulatus* (RC-LPS) and the synthetic Eritoran. The results reported in this paper confirm that the presence of one unsaturation in the fatty acid chains favours the switch to antagonism.¹³⁴

Cationic monosaccharide-based TLR4 antagonists

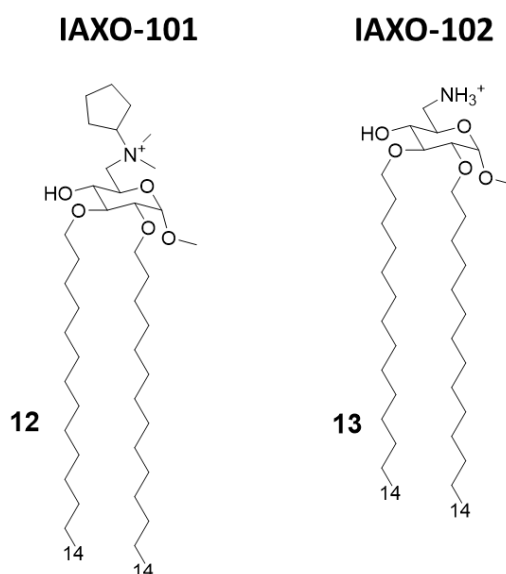


Figure 30 IAXO-101 and IAXO-102 are glycolipid compounds bearing a positive charge. They form stable aggregates with LPS and compete with LPS for TLR4 binding

IAXO compounds are a class of cationic amphiphiles active as TLR4 antagonists. They are formed by a glucopyranose or a benzylamine core linked to two C14 lipid chains through ether bonds (compounds 12 and 13, **Figure 30**).¹³⁵

IAXO's TLR4 antagonism is very likely the combination of two effects: in form of cationic liposomes these molecules form stable co-aggregates with LPS making it less available to bind CD14 and MD-2¹³⁶. On the other hand, mechanism studies clearly show the ability of IAXOs to bind CD14 and MD-2 thus competing with LPS and displacing it from receptors.^{80,137,138}

In a new study on the role of TLRs in Placental Malaria (PM) by Barboza et al., IAXO 101 was used to assess the involvement of TLR4 in infant morbidity and mortality in a group of pregnant mice affected by *Plasmodium berghei* NK65^{GFP}, and its effect was compared with a group of TLR4^{-/-} mice. While TLR4^{-/-} mice did not show PM and their foetuses did not show differences in body weight compared to non-infected WT mice, experiments demonstrated that mice treated with IAXO 101 two weeks after infection showed a partial reverse in placental malaria and their foetuses had an intermediate body weight between infected and non-infected WT mice. In addition to demonstrating the involvement of TLR4 in PM, this study also highlights the viability of IAXO 101 as a treatment for this pathology, which causes high neonatal mortality.¹³⁹

Another recent application of IAXOs has been the prevention of blood brain barrier (BBB) disruption after subarachnoid haemorrhage (SAH). Okada et al. aimed to study the linkage between TLR4

activation and inflammatory BBB disruption.¹⁴⁰ In an animal study, SAH was induced in C57BL/6 male mice, which were eventually treated with two different dosages of IAXO 102 (compound 13, Figure 6) after 30 min. This resulted in a significantly improved neurological score and in clear protection from BBB disruption. A control experiment was conducted involving TAK-242, a well-established TLR4 antagonist, providing similar results. Those experiments highlighted for the first time that BBB disruption after SAH is linked to TLR4 activation and can be efficiently reversed by administration of potent TLR4 antagonists as a treatment for post-SAH BBB disruption.¹⁴⁰

Non-Glycolipid TLR4 Modulators

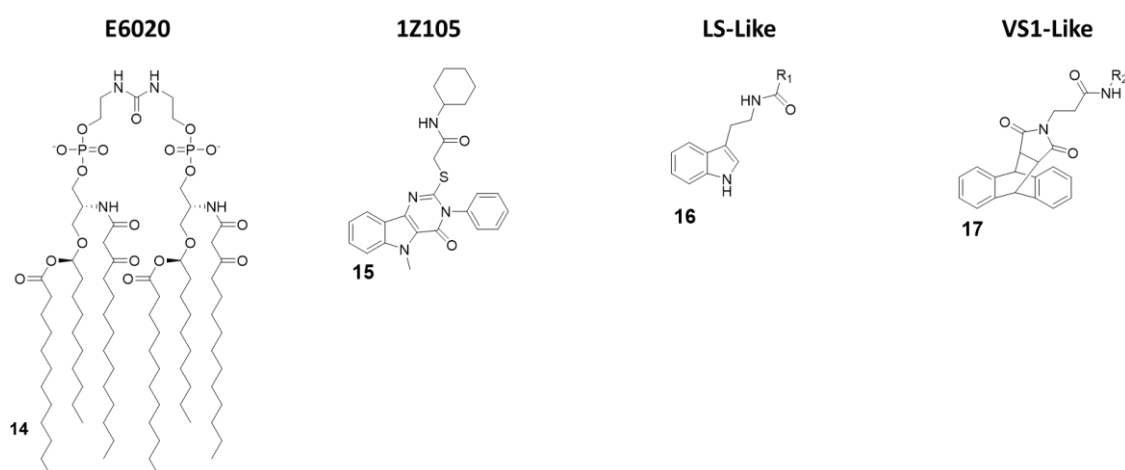


Figure 31 Non-Glycolipid TLR4 agonists. **E6020** is a linear lipid A analogue developed by Eisai Inc., currently in clinical trial in cancer immunotherapy. **1Z105**, a pyrimidoindole, is currently being tested *in vivo* as vaccine adjuvant. **LS-** and **VS1-like** compounds are novel TLR4 agonist structures obtained by computational approach.

Agonists

Linear lipid A analogues (E6020)

E6020 (compound 14, **Figure 31**) is a synthetic agonist patented by Eisai Inc., which has been previously experimented as a vaccine adjuvant *in vivo* and turned out to be a viable alternative to traditional alum adjuvant both on boosting mucosal and systemic antibodies responses and in enhancing vaccine efficacy on a toxic shock syndrome model.^{101,141,142}

Following these successes, it has been recently tested on the central nervous system (CNS) to test its activity in enhancing remyelination in spinal cord white matter following lysolecithin-induced demyelination. Remyelination is mediated by oligodendrocytes, which are vulnerable to a series of pathologies and infection: when their number is low, they can be replaced by oligodendrocyte progenitor cells (OPCs), after differentiation. However, myelin debris prevent OPCs differentiation,

effectively hindering remyelination process. Indeed, it seems that E6020 presence stimulates macrophages to remove myelin debris, which is a vital step, thus allowing and enhancing remyelination in lysolecithin-induced demyelination animal models. The remyelination is therefore linked to TLR4 activation. This novel study opens the possibility to use TLR4 agonists to repair damages caused by aging or injury, thus preventing a series of CNS pathologies included dementia.¹⁴³

Pyrimidoindoles

Pyrimido[5,4-b]indoles are a class of synthetic TLR4 agonists, first identified by H. B. Cottam and coworkers through a high-throughput screening (HTS) approach¹⁴⁴. Subsequently, a structure-activity relationship (SAR) study allowed to select 1Z105 (compound 15, **Figure 31**), as the best agonist compound. 1Z105 has been tested as a vaccine adjuvant in combination with 1V270, a TLR7 agonist.^{144,145}

As a follow-up of these studies, an influenza vaccine formulated with both 1Z105 and 1V270 showed to function *in vivo* through TLR4 and TLR7 activation, without any significant off-target effect, and succeed in inducing protective immunity. The activation of TLR4 by 1Z105 mainly activated the MyD88 pathway. Furthermore, the TLR4 and TLR7 agonists worked synergistically to reach a high adjuvant potency, allowing for a dose reduction of the antigen to achieve equivalent protection, and enhancing vaccines safety profile.¹⁰²

New rationally designed TLR4 agonists

Michaeli et al. recently projected linear and cyclic peptides with the ability to bind MD-2/TLR4 and CD14/TLR4 by computer-assisted drug design (CADD). They used *ab initio* methods coupled with machine learning discovery software, which allowed the finding of a higher percentage of active molecule compared with an HTS approach. New cyclic peptide sequence containing also D-amino acids to increase conformational rigidity and drug-likeness were designed to dock with hMD-2 and the N-terminal region of h-CD14 using the CYCPEP program.¹⁴⁶ Subsequently, *in silico* designed MD-2 and CD14 ligand peptides were synthesized and tested for their activity under physiologically relevant conditions by determining IL-1 β release upon culture in human whole blood. Out of 27 linear and 26 cyclic peptides, 2 peptides (PTC-A-40 and PTC-A-83) showed to be active in stimulating IL-1 β production, validating the use of *ab initio* method to search for TLR4 ligands.¹⁴⁶

Honegr et al. investigated the advantages of *in silico* drug design in the search for TLR4 agonists, by using Ligand- or Structure-Based Virtual Screening (LBVS or SBVS). A large library of molecules (130.000) was screened *in silico* for their capacity to bind to a 3D model of hTLR4/MD2 heterodimer (PDB ID: 4G8A, RCSB Protein Data Bank). Two hit compounds were identified that optimized binding score: a N-(2-(1H-indol-3-yl)ethyl)benzamide (LS-like, compound 16, **Figure 31**) and a anthracene-succinimide hybrid (VS1-like, compound 17, **Figure 31**). Both compounds were then synthesized and chemically modified for SAR studies. While LS and LS-derived molecules didn't achieve a good activity profile (10% of MPLA activity), VS1 and VS1-derived molecules showed a much more promising efficacy when tested *in vitro* and *ex vivo*, scoring 50% of MPLA activation.^{103,147}

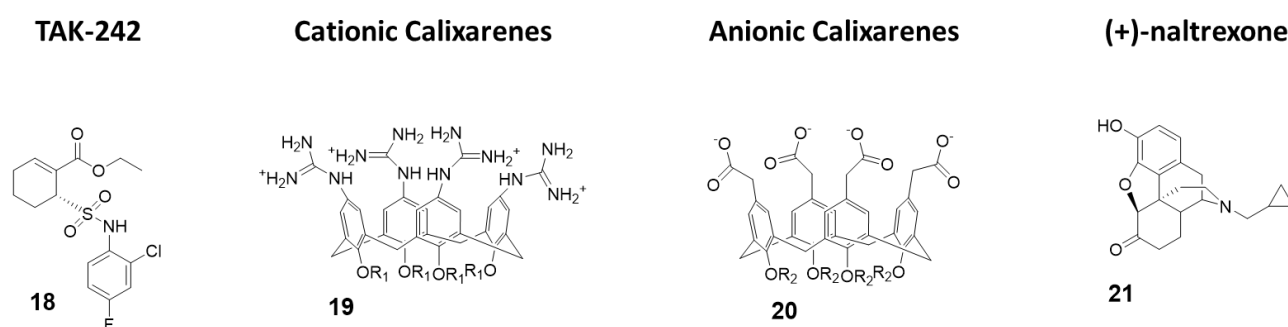


Figure 32 Non-glycolipid TLR4 antagonists. **TAK-242** is a potent TLR4 inhibitor non-competitive toward LPS. Cationic **Calixarenes**, were able to block TLR4 signaling while anionic calixarenes were inactive. (+)-N17-substituted **Naltrexone** derivatives are the only known TLR4 antagonists able to cross the BBB to date and are drug candidate for neuropathic pain.

TLR4 Antagonists

TAK-242

TAK-242 (compound 18, **Figure 32**) is a cyclohexene carboxylic ester derivative produced by Takeda Pharmaceutical Company Ltd which showed a strong action (IC_{50} 1 to 11 nM) as specific TLR4 non-competitive inhibitor.¹⁴⁸ Indeed, studies performed by Takashima (2009) and Matsunaga (2011) demonstrated that TAK-242 binds intracellularly TLR4: it acts as a Michael acceptor for Cys747 residue present in the TIR domain of TLR4. Therefore, TAK-242 disrupts the TIR domain conformation and subsequent interaction with both TIRAP and TRIF, thus inhibiting both MyD88-dependent and MyD88-independent pathways.^{149,150}

TAK-242 was administered on sepsis patients in various intensive care units worldwide in a phase III clinical trial. Unfortunately, trials were terminated because TAK-242 was ineffective in reducing mortality and in suppressing cytokines production. Although failure reasons are unknown, a

combination of individual differences in severity of illnesses and delay in administration of the drug are thought to be the main causes. Furthermore, enrolment in the study of patients without Gram-negative bacteria infections, probably affected the results.⁹⁶

A new study by Wang et al. sought to investigate TAK-242 influence in coronary microembolization (CME)-caused myocardial apoptosis, starting by the fact that TLR4 had been demonstrated to be a promising target for atherosclerotic cardiovascular diseases treatment.¹⁵¹ In the study, the authors were able to reproduce *in vivo* models of CME in mice. CME mice treated with TAK-242 showed a significant improvement in cardiac function and a decrease in micro-infarction area and in apoptotic index when compared with untreated mice, validating TLR4 as a target in this pathology and suggesting treatment with TLR4 inhibitors as an efficient therapeutic approach. However, authors claim the necessity of further studies, as they only experimented short-term effects of TAK-242 and the animal model of CME, obtained by plastic microspheres injection, does not completely mimic microembolization in patients¹⁵²

Calixarene Amphiphiles

Calix[4]arenes are cup-shaped organic molecules formed by 4 or more phenol units linked together by methylene bridges. Calix[4]arenes possess a central hydrophobic conical cavity, and both cavity rims could be chemically functionalized to improve or modulate water solubility. The presence of a cavity and the possibility to synthetically change their chemical structure and therefore modulate water solubility make calix[4]arenes, together with cyclodextrins and cucurbiturils, optimal hosts to carry small molecules and drugs. In recent years, there was a growing interest in calixarenes as drug carriers as they are biocompatible and show low cytotoxicity.^{153–156}

The capacity of amphiphilic calixarenes to modulate TLR4 signal was studied in cationic calix[4]arenes functionalized with guanidine groups on the upper rim (compounds 19, **Figure 32**) and anionic calix[4]arenes with carboxyl groups (compounds 20, **Figure 32**).¹⁵⁷

Surprisingly enough, anionic calix[4]arenes, which should better mimic the negatively charged, amphiphilic lipid A, didn't show any activity on TLR4. On the other hand, positively charged guanidinocalixarenes (compounds 19, **Figure 32**) successfully inhibited TLR4 activity in a dose-dependent manner, with an IC_{50} ranging from 0.7 to 63 μ M. A previous report by K. H. Maio and coworkers¹⁵⁸, described the capacity of similar guanidino calix[4]arenes to neutralize the action of LPS by binding it. The authors sought therefore to verify if the activity of calixarenes in blocking TLR4 signal derives exclusively from LPS binding and neutralization or from a direct action on the

TLR4/MD-2 complex or a combination of these two effects. Cells were treated with a plant lectin, known to activate TLR4 by a mechanism different than LPS, then with different doses of guanidinocalixarenes. A dose-dependent TLR4 inhibition was still observed, thus suggesting a direct effect of calixarenes on the receptor.¹⁵⁷

Opioid Derivatives

The opioid inactive isomer (+)-naltrexone has emerged as the only known TLR4 antagonist having the required LogP to easily cross the blood-brain barrier, making it an interesting lead for the treatment of neuropathic pain and drug addiction. (Northcutt *et al.*, 2015; Wang *et al.*, 2016) While a precedent study by Wang *et al.* confirms that (+)-naltrexone inhibits TRIF/TRAM pathway and binds to MD-2, the molecular mechanism of action and the precise binding to TLR4/MD-2 and/or CD14 interaction is still unclear.¹⁵⁹

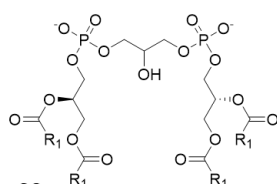
X. Wang and co-workers recently investigated the interaction with MD-2 by molecular docking and experimentally validated the found binding affinity by *in vitro* fluorescence binding studies. Studying a variety of (+)-naltrexones derivatives substituted with different groups on nitrogen N-17, it turned out that the enhancement of the hydrophobic character of the molecules by the introduction of octyl, phenylethyl or methylcyclopropyl groups (compound 21, **Figure 32**) improved MD-2 binding affinity. Adding a methyl group onto N-17 leads to quaternary ammonium cation, which showed poor MD-2 binding affinity ($K_d > 40 \mu\text{M}$) and lost the TLR4 antagonistic activity. Authors concluded that the binding of (+)-naltrexone and its derivatives to MD-2 are primarily driven by hydrophobic interactions. However, polar interactions, which includes both electrostatic interactions and polar solvation free energy, were negatively correlated with experimentally determined binding affinities.¹⁶⁰

Peptide Antagonists PIP2 and cPIP2

A phage display (PD) library of 12-mer peptides was constructed by enriching through six rounds of biopanning against hTLR4. One of the five selected peptides, PIP2, a rather hydrophobic 12-mer, inhibited LPS-stimulated TNF- α and IL-6 production in murine and human macrophages with an IC_{50} of $40 \mu\text{M}$ ¹⁶¹. Besides the relatively weak activity, PIP2 showed some out-of-target inhibitory effects on TLR2. In order to assess PIP2 mechanism of action, fluorescence binding studies, surface plasmon resonance, confocal microscopy with both fluorescently labelled TLR4 and peptide and molecular dynamics experiments were run. All experiments pointed to a direct interaction between PIP2 and

MD-2. Encouraged by these promising results, the authors cyclized PIP2 by a lactam bridge (cPIP2), a common strategy to force α -helix and rigidify small peptides, with the aim to enhance activity and drug-likeness. Indeed, cPIP2 showed better inhibitory profile on TLR4 (IC_{50} 25 μ M) and was further tested *in vivo* in rheumatoid arthritis (RA) mice model. cPIP2 successfully alleviated RA symptoms in mice over a period of 6 weeks, improving histological scores, which suggests the use of cyclic PIP2 as drug lead in RA.¹⁶¹

Saturated Cardiolipins



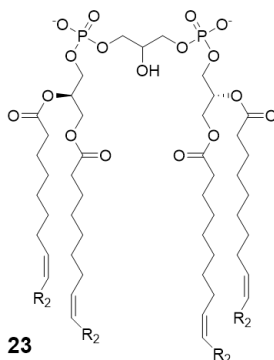
22

22a: R₁: C₁₃H₂₇

22b: R₁: C₁₅H₃₁

22c: R₁: C₁₇H₃₅

Unsaturated Cardiolipins



23

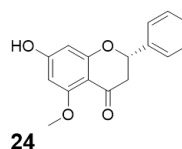
23a: R₁: C₄H₉

23b: R₁: C₆H₁₃

23c: R₁: C₈H₁₇

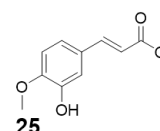
23d: R₁: C₈H₁₅

Alpinetin



24

Ferulic Acid



25

Figure 33 Cardiolipin derivatives 21 and 22 modulate TLR4 activity as agonists or antagonists. The switch between agonism and antagonism seems to be related to the presence of unsaturation on fatty chains. **Alpinetin** is a natural flavonoid which can modulate TLR4 by downregulating its expression by the cell. **Ferulic Acid** showed to antagonize TLR4 by disrupting the TLR4/MD-2 complex.

Cardiolipin

Cardiolipins (CLs) is a family of tetra-acylated diphosphatidylglycerols naturally produced by animals, plants, bacteria and yeasts, with different fatty chains lengths and saturations.¹⁶²

Unsaturated CLs showed activity as TLR4 antagonists although the precise molecular mechanism remains to be studied.^{163,164} As already mentioned in this review, unsaturated fatty acids are present in natural and synthetic TLR4 antagonist. This suggests that the unsaturation of the acyl chains contributes to enhance TLR4 antagonist behaviour. An exhaustive SAR study on CL variants was recently published, focusing on the influence of chain lengths and saturation degree.¹⁶⁵

The activity on cells of a series of saturated and unsaturated derivatives (compounds 22 and 23, **Figure 33**) was tested. Results showed that all unsaturated CLs (compounds 23, **Figure 33**) are active as antagonists on human and murine TLR4 (in HEK-blue cells and murine macrophages), successfully inhibiting receptor signaling with IC_{50} ranging from high nM to low μ M. Saturated CLs (compounds 22, **Figure 33**) can activate TLR4, inducing pro-inflammatory cytokines production.¹⁶⁵ The only

exception to this empirical rule is saturated C14:0 CL, which acted as agonist in murine cells, but as antagonist in human cells, similarly to Lipid IVa.^{165,166}

Alpinetin

Alpinetin (compound 24, **Figure 33**) is a natural flavonoid, extracted from the plant *Alpinia katsumadai* Hayata. It has been demonstrated to possess anti-inflammatory activity, protecting against LPS-related damages both *in vitro* and *in vivo*.¹⁶⁷ Subsequent studies allowed to clarify that alpinetin exert its action as an agonist of PPAR- γ , which in turns down-regulate TLR4 expression, effectively inhibiting receptor signaling¹⁶⁸: it is an indirect TLR4 antagonist. Recent studies proved alpinetin ability to protect mice against kidney damages and endometritis caused by LPS administration. Alpinetin-treated mice showed attenuated LPS-induced histopathological changes; furthermore, alpinetin was showed to inhibit proinflammatory cytokines secretion in a dose-dependent manner.^{169,170}

Ferulic Acid

Ferulic Acid (compound 25, **Figure 33**) is a phenolic compound abundant in various herbs, fruit and vegetables, extracted by *Ligusticum wallichii*. It has been recently shown to have various properties, among which antioxidant and anti-inflammatory effects in murine cells, but its exact mechanism remained unclear.¹⁷¹

Two recent studies claim that FA can protect against LPS-induced bovine endometritis *in vitro* and against LPS-induced acute kidney injury *in vivo* by suppressing NF- κ B and MAPK signaling, which strongly point towards a TLR4-related mechanism of action.^{172,173}

Indeed, Rehman et al., in a recent study in which they demonstrate FA positive effects against LPS-induced neuroinflammation in mice, were able to elucidate FA Activity. By *in silico* molecular docking, the authors reported that FA action is exerted by interfering with MD-2 binding site on TLR4, effectively disrupting the TLR4-MD-2 complex and preventing LPS recognition and formation of the activated dimer (TLR4/MD-2/LPS)₂. However, the proposed mechanism, although intriguing, still lack an experimental proof, as it has only be postulated on the basis of molecular docking.¹⁷⁴

Conclusions

We presented here last advancements in the field of TLR4 modulators, focusing on small molecules of both synthetic and natural origin, as a follow-up of recent reviews on this topic.^{97,175}

All TLR4 modulators described in this review have been validated, or at least evaluated for their capacity to interact specifically with TLR4 and MD-2. For most of the molecules molecular docking calculations and experimental binding studies are available to assess their mechanism of action based on the binding of TLR4/MD-2.

While glycolipid-based TLR4 modulators present a high degree of similarity between them, as they mimic lipid A chemical structure, non-glycolipid TLR4 modulators can have a variety of structures, ranging from smaller bicyclic compounds, as the antagonist TAK-242 approved for clinical use, to larger calix[4]arenes or peptides.

The structural diversity leads inevitably to a diversity in effects, potency and mode of actions, which are reflected in different pharmacodynamics.

TLR4 is the only TLR that initiates two different signal pathways: the MyD88 and the TRAM/TRIF ending up with the production of inflammatory cytokines or type-I interferons.

Interestingly, TLR4 modulators with different chemical structures can activate differentially the two different pathways.

Glycolipid TLR4 agonists, such as MPLA (and its synthetic form GLA) or BECC-derived compounds, were found to preferentially activate the TRIF way, thus skewing lymphocytes towards a T_H1 response, better suited to pathogens and pathogen-infected cells opsonisation and elimination.

On the other hand, the pyrimidoindole derivative 1Z105 was found to activate TLR4 in a MyD88-biased fashion, leading to a T_H2 response, which is better in fighting parasites and extracellular pathogens infections. This difference in the mechanism of action is critical and can be exploited to optimize the rational design of vaccine adjuvants, since they could be more effectively formulated to elicit the most desirable response against a specific pathogen.^{40,102,105,108,109}

The structural diversity of TLR4 modulators leads therefore to different pharmacodynamics, but also to different pharmacokinetic and targeting of different body districts.

Some glycolipid-based compounds, as monosaccharide FP7s, and disaccharide LAMs, can be effectively used systemically, since they are water soluble and have a good distribution. On the other hand, highly hydrophobic non-glycolipid TLR4 antagonists as (+)-naltrexone, are better suited to

target CNS diseases such as neuroinflammation, neuropathic pain, and neurodegenerative diseases including Alzheimer's disease (AD).^{120,134,135,160}

Another intriguing consequence of the structure diversity is the variety of the mechanism of actions. While agonists generally activate TLR4 by direct binding to MD-2, antagonists have much more possibilities to impact on TLR4 activity besides competitive inhibition.

Two interesting examples discussed within this review are TAK-242 and ferulic acid. Thanks to its cyclohexene carboxylic acid ester structure, TAK-242 acts a good electrophilic Michael acceptor, able to form a covalent bond with TLR4. This changes the TLR4 ectodomain conformation thus modifying the conformation of TIR domain and the subsequent interaction with TRIF and MyD88.

¹⁵⁰ Ferulic acid binds in TLR4/MD-2 interaction interface, thus preventing TLR4/MD-2 complex formation, which in turn blocks the formation of the final activated complex (TLR4/MD-2/LPS)₂.¹⁷⁴ Structure refinement and optimization of MD-2 binding *in silico* has proven to be a viable technique in this field, as recently shown by the works of Honegr, Michaeli and Achek reviewed here.^{103,146,147,161}

Novel anti-inflammatory mechanisms indirectly acting on TLR4 have emerged in last years: namely, alpinetin ability to downregulate TLR4 gene expression by enhancing PPAR- γ activity and the activity of LAMs in regulating non-canonical, NLRP3 inflammasome, at the level of caspases 4/11.^{119,168}

The presence of cross-talk between different inflammation pathways, in particular between TLR4 signaling and non-canonical inflammasome initiated by cytosolic LPS, suggest the use of a combination of small molecules to simultaneously block several pathways or, alternatively, the development of dual ligands able to bind to TLR4 and caspases.^{119,120}

AIM OF THE WORK

Vaccines have been a major breakthrough in medicine and public health. Since their introduction in 1798 by Jenner, vaccines dramatically lowered infant and adult mortality rate, extended average life expectancy to level never seen before and reduced incidence of severe diseases such as tetanus, polio, measles and others, while totally eradicating smallpox.¹

After centuries of improvements, vaccines evolved: from attenuated live vaccines, having high efficacy rate but low safety profile as they used alive pathogens, to modern subunit or nucleic acid vaccines. The latter are much safer than attenuated vaccines, as the possibility of adverse events is extremely lower, but without the proper formulation they're also less efficient in eliciting a good immune memory as they lack the immunostimulatory properties of a full-fledged pathogenic cell, with its wide array of possible antigens. Indeed, modern vaccines contains far less antigens than in the past: for example, children undergoing a complete vaccination cycle today (11 vaccinations) are challenged with c.a. 125 antigens, a total amount inferior to the number of antigens present in the 1960s smallpox vaccines (which contained around 200 antigens).¹⁷⁶

Therefore, to reach high efficacy rates, modern vaccines require the presence of adjuvants in their formulation. Vaccine adjuvants are chemical or biological compounds able to induce a proper immune response which enhances antigens ability to generate a good immune memory, so they can rise the overall efficiency of a vaccine, while maintaining a low risk profile.²

For decades, the only vaccine adjuvant approved for human use has been Alum, a mixed salt formed by aluminium hydroxide and aluminium phosphate: its mechanism remained unknown until recently, when its ability to induce DAMPs release upon cell damage was demonstrated.³⁰

In recent decades, however, increased interest on this topic brought to approval of a handful of adjuvants and adjuvant systems, such as oil-in-water emulsions, AS01 or MPL®.²⁹

MPL® is the commercial name of MPLA, a derivative of *Salmonella minnesota* LPS obtained by acid hydrolysis of the entire core and O-antigen portion and of position 1 phosphate. This treatment strongly detoxifies LPS in a way the MPLA only shows c.a. 0.1% of LPS toxicity while retaining the same immunogenic effects. Therefore, MPLA has been approved by FDA and it is used as vaccine adjuvant by itself or in adjuvant systems (AS01, AS04) in human vaccines, such as Pollinex-Quattro, Cervarix®, Fendrix®, Shingrix® and Mosquirix®.⁴⁰

However, MPLA is commonly extracted from bacterial cultures and, as a consequence, it is not a single compound with a well-defined chemical formula, but a mixture of similar and related LPS derivative: not the optimal choice as far as safety is concerned.¹⁰⁹

While a totally synthetic equivalent is available (known as Glucopyranosyl Lipid Adjuvant, GLA, or PHAD®), its synthesis is a long and complex process of 24 steps due to the amount of protective group required for the insertion of biologically active groups. For this reason, the process is extremely expensive as it is shown by the price of the final product, averaging an astounding 200 €/mg: cheaper alternative are therefore needed.^{177,178}

The aim of this work is to develop new, easily synthesizable vaccine adjuvants based on MPLA formula, retaining MPLA strong immunogenic effect but with a much simpler chemical structure which would lead to lower costs when produced industrially.

During the work here presented, two novel classes of monosaccharide MPLA-based vaccine adjuvants acting as TLR4 agonists (FP18 and FP20) were designed, synthesised and tested *in vitro* and *in vivo*. Both FP18 and FP20 resemble MPLA, but they are monosaccharide: consequently, their synthesis is much shorter than MPLA's. This means that both compounds can be mass-produced in less time and with lower cost; therefore, they can be readily available in great quantities for future vaccines.

Both compounds were rationally designed based on previous literature and our own experience on monosaccharide lipid A analogues.

In 1983, Hasegawa at the Gifu University developed a class of monosaccharide derivatives of lipid A called Gifu Lipid A (GLA). Several GLA were synthesized and biologically tested for their inflammatory properties, both as anti-inflammatory and proinflammatory compounds. These early studies were pivotal for assessing a first SAR of monosaccharide TLR4 modulators, but also in elucidating differences in inflammatory pathways in distinct organism: as shown by Matsuura et al., some of the GLA compounds (GLA-26, GLA-47, GLA-64 and GLA-89) have agonist activity in mouse but act as antagonist in human. Interestingly, only GLA-60 and GLA-63 have consistent proinflammatory activity in both species, which suggests that chain length and number, as well as their disposition play a fundamental role in TLR4 activation.^{123,124,179,180}

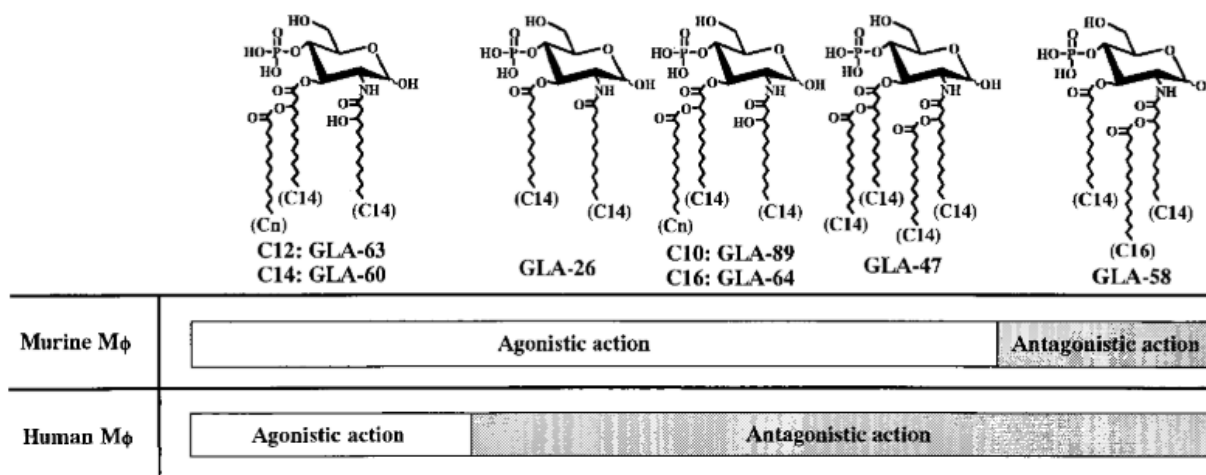


Figure 34 Activities of GLA compounds in human and murine macrophages. Most compounds (GLA-26, GLA-47, GLA-64 and GLA-89) shows different activities in the two systems, while GLA-58 is always a TLR4 antagonist and GLA-60 and GLA-63 are always TLR4 agonists.¹²⁴

In 1999, Johnson et al. developed a new class of TLR4 agonists, called aminoalkyl glucosaminide 4-phosphates (AGPs), also known as Corixa compounds (CRX). These compounds simplified MPLA by substituting the disaccharide backbone with a single sugar unit bound to a serine or a serinol, while featuring the same amount of lipid chains and phosphates. These compounds were meant as vaccine adjuvants, and the SAR performed on these molecules helped understand the effects of bioisostery and stereomery on the biological activity, particularly for the bias toward either MyD88 or TRIF pathway.^{181,182}

Important precursors to our work have been the Sandoz compounds, particularly SDZ MRL 953. A monosaccharide featuring a phosphate and three β -substituted lipid chain, SDZ MRL 953 is derived from the endotoxin of *Salmonella abortus equi*. It showed a potent agonist activity on TLR4, stimulating the release of release of inflammatory cytokines such as interleukin-6 (IL-6), interleukin-8 (IL-8) and TNF- α , while being 10^4 less toxic than the parent molecule.¹⁸³

SDZ MRL 953 was mainly tested as a prophylactic agent against sepsis, due to the known immunostimulatory activity of *Salmonella ebortus equi* endotoxin. Indeed, Kiani et al. conducted a double-blind phase I trial in order to assess the prophylactic properties of SDZ MRL 953 in cancer patients challenged with LPS, as well as its safety profile. The results proved that compound administration can increase G-SCF serum levels as well as the count of granulocytes, while not inducing high and sustained levels of proinflammatory cytokines, which explain the safety and tolerability in human observed during the study.¹⁸⁴

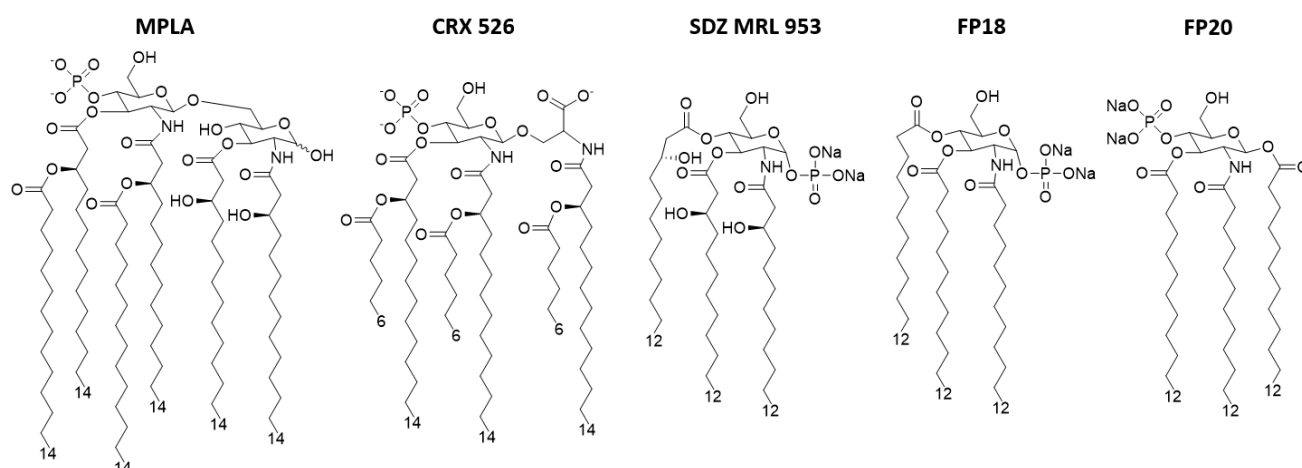


Figure 35 MPLA and some of its derivatives: CRX 526, SDZ MRL 953, FP18 and FP20

Finally, compound formulas were suggested by previous SAR studies performed by our group in the frame of our previous involvement in the TOLLerant project for development of TLR4 antagonists. Particularly, our studies seemed to suggest that, for monosaccharides, TLR4 activity switch depended on the ratio between phosphates and lipid chains: compounds possessing a 1:1 ratio acted as antagonists, while compounds having a 1:3 ratio were agonists.

Eventually, further advances in our understanding of TLR4 agonists mechanism seems to challenge this rule of thumb, though. Our current hypothesis is that what matters for TLR4 activity the three-dimensional shape of the molecule, as it appears to be the case for LPS. The ratio between phosphates and lipid chains does affect the three-dimensional shape, but the relative position between them is important too: a demonstration is the fact that FP200 still retains TLR4 agonist activity, while FP111 is completely inactive (see below).

The results here obtained have been useful both under the industrial/medical and the pure research point of view. The two new classes of compounds here presented represent an advancement in the medical field as they are novel vaccine adjuvants with promising activity and safety profile, comparable or even higher than MPLA ones, while being so much easier and cheaper to synthesize that the patents protecting their intellectual properties are being acquired by Croda Vaccines, a big pharmaceutical company which also produces synthetic MPLA.

Beyond these achievements, FP18 and FP20 have been also used as tools to better understand the biological events leading to inflammation: not only they helped shed light on the minimal requirements to engage TLR4 activations, but they also clarified events leading to LPS internalization and activation of non-canonical inflammasome mediated by NLRP3.

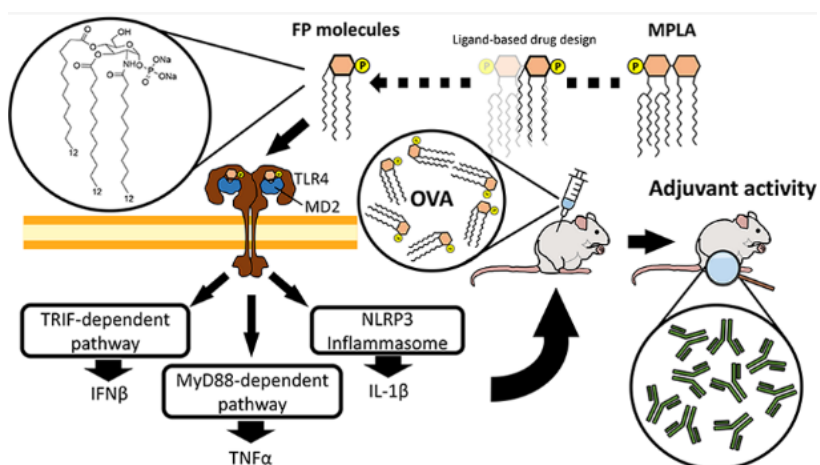
RESULTS AND DISCUSSION

Chapter I: Synthetic Glycolipids as Molecular Vaccine Adjuvants: Mechanism of Action in Human Cells and In Vivo Activity

Fabio A. Facchini, Alberto Minotti, Andrea Luraghi, Alessio Romerio, Nicole Gotri, Alejandra Matamoros-Recio, Andrea Iannucci, Charys Palmer, Guanbo Wang, Rebecca Ingram, Sonsoles Martin-Santamaria, Grisha Pirianov, Marco De Andrea, Miguel A. Valvano, and Francesco Peri

Adapted from Facchini, F. A.; Minotti, A.; Luraghi, A.; Romerio, A.; Gotri, N.; Matamoros-Recio, A.; Iannucci, A.; Palmer, C.; Wang, G.; Ingram, R.; Martin-Santamaria, S.; Pirianov, G.; De Andrea, M.; Valvano, M. A.; Peri, F. Synthetic Glycolipids as Molecular Vaccine Adjuvants: Mechanism of Action in Human Cells and In Vivo Activity. J. Med. Chem. 2021, 64, 12261–12272.

ABSTRACT: Modern adjuvants for vaccine formulations are immunostimulating agents whose action is based on the activation of Pattern Recognition Receptors (PRRs) by well-defined ligands to boost innate and adaptive immune responses. Monophosphoryl lipid



A (MPLA), a detoxified analogue of lipid A, is a clinically approved adjuvant that stimulates Toll-like Receptor 4 (TLR4). The synthesis of MPLA poses manufacturing and quality assessment challenges. Bridging this gap, we report here the development and preclinical testing of chemically simplified TLR4 agonists that could sustainably be produced high purity and in large scale. Underpinned by computational and biological experiments, we show that synthetic monosaccharide-based

molecules (FP compounds) bind to the TLR4/MD-2 dimer with submicromolar affinities stabilizing the active receptor conformation. This results in the activation of MyD88- and TRIF-dependent TLR4 signaling, and the NLRP3 inflammasome. FP compounds lack in vivo toxicity and exhibit adjuvant activity by stimulating antibody responses with a potency comparable to MPLA.

Introduction

Modern subunit vaccines, based on purified or synthetic antigens that are often poorly immunogenic, require combination with adjuvants for optimal immune responses.¹⁸⁵ Molecular adjuvants are single-molecule innate immune stimulants that enhance adaptive immune response against antigens. Adjuvants activate antigen-presenting cells, such as dendritic cells and macrophages. These cells express pathogen recognition receptors that, when activated, initiate immune responses leading to the priming of T cells.¹⁸⁶ Pathogen-associated molecular patterns (PAMPs), the ligands of pathogen recognition receptors, can be exploited as molecular adjuvants. Many well-defined PAMPs have been explored, most of them targeting the Toll-like receptors (TLRs),¹⁸⁷ C-type lectins,¹⁸⁸ and nucleotide-binding oligomerization domain (NOD)-like receptors.¹⁸⁹ Since TLR4 stimulation plays a key role in initiating rapid innate immune responses, TLR4 agonists are promising candidates to develop vaccine adjuvants^{182,190–193} and cancer immunotherapeutics.¹⁹⁴ Lipopolysaccharide (LPS)-stimulated activation of TLR4 promotes the formation of the [TLR4/MD-2/LPS]₂ membrane dimer;¹⁹⁵ which interacts with two important adaptor protein molecules: MyD88 and TRIF. Signaling through the MyD88-dependent pathway results in rapid activation of NF- κ B and MAPK, both of which drive proinflammatory gene expression and cytokine production. Stimulation of the TRIF-dependent arm via the endocytic pathway activates interferon regulatory factors and secondary NF- κ B activation,¹⁹⁶ playing an important role in the stimulation of early T cell responses.¹⁰⁵ TRIF-dependent type I IFN is a central mechanism for TLR4-mediated adjuvant effects on T cell priming by TLR4 agonists.¹⁹⁷ Moreover, the activation of the NLRP3 inflammasome and subsequent caspase-1 activation and release of Interleukin-1 β (IL-1 β) is associated with the potent adjuvant effect by particulate adjuvants, such as alum, chitosan and QuilA/saponin.^{198,199} IL-1 β exerts multiple effects on the immune system,²⁰⁰ which include promoting the differentiation of Th17 cells.²⁰¹

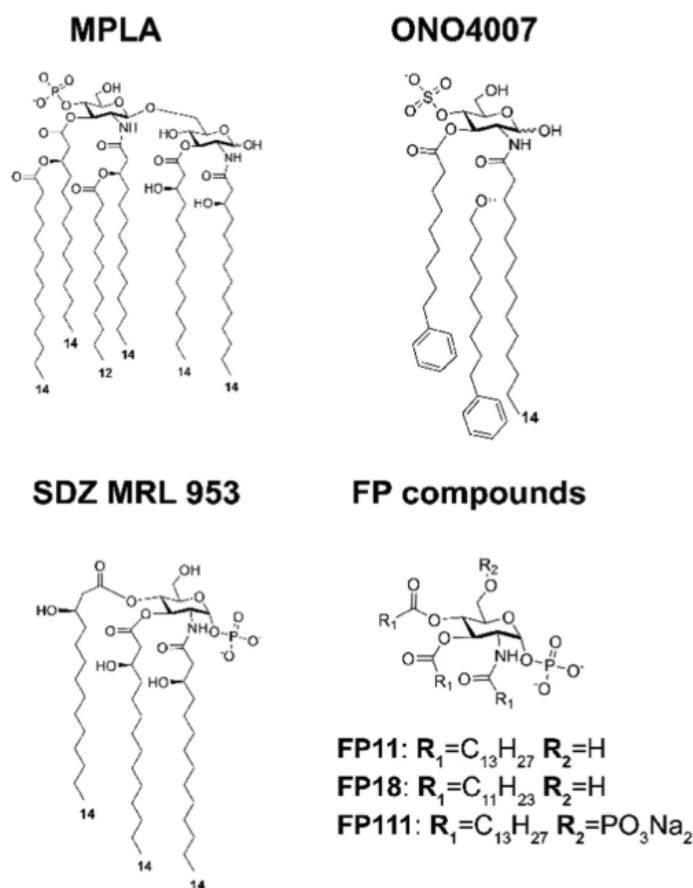


Figure 36 Chemical structure of TLR4 agonists: MPLA, ONO4007, SDZ MRL 953, and FP molecules

Lipid A, the component of LPS that directly binds TLR4/MD-2 is one of the most potent immune-stimulating agents known. The toxicity of lipid A makes it unsuitable for safe use in humans, but the Monophosphoryl lipid A (MPLA, **Figure 36**)¹⁸¹, a lipid A derivative in which the anomeric phosphate has been removed, is an effective adjuvant used in various approved vaccines.^{40,202} MPLA and aminoalkyl glucosaminide phosphates (AGPs)¹⁸¹ are well studied non-toxic TLR4 ligand adjuvants that promote Th1 (cellular)-biased immune responses. MPLA also stimulates the TLR4-mediated activation of the TRIF cascade,¹⁰⁵ which also explains the MPLA's reduced toxicity.²⁰³ However, the production of MPLA is challenging. MPLA derived from modification of bacterial lipid A is not chemically homogeneous, making it difficult to assess its quality. A total synthesis of MPLA has been developed, allowing to obtain a homogeneous compound, which is then named glucopyranosyl lipid A (GLA)^{42,109,204}. However, total synthesis of MPLA is complex (it involves around 24 chemical steps) and expensive. In contrast, easier synthetic access to monosaccharides bearing lipid chains and phosphate groups makes this class of molecules suitable to develop novel TLR4 agonists with simpler and scalable production methods. Synthetic monosaccharide mimetics of Lipid X, a monosaccharide biosynthetic precursor of Lipid A, were developed as TLR4 modulators. Compound SDZ MRL 953

(**Figure 36**), showed powerful immunostimulatory activity both in mice and humans¹⁸³ and was tested in a phase I trial as tumor immunotherapeutic.¹⁸⁴ Also, compound ONO 4007 (**Figure 36**) is a powerful immunostimulant for antitumor therapy.^{205,206} Our group developed synthetic monosaccharides, named FP compounds, which bind to the MD-2 coreceptor and block TLR4 pathway in cells and in animal models.^{60,207–209} Guided by detailed structure-activity information, we predicted new compounds switching from antagonism to agonism by altering the ratio of fatty acid chains and phosphates. Compounds FP11 and FP18 (**Figure 36**), with a triacylated Monophosphoryl glucosamine core and one phosphate group at C1, were designed and synthesized along with compound FP111, which has an additional phosphate group at C6. We present here a preclinical study on the new synthetic TLR4 agonists FP11 and FP18 (compound FP111 turning out to be inactive), their synthesis, computational studies, in vitro binding studies with the TLR4/MD-2 dimer, cell studies on mechanism of action and TLR4 pathways activation, and in vivo assessment of their adjuvant potency, compared to FDA-approved MPLA, in an ovalbumin (OVA) vaccination model.

Results And Discussion

Synthesis of FP molecules

Compounds FP11, FP18 and FP111 were synthesized through a protocol previously developed and optimized for the preparation of TLR4 antagonists of the FP series.²⁰⁸ The synthesis for FP11 and FP18 (**Figure 37**) was carried out starting from the commercially available D-glucosamine hydrochloride, following in part a previously published protocol consisting of the transformation of the amine at C2 into azide (2), followed by protection of sugar's C4-C6 positions as p-methoxybenzylidene (3), silylation of the anomeric position (4), and Staudinger hydrolysis of azide into amine (5).²⁰⁸ Compound 5 was acylated with myristoyl chloride or lauroyl chloride to obtain, respectively, compounds 6 or 7. Regioselective opening of the p-methoxybenzylidene by means of sodium cyanoborohydride (NaBH₃CN) in trifluoroacetic acid (TFA) gave C6 p-methoxybenzyl (PMB)-protected compounds 8 and 9, whose acylation with myristoyl chloride or lauroyl chloride, respectively, afforded triacylated sugars 10 and 11. Cleavage of the anomeric silane with tetrabutylammonium fluoride (TBAF), followed by reaction with phosphoramidite and one-pot oxidation with m-chloroperbenzoic acid (m-CPBA), gave compounds 14 and 15. Catalytic hydrogenation followed by treatment with sodium cation exchange resin, gave final compounds

FP11 and FP18. Similarly, FP111 was synthesized starting from the intermediate compound 13 by removal of the PMB group at C6 through catalytic hydrogenation (16), simultaneous phosphorylation of sugar's C6 and C1 (17) and final removal of benzyl groups again by catalytic hydrogenation.

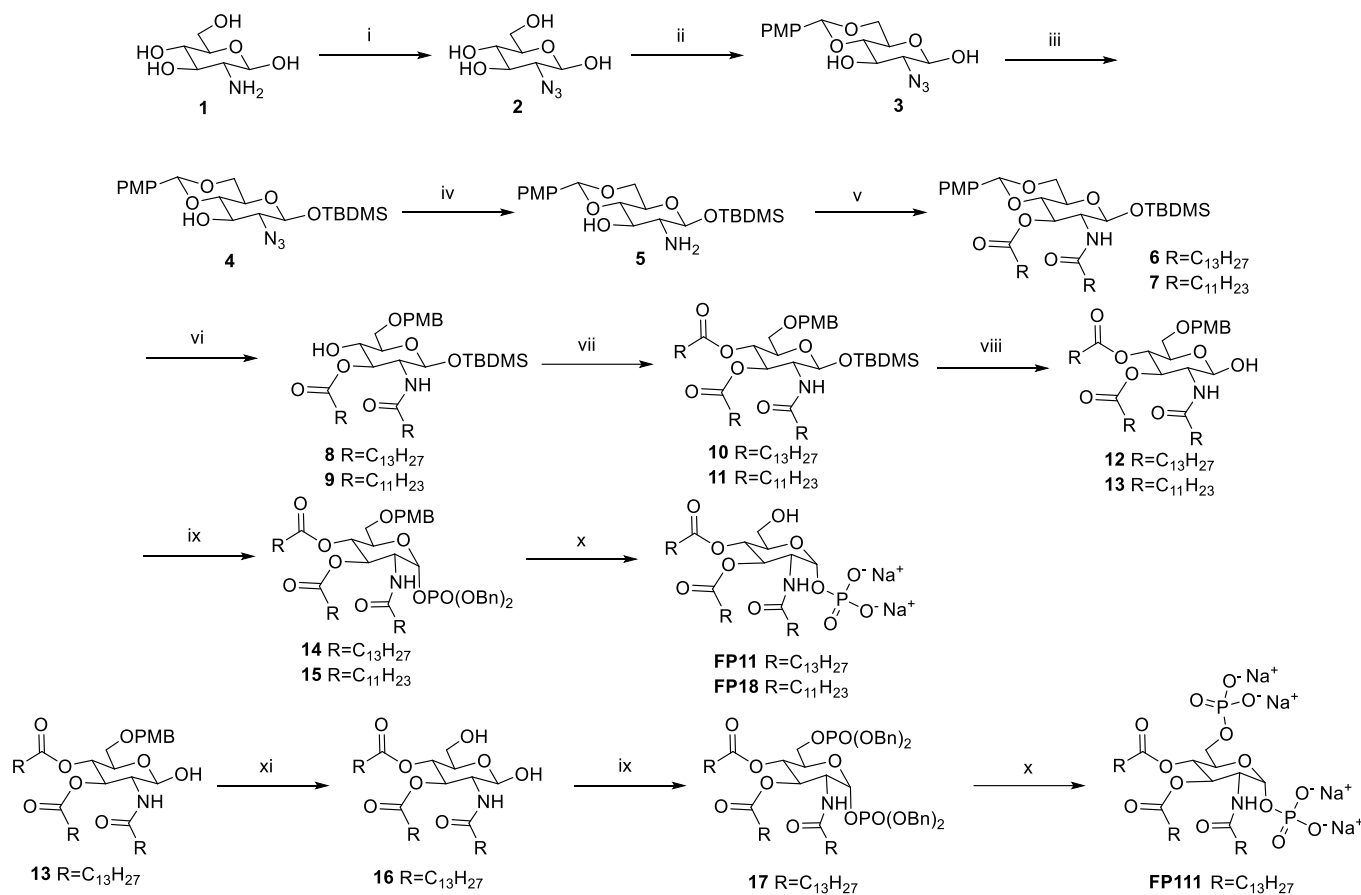


Figure 37 Synthesis of FP11, FP18 and FP111. Conditions: (i) NaN₃, Tf₂O, copper sulphate, Py, H₂O, quant. (ii) Anisaldehyde dimethyl acetal, camphorsulfonic acid (CSA), dimethylformamide (DMF), 50 °C, 68%. (iii) TBDMSCl, imidazole, dichloromethane (DCM), 62%. (iv) PPh₃, tetrahydrofuran (THF), H₂O, quant. In the following steps, the first yield refers to FP11 synthesis and the second to FP18. (v) RCOCl, 4-dimethylaminopyridine (DMAP), triethylamine (TEA), DCM, 75%, 85%. (vi) NaBH₃CN, 4 Å molecular sieves, THF, and then TFA, 83%, 85%. (vii) RCOCl, DMAP, TEA, DCM, 97%, 98%. (viii) TBAF, AcOH, THF, 87%, 90%. (ix) P(OBn)₂N(i-Pr)₂, imidazolium triflate, DCM and then m-CPBA, 50%, 55%. (x) H₂/Pd-C, MeOH, and then IRA78- Na⁺, 80%, 87%. (xi) H₂, Pd-C 10%, MeOH, 95%.

In vitro binding tests: FP11 and FP18 bind to human MD-2

Direct interaction of FP11 and FP18 with human TLR4/MD-2 dimer was investigated by surface plasmon resonance (SPR). The recombinant human TLR4/MD-2 receptor complex was directly immobilized on a NTA sensor chip by amine coupling and probed with increasing amounts of FP11 or FP18. The resulting SPR sensograms (**Figure 38B**) showed a direct interaction between FPs

molecules and the TLR4/MD-2 receptor with similar equilibrium dissociation constants (K_d), 0.18 μM for FP11 and 0.57 μM for FP18. Moreover, these data indicated that both FP11 and FP18 bind to TLR4/MD-2 receptor with fast association (K_a) and slow dissociation (K_d) rates, as reported for LPS and other FPs molecules.^{59,208}

TLR4 Binding of FP11, FP18, and FP111. Computational studies

In order to provide a 3D perspective of the TLR4 binding, FP11 and FP18 were submitted to computational studies to predict their binding modes at atomic level. Also, FP111 was studied. Compounds FP11, FP18, and FP111 were docked into the human TLR4/MD-2 heterodimer in the agonist activated conformation (**Figure 38A**, and Supp. Info.). Preliminary binding poses, obtained with AutoDock Vina, were used as starting geometries for re-docking calculations with AutoDock. The calculations resulted in favorable predicted binding energies for FP11 and FP18 ligands (ranged from -3.8 to -2.7 kcal mol⁻¹, for the best ranked poses), and an unfavorable binding energy for compound FP111 (values greater than 3.0 kcal mol⁻¹). FP11 and FP18 showed predicted binding poses with their fatty acid chains buried inside the MD-2 pocket, interacting with many hydrophobic and aromatic residues, and with the saccharide moiety located at the MD-2 rim, establishing polar interactions (**Figure 38A**). The docking calculations suggested strong affinity and plausible binding modes for compounds FP11 and FP18 with the TLR4/MD-2 system but indicated non-efficient binding for ligand FP111 (**Figure 38A**). The stability of the best FP11 and FP18 predicted binding modes was confirmed by molecular dynamics (MD) simulations. Starting from the best docked TLR4/MD-2/ligand complexes, we constructed full [TLR4/MD-2/ligand]₂ models (Figure S1) that were submitted to 50 ns MD simulations (Supp. Info.). The complexes were stable during the simulations (Figure S2) and none of the ligands underwent orientation flip, all remaining in the agonist orientation predicted from docking calculations (Figure S3). Further, MD-2 Phe126 retained the agonist conformation along the MD simulations (Figure S4). We therefore suggest these complexes as plausible binding modes for FP11 and FP18, accounting for their agonist activity in the TLR4/MD-2 system.

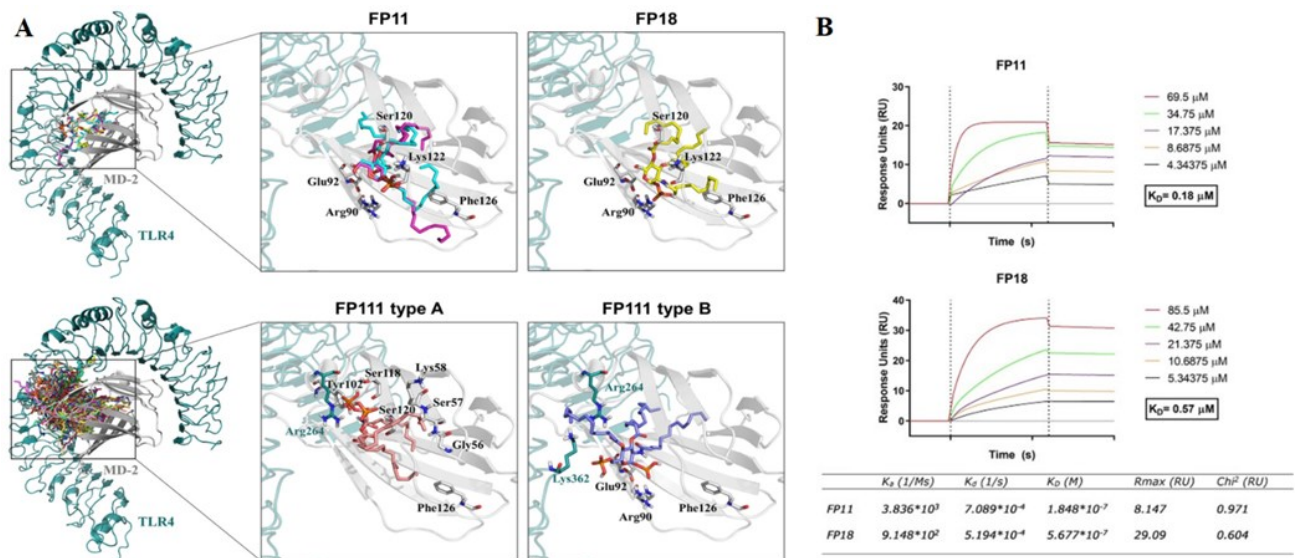


Figure 38 A) Docking studies of compounds FP11, FP18, and FP111. (Top) Best AutoDock predicted binding modes for ligands FP11 and FP18 to the human TLR4/MD-2 heterodimer. On the right are details of the interactions between FP11 (magenta and cyan sticks) and FP18 (yellow sticks) and MD-2 protein. (Bottom) Binding of compound FP111 by means of the AutoDock program to the human TLR4/MD-2 system. On the right are represented detailed poses of FP111 to the TLR4/MD-2 heterodimer, with details of the interactions between FP111 type A antagonist-like (purple sticks) and type B agonist-like (salmon pink sticks) orientations. **B)** Surface plasmon resonance (SPR) analyses of FP11 and FP18 binding to immobilized TLR4/MD2. Increasing concentrations of FP11 (4.34–69.50 μ M, left panel) or FP18 (5.34–85.50 μ M, right panel) diluted in running buffer were injected over a TLR4/MD2-immobilized NTA sensor chip. FP11 and FP18 bind to TLR4/MD2 with equilibrium dissociation constant (K_d) values of 0.18 and 0.57 μ M, respectively. Data are representative of three independent experiments. Binding kinetics are also shown. K_a , association rate constant; M, molarity; s, seconds; K_d , dissociation rate constant; K_D , equilibrium dissociation constant; R_{max} , maximum response; RU, response units; χ^2 , average squared residual.

TLR4 activation by synthetic agonists

The ability of FP molecules to activate human TLR4 was first assessed using HEK-Blue hTLR4 cells. These are a HEK293-derived cell line stably transfected with the LPS receptors CD14, TLR4 and MD-2 and a reporter gene, secreted embryonic alkaline phosphatase (SEAP) placed under the control of two TLR4-dependent transcription factors (NF- κ B and AP-1). The HEK-Blue hTLR4 cells were treated with increasing concentrations (0.1–25 μ M) of FP11, FP18 and FP111 over 18 hours. Stimulation with LPS (smooth chemotype, S-LPS) served as a positive control for the activation of the TLR4-mediated pathway.

Molecules FP11 and FP18 induced the release of the SEAP reporter protein in the medium in a concentration-dependent manner, indicating that both compounds activate NF- κ B and AP-1, while FP111 was inactive (**Figure 39A**). The three compounds did not inhibit LPS-induced SEAP production, suggesting they lack a TLR4 antagonistic activity (**Figure 39B**). A lack of activity on HEK-Blue Null cells, which carry the same SEAP reporter gene but lack the LPS receptors, confirmed that both FP11 and FP18 act via TLR4 (**Figure 39C**). To confirm the selectivity on TLR4 over TLR2, the molecules were

also tested on the HEK-Blue cells expressing hTLR2, and no agonist activity was detected (**Figure 39D**). These data confirm the binding data with purified TLR4/MD-2 and suggest that FP11 and FP18 are specific TLR4 agonists that directly bind to TLR4/MD-2.

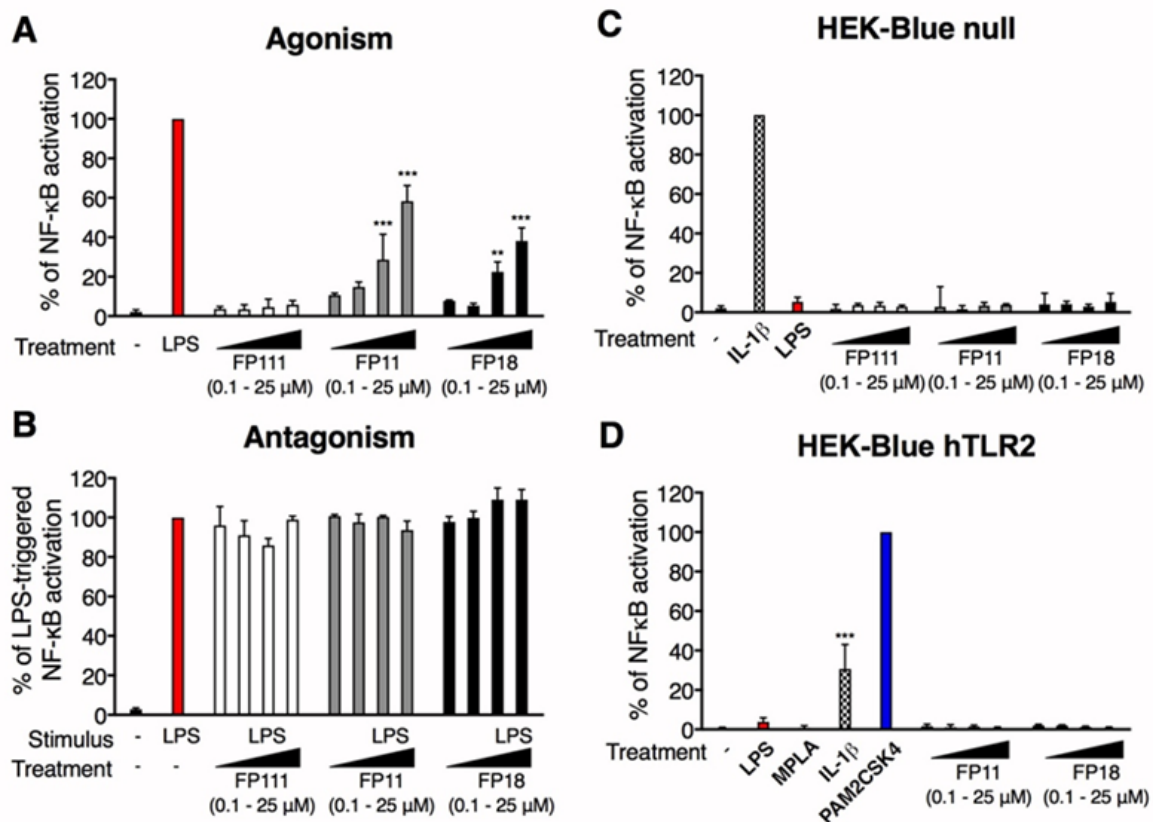


Figure 39 HEK-Blue hTLR4, HEK-Blue Null, and HEK-Blue hTLR2 cells were treated as indicated and incubated for 18 h. Supernatants were collected and SEAP levels were quantified by the QUANTI-blue method. Data were normalized to stimulation with S-LPS (**A**, **B**), IL-1β (**C**), or PAM2CSK4 (**D**) and expressed as the mean percentage ± standard deviation (SD) of three independent experiments (treated versus untreated (-): **p < 0.01 and ***p < 0.001).

Activation of MyD88 and TRIF pathways in human macrophages

We investigated whether the FP compounds are able to induce the same signaling pattern observed with S-LPS and MPLA stimulation in vitro. First, we evaluated whether FP11 and FP18 activate the MyD88-dependent pathway in THP-1-derived macrophages (TDP). The recruitment of MyD88 adaptor protein by the TLR4 cytosolic TIR domain promotes NF-κB and mitogen-activated protein kinases (MAPKs) activation.²¹⁰ Therefore, the phosphorylation status of NF-κB (p65 subunit) and MAPK p38 in response to FP11, FP18, S-LPS and MPLA treatment was assessed over-time. The stimulation with S-LPS, and with FP11 and FP18 triggered p65 phosphorylation after 1 hour, while for MPLA the activation of p65 occurred earlier (**Figure 40A**). The kinetics of p38 activation by FP11

and FP18 was similar to p65 NF- κ B phosphorylation (**Figure 40A**), with the peak of phosphorylation after 1 hour, as also observed upon S-LPS stimulation. In contrast, MPLA showed an earlier peak of phosphorylation at 30 minutes. The quantity of pro-inflammatory cytokines (TNF α , IL-1 β and IL-6) released following treatment with increasing concentrations of FP11 and FP18 were compared with MPLA and S-LPS. S-LPS triggered the release of TNF α , IL-1 β and IL-6 (**Figure 40B**), as did MPLA stimulation albeit in reduced amounts. The effect of MPLA was dose-independent, suggesting that the concentrations used were sufficient to reach receptor saturation. FP11 treatment only triggered a dose-dependent secretion of IL-1 β , while FP18 induced the production of all the three cytokines at levels exceeding those observed with MPLA stimulation (**Figure 40B**). These data clearly show that FP11 and FP18 activate MyD88-dependent intracellular TLR4 signaling in human macrophages.

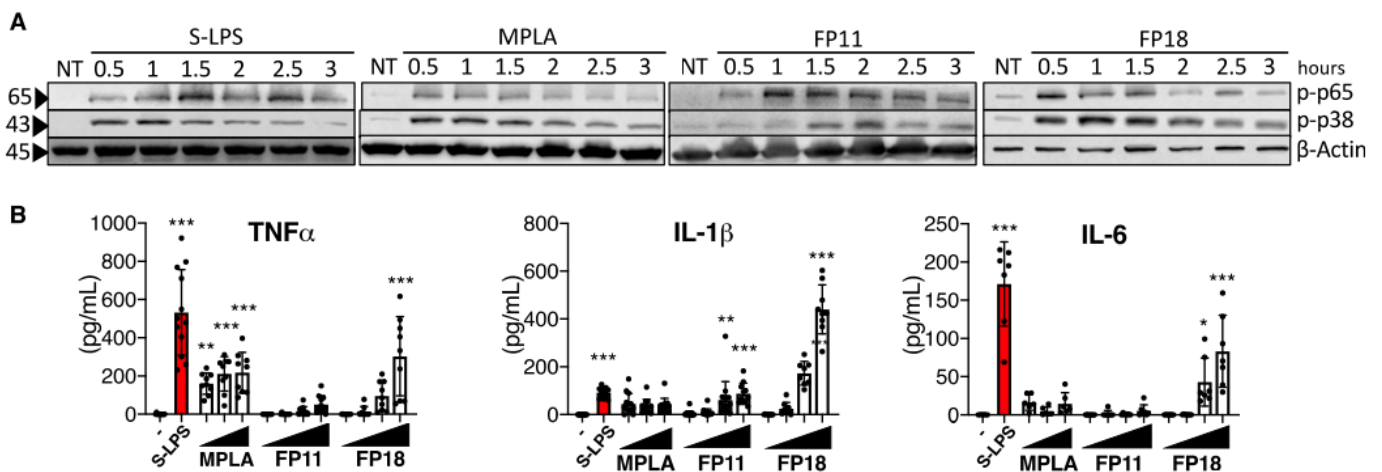


Figure 40 A) TDM were treated with S-LPS (100 ng/mL), MPLA (1 μ g/mL), FP11 (10 μ M), FP18 (10 μ M), or left untreated (NT) and collected after the indicated time. The levels of phospho-p65, phospho-p38, and actin were detected by immunoblotting. **B)** In vitro cytokines released from TDM measured by enzyme-linked immunosorbent assay (ELISA). Cells were treated with S-LPS or with increasing concentrations of MPLA, FP11, and FP18 (0.1–1 to 10–25 μ M) for 18 h. Error bars represent the SD of the mean. TNF α (n = 9), IL-1 β (n = 9), and IL-6 (n = 7), where *p < 0.05, **p < 0.01, and ***p < 0.001. Statistical analysis is between treated vs untreated (-) (one-way analysis of variance (ANOVA) test).

To investigate whether FP11 and FP18 also trigger the TRIF-dependent pathway, four readouts in TDP were selected: the activation of IRF3, the expression and release of IFN β , the activation of STAT1 and the expression of interferon stimulated genes (ISGs). Stimulation with rough chemotype of LPS (R-LPS) was also included as reference in this part of the study.

S-LPS strongly induced IRF3 phosphorylation one hour after treatment, but the effect of FP18 was delayed, with a peak of IRF3 activation observed after 2.5 hours (**Figure 41A**). The peak of IRF3 phosphorylation following R-LPS and MPLA stimulation was of a similar magnitude to that induced

by FP18, appearing between 1-1.5 hours post treatment (**Figure 41A**). In contrast, FP11 did not induce IRF3 phosphorylation (**Figure 41A**). Next, we evaluated whether IFN β induction followed IRF3 activation by examining gene expression and cytokine release. Consistent with previous results, increased IFN β transcription was observed 2 hours post-stimulation with S-LPS, R-LPS and MPLA in comparison with untreated cells, with 600-, 250- and 60-fold increase, respectively, followed by a rapid decline at 6 hours post-treatment (**Figure 41B**, left panel). FP18 showed limited ability to induce the IFN β mRNA expression, with a 20-fold increase at 2 hours post-treatment in comparison with untreated cells. In agreement with the IRF3 phosphorylation status, IFN β mRNA expression was unaffected by FP11 stimulation. The levels of IFN β secreted corroborated the mRNA results, whereby significantly higher levels were detected in the culture supernatants of cells treated with S-LPS and R-LPS than from untreated cells at both 3 and 6 hours post-treatment (**Figure 41B**, right panel). In contrast, induction of IFN β was lower in MPLA and FP18 treated cells, and not observed with FP11 stimulation. Despite the diminished induction of IFN β , downstream STAT1 phosphorylation was detected starting from 2.5 hours upon FP18 and S-LPS stimulation, indicating that IFN β release mediated by FP18 was sufficient to induce ISGs. By comparison, R-LPS and MPLA triggered STAT1 phosphorylation after 1.5 and 2 hours upon stimulation, respectively (**Figure 41A**). The phosphorylation of STAT1 due to IFN β binding to its receptor was confirmed using a specific blocking antibody that prevents IFNAR activation. As predicted, S-LPS and FP18 exposure or direct exogenous IFN β stimulation triggered a significant increase in STAT1 phosphorylation (**Figure 41C**), which was completely abolished by blocking IFNAR in all the three cases, indicating that FP18 can induce type I IFNs release (**Figure 41C**). Finally, STAT1-mediated expression of an ISG (namely, Viperin/RSAD2) was also evaluated. S-LPS induced Viperin/RSAD2 gene expression, reaching a maximum peak 6 hours post treatment (**Figure 41D**). A similar pattern of activation was observed for FP18, R-LPS and MPLA treatments causing increased RSAD2 expression after 6 hours, with a potency similar to S-LPS. In contrast, very low RSAD2 transcription was detected in cells stimulated with FP11 (**Figure 41D**). These results suggest that FP18 triggers both the MyD88- and the TRIF-dependent pathways, while FP11 preferentially activates the MyD88 pathway.

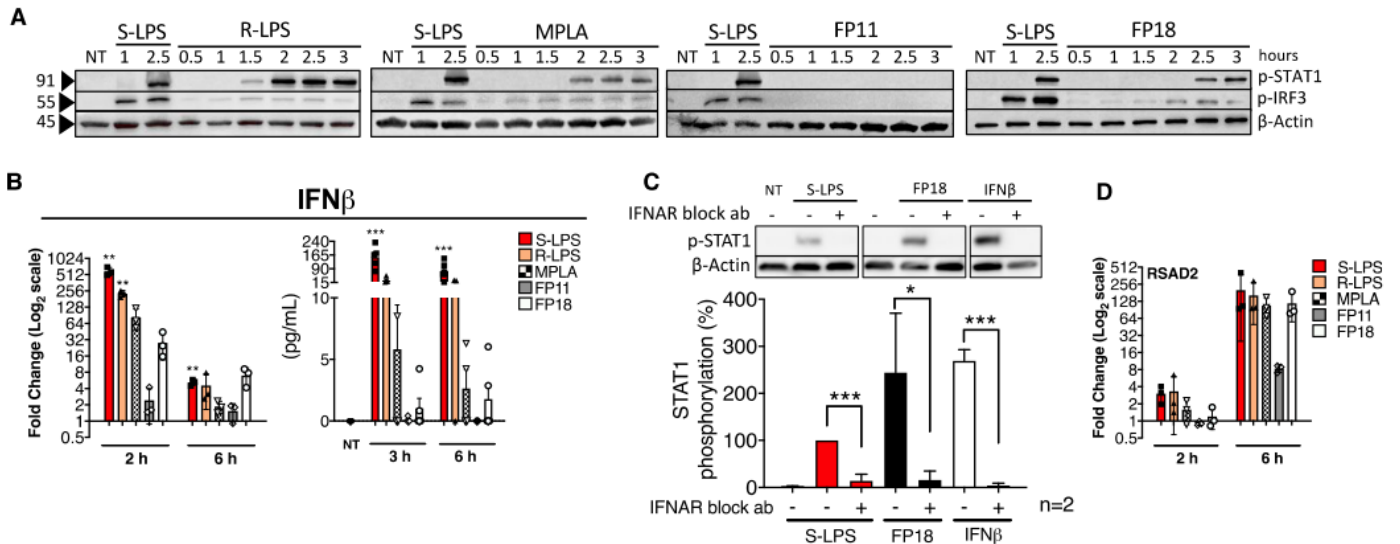


Figure 41 **A)** TDM was treated with S-LPS (100 ng/mL), R-LPS (100 ng/mL), MPLA (1 μ g/mL), FP11 (10 μ M), FP18 (10 μ M), or left untreated (NT) and collected after the indicated time. The levels of phospho-IRF3, phospho-STAT1, and actin were detected by immunoblotting. **B)** TDM were treated as in panel and collected after the indicated time. (Left) IFN β production is expressed as fold change compared to untreated cells. Error bars represent SD of the mean; n = 3, where *p < 0.05, **p < 0.01, and ***p < 0.001. Statistical analysis is between treated vs untreated (Wilcoxon's test). (Right) IFN β release was quantified by ELISA. Error bars represent SD of the mean; n = 4 where *p < 0.05; **p < 0.01; and ***p < 0.001. Statistical analysis is between treated vs untreated (NT) (one-way ANOVA test). **C)** TDM were pretreated with IFNAR2 neutralizing antibody (1 μ g/mL) 1 h prior to exposure to the indicated stimulus. Cell lysates were collected after 3 h and p-STAT1 was measured via immunoblotting. Error bars represent SD of the mean; n = 2 where *p < 0.05 and ***p < 0.001 (one-way ANOVA test). **D)** TDM were treated as in panel B and collected after the indicated time. RSAD2 expression is expressed as fold change compared to untreated cells. Error bars represent SD of the mean; n = 3, where *p < 0.05, **p < 0.01, and ***p < 0.001. Statistical analysis is between treated vs untreated (Wilcoxon's test).

IL-1 β is the predominant pro-inflammatory cytokine induced by FP molecules and its release is normally associated with the activation of NLRP3 inflammasome. The ability of FP11 and FP18 to trigger caspase-1 activation and IL-1 β maturation was investigated using TDP. We first analyzed IL-1 β production by a cell-associated ELISA, which allowed us to compare precursor and mature forms of the cytokine in cell lysates and supernatants, respectively. The accumulation of IL-1 β precursor in cell lysates was induced by FP11 and FP18, as well as the other treatments tested, after 3, 6 and 18 hours (**Figure 42A**). This induction was, however, only significant in the FP18, S-LPS and R-LPS treated cells. Similarly, the analysis of supernatants revealed that although IL-1 β release was triggered by all molecules, only FP18 and S-LPS caused significant secretion of the IL-1 β mature form. The lower level of activity of FP11 is consistent with the previous results (**Figure 42A**). Moreover, IL-1 β levels were higher in cell lysates, suggesting a partial activation of the inflammasome with a limited release of the mature cytokine. For this reason, we evaluated the canonical inflammasome activation by monitoring caspase-1 activation and mature IL-1 β release in the extracellular compartment through western blotting. Caspase-1 was constitutively expressed in differentiated

THP-1 cells, whilst, in agreement with the cell-associated ELISA assay, the IL-1 β precursor was induced after 6 hours by all compounds (**Figure 42B**). It was also demonstrated that only FP18 and S-LPS induced high levels of caspase-1 cleavage and IL-1 β maturation and release, while MPLA and R-LPS stimulation resulted in weaker signaling (**Figure 42B**). To evaluate NLRP3 contribution in FP18-triggered IL-1 β release, TDP were pre-treated for 1 hour with increasing concentration of NLRP3 inhibitor MCC950 (0.01 μ M – 10 μ M) and then stimulated with FP18 or S-LPS for 6 hours. After treatment, cell supernatants were checked for IL-1 β levels by ELISA assay and western blot. MCC950 pre-treatment significantly inhibited IL-1 β release, in a concentration-dependent manner, in both FP18 and S-LPS treated cells (**Figure 42C and D**). Collectively, these data demonstrated that FP18 triggers NLRP3 canonical inflammasome inducing caspase-1 activation and IL-1 β release.

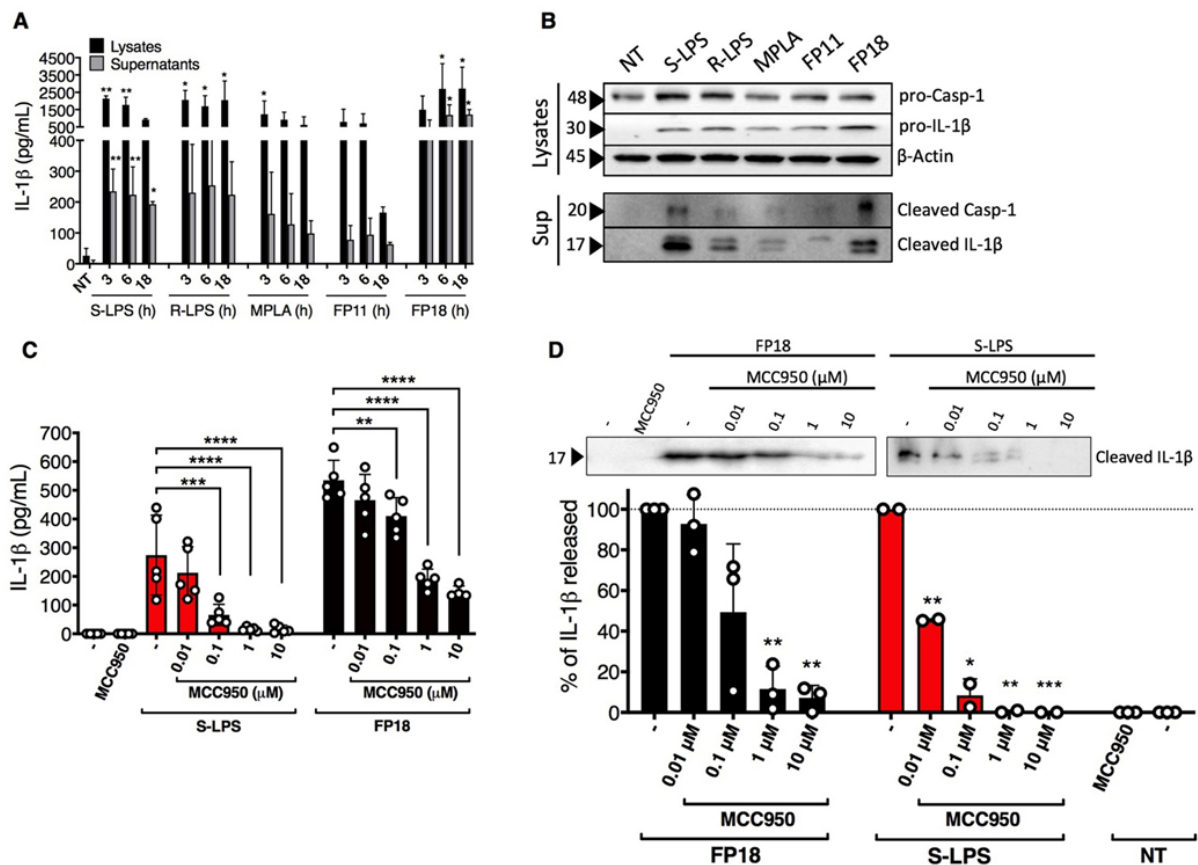


Figure 42 A) TDM were treated with S-LPS (100 ng/mL), R-LPS (100 ng/mL), MPLA (1 μ g/mL), FP11 (20 μ M), FP18 (20 μ M), or left untreated. IL-1 β levels were measured in both cell lysates and supernatants by ELISA. Error bars represent SD of the mean; n = 3 where *p < 0.05, **p < 0.01, and ***p < 0.001. Statistical analysis is between treated vs untreated (NT) (one-way ANOVA test). **B)** TDM were treated as in panel A for 6 h. Levels of pro-casp-1/pro-IL-1 β , and cleaved casp-1/cleaved-IL-1 β were detected by immunoblot in cell lysates and supernatants, respectively. **(C, D)** TDM were pretreated for 1 h with an increasing concentration of MCC950 and then stimulated with S-LPS (100 ng/mL) or FP18 (20 μ M) for 6 h. The effect of MCC950 on LPS- and FP18-triggered IL-1 β secretion was evaluated by ELISA (C) and immunoblot (D). In (C), error bars represent SD of the mean; n = 5 where *p < 0.05, **p < 0.01, and ***p < 0.001 (one-way ANOVA test). In (D), the percentage of IL-1 β release was normalized to stimulation with only S-LPS or only FP18, and error bars represent SD of the mean (*p < 0.05, **p < 0.01, and ***p < 0.001, Wilcoxon's test).

Adjuvant activity of FP11 and FP18 and in vivo toxicity: OVA immunization experiments

The ability of FP11 and FP18 to induce immune responses in vivo was compared to MPLA by evaluating antibody production in C57Bl/6 mice immunized with chicken ovalbumin (OVA) as a model antigen. We first evaluated the toxicity of FPs in a pilot experiment in which mice were injected subcutaneously with 10 µg of the FP11 and FP18. The results showed that the two test adjuvants had no obvious adverse effect on mice, as assessed by the local response at the injection site and by determining the animal weight and state of alertness over 7 days (**Figure 43A**). Next, mice were immunized with the tested adjuvants mixed with ovalbumin (OVA). The induction of antibody was evaluated 21 days post immunization. The results showed that mice immunized with the test adjuvants exhibited marginally higher levels of anti-OVA total IgG after prime immunization compared to OVA-immunized control and significantly lower levels compared to MPLA-OVA immunized animals (**Figure 43B**, prime immunization). In contrast, after a booster immunization given on day 22 and examined for ova-specific antibody titers 14 days later, the IgG levels in the FP18-immunized mice were higher than those in the FP11-immunized group (**Figure 43B**, booster immunization). These data indicate that in agreement with in vitro and in cell results, FP18 is a more effective adjuvant in vivo than FP11 and has a potency comparable or even greater than MPLA.

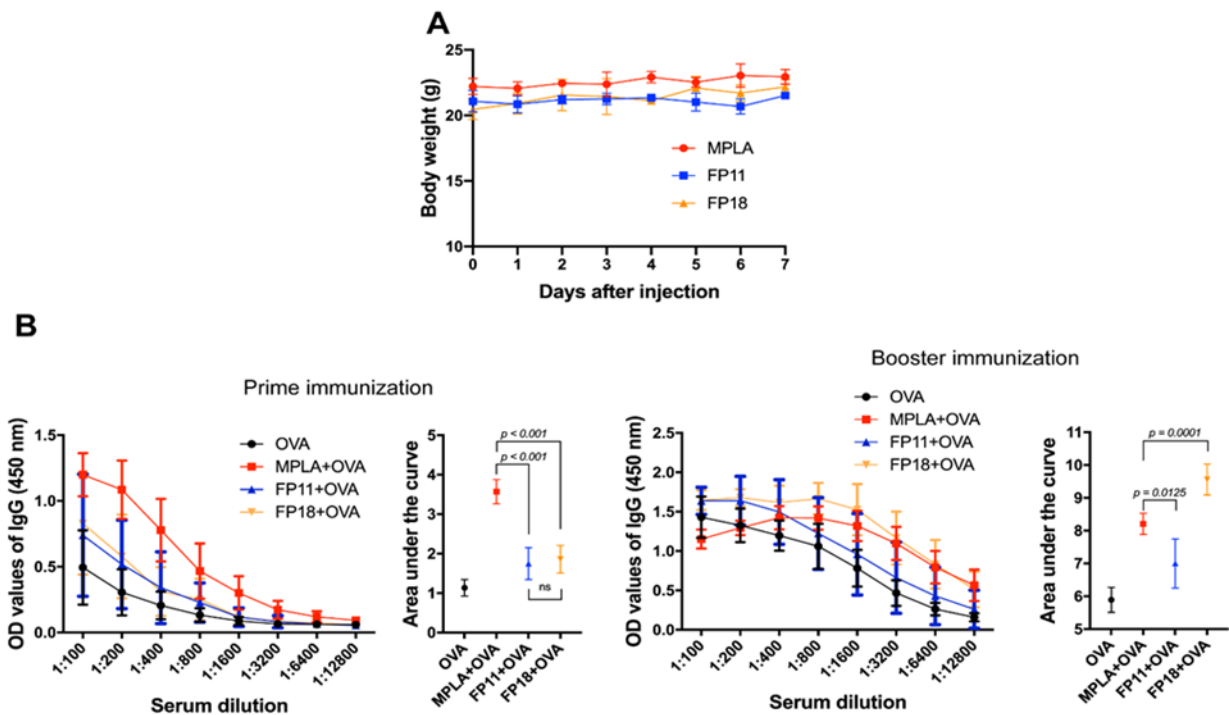


Figure 43 A) Body weight of mice over 7 days after administration of adjuvants (n = 4 per treatment). **B)** Antibody response to OVA immunization using MPLA, FP18, and FP11 as adjuvants after prime (22 days postimmunization) and booster immunization (19 days later) (n = 8 per treatment). For statistical comparisons, the area under each curve was examined by Brown-Forsythe and Welch one-way ANOVA tests with an α of 0.05.

Conclusions

By engaging the TLR4/MD2 endotoxin receptor system, natural adjuvants such as LPS and the LPS derived MPLA modulate adaptive immune responses by influencing early T cell clonal expansion and the cytokine milieu expressed during antigen-dependent proliferation. In addition, inflammasome activation has been associated with the adjuvant efficiency of the first clinically approved combination adjuvants, AS01 and AS04, which contain MPLA, the saponin QS-21, alum^{199,211} and the FDA-approved squalene based oil-in-water emulsion adjuvants MF59 and AS03.^{34,185,212} AS04 and AS01 were used in U.S. vaccine (Cervarix[®]) and in the recombinant Varicella zoster vaccine Shingrix, respectively. Despite showing reassuring overall safety profiles in both vaccines, the lack of chemical homogeneity of MPLA derived from chemical modification of bacterial LPS poses manufacturing and quality control challenges at the industrial level, potentially limiting its use. On the other hand, the chemical synthesis of MPLA, consisting of 24 steps, is expensive and its upscale is challenging. Druggable, chemically simplified MPLA substitutes, such as monosaccharide-based TLR4 agonists could be more attractive compounds to develop adjuvants that can be sustainably produced on a global scale. Therefore, we have worked in the development of new glucosamine derivatives with a phosphate at the β -anomeric position and three lipid chains linked at positions C2, C3 and C4 (termed FP compounds) as TLR4/MD-2 ligands. FP compounds are similar to synthetic agonist SDZ MRL 953, except for the absence of C3 hydroxyl groups on the three fatty acid chains. However, the retention of biological activity after deletion of C-3 is not obvious, and it generally causes reduced activity, as observed with other lipid A derivatives.²¹³ The presence of non-hydroxylated fatty acid chains greatly simplifies FP chemical synthesis, compared to MPLA or other monosaccharide lipid A mimetics, making these compounds scalable at an industrial level. Compounds FP11 and FP18 differ only in the length of fatty acid chains (14 and 12 carbons, respectively). We show here that both compounds have favorable predicted binding energies when docked to the activated TLR4/MD-2 system. Compound FP111, with a second phosphate on sugar's C6, showed unfavorable predicted binding energy. This behavior can be explained by the presence of two phosphates in 1,6-positions that do not allow an LPS-like binding mode at the MD-2 rim, unlike the mono (1- or 6-) phosphate pattern. FP111 binding poses are predicted to be anchored through one phosphate group to MD-2 and the second phosphate to TLR4 chain instead of being completely inserted into the MD-2, accounting for the observed lack of activity. Experiments to assess the capacity of the three molecules to trigger TLR4 activation in HEK-Blue cells confirmed that FP11 and FP18 behave as selective TLR4 agonists, and are not active on TLR2, while the FP111 control molecule was inactive.

FP11 and FP18 bound TLR4 at sub-micromolar affinities and are both capable to stimulate the MyD88-dependent pathway in human THP-1 cells, ultimately leading to the release of TNF α , IL-1 β and IL-6 cytokines, albeit to different extents. FP18 showed a higher potency than FP11 and MPLA in inducing IL-1 β release, due to a greater capacity of activating NLRP3 inflammasome. This activity resembled that of S-LPS, a known potent inflammasome inducer. However, unlike S-LPS, the NLRP3-specific inhibitor MCC950 only partially reversed the efficacy of FP18, as shown by the amount of IL-1 β still released even at the higher concentration of the inhibitor, suggesting this compound causes. In addition, results obtained showed that FP18 stimulatory activity is not limited to the activation of the MyD88-dependent pathway, but also involves activation of the TRIF-dependent pathway leading to a type I IFN signature.¹⁹⁷ The stronger overall activity of FP18 over FP11 is consistent with the higher polarity and solubility in aqueous media of FP18 (calculated log P= 8.3 and 10.2 for FP11 and FP18, respectively, see Table S2), explaining higher efficacy when using this molecule in an aqueous environment. The FP18 and FP11 differences in inflammasome activation were also mirrored in their relative activities as immunization adjuvants. Although both molecules had adjuvant effects *in vivo*, FP18 was significantly more potent than FP11 and also displayed greater potency than MPLA upon boost immunization. In conclusion, we have demonstrated that synthetic FP11 and FP18 show *in vivo* immunostimulatory activity with a potency similar to MPLA and established the molecular mechanisms explaining their action based on the selective TLR4 stimulation with activation of MyD88- and TRIF-dependent pathways and inflammasome. These observations, together with the lack of obvious *in vivo* and *in vitro* (Fig. S18, Supp. Info.) toxicity, and the straightforward synthesis procedure compared to MPLA, support preclinical and clinical development of FP molecules as novel lead compounds for production of effective vaccine adjuvants.

Experimental section

General. All reagents and solvents were purchased from commercial source and used without further purifications, unless stated otherwise. Reactions were carried out under a nitrogen atmosphere unless otherwise noted and were monitored by thin-layer chromatography (TLC) performed over Silica Gel 60 F254 plates (Merck®) and revealed using UV light or staining reagents (H₂SO₄ 5% in EtOH), ninhydrin (5% in EtOH), basic solution of KMnO₄ (0.75% in H₂O), molybdate solution (molybdate phosphorus acid and Ce(IV) sulfate in 4% H₂SO₄). Flash chromatography purifications were performed on silica gel 60 (40-63 μ m) from commercial sources. ¹H and ¹³C NMR

spectra of compounds were recorded with Bruker Advance 400 with TopSpin® software, or with NMR Varian 400 with Vnmrj software. Chemical shifts are reported in parts per million (ppm) relative to the residual solvent; coupling constants are expressed in Hz. The multiplicity in the ¹³C spectra was deduced by APT pulse sequence; peaks were assigned with the help of 2D-COSY and 2D-HSQC experiments. Exact masses were recorded with Orbitrap Fusion™ Tribrid™. Purity of final compounds was about 95% as assessed by quantitative NMR analysis. Reaction conditions and compound characterization are described in the Supporting Information.

Surface plasmon resonance analysis. Real-time binding interaction experiments were performed with a Biacore X100 (GE Healthcare). Recombinant human TLR4/MD2 complex was covalently immobilized onto the surface of sensor chip NTA (cat # BR100034, GE Healthcare) via amine coupling. TLR4/MD2 complex was diluted to a concentration of 20 µg/ml, in 10 mM sodium acetate at pH 4.0, and was injected on NTA chip at a flow rate of 10 µl/min, upon washing with 0.35 M EDTA, injection of NiCl₂ for 60 s, a second wash with 3 mM EDTA and activation of the carboxyl groups on the sensor surface with 7-min injection of a mixture of 0.2 M EDC and 0.05 M NHS. The remaining esters were blocked with 7-min injection of ethanolamine. Based on the ligand (TLR4/MD2) and analytes (FP11, FP18) molecular weights (MW) of 90 kDa, and 934.39 or 850.04 Da, respectively, the appropriate ligand density (RL) on the chip was calculated according as follows: $RL = (\text{ligand MW}/\text{analyte MW}) \times R_{\text{max}} \times (1/S_m)$, where R_{max} is the maximum binding signal and S_m corresponds to the binding stoichiometry. The target capture level of TLR4/MD2 complex was of 1933.5 response units (RUs). The other flow cell was used as a reference and was immediately blocked after the activation. Increasing concentrations of FP11 or FP18 were flowed over the NTA sensor chip coated with TLR4/MD2 at a flow rate of 30 µl/min at 25°C with an association time of 60 s, and a dissociation phase of 180 s. A single regeneration step with 50 mM NaOH and an extra wash with PBS-P+ with 50% DMSO were performed following each analytic cycle. All the analytes tested were sonicated for 15 minutes and then diluted in the PBS-P+ buffer (GE Healthcare) with 5% DMSO. The K_D was evaluated using the Biacore evaluation software (GE Healthcare) after solvent correction and the reliability of the kinetic constants calculated by assuming a 1:1 binding model supported by the quality assessment indicators values.

Cell cultures. HEK-Blue cells and RAW-Blue Cells (InvivoGen) were cultured according to supplier's instructions. Briefly, cells were cultured in DMEM high glucose medium supplemented with 10% heat inactivated fetal bovine serum (FBS), 2 mM glutamine, penicillin (100 U/mL), streptomycin (100 U/mL), and supplemented with the antibiotics indicated in the Table S1. Cells were detached using

a cell scraper, counted, and seeded in a 96-well multiwell plate at the density indicated in the Table S1. After overnight incubation (37 °C, 5% CO₂, 95% humidity), supernatants were removed, and cell monolayers washed with warm PBS. Cells were resuspended in fresh medium supplemented with the molecule to be tested and incubated for 18 hours. THP-1 cells were cultured in RPMI supplemented with 10% heat inactivated FBS, 2 mM glutamine, penicillin (100 U/mL), streptomycin (100 U/mL). Cells were split three times weekly and maintained at a density of 0.5×10^6 cells/mL. For experimental procedures, THP-1 were seeded in multiwell plates at a density of 0.5×10^6 cells/mL, 200 μ L/well (96 wells), 1.5 mL/well (12 wells), and 3 mL/well (6 wells), and differentiated into macrophages with phorbol 12-myristate 13-acetate (PMA, Invivogen) at a final concentration of 25 ng/mL. After 72 hours of differentiation, the culture medium was replaced with fresh medium and cells were rested for another 24 hours before exposure to the molecule to be tested.

Cell Stimulation and treatments. All LPS variants were purchased from Innaxon. Unless otherwise indicated, cells were stimulated with 100 ng/mL ultrapure Smooth-LPS from *S. minnesota* (S-LPS) for 18 hours. Rough-LPS R595 (Re) from *S. minnesota* (R-LPS) was used at 100 ng/mL, while MPLA R595 (Re) from *S. minnesota* (MPLA) was used at 1 μ g/mL. For TLR2 activation PAM2CSK4 (Invivogen) was added at 10 ng/mL for 18 hours. hIL-1 β (Merk) was used as control for NF- κ B activation and added at a final concentration of 100 ng/mL. FP11, FP111 and FP18 compounds were resuspended in ultrapure DMSO and diluted in culture medium. Anti-human IFNAR2 neutralizing antibody (clone MMHAR-20) was purchased from PBL Assay Science, USA and used at 1 μ g/mL. NLRP3 inhibitor MCC950 was purchased from Merck and added to cells at the following concentrations, 0.01, 0.1, 1 and 10 μ M.

HEK-Blue cells reporter assay. After the addition of the molecule to be tested, cells were incubated for 18 hours. Supernatants were collected and SEAP levels were quantified by using QUANTI-Blue assay according to the manufacturer's instruction. Briefly, 20 μ L of the supernatants of SEAP-expressing cells were incubated with 200 μ L of QUANTI-Blue substrate in a 96-well plate for 0.5–4 hours at room temperature. SEAP activity, as indicator of TLR4 activation, was assessed reading the well's optical density (OD) at 630 nm. The results were normalized with positive control (Smooth-LPS for HEK-Blue hTLR4 cells, PAM2CSK4 for HEK-Blue hTLR2 cells and IL-1 β for HEK-Blue Null cells) and expressed as the mean of percentage \pm SEM of at least three independent experiments.

RNA extraction, cDNA synthesis and Real-Time polymerase chain reaction. Total RNA was extracted using Quick-RNA MiniPrep (ZYMO RESEARCH, USA) according to the manufacturer's instruction. Reverse transcription was performed with 1 μ g of total RNA using LunaScript RT SuperMix Kit (New England

BioLabs, Massachusetts, USA) and cDNA was amplified using the Luna Universal qPCR Master Mix (New England BioLabs, Massachusetts, USA) and the following conditions: denaturation for 1 minute at 95°C; annealing for 30 seconds at 62°C for human IFN β , 58°C for human IL-1 β , 60°C for human RSAD2, and 60°C for human β -actin; 30 seconds of extension at 72°C. Primer sequences were as follows: human IFN β forward 5'-CAACTTGCTTGGATTCCTACAAAG-3' reverse 5'-GTATTCAAGCCTCCCATTCAATTG-3'; human IL-1 β forward 5'-AGAATGACCTGAGCACCTTC-3', reverse 5'-GCACATAAGCCTCGTTATCC-3'; human RSAD2 forward 5'-AGAATACCTGGGCAAGTTGG-3', reverse 5'-GTCACAGGAGATAGCGAGAATG-3'; β -actin (forward 5'-AAGATGACCCAGATCATGTTTGAGACC-3', reverse 5'-AGCCAGTCCAGACGCAGGAT-3') was used as a housekeeping gene. Gene expression was calculated using the $\Delta\Delta C_t$ function and expressed as fold change compared to not treated cells

Enzyme-Linked Immunosorbent Assay (ELISA). TNF- α , IL-1 β , IL-6, IFN β levels were measured in TDP supernatants and cell lysates after the indicated timing by using the following sensitive enzyme-linked immunosorbent assays (ELISA) (R&D Systems; #DY210-05, #DY201-05, #DY200-05, #DY206-05, #DY208-05, #DY814-05 Minneapolis, USA). The optical density of each well was determined using a microplate reader set to 450 nm (wavelength correction 570 nm).

Western blot analysis. Immunoblotting of caspase-1 and mature IL-1 β from precipitated supernatant was performed as described.²¹⁴ For cell extracts, cells were washed twice in ice-cold PBS and lysed in RIPA buffer (CST, #9806) supplemented with protease (Roche, Mannheim, Germany) and phosphatase Inhibitors (CST ##5870). After centrifugation at 13000 RCF for 30 min at 4 °C, the supernatants were collected as whole cell lysates. Methanol/chloroform precipitated cell supernatants and cell lysates were resuspended in the Laemmli buffer, denatured for 5 minutes at 100°C and separated on 10% or 13% polyacrylamide gels. Proteins were transferred on PVDF filters (Bio-Rad, USA), blocked in 5% w/v BSA TTBS and incubated with the primary and corresponding secondary antibodies indicated below. Proteins were revealed by chemiluminescence (LiteAbiot EXTEND, Euroclone) and detected by using Odyssey[®] Fc LI-COR Imaging System. The PVDF membrane filters were incubated with the following primary antibodies: anti-phospho NF- κ B (Ser536) (93H1) Rabbit mAb (CST #3033; diluted 1:1000); anti-phospho-p38 MAPK (Thr180/Tyr182) (D3F9) XP[®] Rabbit mAb (CST #4511; diluted 1:1000); anti-phospho-IRF-3 (Ser386) (E7J8G) XP[®] Rabbit mAb (CST #37829 diluted 1:1000); anti-phospho-STAT1 (Tyr701) (58D6) Rabbit mAb (CST #9167 diluted 1:1000); anti-IL-1 β (3A6) Mouse mAb (CST #12242 diluted 1:1000); anti-Cleaved-IL-1 β (Asp116) (D3A3Z) Rabbit mAb (CST #83186 diluted 1:1000); Caspase-1 (D7F10) Rabbit mAb (CST #3866 diluted 1:1000); anti- β -Actin (13E5) Rabbit mAb (CST #4970 diluted 1:1000). Secondary

antibodies used: anti-rabbit or anti-mouse IgG, HRP-linked secondary antibody (Cell Signaling #7074 and #7076, diluted 1:3000). Densitometric analysis was carried out using Image J.

Mice immunization experiments. The in vivo protocols were reviewed by the Queen's University Animal Welfare and Ethical Review Body (AWERB) and the work was carried out under an approved UK Home Office Project License (PPL2807). Chicken ovalbumin (OVA, Sigma-Aldrich) was resuspended in pyrogen-free DPBS (SIGMA-Life Science) at 5mg/ml. Endotoxins were removed by Pierce™ High-Capacity Endotoxin Removal Spin Columns (Thermo Scientific). The endotoxin level of purified OVA was determined by the Limulus Amebocyte Lysate (LAL) Gel-clot method (Associates of Cape Cod; East Falmouth, MA, USA) in the form of single test vials. The samples were assessed at a sensitivity of 0.125 endotoxin unit (EU)/mL. OVA concentration was determined by BioRad Protein Assay Dye Reagent (Bio Rad) and bovine serum albumin (BSA, SIGMA-Aldrich) as reference standard. Six-week-old female C57BL/6 mice were purchased from Envigo, UK. For the pilot toxicity experiment, mice (n=3 per treatment) were injected subcutaneously on the flank with 10 µg adjuvants (FP11, FP18 or MPLA) suspended in 50 µl PBS. The mice were monitored and weighed daily for 7 days. For immunization, C57BL/6 mice (n=8 per treatment) were immunized by subcutaneous injection on the flank with 50 µl of 500 µg OVA mixed with 10 µg of FP11, FP18 or MPLA resuspended in PBS. A control group of OVA without adjuvant was also included. Mice were given a booster immunization on the alternative flank 22 days after prime immunization. Serum, obtained from blood samples drawn from the tail vein, was examined for anti-OVA antibodies at day 21 and 41. The antibody levels in sera were measured by ELISA. Wells of polystyrene microplates Nunc Maxisorp (Thermo Scientific) were coated with 50 µl of OVA at 4 µg/ml diluted in 50 mM carbonate/bicarbonate buffer, pH 9.6, at 4 °C overnight. Coating solution was removed, and plates were washed with 300 µl PBS/Tween 20 (0.05%). Additional blocking was achieved by adding 200 µl of blocking buffer (BSA 5%). Plates were covered and incubated at room temperature for 1 h and then washed 3 times with PBS/Tween20. Fifty microliters of serum diluted in half-strength blocking buffer (from 1:100 to 1:12800) was added to the wells and incubated for 90 min at room temperature. After incubation, plates were washed 4 times with PBS/Tween20. Affinity purified horseradish peroxidase-conjugated goat anti-mouse IgG (catalogue number 170-6516, Bio-Rad, UK) diluted to 1:5000 was added to wells for 1 h at RT. After washing 4 times with PBS/Tween20, 50 µl of the substrate solution 3,3',5,5'-tetramethylbenzidine were added per well and incubated in the dark at room temperature for 10 mins. After sufficient color development, 30 µl of stop solution (2N

H₂SO₄) were added and the absorbance of each well was read with POLARstar Omega microplate reader (BMG LABTECH, Ortenberg, Germany) at 450nm.

All animal experiments performed in the manuscript were conducted in compliance with institutional guidelines.

Statistical information

All experimental results represent the means \pm standard deviation (SD) of at least three independent experiments unless specified. In real-time PCR and western blot experiments, gene expression and protein amount were evaluated in relation to the housekeeping gene β -actin. Gene expression is represented as fold change compared to untreated cells and results evaluated by using one-sample Wilcoxon test. Western blot shown were representative data from at least two independent experiments. For ELISA experiments means were compared by t tests (two groups) or one-way ANOVA (three or more groups). Tukey multiple comparisons testing following one-way ANOVA was performed to obtain adjusted P values. For statistical comparisons of immunization results, the area under the ELISA titration curves were examined by Brown-Forsythe and Welch One way ANOVA tests with an alpha of 0.05. This study includes no data deposited in external repositories.

Chapter II: "NEW SYNTHETIC AGONISTS OF TLR4 RECEPTOR"

Adapted from Italian patent application n. 102021000019544 of 22.07.2021 titled ""New synthetic agonists of TLR4 receptor"" and related PCT application n. PCT/IB2022/056615 of 19.07.2022

DESCRIPTION

The present invention relates to new synthetic molecules with agonist activity of human Toll-like Receptor 4 (TLR4), compositions comprising them and uses thereof, in particular for the treatment of diseases in which it is useful to induce or increase an immune response.

PRIOR ART

Innate immunity is the first line of defense of higher organisms against pathogens and cell damage. It is based on the recognition of specific molecular structures associated with pathogens or cell damage (respectively PAMPs and DAMPs) by specific protein receptors. Such receptors are known as pattern recognition receptors (PRRs) and may be of various typologies, depending on their localization in-cell, in cytosol or on the membrane, and on their function.

Among the most studied receptors are those of the Toll-Like Receptor (TLR) family, whose main role is to recognize different PAMPs, alerting the body to the presence of pathogens through inflammation, recruiting other immune cells to fight infection and thus initiating the process of developing adaptive immunity, which is the most appropriate and specific defense for such menaces.

In fact, innate immunity response to pathogens can be decisive in determining both the nature and the intensity of adaptive immunity response.

For this reason, the development of TLR activators (agonists) has pharmaceutical relevance where an inflammatory stimulus is beneficial from a therapeutic point of view: examples are drugs for cancer immunotherapy and vaccine adjuvants. In the first case, pro-inflammatory activity can lead to the reactivation of the immune system in the tumor environment, which can therefore destroy the tumor.¹¹⁶

In the second case, a pro-inflammatory activity is advantageous because modern vaccines no longer use whole inactivated pathogens, but subunits thereof, which are unable to stimulate a correct inflammatory response without adjuvancy. To date, there are various small molecules able to bind and activate TLR receptors, and some of those are used as adjuvants such as: imidazoquinoline TLR7/8 agonists, like imiquimod and resiquimod, as well as Pam2CS-type TLR2/TLR6 agonist and TLR4 agonists such as Monophosphoryl lipid A (MPL) and aminoalkyl glucosaminide-4-phosphates (AGPs, also referred to as Corixa compounds, CRX).

Among TLRs, TLR4 is of high pharmacological interest: its activation is the most efficient way to stimulate innate and adaptive immunity. Indeed, TLR4 exhibits two different and distinct cellular mechanisms of functioning that lead to the release of a larger and more heterogeneous set of proinflammatory cytokines, causing a more complete immune response.

The natural agonist of TLR4 is lipopolysaccharide (LPS), the main component of the outer membrane of Gram-negative bacteria. It can be divided into three parts: a long polysaccharide chain, called O-Antigen, a shorter oligosaccharide called Core and finally Lipid A (lpd A), the immunogenic portion of the molecule, formed by two glucosamines to which are commonly linked to two phosphates and a variable number of acyl chains.

Lipid A agonistic activity is based on its binding affinity (ability to bind) to the TLR4 co-receptor, Myeloid Differentiation factor 2, MD-2, with the entailed formation of the (TLR4/MD-2/LPS)₂ complex on the surface of innate immunity cells, i.e., macrophages and dendritic cells.

The activation process of the TLR4 receptor by LPS begins with the interaction of individual LPS molecules or aggregates in solution with Lipid Binding Protein (LBP), forming a complex with a LPS molecule. Thereafter, the LPS molecule is transferred from LBP to co-receptor CD14, which in turn transfers it from MD-2.

However, lpd A is toxic even in quantities of the order of picograms, and consequently it cannot be used pharmacologically.⁷⁸

Synthetic and natural molecules with a structure similar to lipid A, but with attenuated endotoxicity, are interesting candidates as vaccine adjuvants in the perspective of maintaining immunostimulatory activity while eliminating the toxic effects.

Monophosphoryl lipid A (MPL) is a molecule identical to lipid A, except for the absence of the C₁ phosphate group. Despite being so similar, the inflammatory activity is only 0.1% of that of the natural molecule, and its pharmacological profile is so good that it has been approved by the FDA for use as a vaccine adjuvant. The molecule is presently used in Cervarix[®] and Fendrix[®] vaccines.

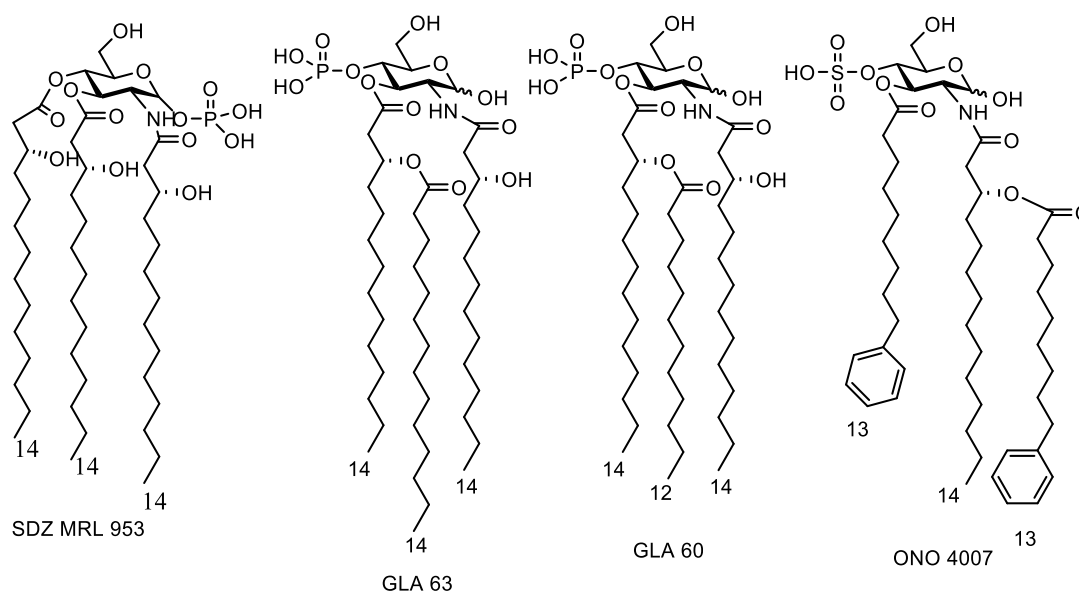
However, the MPL adjuvant used nowadays is chemically heterogeneous, as produced directly from natural LPS.

In addition, the synthesis of these disaccharide compounds is very long and complex, resulting in a final price of about 200 EUR/mg. For this reason, it is interesting to develop further lipid A analogs with a monosaccharide structure, sharing the same advantageous features of the known analogs or even being improved, preferably obtainable through a simpler synthetic route.

An example of monosaccharide lipid A analogs known in the art is represented by the synthetic compounds named AGPs (also known as CRX adjuvants, Corixa) comprising a monosaccharide unit linked by glycosidation to a unit of an aminoalkyl aglycone N-acylate.

AGPs are potent agonists of TLR4 and are chemically homogeneous being produced by chemical synthesis.

Further, simpler, analogs of Lipid A that are still effective in the activation of TLR4 comprise monophosphorylated monosaccharide derivatives mimicking the reducing portion or the non-reducing portion of Lipid A (scheme below).



Another example of compounds known in the art is represented by compounds GLA 63 and GLA 60 (scheme above) comprising a glucopyranoside skeleton, phosphorylated in position C₄, a 14 carbon linear chain in C₂ and a branched chain in C₃ (14 + 14 in GLA 63 or 14 + 12 Carbons in GLA 60).¹²⁴ These monosaccharides that partially mimic lipid A and mimic the monosaccharide lipid X, which is a biosynthetic precursor of lipid A, are active in stimulating TLR4-dependent production of cytokines TNF- α and IL-6, in both murine and human cells.

Also compound SDZ MRL 953, known in the art, showed a potent activity in stimulating the release of inflammatory cytokines such as interleukin-6 (IL-6), interleukin-8 (IL-8) and TNF- α factor in murine macrophages and neutrophil granulocytes, concomitantly exhibiting a toxicity reduced of a factor of at least 10^4 in galactosamine-sensitized mice compared to the parent endotoxin (*Salmonella abortus equi*).

In experimental microbial infection models, the compound proved to have a highly protective effect when administered prophylactically either once or thrice in myelo-suppressed or immunocompetent mice.

Doses effective to reach 50% of response with SDZ MRL 953 vary depending on the infective agent and administration route. In all cases, however, EC_{50} obtained are about 10^3 times greater than those obtained with endotoxin *Salmonella abortus equi*.

However, thanks to the low toxicity, the therapeutic indexes of this molecule, expressed, e.g., as LD_{25}/ED_{75} were significantly improved compared to the endotoxin and range from about 5 to >500, depending on the infective agent and the administration route.

The compound also proved efficient in inducing tolerance to endotoxins: repeated dosages of the compound induce a transient resistance (≥ 1 week) to endotoxin-related lethal risks.

All these positive results were also confirmed in a model of advanced sepsis caused by *Escherichia coli*, in which antibiotic therapy had already proved inefficient: pre-treatment with one dose of SDZ MRL 953 one day prior to microbial inoculation dramatically increased the curative effects of antibiotics administered. For this reason, long-term survival was significantly increased with incremental doses of the immunostimulant in combined therapy.

Due to the tolerability demonstrated by SDZ MRL 953 in animals and *in vitro*, this compound was subsequently tested in human models.

On the basis of the known anti-tumor activity of *Salmonella abortus equi* endotoxin linked to its immunostimulating properties, Kiani et al. conducted a randomized double-blind phase I trial with control medium, administering SDZ MRL 953 in tumor-affected patients in order to assess firstly its biological effects and its safety of administration in humans and, secondly, its influence on the reaction to a subsequent endotoxin (LPS) addition.¹⁸⁴

SDZ MRL 953 administration proved safe and of excellent tolerability. The same SDZ MRL 953 increases granulocyte counts and serum levels of G-CSF and interleukin-6 (IL-6), but not of pro-inflammatory cytokines TNF- α , IL-1b, and IL-8.

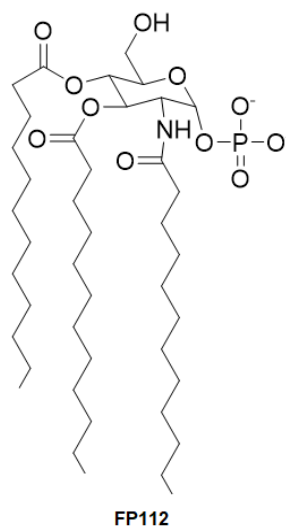
Results and Discussion: Chapter II

Therefore, SDZ MRL 953 has three relevant features, i.e., 1) a high tolerability and low toxicity, 2) the ability to induce G-CSF production, and, as a result, 3) the ability to stimulate an aspecific immune resistance expressed by an increased group of primary defenses in cells.

In spite of these positive results encouraging in the clinical use of SDZ MRL 953, the mechanism of action of this molecule has not yet been studied in molecular detail.

The synthesis of SDZ MRL 953 is complex due to the fact that the glucosamine core binds, in positions C₂, C₃ and C₄, chains of 3(R)-hydroxymyristic acid as pure enantiomer. 3-hydroxymyristic acid is commercially available as racemate, whereas the pure enantiomer 3(R)-hydroxymyristic acid needs to be isolated from the racemate prior to use in the synthesis of SDZ MRL 953.

WO2019/092572 discloses a further class of compounds, with a triacylated Monophosphoryl glucosamine core and one phosphate group on position C₁ in particular FP112.



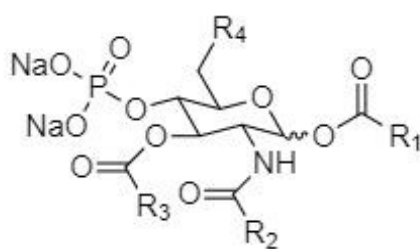
FP112 is a compound similar to the reducing end of lpd A and to SDZ MRL 953, but with three totally saturated and unsubstituted acyl chains. This compound is significantly easier to synthesize than the ones known in the art as the production of optically pure acyl chains is not required for its synthesis. FP112 has an excellent pharmacological profile, as it is able to stimulate the release of numerous proinflammatory cytokines, the most notable of which are IL-1 α , IL-1 β , IL-6, TNF- α and IFN β .

FP112 has been extensively tested in vitro on Hek-Blue, Raw-Blue, THP-1 cells, always demonstrating low toxicity and good pro-inflammatory activity already at a concentration of 10 μ M.

SUMMARY OF THE INVENTION

The authors of the present invention have identified a group of new compounds with a triacylated Monophosphoryl glucosamine core, different from the ones known in the art, which are effective agonists of the TLR4 receptor. Advantageously, said new compounds are more versatile than the ones described in the art as they can be functionalized with various groups of interest. The authors of the present invention have also developed a new method of synthesis of said new compounds as well as of other compounds known in the art, which is simpler, faster and less expensive than the methods disclosed in the art.

The Authors of the present invention herein provide new compounds of formula 1



(Formula 1)

wherein R_1 is a saturated C_5 - C_{15} alkyl chain optionally substituted,

wherein R_2 is a saturated C_5 - C_{15} alkyl chain optionally substituted,

wherein R_3 is a saturated C_5 - C_{15} alkyl chain optionally substituted,

wherein R_4 is any substituent known by the skilled person that can be linked by means of a bond between C_6 and a suitable atom and/or any substituent which possesses an oxygen or a nitrogen atom that can bind to C_6 .

said compounds are apparently similar to the compounds disclosed in WO2019/092572, but have several advantages over the same. A first advantage is represented by the fact that the molecular structure of the compounds of formula 1 makes them more stable: in fact, the phosphate group, which is known to be one of the best leaving groups in organic chemistry, in position C_4 in the compounds of formula 1 has proven to be much more stable than the phosphate group in C_1 , present in the compounds of the prior art discussed above.

As an example, compounds of formula 1 are more stable in the desilylation reaction (reaction 5 of FP20 synthesis and reaction 6 of the FP11 synthesis).

Results and Discussion: Chapter II

During the synthesis of FP112 the lability of C₁ phosphate was a major issue and phosphate degradation was observed also operating under mild conditions, with the formation of two major dephosphorylated byproducts (showed in the experimental section). Moreover, the purification yield is lower in the case of FP112, averaging toward 50%.

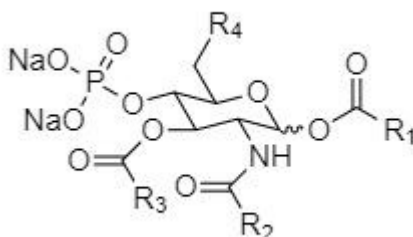
In FP20 the desilylation proceeded with good yields, without the problem of anomeric phosphate cleavage, with 90% yield and negligible byproducts formation.

A second advantage is the simpler method provided for the chemical synthesis of the compounds of the invention that requires only six synthetic steps in order to obtain the final compound; moreover, only three purifications by chromatographic column can be sufficient in the method of the invention thereby avoiding the waste of large quantities of purification solvents. Consequently, this synthesis is cheaper and it is therefore possible to synthesize larger quantities at the laboratory level as well as simplifying the industrial scalability of the process.

Finally, a great advantage of the compound of the present invention, is the possibility of modifying the base molecule with various functional groups in position C₆, thereby allowing the provision of molecules wherein the TLR4 agonist and additional functions may be combined. The different structure of the new compounds of the invention provides a higher stability to the compound and provides position C₆ for functionalization. In FP112 the C₆ functionalization is challenging: most chemical reagents for functionalization cleave the C₁ phosphate, similarly to what happens during the desilylation. In the case of FP20 compound and derivatives the anomeric phosphate is lacking and the C₆ functionalization is feasible. This allows the skilled person to customize the compound for specific desired activities by modifying the functional group in C₆, e.g., by increasing its solubility and/or bioavailability, by adding target-specific substituents, by conjugating the molecule with other functional substituents.

Therefore, objects of the invention are:

1. A compound of formula 1



1

wherein R₁ is a saturated C₅-C₁₅ alkyl chain optionally substituted,

wherein R_2 is a saturated C_5 - C_{15} alkyl chain optionally substituted,

wherein R_3 is a saturated C_5 - C_{15} alkyl chain optionally substituted,

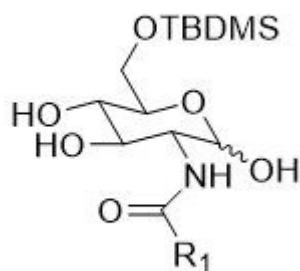
wherein R_4 is any substituent known by the skilled person that can be linked by means of a bond between C_6 and a suitable atom and/or any substituent which possesses an oxygen or a nitrogen atom that can bind to C_6 . and uses thereof;

A vaccine adjuvant consisting of the compound of formula 1;

A vaccine composition comprising the compound of formula 1, at least one pharmaceutically acceptable carrier and at least one pharmaceutically acceptable immunogenic antigen;

A pharmaceutical composition comprising the compound of formula 1 and at least one pharmaceutically acceptable excipient and/or carrier.

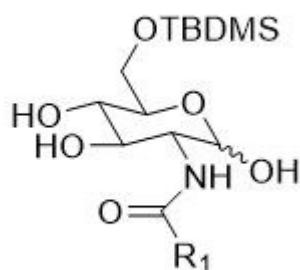
An intermediate of formula 1i



1i

wherein R_1 is a saturated C_5 - C_{15} alkyl chain optionally substituted.

A method for the preparation of an intermediate of formula 1i wherein R_1 is a saturated C_5 - C_{15} alkyl chain optionally substituted



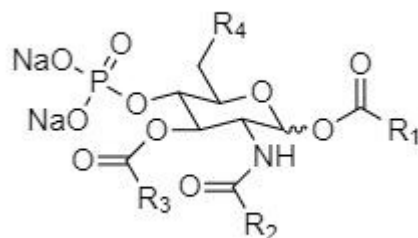
1i

comprising the following steps

1) Selective acylation of the amino group in the C_2 position of glucosamine hydrochloride by reaction with acyl chloride in the presence of sodium bicarbonate.

2) Protection by selective silylation of hydroxyl in position C₆ by reaction with tert-butyldimethylsilyl chloride (TBDMSCl) in the presence of imidazole;

A method for the preparation of a compound of formula 1,



1

wherein R₁ is a saturated C₅-C₁₅ alkyl chain optionally substituted,

wherein R₂ is a saturated C₅-C₁₅ alkyl chain optionally substituted,

wherein R₃ is a saturated C₅-C₁₅ alkyl chain optionally substituted,

wherein R₄ is any substituent known by the skilled person that can be linked by means of a bond between C₆ and a suitable atom and/or any substituent which possesses an oxygen or a nitrogen atom that can bind to C₆., comprising the following steps:

1) Selective acylation of the amino group in the C₂ position of glucosamine hydrochloride by reaction with acyl chloride in the presence of sodium bicarbonate;

2) Protection by selective silylation of hydroxyl in position C₆ by reaction with tert-butyldimethylsilyl chloride (TBDMSCl) in the presence of imidazole, thereby obtaining the intermediate as defined in claim 20;

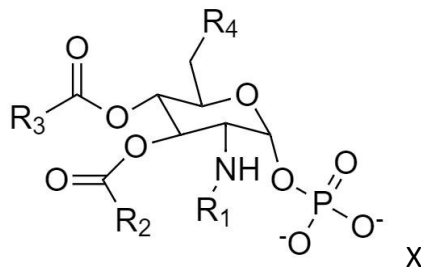
3) Selective acylation of hydroxyls in positions C₁ and C₃ by reaction with acyl chloride in the presence of triethylamine and N, N-dimethyl aminopyridine (DMAP);

4) Phosphorylation of hydroxyl in the C₄ position by reaction with dibenzyl N, N-diisopropylphosphoramidite in the presence of triflate imidazolium, followed by oxidation of phosphite to phosphate *via* metachloroperbenzoic acid;

5) Deprotection of hydroxyl from silane in position C₆ through the presence of sulfuric acid in catalytic quantities; and

6) Deprotection of phosphate from benzyls in position C₄ and optionally in position C₆ through hydrogenation catalysed by Palladium on Carbon (Pd / C).

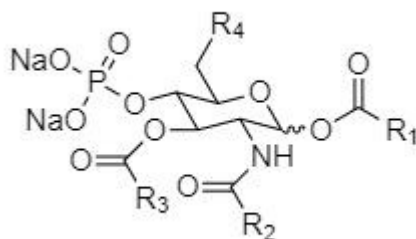
A method for the preparation of a compound of formula X



wherein R₁ is a saturated C₅-C₁₅ alkyl chain optionally substituted,
 wherein R₂ is a saturated C₅-C₁₅ alkyl chain optionally substituted,
 wherein R₃ is a saturated C₅-C₁₅ alkyl chain optionally substituted,
 wherein R₄ is OH and wherein each of R₁, R₂ and R₃ is free from -OH substituents in position C₂.

- 1) Selective acylation of the amino group in the C₂ position of glucosamine hydrochloride by reaction with acyl chloride in the presence of sodium bicarbonate;
- 2) Protection by selective silylation of hydroxyl in position C₆ by reaction with tert-butyldimethylsilyl chloride (TBDMSCl) in the presence of imidazole, thereby obtaining the intermediates defined in claim 20;
- 3) Complete acylation of hydroxyls in positions C₁, C₃ and C₄ by reaction with acyl chloride in the presence of triethylamine and N, N-dimethyl aminopyridine (DMAP);
- 4) Selective deacylation of position C₁ by reaction with ethylenediamine in presence of acetic acid
- 5) Phosphorylation of hydroxyl in the C₁ position by reaction with dibenzyl N, N-diisopropylphosphoramidite in the presence of triflate imidazolium, followed by oxidation of phosphite to phosphate via metachloroperbenzoic acid;
- 6) Deprotection of hydroxyl from silane in position C₆ through the presence of sulfuric acid in catalytic quantities;
- 7) Deprotection of phosphate from benzyls in position C₁ and optionally in position C₆ through hydrogenation catalysed by Palladium on Carbon (Pd / C).

The use of an intermediate compound as defined in claim 22 for the synthesis of compounds of formula 1,

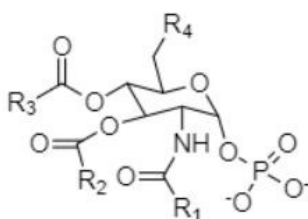


1

wherein R_1 is a saturated C_5 - C_{15} alkyl chain optionally substituted,
 wherein R_2 is a saturated C_5 - C_{15} alkyl chain optionally substituted,
 wherein R_3 is a saturated C_5 - C_{15} alkyl chain optionally substituted,
 wherein R_4 is any substituent known by the skilled person that can be linked by means of a bond between C_6 and a suitable atom and/or any substituent which possesses an oxygen or a nitrogen atom that can bind to C_6 .

And,

The use of an intermediate of formula 1i as defined in any one of the embodiments herein disclosed, for the synthesis of compounds of formula X



X

wherein R_1 is a saturated C_5 - C_{15} alkyl chain optionally substituted,
 wherein R_2 is a saturated C_5 - C_{15} alkyl chain optionally substituted,
 wherein R_3 is a saturated C_5 - C_{15} alkyl chain optionally substituted,
 wherein R_4 is OH and wherein each of R_1 , R_2 and R_3 is free from -OH substituents in position C_2 .

DETAILED DESCRIPTION OF THE FIGURES

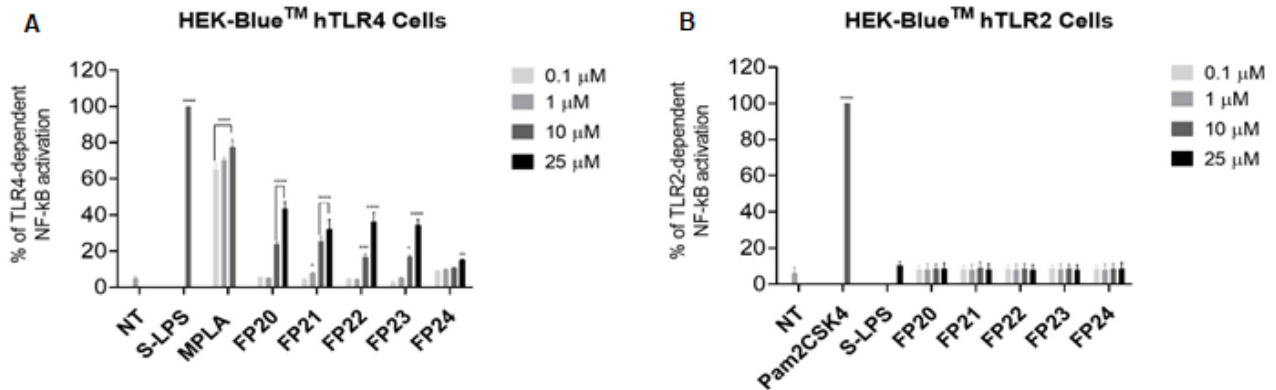


Figure 44 Activity of FP compounds on TLR4 and TLR2. HEK-Blue™ hTLR4 (A) and HEK-Blue™ TLR2 (B) cells were treated with the indicated concentrations of compounds FP20, FP21, FP22, FP23 and FP24, MPLA, LPS (100 ng / mL) and Pam2CSK4 (1 ng / mL) and incubated for 16-18 hours. The results were normalized with respect to stimulation with LPS alone (A) or Pam2CSK4 (B) and were expressed as a percentage of the mean ± SEM of at least three independent experiments. (Treated Vs untreated: * P <0.05; ** P <0.01; *** P <0.001; **** P <0.0001).

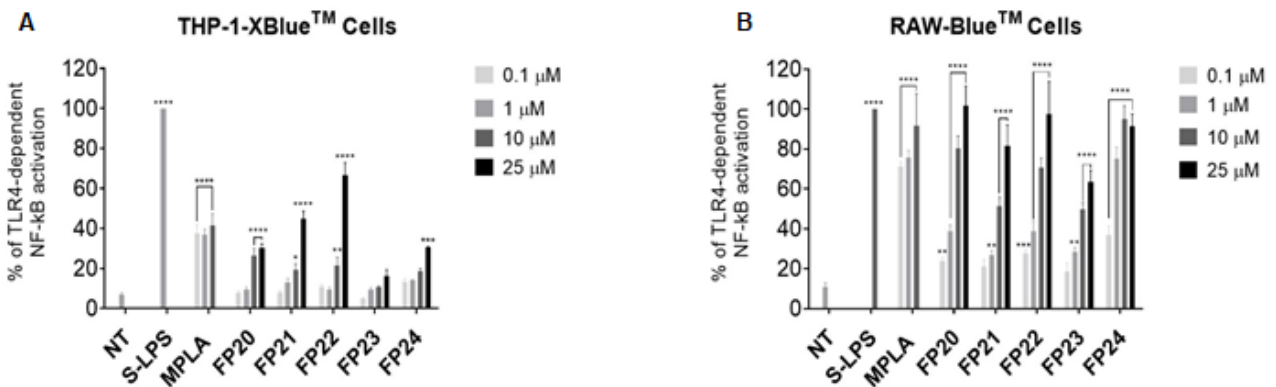


Figure 45 Activity of FP compounds on human and murine macrophages. THP-1-X Blue™ (A) and RAW-Blue™ (B) cells were treated with the indicated concentrations of compounds FP20, FP21, FP22, FP23 and FP24, MPLA and LPS (100 ng / mL) and incubated for 16 -18 hours. The results were normalized with respect to stimulation with LPS alone and were expressed as a percentage of the mean ± SEM of at least three independent experiments. (Treated Vs untreated: * P <0.05; ** P <0.01; *** P <0.001; **** P <0.0001).

THP-1-X-Blue Viability

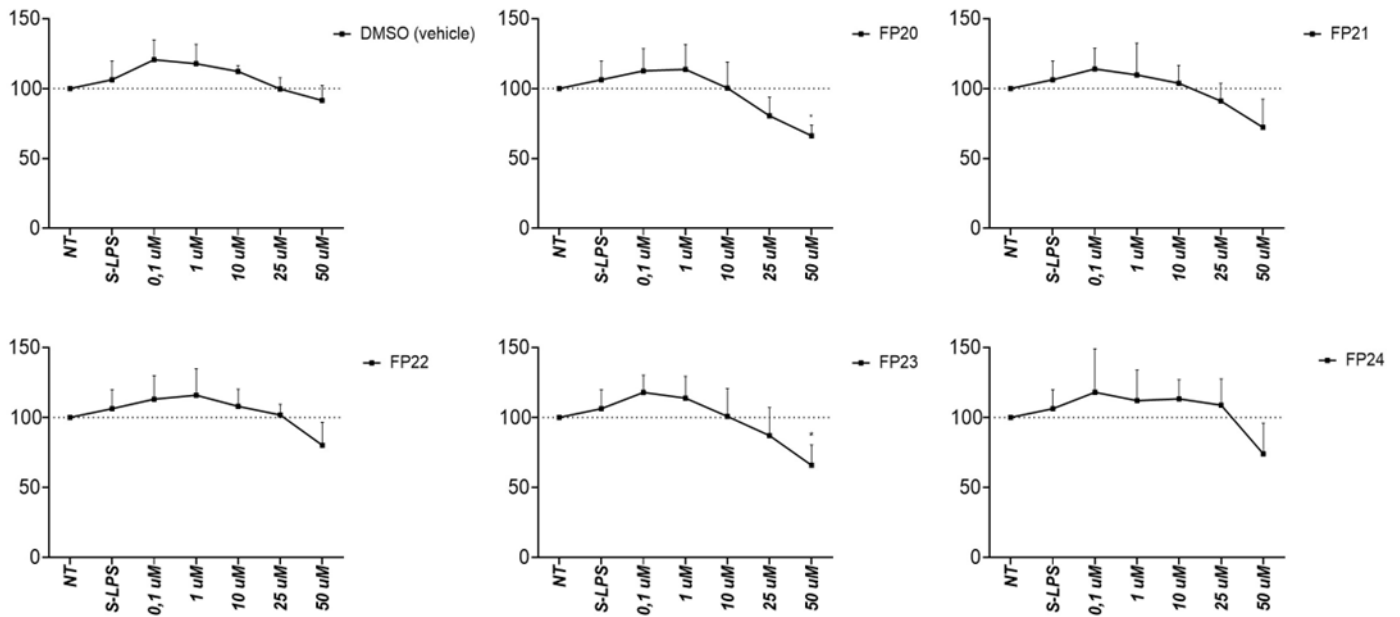


Figure 46 Cell viability. THP-1 cells differentiated into macrophages were treated with increasing concentrations of FP20, FP21, FP22, FP23 and FP24 (0.1-50 μ M) and LPS (100 ng / mL). The vehicle (DMSO) at the same concentrations (0.1-50 μ M) was inserted to evaluate the toxicity of the solvent. Data were normalized to (untreated) control and expressed as a percentage of the mean \pm SEM of at least three independent experiments (Treated Vs untreated: * P <0.05; ** P <0.01; *** P <0.001; **** P <0.0001).

Raw Blue Viability

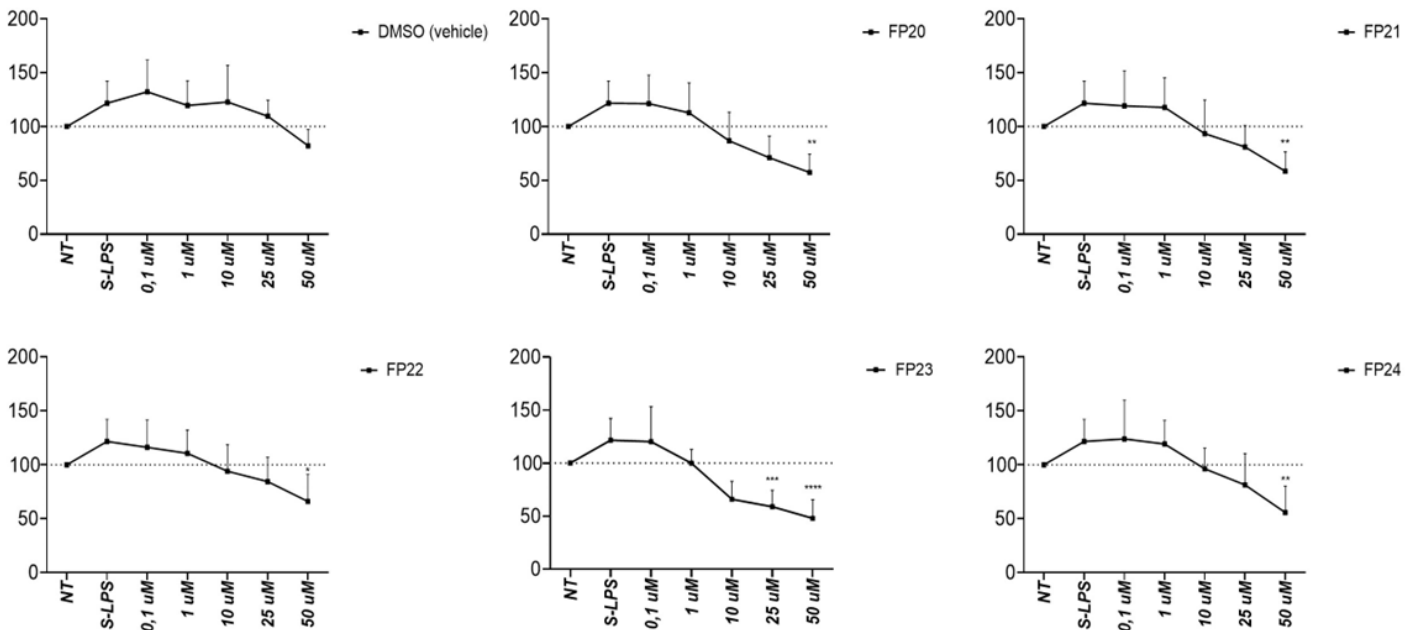


Figure 47 Cell viability. RAW-Blue cells were treated with increasing concentrations of FP20, FP21, FP22, FP23 and FP24 (0.1, 1, 10, 25, 50 μ M) and LPS (100 ng / mL). The vehicle (DMSO) at the same concentrations (0.1, 1, 10, 25, 50 μ M) was inserted to evaluate the toxicity of the solvent. Data were normalized to (untreated) control and expressed as a percentage of the mean \pm SEM of at least three independent experiments. (Treated Vs untreated: * P <0.05; ** P <0.01; *** P <0.001; **** P <0.0001)

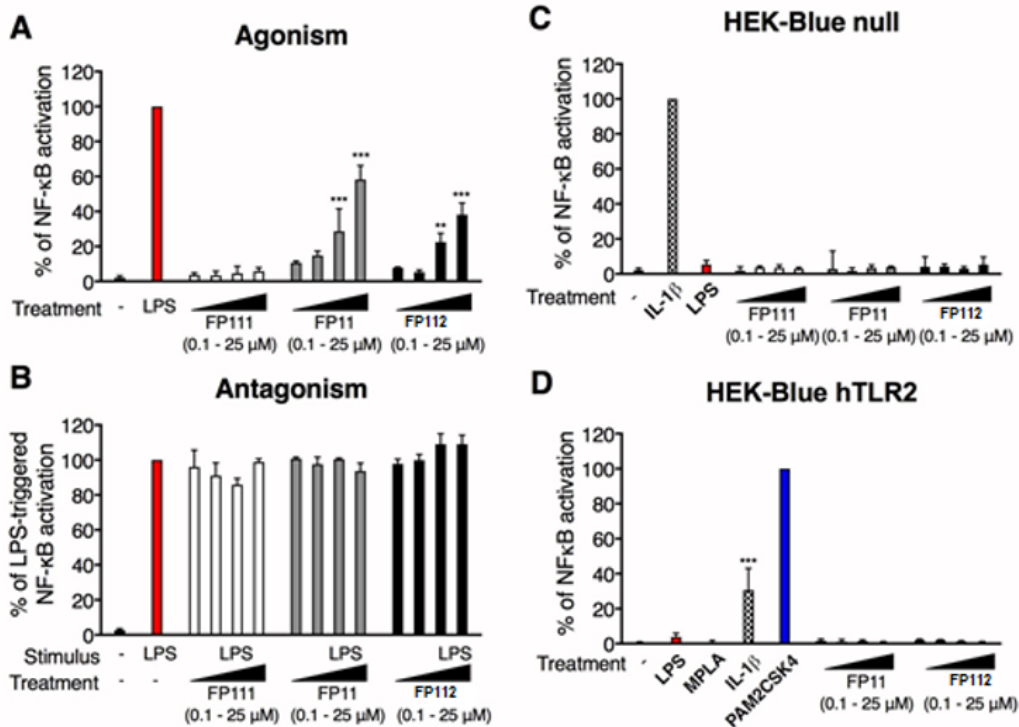


Figure 48 HEK-Blue hTLR4, HEK-Blue Null and HEK-Blue hTLR2 cells were treated as indicated and incubated for 18h. Supernatants were collected and SEAP levels were quantified by QUANTI-blue method. Data were normalized to stimulation with S-LPS (A, B), IL-1β (C) or PAM2CSK4 (D) and expressed as the mean percentage ± SD of three independent experiments. (Treated versus untreated: **p<0.01; ***p<0.001).

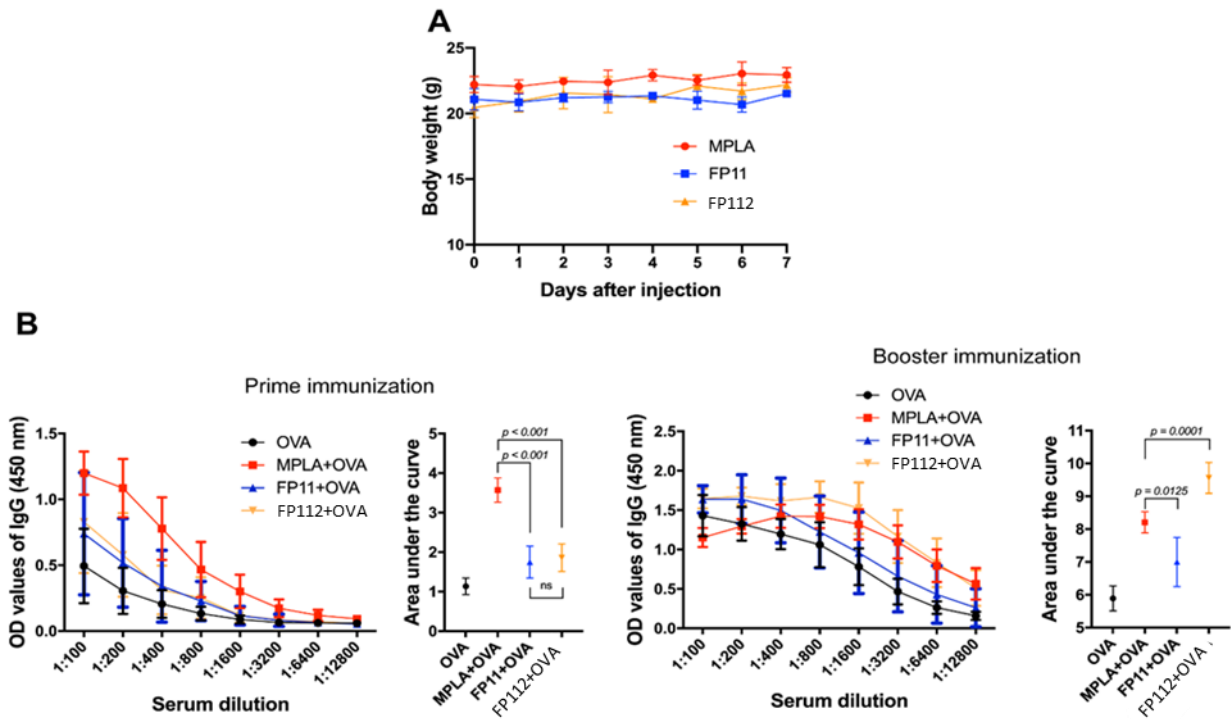


Figure 49 A) Body weight of mice over 7 days after administration of adjuvants (n=4 per treatment). **B)** Antibody response to OVA immunization using MPLA, FP112 and FP11 as adjuvants after prime (22 days post immunization) and booster immunization (19 days later) (n=8 per treatment). For statistical comparisons the area under each curve was examined by Brown-Forsythe and Welch One-way ANOVA tests with an alpha of 0.05.

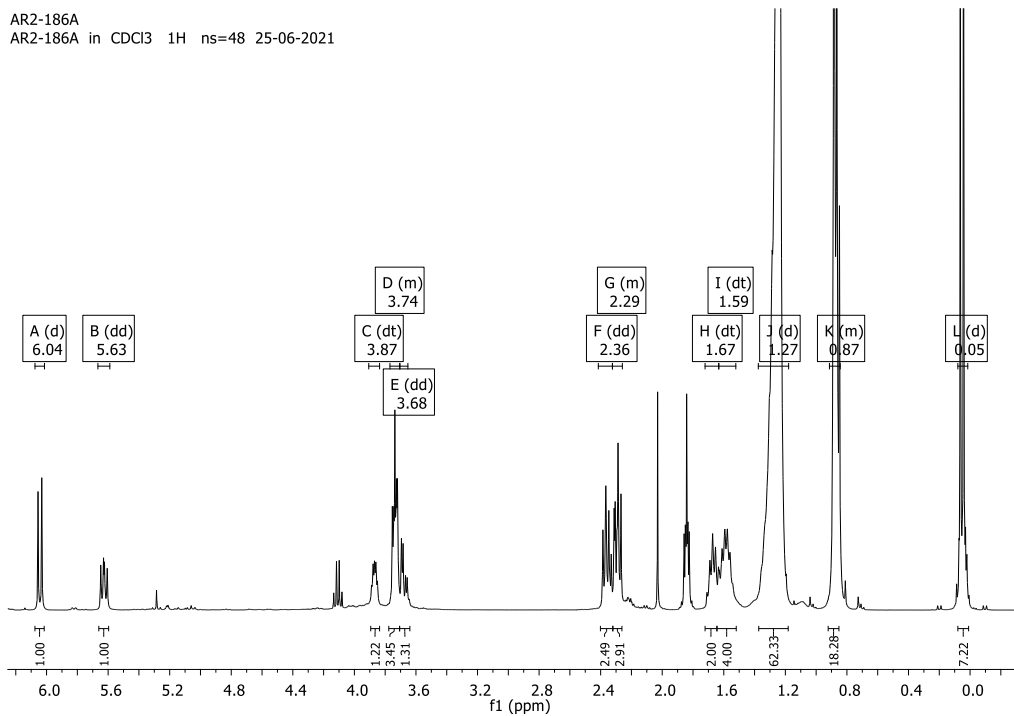


Figure 50 ¹H NMR of compound 25 (Impurity 1 of step 6 in FP11 Synthesis), in which is possible to observe the cleavage of the phosphate in C-1 by the multiplicity (d) of the signal at 6.04 ppm. In the presence of a phosphate in C-1, H-1 would have a dd multiplicity due to the H-P coupling.

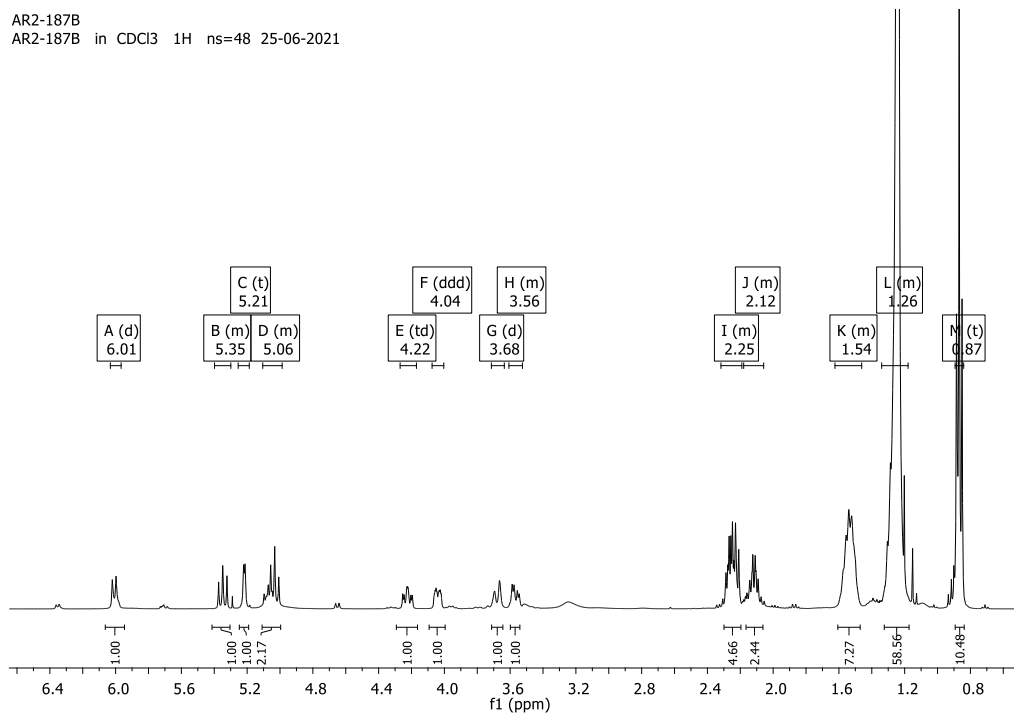


Figure 51 ¹H NMR of compound 26 (Impurity 2 of step 6 in FP11 Synthesis), in which is possible to observe the cleavage of the phosphate in C-1 by the multiplicity (d) of the signal at 6.01 ppm. In the presence of a phosphate in C-1, H-1 would have a dd multiplicity due to the H-P coupling. In this case, also the silane has been cleaved, as observed by the lack of their signals at 0 ppm and 0.85 ppm.

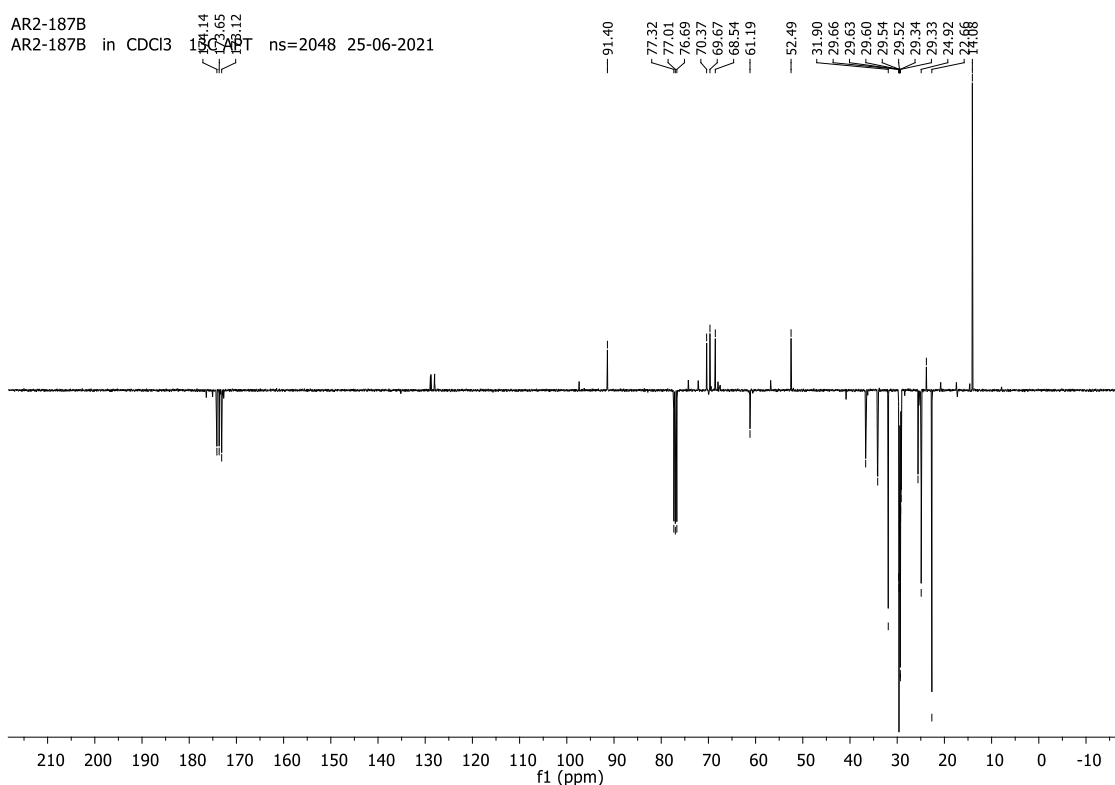


Figure 52 ^{13}C NMR of compound 26 (Impurity 2 of reaction 6 in FP11 Synthesis), which confirms the structure of compound 26 as observed in Figure 51.

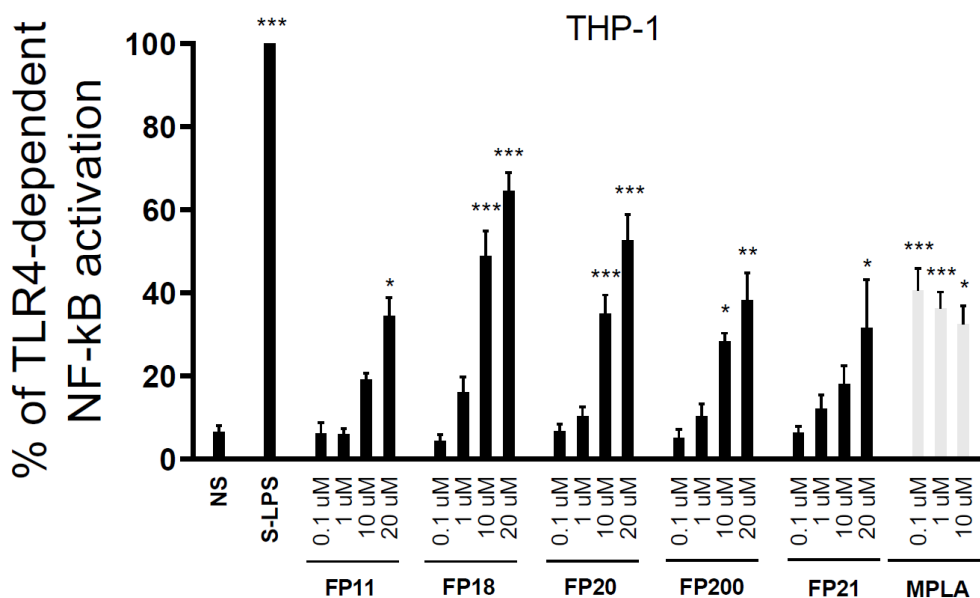


Figure 53 Activity of FP200 diphosphate compounds on human macrophages. Differentiated THP-1-X Blue™ cells were treated with the indicated concentrations of compounds FP11, FP112, FP20, FP200, FP21, MPLA and LPS (100 ng / mL) and incubated for 16 -18 hours. The results were normalized with respect to stimulation with LPS alone and were expressed as a percentage of the mean \pm SEM of at least three independent experiments. (Treated Vs untreated: * P < 0.05; ** P < 0.01; *** P < 0.001; **** P < 0.0001).

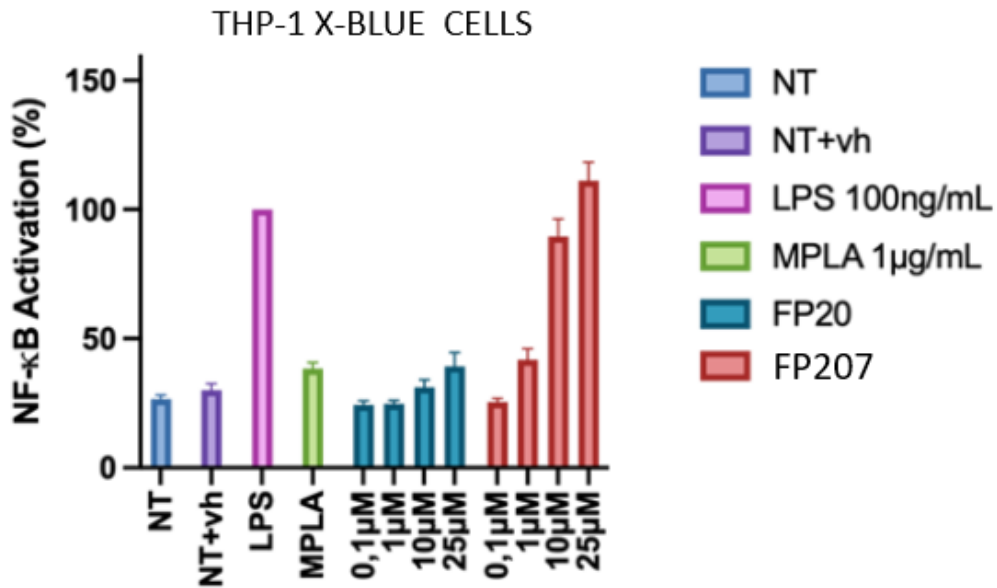


Figure 54 Activity of FP207 on human macrophages Differentiated THP1-XBlue™ were treated with the indicated concentrations of FP20, FP207, MPLA and LPS (100 ng/mL) and incubated for 16-18 hours. The results were normalized with respect to stimulation with LPS alone and were expressed as a percentage of the mean ± SEM of at least three independent experiments. (Treated Vs untreated: * P <0.05; ** P <0.01; *** P <0.001; **** P <0.0001).

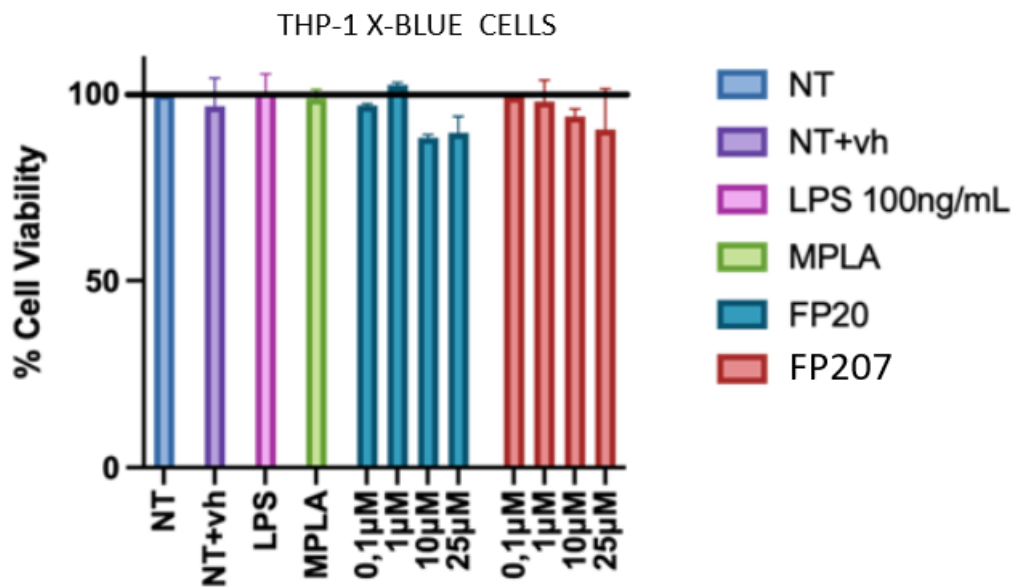
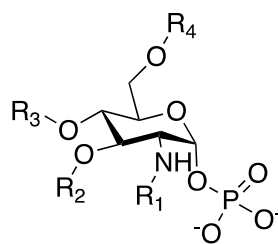


Figure 55 Cell Viability Differentiated THP1-XBlue™ cells were treated with increasing concentrations of FP20 and FP207 (0.1-25 μM), MPLA and LPS (100 ng/mL). Data were normalized to (untreated) control and expressed as a percentage of the mean ± SEM of at least three independent experiments.

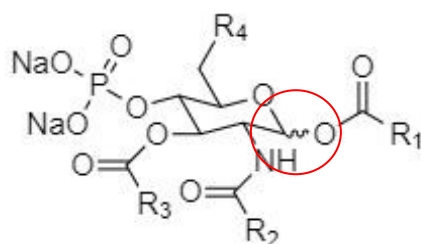
GLOSSARY

In the present description, the term “TLR4 receptor agonist” denotes a compound that selectively binds to the TLR4 receptor inducing a conformational change of said receptor, in turn generating an intracellular stimulation by triggering a response similar to that induced by the natural ligand of said receptor. In the case of TLR4, the substances described as agonists bind to co-receptor MD-2, in turn non-covalently bound to TLR4, thereby generating the receptor complex (TLR4/MD-2/agonist)₂, which from the cell surface initiates a signal cascade leading to activation of nuclear transcription factors and synthesis of pro-inflammatory cytokines (mainly TNF- α and various interleukin types). In the present description, the compound identified as FP112 refers to a compound having the formula represented below



wherein $R_1 = R_2 = R_3 = C=OC_{11}H_{23}$ and $R_4 = H$, disclosed as FP112 in WO2019/092572.

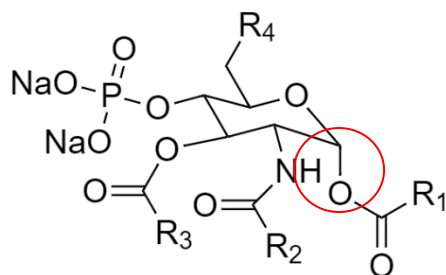
In the present description, the bond in C_1 as represented in Formula 1 below has the meaning commonly intended in organic chemistry



Formula 1

and indicates that the compound can be either in the α or in the β anomer conformation.

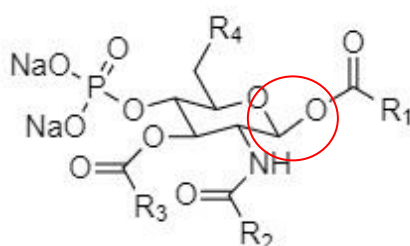
In the present description, the bond in C_1 as represented in Formula 1 α below has the meaning commonly intended in organic chemistry.



Formula 1 α

and indicates that the compound is in the α anomer conformation.

In the present description, the bond in C₁ as represented in Formula 1 α below has the meaning commonly intended in organic chemistry.



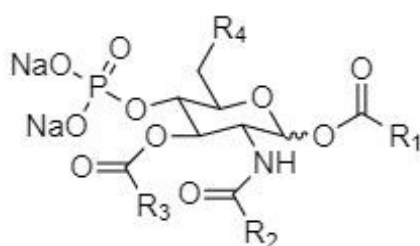
Formula 1 β

and indicates that the compound is in the β anomer conformation.

In the present description, the term “catalytic quantities” means an amount or a concentration of a substance used in a chemical reaction such as to obtain a catalytic effect. In detail, in the description the term “catalytic quantities” can be substituted by “a range from 0.5% to 1% of volume/volume concentration”.

DETAILED DESCRIPTION OF THE INVENTION

The present invention relates to a compound of formula 1



(Formula 1)

wherein R₁ is a saturated C₅-C₁₅ alkyl chain optionally substituted,

wherein R₂ is a saturated C₅-C₁₅ alkyl chain optionally substituted,

wherein R₃ is a saturated C₅-C₁₅ alkyl chain optionally substituted,

wherein R₄ is any substituent known by the skilled person that can be linked by means of a bond between C₆ and a suitable atom and/or any substituent which possesses an oxygen or a nitrogen atom that can bind to C₆.

Therefore, according to the present description, each alkyl chain, R₁, R₂, or R₃, can be a C₅, C₆, C₇, C₈, C₉, C₁₀, C₁₁, C₁₂, C₁₃, C₁₄, C₁₅ alkyl chain.

According to the description each of R₁, R₂, and R₃ can be a different or identical alkyl chain as defined above.

In one embodiment of the invention, at least two of R₁, R₂, and R₃ are identical.

According to the present description one or more of R₁, R₂, or R₃ is substituted or unsubstituted.

In an embodiment of the invention, at least one of R₁, R₂, and R₃ is substituted.

When one or more of R₁, R₂, and R₃ chains are substituted, according to an embodiment of the invention said chain can be free from -OH substituents on position C₂. The absence of hydroxyls in position C₂ advantageously allows a shorter and more efficient synthetic route, eliminating various protection and deprotection steps of the hydroxyl groups thereby, reducing the costs of synthesis and making this synthetic process scalable and industrializable for drugs production.

As described above, the R₄ chain in position C₆ can be any functionalization substituent of interest provided that the TLR4 agonist activity is not disrupted.

According to a non-limiting example, the R₄ can be an hydroxyl group (OH), a phosphate group (PO₄²⁻), an azide group (N₃), an amine group (NH₂), an acyl group (O(C=O)R), an alkyl group (OR) or a glycosyl group.

The suitability of R₄ in position C₆ to functionalization is an extremely advantageous feature of the compounds of the invention. As described above, it is indeed possible to provide molecules in which the agonist function of TLR4 and any other function of interest depending on the selected substituent of R₄ may be combined. For example, it is surprisingly possible to obtain an increase in solubility and bioavailability using a phosphate group (PO₄²⁻). In fact, according to the teachings in the art (WO2019/092572) the presence of two phosphate groups in the agonists described therein

resulted in the absence of TLR4 agonist activity. On the contrary, the new compounds of the invention surprisingly retain the TLR4 agonist activity also with a second phosphate group thereby improving the solubility of the compound itself. As known by the skilled person, improved solubility is an important advantage as it ameliorates the delivery, the bioavailability of the compound and the stability of a composition comprising it. Hence, the simple presence of an additional phosphate in C₆, can significantly improve the efficiency of a pharmaceutical or vaccine composition.

Another important advantage of the possible functionalization in C₆ of the compounds of the invention is that, when used as a vaccine adjuvant it is also possible to conjugate it to an antigen or to an antigenic epitope, or to conjugate it to a different adjuvant to improve and expand its activity. In addition, the compound can be conjugated to a target-specific molecule thereby improving its delivery at a site of preference.

Furthermore, when used in an anti-tumoral composition, the compound of the invention may be functionalized by linking it to additional, different, drugs in order to improve its effectiveness.

By way of example, it is possible to use substituents free of hydrogen atoms capable of forming hydrogen bonds in order to improve the lipophilic effect, or substituents characterized by the presence of hydrogen atoms capable of forming hydrogen bonds in order to improve solubility in water, which is inversely related to lipophilicity.

A further advantage deriving from the possibility of exploiting a large variety of substituents as R₄, is the steric effect that can derive for example by using a substituent which tends to limit the free rotation around simple bonds, and therefore to reduce the number of energetically accessible conformations.

When the bioactive one is present among these conformations, the "stiffening" effect can increase the affinity of the molecule for the receptor.

Another important example may be represented by the functionalization with a linker in position C₆. A non-limiting example of suitable linkers is represented by a disulfide (R-S-S-R'), a hydrazone (R'R''C=N-NH₂), a peptide or a thioether (R'-S-R'') or the like.

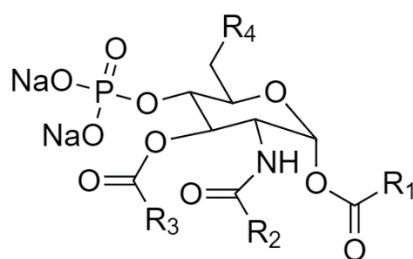
Linkers such as the ones described above allow the preparation of an Antibody-Drug-Conjugate (ADC) which is a complex molecule comprising an antibody linked to a biologically active anticancer payload or drug (such as the compounds of the invention), allowing to obtain a combination effect between the antibody and the compound of the present invention.

A further interesting instance is the possibility to insert a glycosyl group in C₆, as the resulting compound would have two advantages: an improved water solubility due to the presence of the

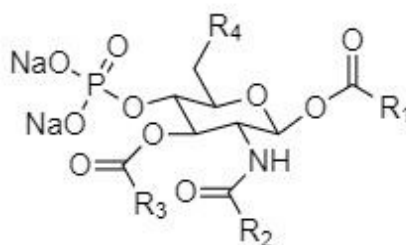
hydrophilic glycosyl group and theoretically a better affinity for the receptor due to the mimicking of the core portion of LPS.

Suitable substituents depending on the desired property are known to the skilled person.

According to the present invention, the compound of formula 1 may be an α -anomer having formula 1 α or an β -anomer having formula 1 β .



(Formula 1 α)



(Formula 1 β)

According to some possible non-limiting embodiments, the compound of formula 1 may be selected from compounds in the form of α -anomer or β -anomer of compounds of Formula 1, wherein

- $R_1 = R_2 = R_3 = C_{11}H_{23}$ and $R_4 = OH$, or
- $R_1 = R_3 = C_{13}H_{27}$; $R_2 = C_{11}H_{23}$ and $R_4 = OH$, or
- $R_1 = R_2 = R_3 = C_9H_{19}$ and $R_4 = OH$, or
- $R_1 = R_2 = R_3 = C_{13}H_{27}$ and $R_4 = OH$, or
- $R_1 = R_3 = C_9H_{19}$; $R_2 = C_{11}H_{23}$ and $R_4 = OH$, or
- $R_1 = R_2 = R_3 = C_{11}H_{23}$ and $R_4 = PO_4^{2-}$, or
- $R_1 = R_2 = R_3 = C_9H_{19}$ and $R_4 = PO_4^{2-}$, or
- $R_1 = R_2 = R_3 = C_{13}H_{27}$ and $R_4 = PO_4^{2-}$, or
- $R_1 = R_2 = R_3 = C_{11}H_{23}$ and $R_4 = OC_3H_7$, or
- $R_1 = R_2 = R_3 = C_{11}H_{23}$ and $R_4 = O(C=O)C_6H_8(OH)_3$, or

$R_1 = R_2 = R_3 = C_{11}H_{23}$ and $R_4 = NH_2$

$R_1 = R_2 = R_3 = C_{11}H_{23}$ and $R_4 = O(C=O)CCH_3(CH_2OH)_2$

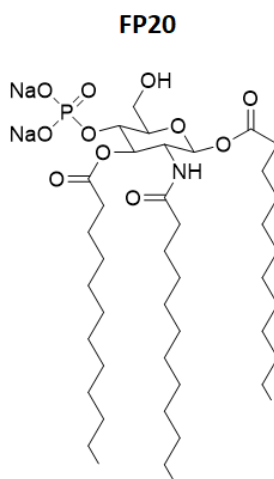
$R_1 = R_2 = R_3 = C_{11}H_{23}$ and $R_4 = OCH(CHOH)_3CH(CH_3)O$

$R_1 = R_2 = R_3 = C_{11}H_{23}$ and $R_4 = OCH(CHOH)_3CH(CH_2OH)O$

$R_1 = R_2 = R_3 = C_{11}H_{23}$ and $R_4 = OCH(CHOH)_3(CH_2)O$.

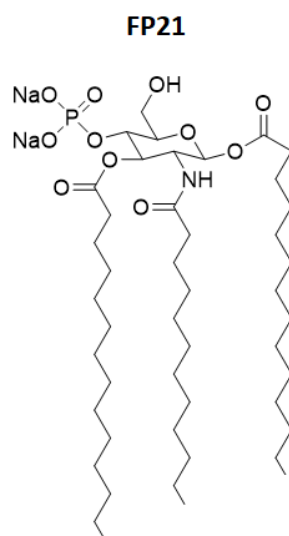
In a preferred embodiment the compounds are β -anomer of compounds of Formula 1 such as:

Compound FP20: with $R_1 = R_2 = R_3 = C_{11}H_{23}$ $R_4 = OH$



(Formula 2)

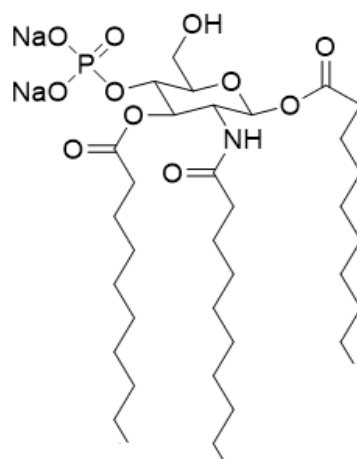
compound FP21: with $R_1 = R_3 = C_{13}H_{27}$ $R_2 = C_{11}H_{23}$ $R_4 = OH$



(Formula 3)

compound FP22: with $R_1 = R_2 = R_3 = C_9H_{19}$ $R_4 = OH$

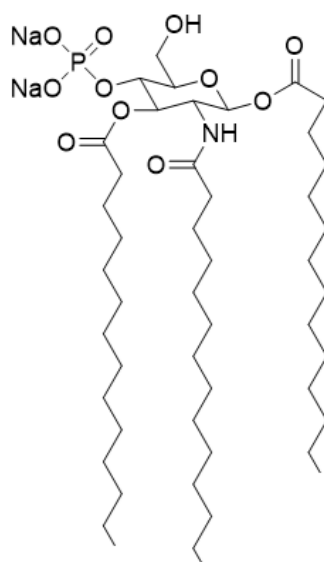
FP22



(Formula 4)

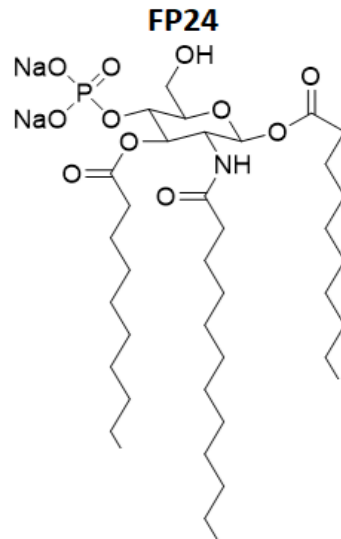
compound FP23: with $R_1 = R_2 = R_3 = C_{13}H_{27}$ $R_4 = OH$

FP23



(Formula 5)

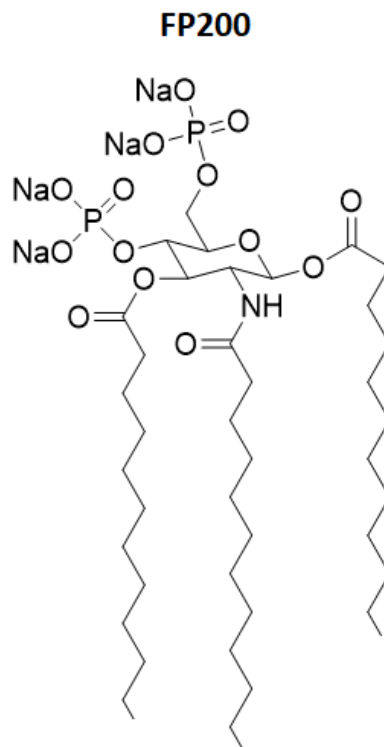
compound FP24: with $R_1 = R_3 = C_9H_{19}$ $R_2 = C_{11}H_{23}$ $R_4 = OH$



(Formula 6)

compound FP200: with $R_1 = R_2 = R_3 = C_{11}H_{23}$

$R_4 = PO_4^{2-}$

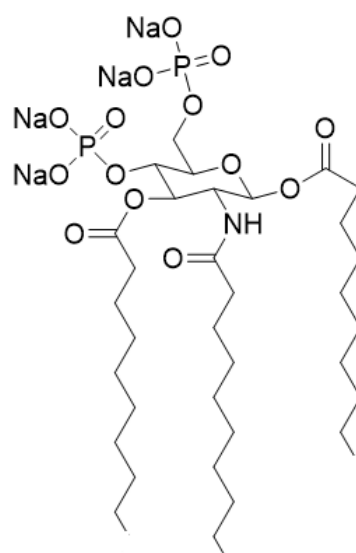


(Formula 7)

compound FP202: with $R_1 = R_2 = R_3 = C_9H_{19}$

$R_4 = PO_4^{2-}$

FP202

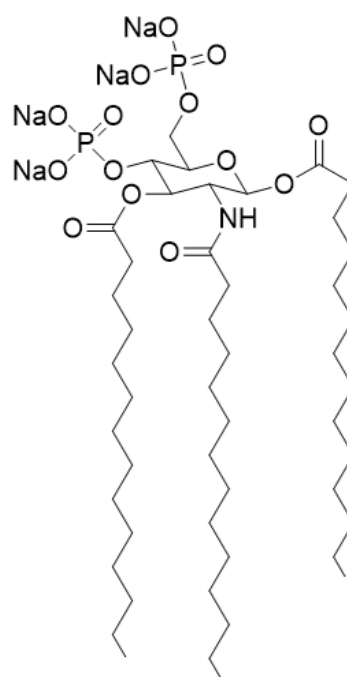


(Formula 8)

compound FP203: with $R_1 = R_2 = R_3 = C_{13}H_{27}$

$R_4 = PO_4^{2-}$

FP203



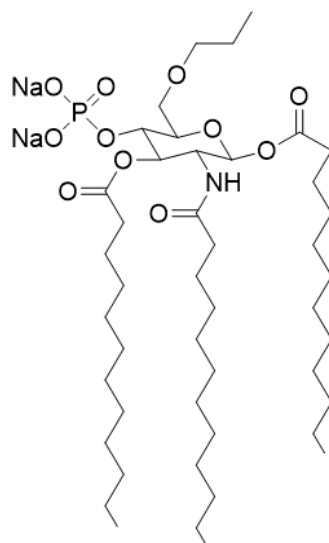
(Formula 9)

Results and Discussion: Chapter II

Further embodiments according to the present invention, wherein the compound of formula 1 having additional substituent on position C₆ may be selected from the following ones:

compound FP204: with $R_1 = R_2 = R_3 = C_{11}H_{23}$

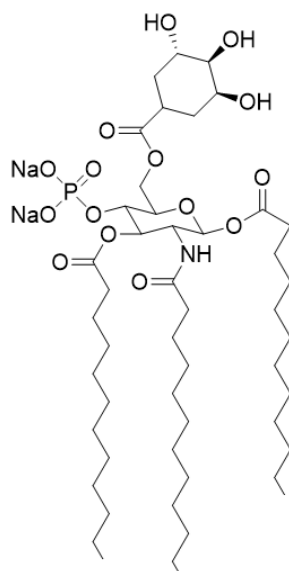
$R_4 = OC_3H_7$



(Formula 10)

compound FP205: with $R_1 = R_2 = R_3 = C_{11}H_{23}$

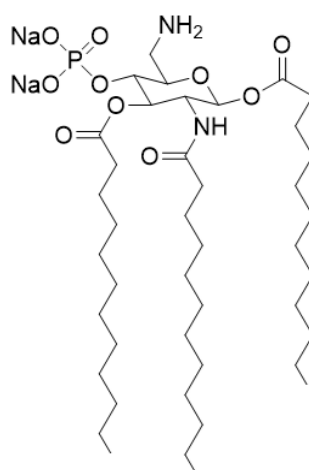
$R_4 = O(C=O)C_6H_8(OH)_3$



(Formula 11)

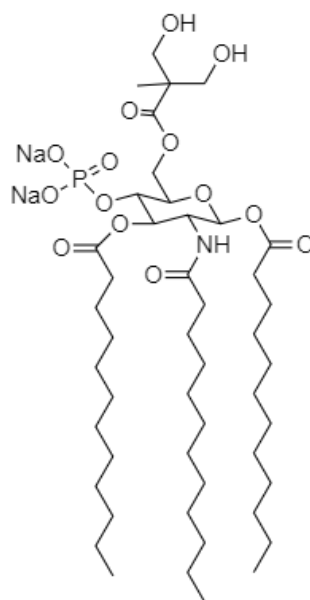
compound FP206: with $R_1 = R_2 = R_3 = C_{11}H_{23}$

$R_4 = NH_2$



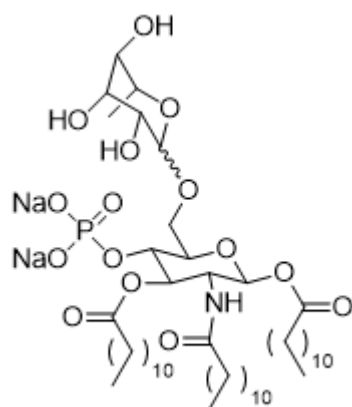
(Formula 12)

compound FP207: with $R_1 = R_2 = R_3 = C_{11}H_{23}$ $R_4 = O(C=O)CCH_3(CH_2OH)_2$



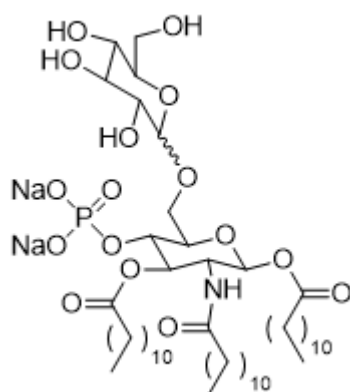
(Formula 13)

compound FP20Rha: with $R_1 = R_2 = R_3 = C_{11}H_{23}$ $R_4 = OCH(CHOH)_3CH(CH_3)O$



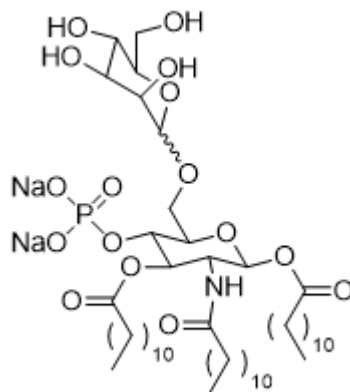
(Formula 14)

compoundFP20Glc: with $R_1 = R_2 = R_3 = C_{11}H_{23}$ $R_4 = OCH(CHOH)_3CH(CH_2OH)O$



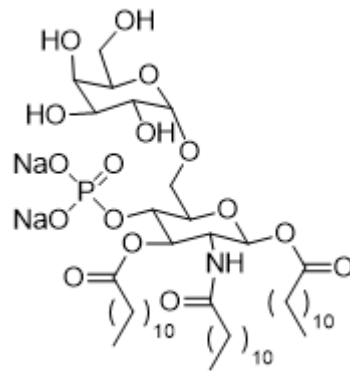
(Formula 15)

Compound FP20Man: with $R_1 = R_2 = R_3 = C_{11}H_{23}$ $R_4 = OCH(CHOH)_3CH(CH_2OH)O$



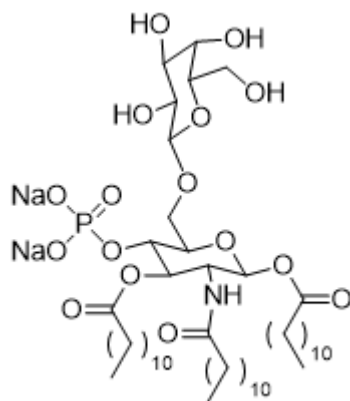
(Formula 16)

Compound FP20Gal- α : with $R_1 = R_2 = R_3 = C_{11}H_{23}$ $R_4 = OCH(CHOH)_3CH(CH_2OH)O$



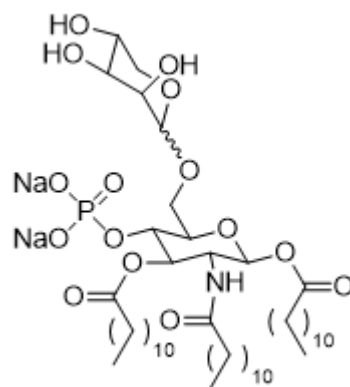
(Formula 17)

Compound FP20Gal- β : with $R_1 = R_2 = R_3 = C_{11}H_{23}$ $R_4 = OCH(CHOH)_3CH(CH_2OH)O$



(Formula 18)

Compound FP20Lyx: with $R_1 = R_2 = R_3 = C_{11}H_{23}$ $R_4 = OCH(CHOH)_3CH_2O$



(Formula 19)

Compounds of the present invention having formula 14, 15, 16 or 19 are mixtures of anomers (diastereomers) of the sugars bound to C₆.

Compounds of the present invention having formula 17 or 18 are respectively the pure alpha and beta anomers of glucose bound in C₆.

In one embodiment, the compound having formula 2 is preferred.

In the present description, such a compound is also referred as compound FP20, wherein R₁, R₂ and R₃ are -C₁₁H₂₃ and R₄ is -OH.

Data reported in the Examples section show the peculiar advantageous features of the aforementioned compounds.

According to the present description, and on the basis of experimental data obtained, it is evident that the compounds as described and claimed are effective agonists of TLR4 receptor. By "agonist of a receptor" (receptor agonist) it is meant as is commonly defined in the literature, i.e., a substance able to bind a specific receptor in the binding site for the endogenous ligand. Therefore, as the name suggests, the former competes with the latter for the binding with said site.

Following binding with the natural ligand, the receptor encounters conformational changes that mediate its biological activity at cell level. Agonists are molecules having inherent activity able to mimic ligand effects. When binding to the receptor, they cause conformational changes of an extent similar to those caused by binding with the endogenous ligand.

In the case of the present description, each agonist disclosed and claimed is an agonist selective for the TLR4 receptor.

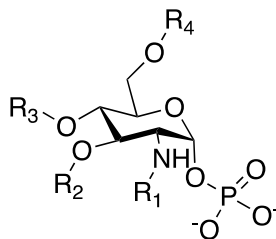
Given the technical features observed for compounds of formula (1) as defined in the present description and in the claims, said compounds are useful as active principles or as adjuvants in the treatment of diseases benefiting from a TLR4 receptor activation, i.e., in diseases in which an activation of the immune system, particularly of the innate activity, has a therapeutic or prophylactic effect.

Therefore, among diseases requiring or benefiting from a TLR4 receptor activation are included all the diseases whose treatment or whose prevention are improved by TLR4 receptor activation and by the innate immune response triggered by the activation of said receptor.

A non-limiting example of such diseases is represented by tumors, allergies, infectious diseases such as viral infections, cardiovascular diseases, obesity-dependent metabolic diseases, neuronal degeneration, autoimmune disorders, bacterial infections autoimmune diseases. An example of autoimmune diseases is represented by IBD, Chron's disease or rheumatoid arthritis.

Results and Discussion: Chapter II

The compound of formula 2, herein also identified as compound FP20, can be compared with the compound of formula FP112 having the formula represented below



wherein $R_1 = R_2 = R_3 = C=OC_{11}H_{23}$ $R_4 = H$, disclosed in WO2019/092572, named therein as FP112, due to the fact that they have the same R_1 , R_2 , R_3 and R_4 substituents, but the phosphate group is on position C_1 for FP112 and on position C_4 for FP20.

Experiments *in vitro* conducted for FP112 on cells Hek-Blue, Raw-Blue and THP-1 briefly reported in the examples below, demonstrated a low toxicity and a good pro-inflammatory activity at a concentration of 10 μ M. Furthermore, experiments *in vivo* conducted with FP112 to test its tolerability and effectiveness as vaccine adjuvant, demonstrated no collateral damage from the administration of 10 μ g of FP112, and an effectiveness as vaccine adjuvant comparable to that of MPLA. Data reported in the Examples section show that for experiments conducted on Hek-Blue, Raw-Blue and THP-1 cells, the activity of the compounds of the invention is comparable with the activity of the agonist compounds disclosed in WO2019/092572 which proved to be also non cytotoxic and effective as vaccine adjuvants *in vivo*.

Additionally, the compounds of the present invention are improved with respect to the compounds disclosed in WO2019/092572 due to the relocation of the phosphate group in C_1 in the prior art, in position C_4 in the present invention, thereby allowing the positioning of the alkyl chains in C_1 in the compounds of the present invention rather than in C_4 , which resulted in an enhanced activity of the substituents in C_6 . In fact, WO2019/092572 discloses in Experiment 2 that a compound named therein as FP111, having two phosphate groups: one in position C_1 and the other one in position C_6 proved completely inactive as TLR4 agonist in a test conducted on HEK-Blue™ hTLR4 cells. In WO2019/092572 it was speculated that the absence of activity could be due to the presence of two phosphates in the molecule and that the number of phosphates in the molecule had to be no more than 1 in order to maintain their TLR4 agonist activity.

Surprisingly, the Authors of the present invention discovered that the compounds disclosed and claimed in the present application, such as, by way of example compounds of formula 7, 8 and 9, bearing two phosphate group, one in position C_4 and another one in position C_6 , maintained the

TLR4 agonist activity in the same tests in which compound FP111 disclosed in WO2019/092572 resulted completely inactive. This finding was unexpected and proves a relevant advantage of the compounds of the invention over the prior art as it demonstrates that the position of phosphate groups in a triacylated Monophosphoryl glucosamine core can significantly vary the activity of such compound.

The invention therefore also provides the compound of formula 1 in any one of the embodiments disclosed in the description or in the claims as vaccine adjuvant.

The relevance of immune response adjuvants in vaccine composition is known. Vaccine adjuvants, indeed, substantially increase vaccine effectiveness and development of immunity toward antigens present in the vaccine, in the treated subject.

Therefore, object of the present invention is also a vaccine composition comprising the compound of formula 1 as defined in any one of the embodiments in the description or in the claims or a mixture thereof.

The vaccine composition according to the invention can therefore comprise the compound of formula 1 as described herein or a mixture thereof, in any one of the aforementioned embodiments, at least one pharmaceutically acceptable carrier and at least one antigenic compound able to induce a desired immune response, such as an immunogenic antigen.

Suitable vaccine carriers are known to the skilled person.

The pharmaceutical carrier may be selected to assist release of the antigen component(s) over an extended period of time from the composition. The carrier may include a water-soluble or water-insoluble substance.

A water-soluble substance is a substance which plays a role in controlling infiltration of water into the interstices of the drug dispersion.

One water-soluble substance, or a combination of two or more water-soluble substances may be used.

The water-soluble substance specifically may be selected from one or more of the groups consisting of synthetic polymers (e.g., polyethylene glycol, polyethylene polypropylene glycol), sugars (e.g., sucrose, mannitol, glucose, sodium chondroitin sulfate), polysaccharides (e.g., dextran), amino acids (e.g., glycine and alanine), mineral salts (e.g., sodium chloride), organic salts (e.g., sodium citrate) and proteins (e.g., gelatin and collagen and mixtures thereof).

In addition, when the water-soluble substance is an amphiphilic substance, which dissolves in both an organic solvent and water, it has an effect of controlling the release of, for example, a lipophilic

drug by altering the solubility thereof. An amphiphilic substance includes, but not limited to, one or more selected from the group consisting of polyethylene glycol or a derivative thereof, polyoxyethylene polyoxypropylene glycol or a derivative thereof, fatty acid ester and sodium alkylsulfate of sugars, and more specifically, polyethylene glycol, polyoxy stearate 40, polyoxyethylenepolyoxypropylene-glycol sucrose esters of fatty acids, polyoxyethylene-polyoxypropylene-glycol, polyoxyethylene-polyoxypropylene-glycol, , sodium lauryl sulfate, sodium oleate, sodium chloride, sodium desoxycholic acid (or sodium deoxycholic acid (DCA)) of which mean molecular weights are more than 1500.

In addition, the water-soluble substance may include a substance selected from one or more of the groups consisting of drugs, peptides, proteins, glycoproteins, polysaccharides, or an antigenic substance used as vaccines.

A water-insoluble carrier, when present, may include a substance which plays a role in controlling infiltration of water into the interstices of the drug dispersion. One water-insoluble substance, or a combination of two or more water-insoluble substances may be used.

The water-insoluble substance specifically may be selected from one or more of the groups of water insoluble polymers, resins and latexes including water-insoluble acrylates, methacrylates and other carboxy polymers, waxes, lipids including phospholipids and lipoproteins.

The skilled person knows the amount of carrier and optional further excipients commonly used in a pharmaceutical or in a vaccine composition.

In an embodiment, the pharmaceutical carrier may constitute from approximately 1% to 20% by weight, preferably approximately 10% to 20% by weight, based on the total weight of the vaccine composition.

The composition according to the invention may comprise one of the compounds as defined and claimed herein, or a mixture thereof.

The composition of the invention may be prepared in the form of a single mixture of adjuvant and antigen or in the form of different mixtures for a concomitant or sequential administration of the components.

In a particular embodiment, the compound of formula 1 described in the present invention is the sole adjuvant present in the vaccine composition.

The present invention also relates to a pharmaceutical composition, comprising a compound of formula 1 described in any one of the embodiments provided in the description or in the claims or a mixture thereof and at least one pharmaceutically acceptable excipient and/or carrier.

Results and Discussion: Chapter II

The composition may further comprise one or more additional therapeutically active principle.

Said pharmaceutical composition can also be formulated in the form of an association of a plurality of active principles.

The pharmaceutical composition of the invention may comprise as sole active principle one or more compounds of formula 1 according to any one of the embodiments provided in the description or in the claims, or could also comprise additional active principles, such as anti-tumor active principles, kinase inhibitors, cytotoxic compounds and at least one pharmaceutically acceptable carrier or excipient.

The pharmaceutical composition may be formulated for oral, parenteral, nasal, aerosol, sublingual, rectal, vaginal, topical, endovenous or systemic administration.

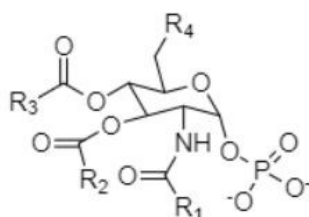
Suitable conventional carriers and/or excipients for suspension, emulsion, ointment, cream, spray, granulate, powder, solution, capsule, pill, tablet, lyophilized product, lozenge, aerosol, nebulization, injection, or others can be selected by the person skilled in the art.

Further object of the present invention is the pharmaceutical composition according to any one of the embodiments herein disclosed for use in the treatment, or as an adjuvant in the treatment, of diseases that require or benefit from an immune stimulation by activating the TLR4 receptor.

Diseases that require or benefit from an immune stimulation by activating the TLR4 receptor, are known in the art and comprise cancer, allergies, infectious diseases, cardiovascular diseases, obesity-dependent metabolic diseases, neuronal degeneration, apoptotic diseases, autoimmune disorders, viral infections, bacterial infections, autoimmune diseases. An example of autoimmune diseases is represented by IBD, Chron's disease or rheumatoid arthritis.

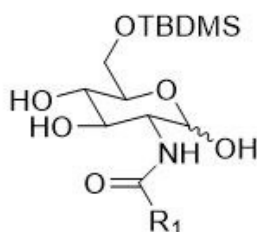
According to the invention, the composition may comprise 0.01 to 50 mg of compound of the invention or of a mixture thereof per daily dosage, by way of example 0.01 to 50 mg of substance per Kg of body weight (test on animals).

The invention also provides a new method for the synthesis of compounds of formula 1 as herein defined as well as for the synthesis of the compounds disclosed in WO2019/092572 of formula X



Formula X

wherein R_1 is a saturated C_7 - C_{15} alkyl chain optionally substituted,
wherein R_2 is a saturated C_7 - C_{15} alkyl chain optionally substituted,
wherein R_3 is a saturated C_7 - C_{15} alkyl chain optionally substituted,
wherein R_4 is OH and wherein each of R_1 , R_2 and R_3 is free from -OH substituents in position C_2 , and
for the synthesis of an intermediate of of formula 1i



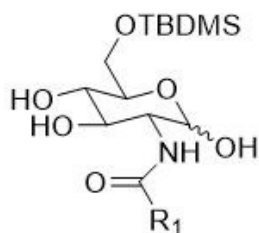
Formula 1i

wherein R_1 is a saturated C_5 - C_{15} alkyl chain optionally substituted.

The compounds of formula 1, as well as the compounds disclosed in WO2019/092572, can be synthesized in a simpler and industrially scalable way compared to the synthesis methods known in the art for the compounds of WO2019/092572 as well as for SDZ MRL 953. The latter requires the insertion of three acyl chains of (R)-3-hydroxymyristic acid. The optically pure compound (R-enantiomer) is not commercially available, as only the racemic mixture is marketed. Moreover, (R)-3-hydroxymyristic acid requires a reaction of protection of the hydroxyl group in position 3 prior to the condensation reaction with the sugar. The method disclosed in WO2019/092572 for the synthesis of compounds of formula X as defined above, although already simplified with respect to the synthesis method disclosed for SDZ MRL 953, due to the absence of substituents on the acyl chains, still comprises 10 steps, several purifications by chromatographic column and some critical steps, such as the formation of a low molecular weight azide. Additionally, the method disclosed in WO2019/092572 has an extremely low yield (about 8-9%), which makes the whole process uneconomic.

The compounds provided in the present invention exhibit biological activities comparable to, if not even better than, the compounds of the art and can be synthesized in a much simpler and industrially scalable way.

Hence, an object of the present invention is a method for the preparation of an intermediate of formula 1i

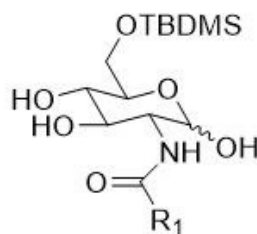


1i

wherein R_1 is a saturated C_5 - C_{15} alkyl chain optionally substituted, comprising the following steps

- 1) Selective acylation of the amino group in the C_2 position of glucosamine hydrochloride by reaction with acyl chloride in the presence of sodium bicarbonate.
- 2) Protection by selective silylation of hydroxyl in position C_6 by reaction with tert-butyldimethylsilyl chloride (TBDMSCl) in the presence of imidazole.

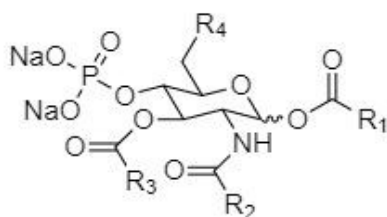
Therefore, present invention also relates to an intermediate of formula 1i



1i

wherein R_1 is a saturated C_5 - C_{15} alkyl chain optionally substituted.

Furthermore, the present invention relates to a method for the preparation of compounds of formula 1 as defined in any of the embodiments above and in the claims



wherein R_1 is a saturated C_5 - C_{15} alkyl chain optionally substituted,

wherein R_2 is a saturated C_5 - C_{15} alkyl chain optionally substituted,

wherein R_3 is a saturated C_5 - C_{15} alkyl chain optionally substituted,

wherein R_4 is any substituent known by the skilled person that can be linked by means of a bond between C_6 and a suitable atom and/or any substituent which possesses an oxygen or a nitrogen atom that can bind to C_6

comprising the following steps:

- 1) Selective acylation of the amino group in the C_2 position of glucosamine hydrochloride by reaction with acyl chloride in the presence of sodium bicarbonate.
- 2) Protection by selective silylation of hydroxyl in position C_6 by reaction with tert-butyldimethylsilyl chloride (TBDMSCl) in the presence of imidazole obtaining the intermediate of formula 1i as defined in the previous described embodiments.
- 3) Selective acylation of hydroxyls in positions C_1 and C_3 by reaction with acyl chloride in the presence of triethylamine and N, N-dimethyl aminopyridine (DMAP).
- 4) Phosphorylation of hydroxyl in the C_4 position by reaction with dibenzyl N, N-diisopropylphosphoramidite in the presence of triflate imidazolium, followed by oxidation of phosphite to phosphate via metachloroperbenzoic acid.
- 5) Deprotection of hydroxyl in position C_6 from silane through the presence of sulfuric acid in catalytic quantities.
- 6) Deprotection of phosphate from benzyls in position C_4 and optionally deprotection of benzyls on any substituent in position C_6 through hydrogenation catalyzed by Palladium on Carbon (Pd / C).

The method can alternatively start from the intermediate of formula 1i as defined above and in the claims and may comprise steps 3-6.

In one embodiment, the method of synthesis described above may comprise an additional step 5i) after step 5) and before step 6)

5i) Phosphorylation of hydroxyl in position C_6 by reaction with dibenzyl N, N-diisopropylphosphoramidite in the presence of triflate imidazolium, followed by oxidation of phosphite to phosphate via metachloroperbenzoic acid, and wherein the resulting R_4 is a phosphate group (PO_4^{2-}).

When carried out, this method leads to compounds of formula 1 wherein R_4 is a phosphate group, such as compounds of formulas 7, 8 and 9.

Alternatively, the method of synthesis may further comprise a step 5ii) instead of step 5i) after step

5) and before step 6):

5ii) Acylation of hydroxyl in C₆ position either by reaction with carboxylic acid in the presence of a suitable condensing agent and catalyst, such as 1-ethyl-3-(3-dimethylaminopropyl) carbodiimide (EDC) and N, N-dimethyl aminopyridine (DMAP), or by reaction with acyl chloride in the presence of a suitable catalyst, such as N, N-dimethyl aminopyridine (DMAP).

wherein the resulting R₄ is an acyl group. When carried out, this method leads to compounds of formula 1 wherein R₄ is an acyl group, such as compounds of formulas 10 and 11.

In a preferred embodiment, said suitable condensing agent and catalyst are 1-ethyl-3-(3-dimethylaminopropyl) carbodiimide (EDC) and N, N-dimethyl aminopyridine (DMAP).

Alternatively, the method of synthesis may further comprise a step 5iii) instead of step 5i) and 5ii) after step 5) and before step 6):

5iii) Glycosylation of hydroxyl in C₆ position by reaction of a glycosyl chloride donor in the presence of silver (I) oxide as activator, of triflic acid as catalyst and molecular sieves as water scavenger

Or

Glycosylation of hydroxyl in C₆ position by reaction of a glycosyl thioethyl (Set) donor in the presence of NIS (N-iodosuccinimide) as activator and HOFox (3,3-difluoroxindole) as catalyst and molecular sieves as water scavenger wherein the resulting R₄ is a glycosyl group.

Alternatively, the method of synthesis may further comprise a step 5iv) instead of step 5i), 5ii) and 5iii) after step 5) and before step 6):

5iv) Alkylation of hydroxyl in C₆ by reaction of a stabilized alkyl chloride in the presence of silver (I) oxide as activator, of triflic acid as catalyst and molecular sieves as water scavenger

wherein the resulting R₄ is n alkyl group.

Alternatively, the method of synthesis may further comprise a step 5v) and a step 5vi) instead of step 5i), 5ii), 5iii) and 5iv) after step 5) and before step 6):

5v) Tosylation of position C₆ by reaction of tosyl chloride in presence of triethylamine as base and of DMAP as catalyst

5vi) azide insertion in position C₆ by reaction with sodium azide in the presence of tetrabutylammonium iodide

wherein the resulting R₄ is an azide group.

Alternatively, the method of synthesis may further comprise a step 5vii) and a step 5viii) instead of step 5i), 5ii), 5iii) and 5iv) after step 5) and before step 6):

5vii) Glycosylation of hydroxyl in C₆ position by reaction of a glycosyl chloride donor bearing a picoloyl group in the presence of Bi(OTf)₃ as sole activator.

wherein the resulting R₄ is a glycosyl group.

5viii) Picoloyl group removal by reaction with Cu(OAc)₂.

According to the present description, the acylations described in reactions 1), 3), 5ii) can be carried out according to methods commonly used by technicians in the chemical field. By way of example, acylations can be carried out using acyl chloride or carboxylic acid in presence other common condensing agents, such as 1-ethyl-3-(3-dimethylaminopropyl) carbodiimide (EDC) or dicyclohexylcarbodiimide (DCC).

The condensations referred to in reactions 1) and 3) can be carried out using alkyl chains of different lengths, between 5 and 15 carbon atoms, thereby obtaining different derivatives of the molecule described by formula 1.

The protection of C₆ described by reaction 2) can be carried out in accordance with the most common techniques known to those skilled in the chemical field. One of said common techniques is silylation in the presence of various non nucleophilic bases, such as triethylamine, diisopropylethylamine or sodium bicarbonate and catalyst such as N, N-dimethyl aminopyridine (DMAP).

The phosphorylation of C₄ described by reaction 4) can be carried out according to the most common techniques known to those skilled in the chemical field, such as phosphite insertion in presence of different acidic pH buffers, such as, but not limited to, tetrazole or 4,5-Dicyanoimidazole. The subsequent oxidation can be carried out by reaction with different mild oxidants, such as but not limited to dimethyldioxirane (DMDO) or tert-Butyl peroxide (tBuOOH).

The deprotection of C₆ described by reaction 5) can be carried out according to the most common techniques known to those skilled in the chemical field. such as desilylation in the presence of tetrabutylammonium fluoride (TBAF), acetic acid (AcOH) or various types of acidic resins, i.e., IRA 120 H⁺, IRC 120 H⁺ or Dowex® 50W.

The process of synthesis according to the invention enables to make in an easy and industrially scalable way the compounds of formula 1.

As stated above, the invention encompasses both α as well as β anomers of the compound of formula 1 as defined above. The inventors have surprisingly found that, depending on the temperature and amount of a suitable catalyst of the acylation step 3, α or β anomers can be obtained.

Therefore, when a β anomer is desired, the acylation step 3) is carried out at a temperature ranging from $-78\text{ }^{\circ}\text{C}$ to $0\text{ }^{\circ}\text{C}$ and with an amount of DMAP ranging from 0.05 to 0.2 equivalents.

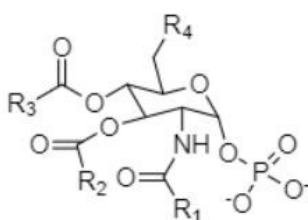
In a preferred embodiment, to synthesise a β anomer acylation step 3 is carried out at $-20\text{ }^{\circ}\text{C}$ with 0.1 equivalents of DMAP.

On the other hand, when an α anomer is desired, the acylation step 3) is carried out at a temperature ranging from $20\text{ }^{\circ}\text{C}$ to $50\text{ }^{\circ}\text{C}$ with an amount of DMAP ranging from 2 to 2.5 equivalents.

In a preferred embodiment, to synthesise an α anomer acylation step 3 is carried out at a temperature of about $30\text{ }^{\circ}\text{C}$ with 2.02 equivalents of DMAP.

The methods as defined herein allow the synthesis of each one of the embodiments of the compounds of formula 1 (such as compounds of formulas 2-12) as disclosed in the present specification. The skilled person will know the substituents to use based on the common knowledge in organic chemistry.

Advantageously, the invention also provides a method for the synthesis of a compound of formula X



X

wherein R_1 is a saturated C_5 - C_{15} alkyl chain optionally substituted,

wherein R_2 is a saturated C_5 - C_{15} alkyl chain optionally substituted,

wherein R_3 is a saturated C_5 - C_{15} alkyl chain optionally substituted,

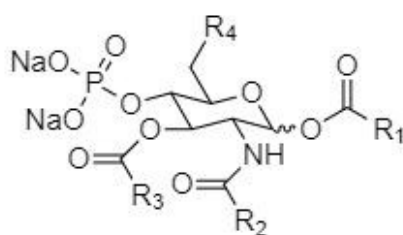
wherein R_4 is OH and wherein each of R_1 , R_2 and R_3 is free from -OH substituents in position C_2

comprising the following steps:

1) Selective acylation of the amino group in the C_2 position of glucosamine hydrochloride by reaction with acyl chloride in the presence of sodium bicarbonate.

- 2) Protection by selective silylation of hydroxyl in position C₆ by reaction with tert-butyldimethylsilyl chloride (TBDMSCl) in the presence of imidazole obtaining the intermediate of formula 1i as defined in the previous described embodiments.
- 3) Complete acylation of hydroxyls in positions C₁, C₃ and C₄ by reaction with acyl chloride in the presence of triethylamine and N, N-dimethyl aminopyridine (DMAP).
- 4) Selective deacylation of position C₁ by reaction with ethylenediamine in the presence of acetic acid
- 5) Phosphorylation of hydroxyl in the C₁ position by reaction with dibenzyl N, N-diisopropylphosphoramidite in the presence of triflate imidazolium, followed by oxidation of phosphite to phosphate via metachloroperbenzoic acid.
- 6) Deprotection of hydroxyl from silane in position C₆ through the presence of a 5% solution of sulfuric acid in water in catalytic quantities.
- 7) Deprotection of phosphate from benzyls in position C₄ and optionally deprotection of benzyls on any substituent in position C₆ through hydrogenation catalyzed by Palladium on Carbon (Pd/C).

The present invention also relates to the use of an intermediate compound of formula 1i, as defined in any one of the embodiments herein disclosed, for the synthesis of compounds of formula 1

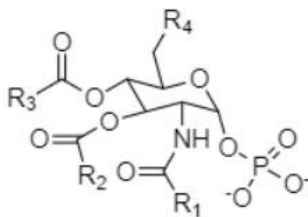


(Formula 1)

wherein R₁ is a saturated C₅-C₁₅ alkyl chain optionally substituted,
wherein R₂ is a saturated C₅-C₁₅ alkyl chain optionally substituted,
wherein R₃ is a saturated C₅-C₁₅ alkyl chain optionally substituted,
wherein R₄ is any substituent known by the skilled person that can be linked by means of a bond between C₆ and a suitable atom and/or any substituent which possesses an oxygen or a nitrogen atom that can bind to C₆.

Results and Discussion: Chapter II

Furthermore, the present invention relates to the use of an intermediate of formula 1i as defined in any one of the embodiments herein disclosed, for the synthesis of compounds of formula X



X

wherein R₁ is a saturated C₅-C₁₅ alkyl chain optionally substituted,
wherein R₂ is a saturated C₅-C₁₅ alkyl chain optionally substituted,
wherein R₃ is a saturated C₅-C₁₅ alkyl chain optionally substituted,
wherein R₄ is OH and wherein each of R₁, R₂ and R₃ is free from -OH substituents in position C₂.

Object of the invention is also a process for the preparation of pharmaceutical formulations or of vaccine compositions comprising the steps of the above process, and at least one step wherein the product obtained at 6) in a pharmaceutically acceptable grade is mixed with at least one pharmaceutically acceptable carrier and/or excipient.

In any part of the present description and claims the term comprising can be substituted by the term "consisting of".

In compliance with Art. 170bis of the Italian patent law it is herein declared that:

all experiments involving cells were carried out on commercially available cells

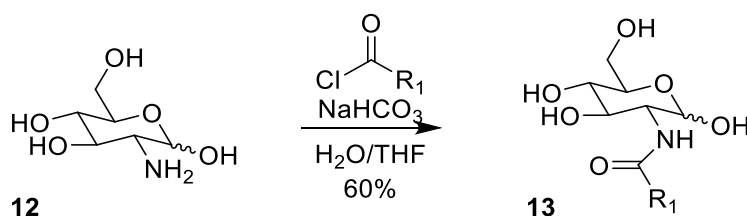
with reference to model mice used in the described experiments, the obligations deriving from the national or EU regulations and, in particular, from the provisions referred to in paragraph 6 of Legislative Decree No. 206 of 12 April 2001 and 8 July 2003 no. 224, have been fulfilled.

EXAMPLES

Chemistry

All reagents and solvents were purchased from commercial source and used without further purifications, unless stated otherwise. Reactions were monitored by thin-layer chromatography (TLC) performed over Silica Gel 60 F254 plates (Merck®). Flash chromatography purifications were performed on silica gel 60 60-75 μ m from commercial source.

¹H and ¹³C NMR spectrum were recorded with Bruker Advance 400 with TopSpin® software, or with NMR Varian 400 with Vnmrj software. Chemical shifts are expressed in ppm respect Me₄Si; coupling constants are expressed in Hz. The multiplicity in the ¹³C spectra was deduced by APT experiments.

Synthesis of **13**

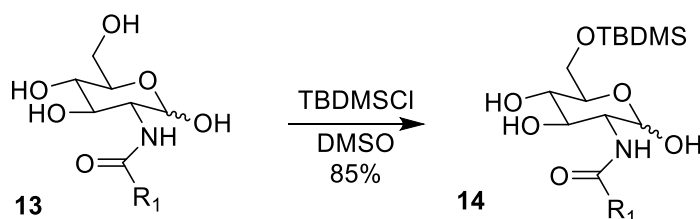
Glucosamine hydrochloride **12** (10 g, 46.5 mmol, 1 eq.) and NaHCO₃ (10.54 g, 126 mmol, 2.7 eq.) were dissolved in water (120 ml). Then, previously dissolved lauroyl chloride (11.20 g, 51.2 mmol, 1.1 eq.) in THF (120 ml) was added dropwise to the solution at 0 °C. Reaction was stirred for 5 h, then solution was filtered. A white solid was obtained, which was washed with 4 °C water and THF. Excess water was then coevaporated with toluene under reduced pressure, to obtain the desired product **13** as a white powder in 60% yield (10.10 g). Compound was used without further purification.

¹H NMR (400 MHz, DMSO) δ 7.68 (d, J = 8.1 Hz, 1H), 7.52 (d, J = 7.7 Hz, 3H), 6.46 (d, J = 6.3 Hz, 1H), 6.37 (d, J = 4.0 Hz, 3H), 4.97 – 4.86 (m, 7H), 4.81 (d, J = 4.7 Hz, 1H), 4.62 (d, J = 5.0 Hz, 3H), 4.53 (t, J = 5.7 Hz, 1H), 4.43 (dd, J = 9.5, 4.3 Hz, 4H), 3.73 – 3.42 (m, 18H), 3.34 – 3.22 (m, 2H), 3.16 – 3.09 (m,

3H), 3.04 (d, $J = 14.1$ Hz, 2H), 2.13 – 2.03 (m, 8H), 1.56 – 1.37 (m, 9H), 1.26 (d, $J = 14.5$ Hz, 6H), 0.86 (t, $J = 6.8$ Hz, 13H).

^{13}C NMR (101 MHz, DMSO) δ 173.31, 172.82, 96.11, 91.05, 77.21, 74.74, 72.49, 71.59, 71.32, 70.83, 61.58, 57.57, 54.73, 40.59, 40.38, 40.17, 39.96, 39.75, 39.54, 39.33, 36.18, 35.74, 31.77, 29.53, 29.49, 29.43, 29.37, 29.23, 29.18, 29.14, 25.78, 22.56, 14.42.

Synthesis of **14**

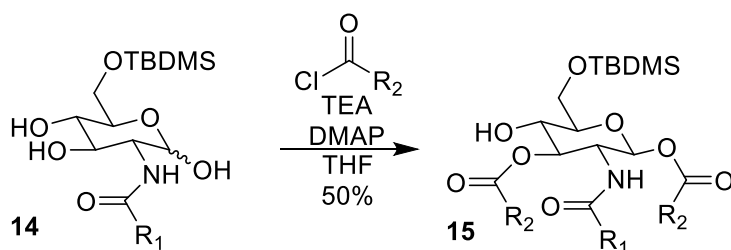


To a solution of **13** (3 g, 8.3 mmol, 1 eq.) and imidazole (850 mg, 12.4 mmol, 1.5 Eq.) in dimethylsulfoxide (166 ml, 0.05 M) a solution of TBDMSCl (1.4 g, 9.1 mmol, 1.1 eq.) in DCM (15 ml) was added dropwise under inert atmosphere in ice bath. Subsequently, the solution was allowed to return at room temperature and stirred overnight. Reaction, monitored by TLC (DCM/MeOH 9:1), was then stopped and the solution concentrated under reduced pressure. Then it was diluted with AcOEt and washed three times with NH_4Cl . Organic phase thus obtained was dried with Na_2SO_4 and solvent was removed by rotavapor. Raw product thus obtained (3.65 g) was resuspended in EtPet at 0 °C for 30 min. Then, suspension was filtered under vacuum and desired compound was recovered as a white solid. After purification, 3.5 g of compound **14** as a whiteish solid were obtained, in 85% yield.

^1H NMR (400 MHz, DMSO) δ 7.62 (d, $J = 7.9$ Hz, 1H), 6.43 (d, $J = 6.4$ Hz, 1H), 4.90 (t, $J = 6.5$ Hz, 1H), 4.77 (t, $J = 9.1$ Hz, 1H), 4.42 (t, $J = 7.0$ Hz, 1H), 3.86 (d, $J = 10.8$ Hz, 1H), 3.66 (dd, $J = 11.0, 4.6$ Hz, 1H), 3.30 (d, $J = 7.9$ Hz, 1H), 3.14 – 2.98 (m, 1H), 2.06 (t, $J = 7.4$ Hz, 1H), 1.48 (s, 1H), 1.24 (s, 3H), 0.94 – 0.74 (m, 2H), 0.05 (d, $J = 3.0$ Hz, 1H).

^{13}C NMR (101 MHz, DMSO) δ 173.21, 95.93, 77.09, 74.83, 70.82, 63.61, 57.54, 40.61, 40.40, 40.20, 39.99, 39.78, 39.57, 39.36, 36.20, 31.78, 29.54, 29.51, 29.45, 29.39, 29.20, 29.14, 26.41, 25.76, 22.57, 18.64, 14.41, -4.66, -4.67.

Synthesis of 15

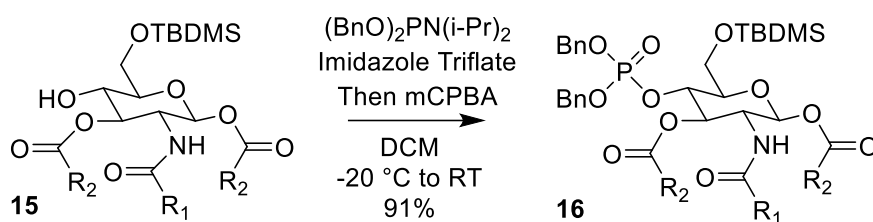


Compound **14** (2.0 g, 4.2 mmol, 1 eq.) and 4-dimethylaminopyridine (26 mg, 0.2 mmol, 0.05 Eq.) were dissolved in anhydrous THF (84 ml, 0.05 M) under Ar atmosphere. Triethylamine (2.4 ml, 17.2 mmol, 4.1 Eq.) and lauroyl chloride (2.10 ml, 8.5 mmol, 2.0 eq.) were added dropwise to the solution at $-20\text{ }^{\circ}\text{C}$. Reaction was stirred for two hours at $-20\text{ }^{\circ}\text{C}$, then controlled by TLC (EtPet/AcOEt 6:4). Subsequently, solution was diluted in AcOEt and washed with 1M HCl. Organic phase thus obtained was dried with Na_2SO_4 and solvent was removed by rotavapor. Raw product thus obtained (4 g) was purified using flash column chromatography (Tol/AcOEt 9:1). After purification, 2.1 g of compound **15** were obtained, in 50% yield.

^1H NMR (400 MHz, DMSO) δ 7.80 (d, $J = 9.5$ Hz, 1H), 5.56 (d, $J = 8.9$ Hz, 1H), 5.38 (d, $J = 5.9$ Hz, 1H), 4.92 (dd, $J = 10.6, 8.6$ Hz, 1H), 3.83 (dd, $J = 10.4, 5.8$ Hz, 2H), 3.76 – 3.70 (m, 1H), 3.38 (dd, $J = 14.3, 8.5$ Hz, 2H), 2.30 – 2.14 (m, 7H), 1.94 (t, $J = 7.3$ Hz, 2H), 1.44 (dd, $J = 25.9, 6.4$ Hz, 10H), 1.24 (d, $J = 2.4$ Hz, 75H), 0.90 – 0.81 (m, 24H), 0.07 – -0.01 (m, 6H).

^{13}C NMR (101 MHz, DMSO) δ 174.93, 172.72, 172.34, 171.74, 92.49, 77.48, 75.66, 67.73, 62.54, 52.26, 40.65, 40.44, 40.23, 40.02, 39.82, 39.61, 39.40, 36.08, 34.13, 33.94, 31.78, 31.74, 29.59, 29.52, 29.50, 29.44, 29.39, 29.35, 29.30, 29.19, 29.00, 28.93, 28.75, 26.26, 25.70, 24.95, 24.77, 22.55, 18.54, 14.39, 14.36, -4.71, -4.78.

Synthesis of 16



Compound **15** (2.12 g, 2.4 mmol, 1 Eq.) and imidazole triflate (1.4 g, 5.4 mmol, 2.25 Eq.) were dissolved in DCM (121 mL, 0.02 M) under inert atmosphere. Dibenzyl N,N-diisopropylphosphoramidite (1.83 g, 5.3 mmol, 2.2 Eq.) was added to the solution at 0 °C. Reaction was monitored by TLC (EtPet/acetone 9:1); after 30 min, substrate depletion was detected. Solution was then cooled at -20 °C and meta-chloroperbenzoic acid (1.66 g, 9.7 mmol, 4 Eq.), dissolved in 17 ml of DCM, was added dropwise. After 30 min the reaction was allowed to return to RT and left stirring overnight.

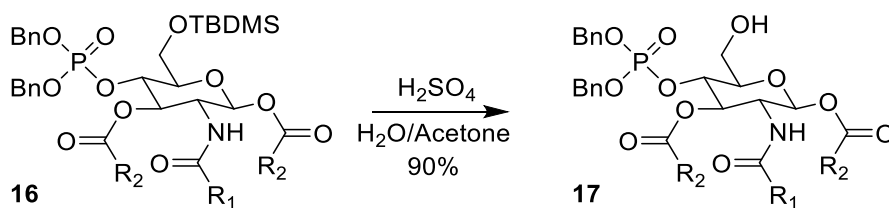
After TLC analysis, reaction was quenched with 15 ml of a saturated NaHCO_3 solution and concentrated by rotavapor. The mixture was then diluted in AcOEt and washed 3 times with a saturated NaHCO_3 solution and three times with a 1 M HCl solution. The organic phase was recovered, dried with Na_2SO_4 and solvent was removed by rotavapor.

Crude thus obtained was purified by flash column chromatography (EtPet/acetone 9:1). 2.41 g of pure compound **16** were obtained as a yellow oil in a 91% yield.

$^1\text{H NMR}$ (400 MHz, CDCl_3) δ 7.34 – 7.25 (m, 10H), 5.61 (d, $J = 8.7$ Hz, 1H), 5.44 (d, $J = 9.6$ Hz, 1H), 5.16 (dd, $J = 10.8, 9.1$ Hz, 1H), 5.00 (dd, $J = 8.1, 2.8$ Hz, 2H), 4.96 – 4.91 (m, 2H), 4.53 (q, $J = 9.2$ Hz, 1H), 4.23 (dt, $J = 10.8, 9.5$ Hz, 1H), 3.91 (dd, $J = 11.9, 1.8$ Hz, 1H), 3.78 (dd, $J = 11.9, 4.6$ Hz, 1H), 3.56 (ddd, $J = 9.6, 4.4, 1.7$ Hz, 1H), 2.31 (td, $J = 7.5, 3.5$ Hz, 2H), 2.19 (t, $J = 7.7$ Hz, 2H), 2.07 – 2.01 (m, 2H), 1.61 – 1.37 (m, 6H), 1.33 – 1.10 (m, 50H), 0.92 – 0.83 (m, 19H), 0.03 – -0.03 (m, 6H).

$^{13}\text{C NMR}$ (101 MHz, CDCl_3) δ 174.43, 172.75, 172.40, 135.52, 128.60, 128.56, 127.88, 127.83, 92.59, 77.31, 77.00, 76.68, 76.23, 76.16, 72.94, 72.89, 69.56, 69.51, 69.46, 61.63, 52.79, 36.76, 34.08, 33.94, 31.89, 29.65, 29.60, 29.49, 29.47, 29.43, 29.37, 29.33, 29.25, 29.11, 29.01, 25.82, 25.58, 24.63, 24.58, 22.66, 18.32, 14.07, -5.19, -5.32.

Synthesis of 17

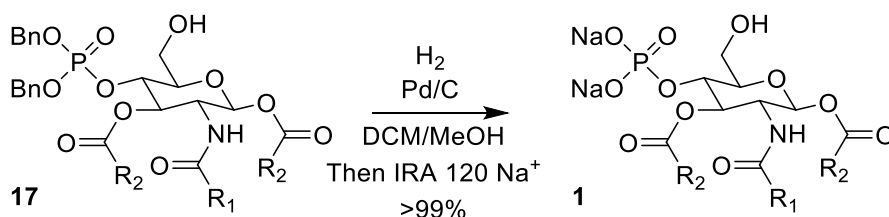


Compound **16** (2.41 g, 2.4 mmol, 1 Eq.) was dissolved in acetone (48 mL) and a 5% v/v solution of H_2SO_4 in H_2O was added at RT (480 μL , 1% v/v). Solution was left stirring for 8 h and monitored by TLC (EtPet/Acetone 8:2). After reaction completion, solution was diluted in AcOEt and washed three times with a saturated NaHCO_3 solution. Organic phase thus obtained was dried with Na_2SO_4 and solvent was removed by rotavapor. Raw product thus obtained was purified by flash column chromatography (EtPet/Acetone 85:15). After purification (2.1 g) of compound **17** was obtained as a white solid in a 90% yield.

^1H NMR (400 MHz, CDCl_3) δ 7.40 – 7.27 (m, 1H), 5.63 (d, $J = 8.8$ Hz, 1H), 5.45 (d, $J = 9.6$ Hz, 1H), 5.18 (dd, $J = 10.7, 9.3$ Hz, 1H), 5.08 – 4.91 (m, 1H), 4.54 (q, $J = 9.5$ Hz, 1H), 4.26 (dd, $J = 19.9, 9.3$ Hz, 1H), 3.87 – 3.74 (m, 1H), 3.47 (d, $J = 9.7$ Hz, 1H), 2.40 – 2.24 (m, 1H), 2.10 – 1.91 (m, 1H), 1.61 – 1.46 (m, 1H), 1.46 – 1.33 (m, 1H), 1.33 – 1.01 (m, 5H), 0.92 – 0.83 (m, 1H).

^{13}C NMR (101 MHz, CDCl_3) δ 174.11, 172.77, 172.49, 128.94, 128.84, 128.72, 128.66, 128.26, 127.95, 92.61, 77.33, 77.01, 76.69, 75.90, 75.87, 72.46, 72.42, 72.15, 72.10, 70.23, 70.17, 70.10, 60.23, 52.78, 36.71, 34.03, 33.71, 31.90, 29.67, 29.62, 29.49, 29.44, 29.38, 29.34, 29.32, 29.26, 29.23, 29.04, 29.01, 25.56, 24.59, 24.48, 22.66, 14.09.

Synthesis of **1**



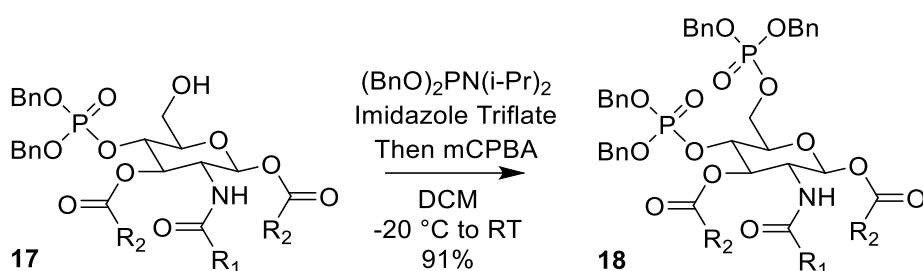
Compound **17** (50 mg, 0.05 mmol, 1 Eq.) was dissolved in a mixture of DCM (2.5 mL) and MeOH (2.5 mL) and put under Ar atmosphere. Pd/C catalyser (10 mg, 20% m/m) was then added to the solution. Gases were then removed in reaction environment, which was subsequently put under H₂ atmosphere. The solution was allowed to stir for 2 h, then H₂ was removed and reaction monitored by TLC (EtPet/acetone 8:2).

Triethylamine (100 µL) was then added to reaction, which was stirred for 15 min. Solution was subsequently filtered on syringe filters PALL 4549T Acrodisc 25 mm with GF/0.45 µm Nylon to remove Pd/C catalyser and solvents were evaporated by rotavapor. Crude product was resuspended in a DCM/MeOH solution and IRA 120 H⁺ was added. After 30 min stirring, IRA 120 H⁺ was filtered, solvents were removed by rotavapor, the crude resuspended in DCM/MeOH and IRA 120 Na⁺ was added. After 30 min stirring, IRA 120 Na⁺ was filtered and solvents were removed by rotavapor. (45 mg) of **1** were obtained as a white powder in a quantitative yield.

¹H NMR (400 MHz, MeOD) δ 5.75 (d, J = 8.9 Hz, 1H), 5.28 (t, J = 9.8 Hz, 1H), 4.28 (q, J = 9.7 Hz, 1H), 4.06 (t, J = 9.6 Hz, 1H), 3.89 – 3.74 (m, 2H), 3.62 (t, J = 9.2 Hz, 1H), 2.42 – 2.25 (m, 5H), 2.09 (t, J = 7.6 Hz, 2H), 1.56 (d, J = 6.4 Hz, 7H), 1.29 (s, 53H), 0.90 (t, J = 6.6 Hz, 9H).

¹³C NMR (101 MHz, MeOD) δ 174.69, 173.32, 172.00, 92.16, 76.22, 76.17, 72.81, 72.78, 72.20, 72.14, 60.30, 52.82, 48.23, 48.02, 47.81, 47.59, 47.38, 47.17, 46.96, 36.05, 33.64, 33.55, 31.67, 31.66, 29.45, 29.39, 29.38, 29.35, 29.26, 29.20, 29.19, 29.14, 29.07, 29.05, 29.02, 28.92, 28.74, 25.58, 24.38, 22.31, 13.00.

Synthesis of 18



Compound **17** (2.36 g, 2.4 mmol, 1 Eq.) and imidazole triflate (1.4 g, 5.4 mmol, 2.25 Eq.) were dissolved in DCM (121 mL, 0.02 M) under inert atmosphere. Dibenzyl N,N-

diisopropylphosphoramidite (1.83 g, 5.3 mmol, 2.2 Eq.) was added to the solution at 0 °C. Reaction was monitored by TLC (EtPet/acetone 9:1); after 30 min, substrate depletion was detected. Solution was then cooled at -20 °C and meta-chloroperbenzoic acid (1.66 g, 9.7 mmol, 4 Eq.), dissolved in 17 ml of DCM, was added dropwise. After 30 min the reaction was allowed to return to RT and left stirring overnight.

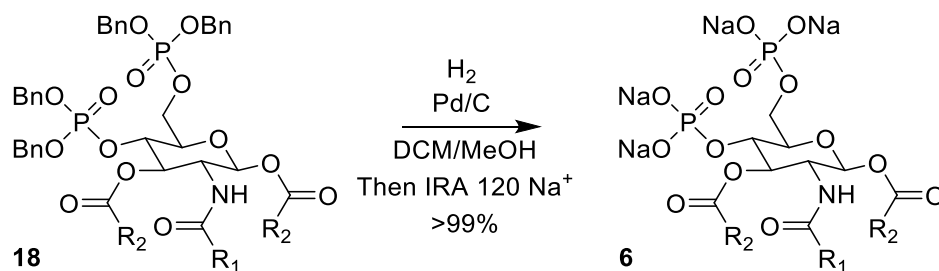
After TLC analysis, reaction was quenched with 15 ml of a saturated NaHCO₃ solution and concentrated by rotavapor. The mixture was then diluted in AcOEt and washed 3 times with a saturated NaHCO₃ solution and three times with a 1 M HCl solution. The organic phase was recovered, dried with Na₂SO₄ and solvent was removed by rotavapor.

Crude thus obtained was purified by flash column chromatography (EtPet/acetone 9:1). 2.41 g of pure compound **18** were obtained as a yellow oil in a 91% yield.

¹H NMR (400 MHz, CDCl₃) δ 7.33 – 7.18 (m, 21H), 5.66 (d, J = 8.8 Hz, 1H), 5.51 (d, J = 9.5 Hz, 1H), 5.18 (dd, J = 10.6, 9.2 Hz, 1H), 5.02 (dd, J = 10.8, 3.3 Hz, 4H), 5.00 – 4.95 (m, 2H), 4.94 – 4.88 (m, 2H), 4.49 – 4.43 (m, 1H), 4.42 – 4.36 (m, 1H), 4.25 (dd, J = 19.8, 9.3 Hz, 1H), 4.16 (ddd, J = 11.8, 7.1, 5.0 Hz, 1H), 3.74 (dd, J = 9.5, 4.2 Hz, 1H), 2.19 (dt, J = 15.9, 7.0 Hz, 5H), 2.07 – 2.01 (m, 2H), 1.49 (dt, J = 14.0, 7.1 Hz, 4H), 1.45 – 1.36 (m, 2H), 1.34 – 1.11 (m, 54H), 0.88 (t, J = 6.8 Hz, 10H).

¹³C NMR (101 MHz, CDCl₃) δ 174.22, 172.82, 172.18, 135.79, 135.72, 135.33, 128.62, 128.58, 128.52, 128.05, 128.00, 127.96, 92.44, 74.11, 72.59, 72.39, 69.38, 65.25, 52.68.

Synthesis of 6



Compound **18** (57 mg, 0.05 mmol, 1Eq.) was dissolved in a mixture of DCM (2.5 mL) and MeOH (2.5 mL) and put under Ar atmosphere. Pd/C catalyser (10 mg, 20% m/m) was then added to the solution. Gases were then removed in reaction environment, which was subsequently put under H₂

atmosphere. The solution was allowed to stir for 2 h; then H₂ was removed and reaction monitored by TLC (EtPet/acetone 8:2).

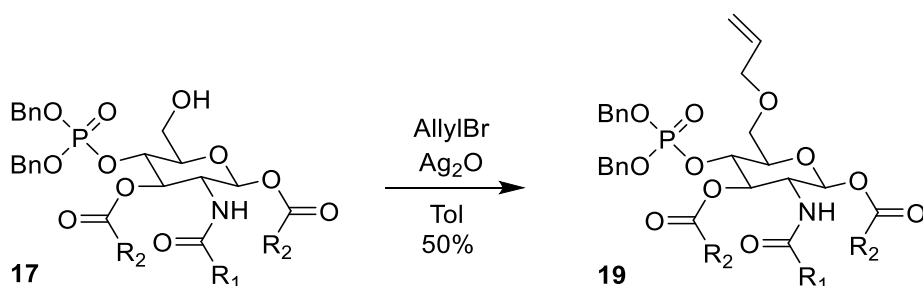
Triethylamine (100 μL) was then added to reaction, which was stirred for 15 min. Solution was subsequently filtered on syringe filters PALL 4549T Acrodisc 25 mm with GF/0.45 μm Nylon to remove Pd/C catalyser and solvents were evaporated by rotavapor. Crude product was resuspended in a DCM/MeOH solution and IRA 120 H⁺ was added. After 30 min stirring, IRA 120 H⁺ was filtered, solvents were removed by rotavapor, the crude resuspended in DCM/MeOH and IRA 120 Na⁺ was added. After 30 min stirring, IRA 120 Na⁺ was filtered and solvents were removed by rotavapor.

(45 mg) of **6** were obtained as a white powder in a quantitative yield.

¹H NMR (400 MHz, MeOD) δ 5.77 (d, J = 8.8 Hz, 1H), 5.32 – 5.23 (m, 1H), 4.39 (dd, J = 18.9, 9.5 Hz, 1H), 4.21 (d, J = 9.7 Hz, 3H), 4.10 – 4.00 (m, 1H), 3.80 (d, J = 9.2 Hz, 1H), 2.44 – 2.24 (m, 6H), 2.09 (t, J = 7.6 Hz, 2H), 1.55 (dd, J = 13.5, 6.9 Hz, 10H), 1.39 – 1.24 (m, 79H), 0.96 – 0.82 (m, 33H).

¹³C NMR (101 MHz, MeOD) δ 174.87, 173.81, 91.22, 72.86, 72.80, 71.25, 68.94, 68.86, 68.80, 64.65, 64.61, 52.10, 48.24, 48.03, 47.82, 47.61, 47.39, 47.18, 46.97, 36.10, 35.63, 33.76, 33.64, 33.55, 33.40, 31.69, 31.63, 29.26, 29.22, 29.18, 29.15, 29.11, 29.06, 29.03, 28.98, 28.84, 28.78, 25.68, 25.62, 24.69, 24.63, 24.38, 22.35, 22.32, 13.06, 13.03, 7.82.

Synthesis of **19**



Compound **17** (100 mg, 0.1 mmol, 1 Eq.) and silver (I) oxide (140 mg, 0.6 mmol, 6 Eq.) were dissolved in toluene (1 mL, 0.1 M) under inert atmosphere. Allyl bromide (51 μL, 0.6 mmol, 6 Eq.) was added to the solution at RT. Reaction was left stirring overnight.

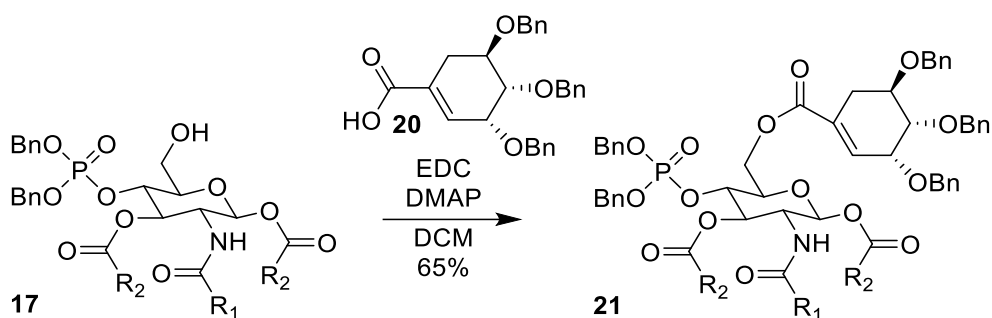
After TLC analysis (EtPet/acetone 8:2), reaction was halted and solution filtered on a celite pad. The organic liquid phase was recovered and solvent was removed by rotavapor.

Crude thus obtained was purified by flash column chromatography (EtPet/acetone 8:2). 50 mg of pure compound **19** were obtained as a yellow oil in a 50% yield.

¹H NMR (400 MHz, CDCl₃) δ 7.38 – 7.22 (m, 10H), 5.91 – 5.77 (m, 1H), 5.64 (d, J = 8.8 Hz, 1H), 5.25 – 5.07 (m, 3H), 5.04 – 4.91 (m, 4H), 4.56 (q, J = 9.3 Hz, 1H), 4.26 (dd, J = 19.8, 9.3 Hz, 1H), 3.99 – 3.90 (m, 2H), 3.73 (dd, J = 11.0, 1.5 Hz, 1H), 3.69 (dd, J = 9.6, 4.4 Hz, 1H), 3.60 (dd, J = 11.0, 4.4 Hz, 1H), 2.40 – 2.24 (m, 2H), 2.18 (dd, J = 16.1, 8.4 Hz, 2H), 2.03 (dd, J = 15.1, 7.1 Hz, 2H), 1.62 – 1.53 (m, 2H), 1.49 (dd, J = 14.2, 7.2 Hz, 2H), 1.41 (dt, J = 13.2, 6.8 Hz, 2H), 1.34 – 1.10 (m, 51H), 0.88 (t, J = 6.8 Hz, 9H).

¹³C NMR (101 MHz, CDCl₃) δ 174.33, 172.77, 172.41, 135.48, 134.43, 128.64, 128.59, 127.92, 117.20, 92.70, 77.32, 77.00, 76.68, 75.29, 75.23, 73.21, 73.15, 72.83, 72.47, 69.67, 69.63, 67.81, 52.83, 36.74, 34.05, 33.93, 31.89, 29.65, 29.62, 29.60, 29.49, 29.44, 29.36, 29.33, 29.31, 29.27, 29.23, 29.10, 29.00, 25.55, 24.57, 24.50, 22.65, 14.07.

Synthesis of **21**

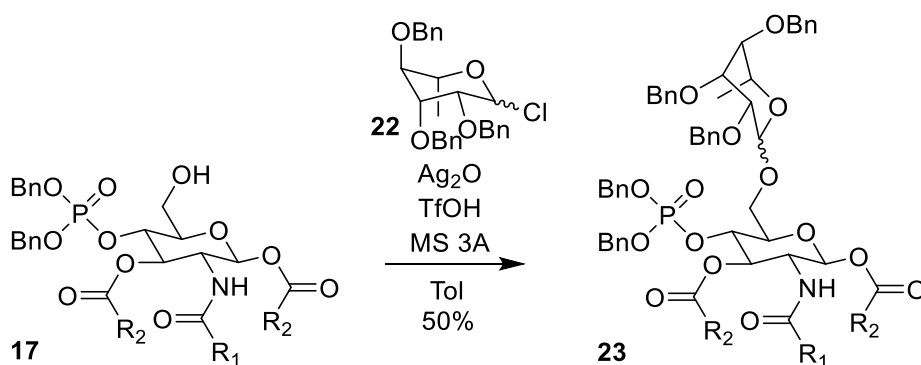


Compound **17** (100 mg, 0.1 mmol, 1 Eq.) and compound **20** (48 mg, 0.11 mmol, 1.1 Eq.) were dissolved in DCM (1 mL, 0.1 M) under inert atmosphere. 1-Ethyl-3-(3-dimethylaminopropyl) carbodiimide (EDC) (192 mg, 0.12 mmol, 1.2 Eq.) and N,N-dimethylaminopyridine (DMAP) was added to the solution at 0° C. Reaction was allowed to return to RT and left stirring overnight.

After reaction completion, solution was diluted in AcOEt and washed three times with a saturated NaHCO₃ solution. Organic phase thus obtained was dried with Na₂SO₄ and solvent was removed by rotavapor.

Crude thus obtained was purified by flash column chromatography (EtPet/acetone 85:15). 100 mg of pure compound **21** were obtained as a white powder in a 65% yield.

Synthesis of **23**



Compound **17** (100 mg, 0.1 mmol, 1 Eq.), compound **22** (57 mg, 0.13 mmol, 1.25 Eq.) and powdered 3 Å molecular sieves (50 mg) were dissolved in toluene (1 mL, 0.1 M) under inert atmosphere and allowed to stir for 1 h. Silver (I) oxide (46 mg, 0.2 mmol, 2 Eq.) was then added to the solution at RT, which was then cooled to 0 °C and triflic acid (4.4 μL, 0.05 mmol, 0.5 Eq.) was added. Reaction was then left stirring overnight at RT.

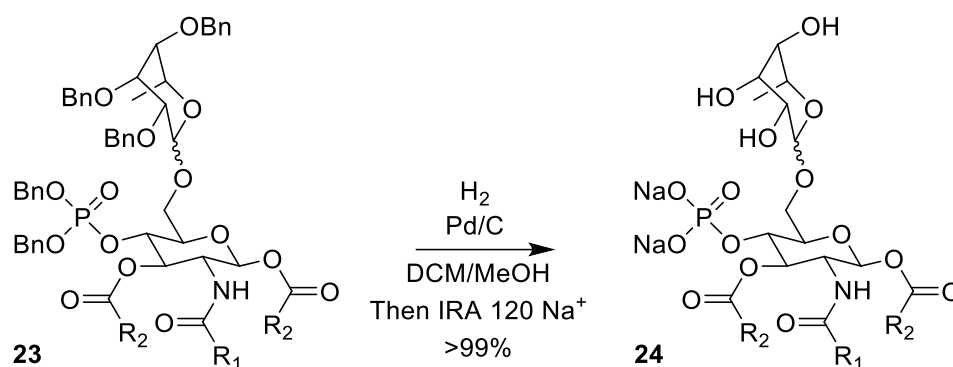
After TLC analysis (EtPet/acetone 8:2), reaction was halted and solution filtered on a celite pad. The organic liquid phase was recovered, diluted in AcOEt and washed three times with NaHCO₃. Organic phase was recovered, dried over Na₂SO₄ and evaporated.

Crude thus obtained was purified by flash column chromatography (toluene/acetone 85:15). 50 mg of a mixture of diastereomers of compound **23** were obtained as a yellow oil in a 40% yield.

¹H NMR (400 MHz, CDCl₃) δ 7.40 – 7.20 (m, 38H), 5.65 (d, J = 8.8 Hz, 1H), 5.61 (s, 1H), 5.40 (s, 1H), 5.24 – 5.18 (m, 1H), 5.14 (s, 1H), 4.91 (d, J = 11.6 Hz, 9H), 4.69 (s, 2H), 4.62 (d, J = 2.2 Hz, 4H), 4.57 – 4.37 (m, 2H), 4.23 (s, 1H), 2.40 – 2.26 (m, 3H), 2.13 (ddd, J = 13.7, 7.6, 4.4 Hz, 3H), 2.05 (s, 3H), 1.57 (s, 6H), 1.47 – 1.36 (m, 3H), 1.29 (s, 79H), 0.88 (t, J = 6.8 Hz, 14H).

¹³C NMR (101 MHz, CDCl₃) δ 174.23, 172.81, 172.43, 138.66, 138.63, 135.24, 128.75, 128.69, 128.67, 128.62, 128.50, 128.40, 128.31, 128.27, 128.20, 128.06, 127.92, 127.88, 127.71, 127.64, 127.56, 127.41, 127.39, 98.55, 92.54, 80.36, 79.72, 77.32, 77.00, 76.68, 75.36, 74.99, 72.76, 72.51, 71.93, 69.72, 69.66, 69.63, 69.58, 68.09, 64.99, 52.74, 36.77, 34.03, 33.89, 31.89, 30.90, 29.66, 29.60, 29.49, 29.46, 29.36, 29.34, 29.22, 29.09, 29.02, 25.59, 24.58, 24.46, 22.66, 17.97, 14.09.

Synthesis of **24**



Compound **23** (70 mg, 0.05 mmol, 1 Eq.) was dissolved in a mixture of DCM (2.5 mL) and MeOH (2.5 mL) and put under Ar atmosphere. Pd/C catalyser (10 mg, 20% m/m) was then added to the solution. Gases were then removed in reaction environment, which was subsequently put under H₂ atmosphere. The solution was allowed to stir for 2 h, then H₂ was removed and reaction monitored by TLC (EtPet/acetone 8:2).

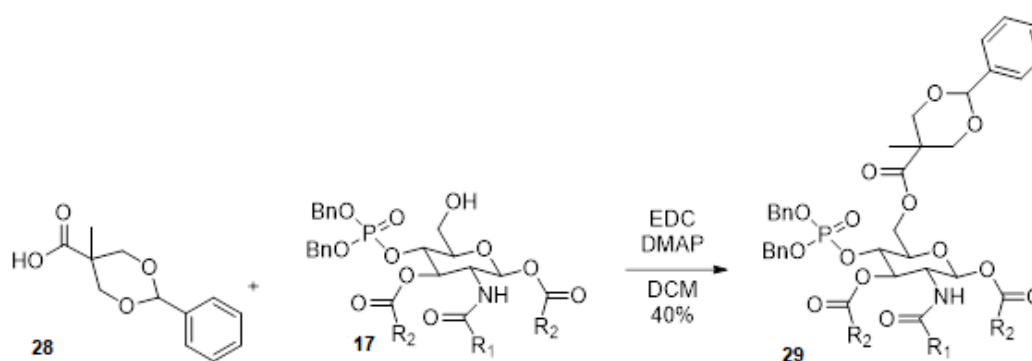
Triethylamine (100 μL) was then added to reaction, which was stirred for 15 min. Solution was subsequently filtered on syringe filters PALL 4549T Acrodisc 25 mm with GF/0.45 μm Nylon to remove Pd/C catalyser and solvents were evaporated by rotavapor. Crude product was resuspended in a DCM/MeOH solution and IRA 120 H⁺ was added. After 30 min stirring, IRA 120 H⁺ was filtered, solvents were removed by rotavapor, the crude resuspended in DCM/MeOH and IRA 120 Na⁺ was added. After 30 min stirring, IRA 120 Na⁺ was filtered and solvents were removed by rotavapor. (50 mg) of **24** were obtained as a white powder in a quantitative yield, as a mixture of diastereomers.

¹H NMR (400 MHz, MeOD) δ 5.76 (dd, J = 8.8, 4.7 Hz, 1H), 5.29 (dd, J = 10.5, 9.1 Hz, 1H), 4.76 (d, J = 1.2 Hz, 1H), 4.36 (dd, J = 18.8, 9.4 Hz, 1H), 4.08 (ddt, J = 19.6, 14.2, 5.9 Hz, 4H), 3.91 (dd, J = 3.4, 1.6

Hz, 2H), 3.83 – 3.75 (m, 2H), 3.75 – 3.62 (m, 5H), 3.44 – 3.34 (m, 3H), 2.48 – 2.27 (m, 7H), 2.14 – 2.08 (m, 2H), 1.60 (s, 11H), 1.40 – 1.21 (m, 96H), 0.92 (t, $J = 6.8$ Hz, 17H).

^{13}C NMR (101 MHz, MeOD) δ 174.68, 173.39, 171.99, 101.03, 92.10, 75.14, 72.96, 72.66, 72.32, 70.90, 70.57, 68.47, 65.71, 52.71, 48.23, 48.02, 47.81, 47.59, 47.38, 47.17, 46.96, 36.06, 33.66, 33.57, 31.69, 29.39, 29.30, 29.09, 28.95, 28.76, 28.44, 25.59, 24.42, 22.33, 16.62, 13.03.

Synthesis of 29

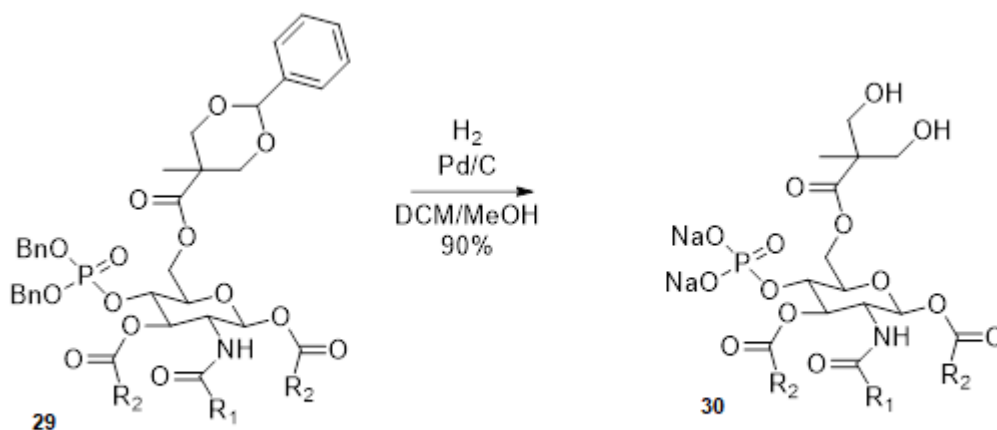


Compound **17** (100 mg, 0.11 mmol, 1 Eq.) and compound **28** (24 mg, 0.11 mmol, 1.1 Eq.) were dissolved in dry DCM (1 ml, 0.1 M) under Ar atmosphere. Then, EDC (23 mg, 0.12 mmol, 1.2 Eq.) and DMAP (0.112 mg, 0.01 mmol, 0.1 Eq.) were added to the solution at 0° C. Subsequently, the solution was allowed to return at room temperature and was stirred overnight. Reaction, monitored by TLC (EtPet/Acetone 8:2), was then stopped and the solution concentrated under reduced pressure. Then it was diluted with AcOEt and washed three times with HCl. Organic phase thus obtained was dried with Na_2SO_4 and solvent was removed by rotavapor. Raw product thus obtained (550 mg) was purified using flash column chromatography (EtPet/Acetone 85:15). After purification, 17 mg of compound **29** were obtained, in 40% yield.

^1H NMR (400 MHz, CDCl_3) δ 7.43 (dd, $J = 6.8, 2.9$ Hz, 1H), 7.36 – 7.19 (m, 10H), 5.60 (d, $J = 8.7$ Hz, 1H), 5.45 (s, 1H), 5.36 (d, $J = 9.7$ Hz, 1H), 5.15 (dd, $J = 10.7, 9.1$ Hz, 1H), 4.97 (t, $J = 9.9$ Hz, 1H), 4.93 – 4.80 (m, 1H), 4.67 (ddd, $J = 18.4, 12.5, 2.3$ Hz, 2H), 4.51 (q, $J = 9.3$ Hz, 1H), 4.22 (td, $J = 12.5, 7.2$ Hz, 1H), 3.79 (dd, $J = 9.5, 3.1$ Hz, 1H), 3.64 (d, $J = 10.2$ Hz, 1H), 2.36 – 2.23 (m, 1H), 2.21 – 2.09 (m, 1H), 2.09 – 1.99 (m, 1H), 1.04 (s, 2H), 0.98 – 0.75 (m, 5H).

^{13}C NMR (101 MHz, CDCl_3) δ 172.86, 134.44, 129.73, 128.98, 128.68, 128.27, 128.08, 127.97, 127.89, 126.22, 126.09, 101.61, 92.55, 77.31, 76.99, 76.67, 73.09, 72.47, 72.27, 69.82, 67.34, 61.47, 52.67, 50.48, 42.54, 36.74, 34.02, 31.89, 29.60, 29.44, 29.33, 28.99, 25.57, 24.50, 22.66, 19.14, 17.39, 14.08.

Synthesis of 30

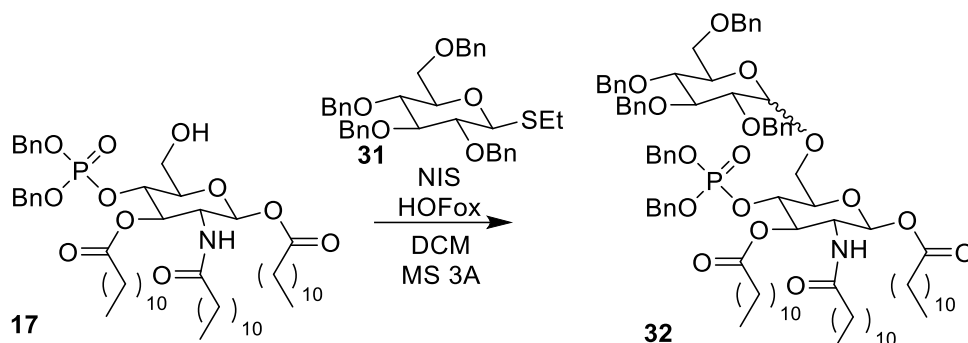


Compound **29** (30 mg, 0.03 mmol, 1 Eq.) was dissolved in a 1:1 mixture of dry DCM and dry MeOH (3 ml, 0.01 M) under Ar atmosphere. Then, Pd/C catalyst (6 mg, 20% m/m) was added always under inert atmosphere. The reaction is left under vacuum for some minutes. Then, the hydrogen was added, and the reaction stirred overnight at room temperature. Reaction, monitored by TLC (Toluene/Acetone 85:15), was then stopped. The hydrogen was completely removed and the Ar atmosphere restored. Triethylamine (60 μl , 2% v/v) was added to the solution that stirred for 30 minutes. Then, the catalyst was removed by filtration on syringe filters PALL 4549T Acrodisc 25 mm with GF/0.45 μm Nylon to remove Pd/C catalyser and solvents were evaporated by rotavapor. Raw compound was resuspended in DCM/MeOH 1:1 and IRA 120 H+ was added to the solution. After 30 minutes, the acid resin was removed, and sodic resin was added instead. The solution was stirred again for 30 minutes; then Solvent was removed by rotavapor, obtaining 52,9 mg of compound **30** were obtained, in >99% yield.

^1H NMR (400 MHz, MeOD) δ 5.76 (d, $J = 8.9$ Hz, 1H), 5.33 – 5.24 (m, 1H), 4.54 – 4.38 (m, 2H), 4.37 – 4.29 (m, 1H), 4.14 – 4.05 (m, 1H), 3.89 (d, $J = 7.3$ Hz, 1H), 3.78 (q, $J = 9.0$ Hz, 1H), 3.67 (dd, $J = 16.4$,

11.6 Hz, 4H), 3.56 (t, $J = 6.6$ Hz, 1H), 2.49 – 2.27 (m, 5H), 2.23 – 2.08 (m, 2H), 1.59 (d, $J = 6.4$ Hz, 7H), 1.22 – 1.15 (m, 3H).

Synthesis of **32**



Compound **17** (100 mg, 0.1 mmol, 1 Eq.), compound **31** (110 mg, 0.2 mmol, 2 Eq.) and powdered 3a molecular sieves (330 mg) were dissolved in DCM (2 mL, 0.2 M) under inert atmosphere and allowed to stir for 1 h. NIS (45 mg, 0.2 mmol, 2 Eq.) and HOFox (8.5 mg, 0.5 mmol, 0.5 Eq.) were then added to the solution at RT. Reaction was then left stirring c.a 1.5h at RT.

After TLC analysis (EtPet/acetone 8:2), reaction was stopped and solution filtered on a cotton pad. The organic liquid phase was recovered, diluted in AcOEt and washed three times with $\text{Na}_2\text{S}_2\text{O}_3$. Organic phase was recovered, dried over Na_2SO_4 and evaporated.

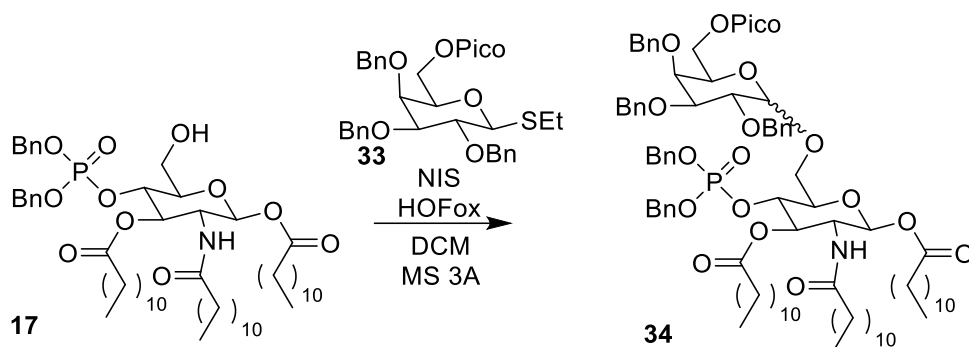
Crude thus obtained was purified by flash column chromatography (EtPet/acetone 80:20). 120 mg of a mixture of diastereomers of compound **32** were obtained as a yellow oil in an 84% yield.

^1H NMR (400 MHz, CDCl_3) δ 7.40 – 7.20 (m, 32H), 7.11 (ddd, $J = 13.3, 6.8, 2.7$ Hz, 2H), 5.62 (dd, $J = 8.8, 3.8$ Hz, 1H), 5.34 (d, $J = 9.5$ Hz, 1H), 5.27 (d, $J = 9.6$ Hz, 0H), 5.13 (td, $J = 10.9, 8.9$ Hz, 1H), 5.00 – 4.85 (m, 6H), 4.79 (dd, $J = 10.9, 2.5$ Hz, 1H), 4.73 (d, $J = 11.0$ Hz, 1H), 4.70 – 4.64 (m, 2H), 4.63 – 4.54 (m, 2H), 4.53 – 4.45 (m, 1H), 4.44 – 4.21 (m, 4H), 3.93 (t, $J = 9.3$ Hz, 1H), 3.87 – 3.75 (m, 3H), 3.70 – 3.51 (m, 5H), 3.46 – 3.33 (m, 1H), 2.22 (t, $J = 7.6$ Hz, 1H), 2.13 (dt, $J = 17.2, 7.7$ Hz, 3H), 2.03 (q, $J = 7.3$ Hz, 3H), 1.50 (s, 3H), 1.40 (p, $J = 7.1$ Hz, 3H), 1.22 (d, $J = 16.1$ Hz, 52H), 0.88 (t, $J = 6.7$ Hz, 10H).

^{13}C NMR (101 MHz, CDCl_3) δ 174.35, 172.75, 172.22, 138.97, 138.22, 138.03, 128.74, 128.69, 128.67, 128.59, 128.45, 128.35, 128.29, 128.22, 128.12, 128.02, 127.91, 127.89, 127.83, 127.80,

127.73, 127.69, 127.63, 127.48, 127.43, 103.88, 97.27, 92.65, 92.54, 84.49, 81.90, 79.78, 77.61, 77.50, 77.34, 77.02, 76.70, 75.58, 74.95, 74.64, 73.43, 73.33, 73.27, 72.80, 72.71, 70.19, 69.73, 68.41, 52.92, 36.83, 34.03, 33.94, 31.93, 29.69, 29.64, 29.51, 29.47, 29.39, 29.37, 29.33, 29.26, 29.14, 29.04, 25.64, 24.60, 24.53, 24.36, 22.69, 14.12.

Synthesis of **34**



Compound **17** (100 mg, 0.1 mmol, 1 Eq.), compound **33** (110 mg, 0.2 mmol, 2 Eq.) and powdered 3a molecular sieves (330 mg) were dissolved in DCM (2 mL, 0.2 M) under inert atmosphere and allowed to stir for 1 h. Reaction was cooled at 0° C and Bi(OTf)₃ (50 mg, 0.075 mmol, 0.75 Eq.) and was then added to the solution. Reaction was then left stirring overnight at RT.

After TLC analysis (EtPet/acetone 7:3), reaction was stopped and solution filtered on a celite pad. The organic liquid phase was recovered, diluted in AcOEt and washed three times with NaHCO₃. Organic phase was recovered, dried over Na₂SO₄ and evaporated.

Crude thus obtained was purified by flash column chromatography (EtPet/acetone 70:30), which allowed to separate the two diastereomers. 125 mg of total compound **34** (α+β) were obtained as a yellow oil in a 94% yield.

34α

¹H NMR (400 MHz, CDCl₃) δ 8.75 (dt, J = 4.6, 1.4 Hz, 1H), 8.06 (d, J = 7.8 Hz, 1H), 7.89 (td, J = 7.7, 1.8 Hz, 1H), 7.47 (ddd, J = 7.6, 4.7, 1.2 Hz, 1H), 7.40 – 7.13 (m, 30H), 5.53 (d, J = 8.8 Hz, 1H), 5.32 (d, J = 9.7 Hz, 1H), 5.10 (dd, J = 10.8, 8.9 Hz, 1H), 4.99 – 4.90 (m, 5H), 4.89 (d, J = 3.5 Hz, 1H), 4.83 (d, J = 11.7 Hz, 1H), 4.75 (d, J = 11.8 Hz, 1H), 4.68 (dd, J = 11.7, 6.1 Hz, 2H), 4.61 (d, J = 11.4 Hz, 1H), 4.40 – 4.30 (m, 2H), 4.30 – 4.25 (m, 1H), 4.16 – 4.09 (m, 1H), 4.05 (dd, J = 10.2, 2.9 Hz, 2H), 3.98 (dd, J =

Results and Discussion: Chapter II

10.1, 2.7 Hz, 1H), 3.90 (d, $J = 2.5$ Hz, 1H), 3.78 (td, $J = 9.5, 5.4$ Hz, 3H), 2.26 (q, $J = 7.4$ Hz, 2H), 2.15 (d, $J = 7.8$ Hz, 2H), 2.06 – 1.99 (m, 3H), 1.49 (q, $J = 7.4$ Hz, 4H), 1.41 (p, $J = 7.3$ Hz, 1H), 1.23 (d, $J = 7.7$ Hz, 61H), 0.88 (qt, $J = 3.8, 1.8$ Hz, 12H).

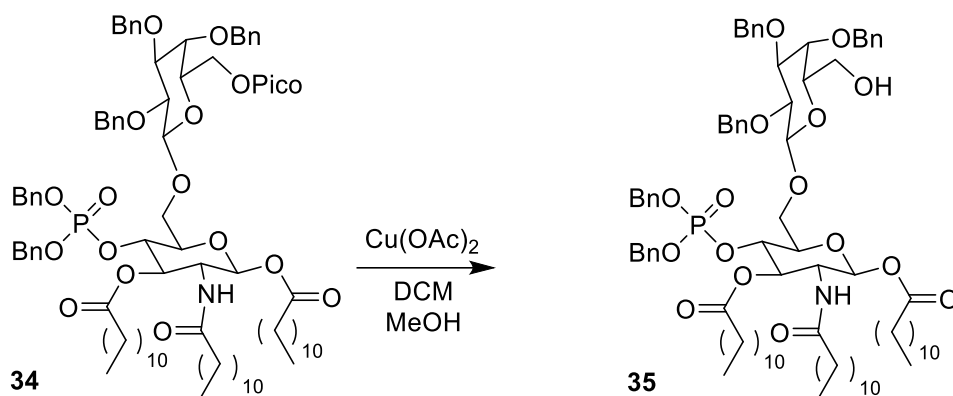
^{13}C NMR (101 MHz, CDCl_3) δ 174.24, 172.55, 172.30, 164.62, 149.93, 147.89, 138.46, 138.29, 137.14, 128.66, 128.39, 128.30, 128.07, 127.87, 127.69, 127.63, 127.46, 126.92, 125.40, 97.29, 92.61, 79.00, 76.34, 75.16, 74.57, 73.59, 73.19, 72.81, 69.70, 68.80, 65.18, 65.03, 52.82, 36.82, 33.97, 31.92, 29.64, 29.52, 29.36, 29.30, 29.14, 29.06, 25.63, 24.60, 22.69, 14.11.

34 β

^1H NMR (400 MHz, CDCl_3) δ 8.73 (dd, $J = 4.9, 1.7$ Hz, 1H), 7.95 (d, $J = 7.8$ Hz, 1H), 7.78 (td, $J = 7.8, 1.8$ Hz, 1H), 7.46 – 7.41 (m, 1H), 7.29 (dddd, $J = 21.3, 16.3, 13.5, 8.4, 4.4$ Hz, 27H), 5.63 (d, $J = 8.8$ Hz, 1H), 5.36 (d, $J = 9.6$ Hz, 1H), 5.12 (dd, $J = 10.8, 8.9$ Hz, 1H), 4.97 (d, $J = 11.7$ Hz, 1H), 4.95 – 4.86 (m, 5H), 4.81 (d, $J = 11.8$ Hz, 1H), 4.71 (d, $J = 11.9$ Hz, 1H), 4.65 (dd, $J = 11.2, 5.6$ Hz, 2H), 4.39 (d, $J = 8.0$ Hz, 1H), 4.48 – 4.34 (m, 2H), 4.34 – 4.22 (m, 2H), 3.90 – 3.82 (m, 3H), 3.68 (t, $J = 4.6$ Hz, 1H), 3.64 (dd, $J = 9.2, 5.7$ Hz, 1H), 3.51 (dd, $J = 9.8, 2.9$ Hz, 1H), 2.19 – 2.06 (m, 3H), 2.02 (t, $J = 7.7$ Hz, 2H), 1.49 (t, $J = 7.3$ Hz, 2H), 1.40 (p, $J = 7.2$ Hz, 1H), 1.35 – 1.04 (m, 55H), 0.88 (td, $J = 6.8, 2.1$ Hz, 10H).

^{13}C NMR (101 MHz, CDCl_3) δ 174.24, 172.75, 172.16, 164.53, 149.91, 147.67, 138.78, 138.53, 138.20, 137.00, 128.65, 128.62, 128.51, 128.36, 128.28, 128.25, 128.04, 127.98, 127.62, 127.57, 127.51, 126.90, 125.35, 104.08, 92.54, 81.88, 79.16, 74.41, 73.25, 72.85, 72.11, 69.77, 68.46, 64.19, 52.87, 36.77, 33.89, 31.92, 29.69, 29.63, 29.36, 29.34, 29.22, 29.12, 28.99, 25.59, 24.60, 24.34, 22.69, 14.12.

Synthesis of 35



To a solution of **34** (75 mg, 0.5 mmol, 0.5 Eq.) in a 3:1 mixture of DCM/MeOH (5 mL, 0.1 M) under inert atmosphere, Cu(OAc)_2 (15 mg, 0.75 mmol, 1.5 Eq.) was added at RT.

Solution is left stirring for c.a. 2h and then monitored by TLC (EtPet/AcOEt 6:4).

Solvent is evaporated by rotavapor and solution is purified by flash chromatography (EtPet/AcOEt 6:4) without further purification.

55 mg of compound **35** were recovered in an 80% yield

$^1\text{H NMR}$ (400 MHz, CDCl_3) δ 7.40 – 7.22 (m, 29H), 5.62 (d, $J = 8.7$ Hz, 1H), 5.38 (d, $J = 9.6$ Hz, 1H), 5.12 (dd, $J = 10.8, 8.9$ Hz, 1H), 4.97 – 4.88 (m, 6H), 4.80 (d, $J = 11.9$ Hz, 1H), 4.71 (d, $J = 11.9$ Hz, 1H), 4.65 (dd, $J = 13.1, 11.3$ Hz, 2H), 4.39 – 4.36 (m, 1H), 4.35 (d, $J = 5.5$ Hz, 1H), 4.33 (d, $J = 7.4$ Hz, 1H), 4.27 (dt, $J = 10.8, 7.4$ Hz, 1H), 3.86 – 3.80 (m, 2H), 3.72 (d, $J = 3.3$ Hz, 2H), 3.72 – 3.63 (m, 2H), 3.47 (dd, $J = 9.7, 2.9$ Hz, 1H), 3.39 (dd, $J = 11.5, 4.8$ Hz, 1H), 3.31 (dd, $J = 7.2, 4.9$ Hz, 1H), 2.16 (dd, $J = 8.8, 7.1$ Hz, 2H), 2.09 (ddd, $J = 8.7, 7.2, 5.1$ Hz, 2H), 2.03 (t, $J = 7.7$ Hz, 2H), 1.51 (q, $J = 7.3$ Hz, 2H), 1.41 (dq, $J = 14.9, 7.0$ Hz, 4H), 1.33 – 1.09 (m, 55H), 0.88 (td, $J = 6.9, 2.0$ Hz, 10H).

$^{13}\text{C NMR}$ (101 MHz, CDCl_3) δ 174.21, 172.80, 172.24, 138.79, 138.52, 138.27, 135.34, 128.72, 128.66, 128.64, 128.53, 128.40, 128.26, 128.10, 128.06, 127.89, 127.64, 127.59, 127.51, 103.82, 92.52, 82.12, 79.15, 75.18, 75.09, 74.94, 74.20, 73.75, 73.69, 73.44, 73.24, 72.79, 69.87, 69.81, 67.94, 62.16, 52.74, 36.77, 33.91, 33.86, 31.93, 29.69, 29.64, 29.51, 29.47, 29.36, 29.33, 29.29, 29.23, 29.11, 29.00, 25.59, 24.59, 24.39, 22.70, 14.12.

Biology

The ability of compounds FP20, FP21, FP22, FP23 and FP24 to selectively activate TLR4 was initially investigated on specific HEK reporter cell lines. HEK-Blue™ hTLR4 and HEK-Blue™ hTLR2 (InvivoGen) are cell lines designed to study the activation of human TLR4 and TLR2 receptors, respectively, by monitoring the activation of transcription factors NF-κB and AP-1. Stimulation with TLR4 ligands (in the case of HEK-Blue hTLR4) or with TLR2 ligands (in the case of HEK-Blue hTLR2) activates NF-κB and AP-1, inducing the production and release of the SEAP reporter gene (phosphatase secreted embryonic alkaline) in the extracellular environment. The analysis of the reporter gene was performed using the QUANTI-Blue™ colorimetric assay (InvivoGen), a substrate of SEAP, which generates a chromogenic product whose absorbance is read at 630 nm. The agonist activity of the molecules was tested by treating HEK-Blue hTLR4 cells for 18 hours with increasing concentrations of the compounds (0.1-1-10-25μM) and using MPLA (0.1-1-10 μM) and S-LPS (100 ng / mL) as a reference and positive receptor activation control, respectively. The results obtained show that the molecules FP20, FP21, FP22, FP23 and FP24 are able to induce the activation of TLR4 in a dose-dependent manner (**Figure 44A**). The molecules were subsequently tested on the HEK-Blue hTLR2 cell line with the aim of excluding the activation of this receptor. In this regard, HEK-Blue hTLR2 cells were treated with the same compounds and at the same concentrations as the tests conducted previously and the compound PAM2CSK4 was used as a positive control for TLR2 activation. As expected, stimulation with PAM2CSK4 induced a strong activation of TLR2, while treatment with compounds FP20, FP21, FP22, FP23 and FP24 did not produce any activation (**Figure 44B**).

Following the results obtained from screening tests on HEK cells, the biological activity of compounds FP20, FP21, FP22, FP23 and FP24 was investigated in human and mouse macrophage cell lines. THP-1-X Blue™ cell lines, monocytes differentiated into macrophages following treatment with PMA 100 ng / mL, and RAW-Blue™ were used. Similarly to HEK-Blue™ cells, THP-1 X-Blue™ and RAW-Ox stably express the SEAP reporter gene, under the control of transcription factors NF-κB and AP-1. The cells were treated as previously described. The results show that all compounds induce the activation of NF-κB, both on human (**Figure 45A**) and murine macrophages (**Figure 45B**); the FP23 compound is the only one statistically insignificant on the human macrophage line. Furthermore, on the RAW-blue line the compounds are active at the lowest concentration tested (0.1 μM), while on the THP-1-X-Blue™ the compounds activate significantly starting from a concentration 100 times higher (10 μM).

To evaluate the cytotoxicity of compounds FP20, FP21, FP22, FP23 and FP24, THP-1-X-Blue cells differentiated into macrophages (**Figure 46**) and RAW-Blue (**Figure 47**) were treated with increasing concentrations of the test compounds (0.1, 1, 10, 25, 50 μM). The toxicity of the compounds was evaluated by MTT viability assay (3- (4,5-dimethylthiazol-2-yl) -2,5-diphenyltetrazolium bromide). The results obtained show that the compounds are non-toxic on the THP-1-X-Blue cell line, however at the highest concentration tested (50 μM) there is a decrease in cell viability following treatment with FP20 and FP23 (**Figure 46**). The results on the mouse macrophage line show an increase in the toxicity of the compounds at a concentration of 50 μM , while the compound FP23 is the only one to show toxicity at a concentration of 25 μM .

FP200 activity was then assessed on human monocytes cell line THP-1-X-Blues, described before. Cells were treated with compounds FP11, FP112, FP20, FP200 and FP21 in increasing concentrations (0.1, 1, 10, 20 μM) and using MPLA (0.1-1-10 μM) and S-LPS (100 ng / mL) as a reference and positive receptor activation control, respectively. The result shows that all compounds induce the activation of NF- κB in a dose dependent manner.

Compound FP207, functionalized with MPA, was tested *in vitro* on human THP-1-X-Blue cells to evaluate the NF- κB activation. The molecule was tested at the same concentrations used for FP22 and FP23.

Also in this case, the results revealed that compound **FP207** is active on TLR4 and induces the production of the transcription factor. Its agonist activity has a concentration-dependent manner as the previous case. Astonishingly, it is more active than FP20 and also comparable to LPS at 25 μM . This is a great result because it will be possible to use less quantity of product to obtain the same inflammatory effect compared to FP20, which will be advantageous in two ways: pharmacologically any possible collateral effect is reduced; while economically this means that less expenses are required to achieve greater results and larger public.

A preliminary test to investigate the toxicity of this functionalized compound was performed, even though without a triplicate. However preliminary, those data suggest that the molecule is non-toxic in the concentration range from 1 to 25mM.

In vitro and *vivo* data regarding the compounds disclosed in WO2019/092572 are provided below.

TLR4 activation by synthetic agonists

The ability of FP molecules to activate human TLR4 was assessed using HEK-Blue hTLR4 cells. These are a HEK293-derived cell line stably transfected with the LPS receptors CD14, TLR4 and MD-2 and a reporter gene, secreted embryonic alkaline phosphatase (SEAP) placed under the control of two TLR4-dependent transcription factors (NF- κ B and AP-1). The HEK-Blue hTLR4 cells were treated with increasing concentrations (0.1-25 μ M) of FP11, FP112 and FP111 over 18 hours. Stimulation with smooth chemotype of LPS (S-LPS) served as a positive control for the activation of the TLR4-mediated pathway.

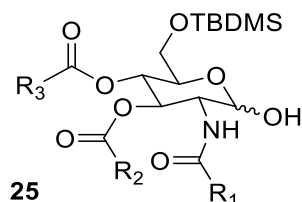
Molecules FP11 and FP112 induced the release of the SEAP reporter protein in the medium in a concentration-dependent manner, indicating that both compounds activate NF- κ B and AP-1, while FP111 was inactive (**Figure 48A**). The three compounds did not inhibit LPS-induced SEAP production, suggesting they lack a TLR4 antagonistic activity (**Figure 48B**). A lack of activity on HEK-Blue Null cells, which carry the same SEAP reporter gene but lack the LPS receptors, confirmed that both FP11 and FP112 act via TLR4 (**Figure 48C**). To confirm the selectivity on TLR4 over TLR2, the molecules were also tested on the HEK-Blue cells expressing the human Toll-like receptor 2 (hTLR2), resulting in no agonist activity (**Figure 48D**). These data agree with the *in vitro* binding results and suggest that FP11 and FP112 are specific TLR4 agonists that directly interact with the co-receptor MD-2.

Adjuvant activity of FP11 and FP112 and in vivo toxicity: OVA immunization experiments

The ability of FP11 and FP112 to induce immune responses *in vivo* was compared to MPLA by evaluating antibody production in C57Bl/6 mice immunized with chicken ovalbumin (OVA) as a model antigen. Has been first evaluated the toxicity of FPs in a pilot experiment in which mice were injected subcutaneously with 10 μ g of the FP11 and FP112. The results showed that the two test adjuvants had no obvious adverse effect on mice, as assessed by the local response at the injection site and by determining the animal weight and state of alertness over 7 days (**Figure 49A**). Next, mice were immunized with the tested adjuvants mixed with ovalbumin (OVA). The induction of antibody was evaluated 21 days post immunization. The results showed that mice immunized with the test adjuvants exhibited marginally higher levels of anti-OVA total IgG after prime immunization compared to OVA-immunized control and significantly lower levels compared to MPLA-OVA immunized animals (**Figure 49B**, Prime Immunization). In contrast, after a boost immunization given on day 22 and examined for ova-specific antibody titers 14 days later, the IgG levels in the FP112-immunized mice were higher than those in the FP11-immunized group (**Figure 49B**, Booster

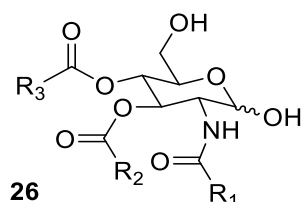
immunization). These data indicate that in agreement with in vitro and in cell results, FP112 is a more effective adjuvant in vivo than FP11 and has a potency comparable or even greater than MPLA.

Impurity 1 of step 6 in FP11 Synthesis, reference Figure 50



¹H NMR (400 MHz, CDCl₃) δ 6.04 (d, *J* = 9.7 Hz, 1H), 5.63 (dd, *J* = 9.7, 7.3 Hz, 1H), 3.87 (dt, *J* = 7.5, 3.9 Hz, 1H), 3.77 – 3.70 (m, 3H), 3.68 (dd, *J* = 10.5, 4.3 Hz, 1H), 2.36 (dd, *J* = 14.7, 6.9 Hz, 2H), 2.32 – 2.26 (m, 3H), 1.67 (dt, *J* = 15.3, 7.7 Hz, 2H), 1.59 (dt, *J* = 20.5, 7.1 Hz, 4H), 1.27 (d, *J* = 16.5 Hz, 62H), 0.91 – 0.84 (m, 20H), 0.05 (d, *J* = 8.4 Hz, 7H).

Impurity 2 of step 6 in FP11 Synthesis, reference Figure 51 (¹H NMR) Figure 52 (¹³C NMR)

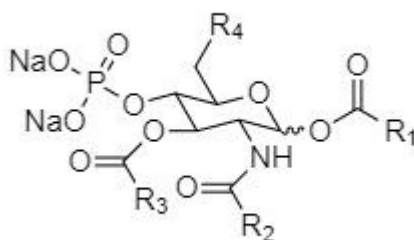


¹H NMR (400 MHz, CDCl₃) δ 6.01 (d, *J* = 9.1 Hz, 1H), 5.40 – 5.30 (m, 1H), 5.21 (t, *J* = 6.7 Hz, 1H), 5.10 – 4.99 (m, 2H), 4.22 (td, *J* = 10.7, 3.4 Hz, 1H), 4.04 (ddd, *J* = 10.2, 4.3, 2.0 Hz, 1H), 3.68 (d, *J* = 11.7 Hz, 1H), 3.61 – 3.53 (m, 1H), 2.32 – 2.19 (m, 5H), 2.18 – 2.06 (m, 3H), 1.62 – 1.46 (m, 8H), 1.34 – 1.18 (m, 62H), 0.87 (t, *J* = 6.8 Hz, 11H).

¹³C NMR (101 MHz, CDCl₃) δ 174.14, 173.65, 173.12, 91.40, 77.32, 77.01, 76.69, 70.37, 69.67, 68.54, 61.19, 52.49, 36.68, 34.19, 34.13, 31.90, 29.66, 29.63, 29.60, 29.54, 29.52, 29.46, 29.39, 29.34, 29.33, 29.29, 29.27, 29.19, 29.15, 25.60, 24.92, 23.82, 22.66, 14.08.

CLAIMS

1. A compound of formula 1



wherein R_1 is a saturated C_5 - C_{15} alkyl chain optionally substituted,

wherein R_2 is a saturated C_5 - C_{15} alkyl chain optionally substituted,

wherein R_3 is a saturated C_5 - C_{15} alkyl chain optionally substituted,

wherein R_4 is any substituent that can be linked by means of a bond between C_6 and a suitable atom and/or any substituent which possesses an oxygen or a nitrogen atom that can bind to C_6 .

2. The compound according to claim 1, wherein R_4 chain is an hydroxyl group (OH), a phosphate group (PO_4^{2-}), an azide group (N_3), an amine group (NH_2), an acyl group ($O(C=O)R$) or an alkyl group (OR) or a glycosyl group.

3. The compound according to claims 1 or 2, wherein R_1 , R_2 , R_3 , different from each other.

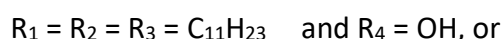
4. The compound according to claims 1 or 2, wherein at least two of R_1 , R_2 , and R_3 , are identical.

5. The compound according to any one of claims 1 to 4, wherein at least one of R_1 , R_2 , and R_3 , is substituted.

6. The compound according to any one of claims 1 to 5, wherein at least one of R_1 , R_2 , and R_3 , is free from $-OH$ substituents on position 2.

7. The compound according to any one of claims 1 to 4, wherein at least one of R_1 , R_2 or R_3 , is unsubstituted.

8. The compound according to any one of claims 1 to 7, wherein



- $R_1 = R_3 = C_{13}H_{27}$; $R_2 = C_{11}H_{23}$ and $R_4 = OH$, or
- $R_1 = R_2 = R_3 = C_9H_{19}$ and $R_4 = OH$, or
- $R_1 = R_2 = R_3 = C_{13}H_{27}$ and $R_4 = OH$, or
- $R_1 = R_3 = C_9H_{19}$; $R_2 = C_{11}H_{23}$ and $R_4 = OH$, or
- $R_1 = R_2 = R_3 = C_{11}H_{23}$ and $R_4 = PO_4^{2-}$, or
- $R_1 = R_2 = R_3 = C_9H_{19}$ and $R_4 = PO_4^{2-}$, or
- $R_1 = R_2 = R_3 = C_{13}H_{27}$ and $R_4 = PO_4^{2-}$, or
- $R_1 = R_2 = R_3 = C_{11}H_{23}$ and $R_4 = OC_3H_7$, or
- $R_1 = R_2 = R_3 = C_{11}H_{23}$ and $R_4 = O(C=O)C_6H_8(OH)_3$, or
- $R_1 = R_2 = R_3 = C_{11}H_{23}$ and $R_4 = NH_2$
- $R_1 = R_2 = R_3 = C_{11}H_{23}$ and $R_4 = O(C=O)CCH_3(CH_2OH)_2$
- $R_1 = R_2 = R_3 = C_{11}H_{23}$ and $R_4 = OCH(CHOH)_3CH(CH_3)O$
- $R_1 = R_2 = R_3 = C_{11}H_{23}$ and $R_4 = OCH(CHOH)_3CH(CH_2OH)O$
- $R_1 = R_2 = R_3 = C_{11}H_{23}$ and $R_4 = OCH(CHOH)_3(CH_2)O$.

9. The compound of anyone of claims 1 to 8 wherein said compound is an α anomer of the compound of formula 1.
10. The compound of anyone of claims 1 to 8 wherein said compound is an β anomer of the compound of formula 1.
11. The compound according to any one of claims 1 to 10 for use as an active principle or as adjuvant in the treatment of diseases that require or benefit from an immune stimulation by activating the TLR4 receptor.
12. The compound for use according to claim 11 wherein said diseases are cancer, allergies, infectious diseases, cardiovascular diseases, obesity-dependent metabolic diseases, neuronal degeneration, apoptosis, autoimmune disorders, viral infections, bacterial infections, autoimmune diseases.
13. A vaccine adjuvant consisting of the compound as defined in anyone of claims 1 to 10.

14. A vaccine composition comprising the compound as defined in any one of claims 1 to 13, at least one pharmaceutically acceptable carrier and at least one pharmaceutically acceptable immunogenic antigen.

15. The vaccine composition according to claim 14, wherein said compound is the sole adjuvant present in said composition.

16. A pharmaceutical composition comprising the compound as defined in any one of claims 1 to 10 and at least one pharmaceutically acceptable excipient and/or carrier.

17. The pharmaceutical composition according to claim 16, further comprising at least one additional active principle.

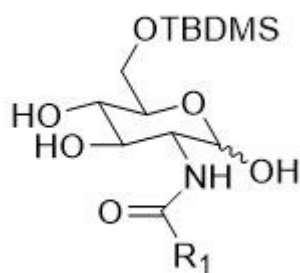
18. The pharmaceutical composition according to claims 16 or 17, in a form for oral, parenteral, nasal, aerosol, sublingual, rectal, vaginal, topical or systemic administration.

19. The pharmaceutical composition according to any one of claims 16 to 18 in the form of suspension, emulsion, ointment, cream, spray, granulate, powder, solution, capsule, pill, tablet, lyophilized product, lozenge, aerosol, nebulization, or injection.

20. The pharmaceutical composition according to any of claims 16 to 19, for use as an active ingredient or as an adjuvant, in the treatment of diseases that require or benefit from an immune stimulation by activating the TLR4 receptor.

21. The pharmaceutical composition for use according to claim 20, wherein said diseases are cancer, allergies, infectious diseases, cardiovascular diseases, obesity-dependent metabolic diseases, neuronal degeneration, apoptosis, autoimmune disorders, viral infections, bacterial infections, autoimmune diseases.

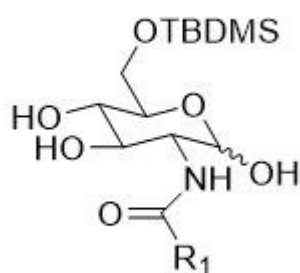
22. An intermediate of formula 1i



1i

wherein R_1 is a saturated C_5 - C_{15} alkyl chain optionally substituted.

23. A method for the preparation of an intermediate of formula 1i

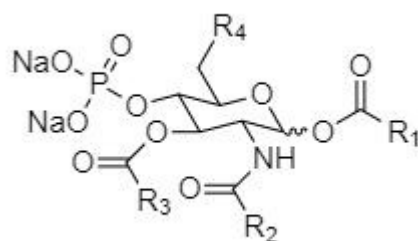


1i

comprising the following steps

- 1) Selective acylation of the amino group in the C_2 position of glucosamine hydrochloride by reaction with acyl chloride in the presence of sodium bicarbonate.
- 2) Protection by selective silylation of hydroxyl in position C_6 by reaction with tert-butyldimethylsilyl chloride (TBDMSCl) in the presence of imidazole.

24. A method for the preparation of a compound of formula 1,



1

wherein R_1 is a saturated C_5 - C_{15} alkyl chain optionally substituted,

wherein R_2 is a saturated C_5 - C_{15} alkyl chain optionally substituted,

wherein R₃ is a saturated C₅-C₁₅ alkyl chain optionally substituted,

wherein R₄ is any substituent that can be linked by means of a bond between C₆ and a suitable atom and/or any substituent which possesses an oxygen or a nitrogen atom that can bind to C₆, comprising the following steps:

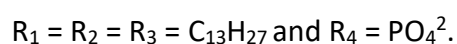
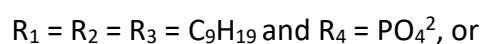
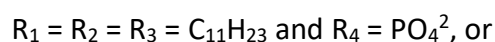
- 1) Selective acylation of the amino group in the C₂ position of glucosamine hydrochloride by reaction with acyl chloride in the presence of sodium bicarbonate;
- 2) Protection by selective silylation of hydroxyl in position C₆ by reaction with tert-butyldimethylsilyl chloride (TBDMSCl) in the presence of imidazole, thereby obtaining the intermediate as defined in claim 22;
- 3) Selective acylation of hydroxyls in positions C₁ and C₃ by reaction with acyl chloride in the presence of triethylamine and N, N-dimethyl aminopyridine (DMAP);
- 4) Phosphorylation of hydroxyl in the C₄ position by reaction with dibenzyl N, N-diisopropylphosphoramidite in the presence of triflate imidazolium, followed by oxidation of phosphite to phosphate via metachloroperbenzoic acid;
- 5) Deprotection of hydroxyl from silane in position C₆ through the presence of sulfuric acid in catalytic quantities; and
- 6) Deprotection of phosphate from benzyls in position C₄ and optionally deprotection of benzyls on any substituent in position C₆ through hydrogenation catalysed by Palladium on Carbon (Pd / C).

25. The method of claim 24, further comprising a step 5i) after step 5) and before step 6):

5i) Phosphorylation of hydroxyl in position C₆ by reaction with dibenzyl N, N-diisopropylphosphoramidite in the presence of triflate imidazolium, followed by oxidation of phosphite to phosphate via metachloroperbenzoic acid wherein said deprotection step 6) is carried out in position C₄ and C₆, and

wherein the resulting R₄ is a phosphate group (PO₄²⁻).

26. The method of claim 24 wherein the compound of formula 1 is one of



27. The method of claim 24, further comprising a step 5ii) after step 5) and before step 6):

5ii) Acylation of hydroxy in C₆ position by reaction with carboxylic acid in the presence of a suitable condensing agent and catalyst, or with acyl chloride in the presence of a suitable catalyst, wherein said deprotection step 6) is carried out in position C₄ wherein the resulting R₄ is an acyl group.

28. The method of claim 27 wherein in said acylation step 5ii) said suitable condensing agent and catalyst are 1-ethyl-3-(3-dimethylaminopropyl) carbodiimide (EDC) and N, N-dimethylaminopyridine (DMAP).

29. The method of claim 24, further comprising a step 5iii) after step 5) and before step 6):

5iii) Glycosylation of hydroxyl in C₆ position by reaction of a glycosyl chloride donor in the presence of a suitable activator, catalyst and a molecular sieve wherein the resulting R₄ is a glycosyl group.

30. The method of claim 24, further comprising a step 5iv) after step 5) and before step 6):

5iv) Alkylation of hydroxyl in C₆ by reaction of a stabilized alkyl chloride in the presence of a suitable activator, catalyst and a molecular sieve wherein the resulting R₄ is n alkyl group.

31. The method of claim 29 and 30, wherein in said glycosylation step 5iii) and alkylation step 5iv) said suitable activator is silver (I) oxide, said suitable catalyst is triflic acid and said suitable molecular sieve is a water scavenger.

32. The method of claim 24, further comprising a step 5v) and a step 5vi) after step 5) and before step 6):

5v) Tosylation of position C₆ by reaction of tosyl chloride in presence of triethylamine as base and of a suitable catalyst

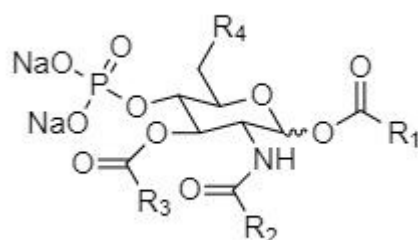
5vi) Azide insertion in position C₆ by reaction with sodium azide in the presence of tetrabutylammonium iodide.

33. The method of claim 32, wherein in said tosylation step 5v) said suitable catalyst is N, N-dimethylaminopyridine (DMAP).

34. The method of anyone of claims 24 to 33 wherein said acylation step 3) is carried out at a temperature ranging from -78°C of 0°C and an amount of catalyst ranging from 0.05 to 0.2 equivalents thereby obtaining a β -anomer of said compound of formula 1, preferably a temperature of -20°C and an amount of catalyst of 0.1 equivalents.

35. The method of anyone of claims 24 to 33, wherein said acylation step 3) is carried out at a temperature ranging from 20°C to 50°C and an amount of catalyst ranging from 2 to 2.5 equivalents thereby obtaining an α -anomer of said compound of formula 1, preferably a temperature of 30°C and an amount of catalyst of 2.02 equivalents.

36. Use of an intermediate compound as defined in claim 22 for the synthesis of compounds of formula 1,



1

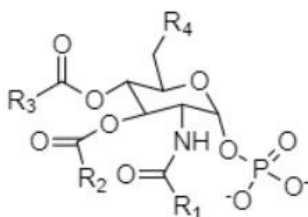
wherein R_1 is a saturated C_5 - C_{15} alkyl chain optionally substituted,

wherein R_2 is a saturated C_5 - C_{15} alkyl chain optionally substituted,

wherein R_3 is a saturated C_5 - C_{15} alkyl chain optionally substituted,

wherein R_4 is any substituent that can be linked by means of a bond between C_6 and a suitable atom and/or any substituent which possesses an oxygen or a nitrogen atom that can bind to C_6 .

37. A method for the preparation of a compound of formula X

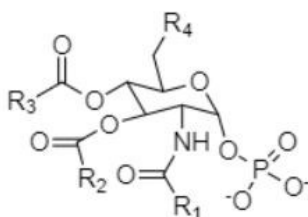


X

wherein R_1 is a saturated C_5 - C_{15} alkyl chain optionally substituted,
 wherein R_2 is a saturated C_5 - C_{15} alkyl chain optionally substituted,
 wherein R_3 is a saturated C_5 - C_{15} alkyl chain optionally substituted,
 wherein R_4 is OH and wherein each of R_1 , R_2 and R_3 is free from -OH substituents in position C_2
 comprising the following steps:

- 1) Selective acylation of the amino group in the C_2 position of glucosamine hydrochloride by reaction with acyl chloride in the presence of sodium bicarbonate.
- 2) Protection by selective silylation of hydroxyl in position C_6 by reaction with tert-butyldimethylsilyl chloride (TBDMSCl) in the presence of imidazole obtaining the intermediate of formula 1i as defined in claim 22.
- 3) Complete acylation of hydroxyls in positions C_1 , C_3 and C_4 by reaction with acyl chloride in the presence of triethylamine and N, N-dimethyl aminopyridine (DMAP).
- 4) selective diacylation of position C_1 by reaction with ethylenediamine in presence of acetic acid
- 5) Phosphorylation of hydroxyl in the C_1 position by reaction with dibenzyl N, N-diisopropylphosphoramidite in the presence of triflate imidazolium, followed by oxidation of phosphite to phosphate via metachloroperbenzoic acid.
- 6) Deprotection of hydroxyl from silane in position C_6 through the presence of sulfuric acid in catalytic quantities.
- 7) Deprotection of phosphate from benzyls in position C_4 and optionally deprotection of benzyls on any substituent in position C_6 through hydrogenation catalyzed by Palladium on Carbon (Pd / C).

38. Use of an intermediate compound as defined in claim 22 for the synthesis of compounds of formula X,



X

wherein R_1 is a saturated C_5 - C_{15} alkyl chain optionally substituted,
 wherein R_2 is a saturated C_5 - C_{15} alkyl chain optionally substituted,
 wherein R_3 is a saturated C_5 - C_{15} alkyl chain optionally substituted,

wherein R₄ is OH and wherein each of R₁, R₂ and R₃ is free from -OH substituents in position C₂.

ABSTRACT

The present invention relates to new synthetic molecules with agonist activity of human Toll-like Receptor 4 (TLR4), compositions comprising them and uses thereof for the treatment of diseases in which it is useful to induce or increase an immune response. These new synthetic molecules differ from other similar agonists due to the simplicity of the formula, the ease and cheapness of preparation and the possibility of further chemical processing to modify the physicochemical properties and allow conjugation to other molecules (for example protein antigens).

Chapter III: Unpublished Chemical and Biological Work

FP20 *ex vivo* and *in vivo* Biological Data

In Chapter II we discussed FP20 and its derivatives design, synthesis and initial biological evaluation. However, due to the promising results obtained in the initial screening, FP20 and its most active analogues (FP21 and FP22) were further tested and their activity and toxicity evaluated also *ex vivo* and *in vivo*.

Ex vivo experiments were carried on Peripheral Blood Mononuclear Cells (PBMC), a mixture of peripheral blood cells presenting one single round nucleus, consisting mainly of lymphocytes and monocytes, which were obtained by separation from healthy blood donors. These cells were subsequently treated with either a 10 or 25 μM concentration of FP20, FP21 and FP22, 1 $\mu\text{g}/\text{mL}$ of MPLA as comparison and 100 ng/mL of S-LPS as positive control.

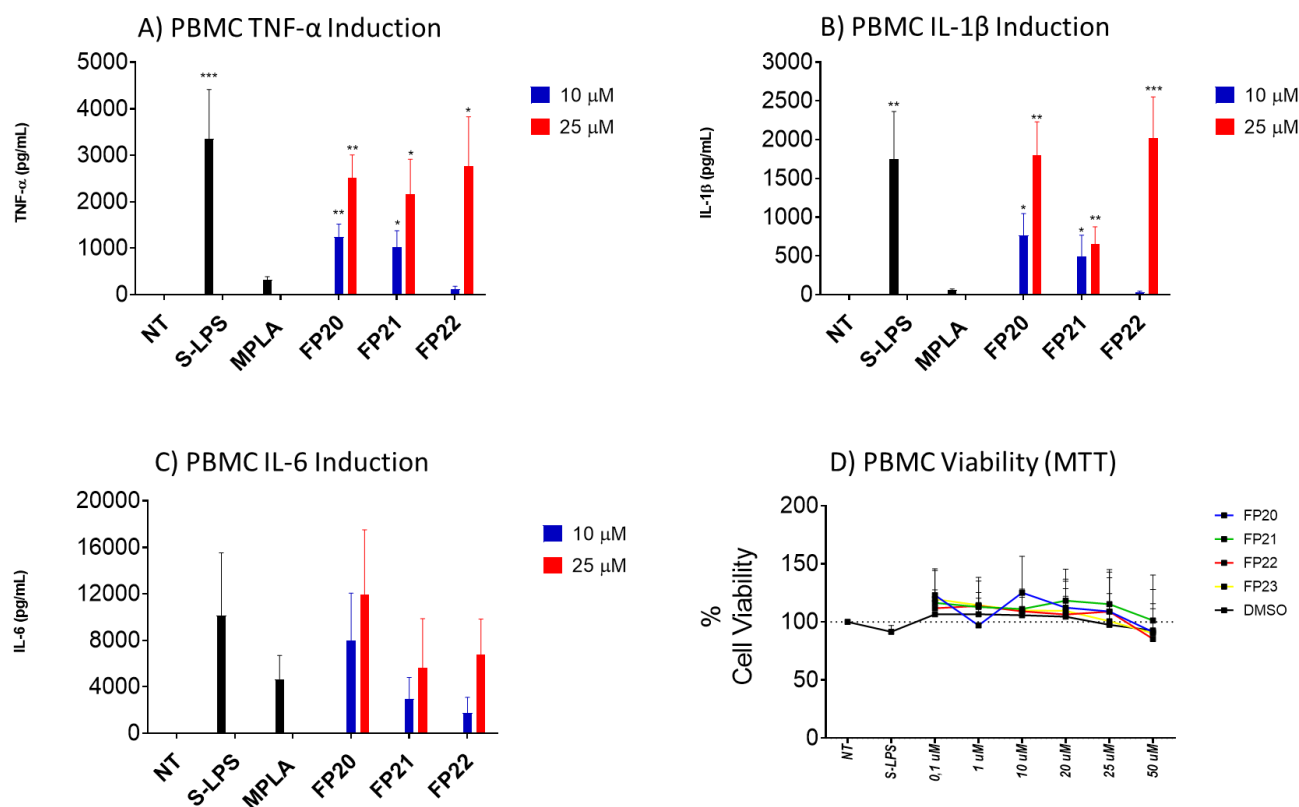


Figure 56 *Ex vivo* biological evaluation of FP20, FP21 and FP22. PBMC were treated either with a 10 or 25 μM concentration of FP20, FP21 and FP22, 1 $\mu\text{g}/\text{mL}$ of MPLA as comparison and 100 ng/mL of S-LPS as positive control. All cytokine induction levels are expressed in pg/mL **A)** TNF- α induction. **B)** IL-1 β induction. **C)** IL-6 induction **D)** Viability screening through MTT assay.

Results show as all the three molecules are non-toxic at the tested doses and can induce a larger production of TNF- α and IL-1 β than MPLA, a trend confirmed also for IL-6 induction in the case of FP20. This may suggest that our compounds lead to a stronger MyD88 activation than MPLA, which is instead a TRIF-skewed TLR4 agonist; however, it may also underlie that FP20 and its analogues also act through the non-canonical inflammasome, as suggested by the high levels of IL-1 β induction. Furthermore, FP22 behavior is noteworthy, due to the marked difference in activity between the two doses here tested.

FP20 and FP22, being the most active molecules both *in vitro* and *ex vivo* were selected for further evaluation *in vivo*, which were carried out in collaboration with the group of Dr. Anguita at CICBiogune in Bilbao. 37 C57BL/6 mice divided in five groups (5, 8, 8, 8, 8) were immunized with either 10 μ g of OVA (control group) or 10 μ g of OVA and 10 μ g of a vaccine adjuvant (MPLA, FP18, FP20 or FP22) on day 0 and day 21. Serum was collected and analyzed for IgG titers and transaminases levels on day 0, 21 and 42.

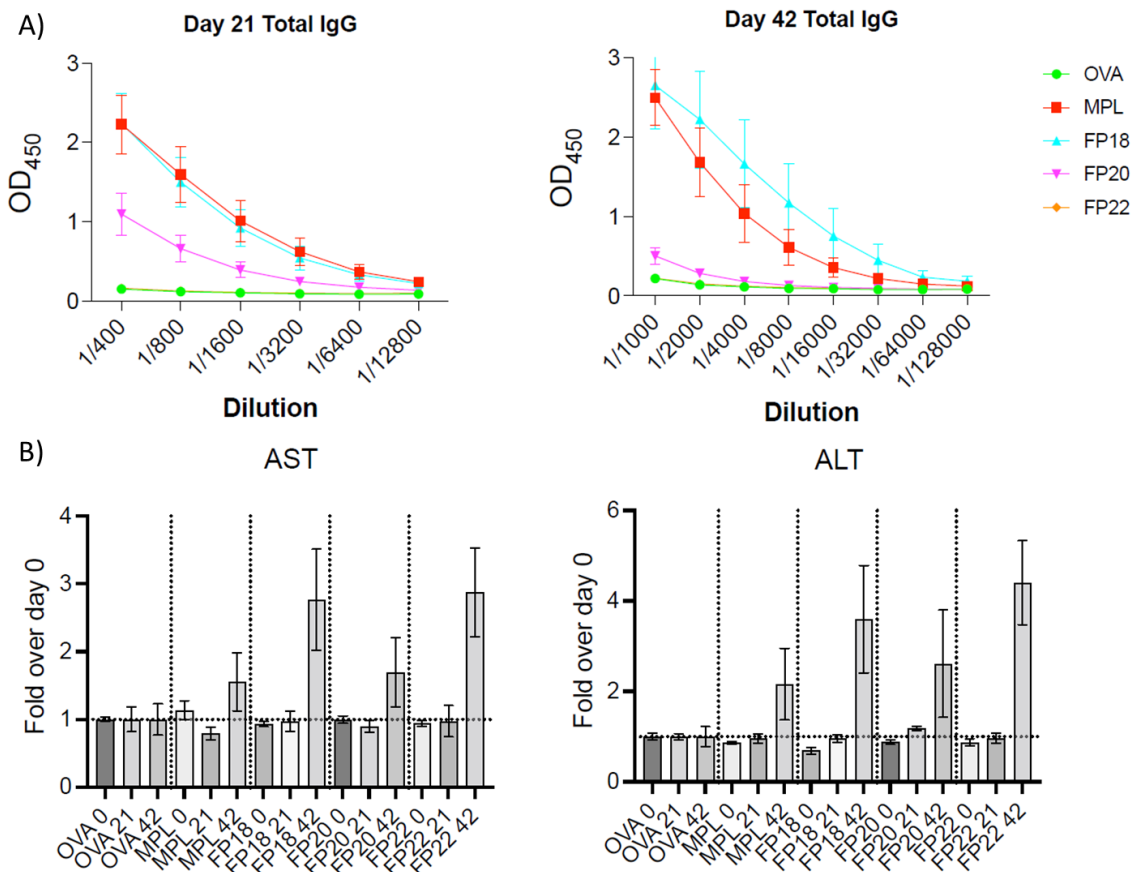


Figure 57 *In vivo* results. C57BL/6 mice were treated with either 10 μ g of OVA (control group) or 10 μ g of OVA and 10 μ g of a vaccine adjuvant (MPLA, FP18, FP20 or FP22) on day 0 and day 21. Serum was collected and analysed on day 0, 21 and 42. **A)** Total IgG titers induced after immunization. Results are expressed in OD450. **B)** Aspartate and alanine transaminases levels at day 0, 21 and 42. Results are expressed as fold increase.

All the adjuvants tested seems to show the same levels of transaminases activity induction, as in all the four groups (MPLA, FP18, FP20 and FP22) there is no significant transaminase activity increase until the end of the experiment. Furthermore, on day 42 the maximum level reached is a four-fold increase when compared to control group; however, these levels aren't yet indicative of a significant liver toxicity: liver damages are normally associated to an 8 or 10-fold increase in transaminase activity. These data suggest that all the adjuvants tested are viable in mice, and that FP18, FP20 and FP22 are on par with MPLA as toxicity.

Total IgG titers again demonstrate the validity of FP18 as a vaccine adjuvant, as this compound induces levels of IgG comparable to MPLA on day 21 and slightly higher levels on day 42. Unfortunately, FP22 seems to be totally unable to induce a significant IgG production: this may be connected to the peculiar behavior shown in the *ex vivo* experiments, during which the immunogenic activity of the molecules was suppressed at lower concentration; it is thus possible that the 10 µg dose injected was too low to lead to proper adjuvancy. The results obtained also show the viability of FP20 as a possible vaccine adjuvant, even though the induction of IgG is lower than MPLA or FP18 and it seems not to increase after the booster immunization. This behavior may be due to differences in the mechanism of action between FP20 and MPLA, as highlighted during the *ex vivo* tests: while MPLA is a TRIF-biased adjuvant, FP20 may act through a different mechanism (as showed by the different cytokines profile), and therefore also its adjuvancy may be influenced.

FP20 Glycosylation

First Attempts and Modified Koenigs-Knorr Protocol

As shown by results in Chapter II and in the previous paragraph, FP20 was demonstrated to possess high TLR4 agonist activity, low to no toxicity and to be easy and cheap to synthesize. For this reason, it was patented nationally and internationally, attracting the interest of big pharmaceuticals corporations such as Croda.

However, FP20 still suffers from its limited solubility in water due to the large hydrophobic moiety it possesses. Our solution to this issue has been to try and functionalize FP20 6-OH with a polar moiety, in order to enhance biologically relevant properties such as bioavailability or, indeed, solubility. Furthermore, this solution would allow our molecules to better mimic the highly

hydrophilic core oligosaccharide portion of LPS, hopefully improving the TLR4 agonist character of the molecule.

These results can be obtained with different chemical modifications, such as acylation, which has been achieved in a straightforward way (*vide supra*, FP207) or glycosylation, which could be advantageous because the final compound will closely resemble TLR4 natural ligand. In order to enhance this latter effect, L-rhamnose was chosen as the first glycoside donor, due to the peculiar interactions between said sugar and CD14: indeed, not only CD14 is one of the three ancillary proteins of TLR4 pathway, responsible for shuttling LPS to MD-2, but mCD14 involvement in the recognition is the discriminating event for the selection of either MyD88 or TRIF downstream signaling pathway.^{66,215}

Even though this topic was briefly covered in chapter II, it is worth expanding on it due to the unique challenges that had to be overcome to successfully glycosylate FP20: hasn't been possible to just straightforwardly choose one of the many glycosylation methods available and apply it to our case, as most of them are too harsh on our molecule.

Indeed, while FP20 is significantly more stable and resistant than FP18, it still retains a delicate group: the acyl chain in 1-OH, which could act as an anomeric leaving group when treated with glycosylating conditions. In fact, we observed this very phenomenon during our early glycosylation attempts using several of the most common conditions. As examples, we used TCA donors in presence of various strong acids (e.g., TMSOTf, TfOH) or chloride donors in presence of Lewis acids (e.g., FeCl₃) in various concentrations and temperatures; however, all these conditions resulted in the cleavage of the 1-OH acyl chain (**Table 6**).

We then started screening milder conditions, and we finally managed to achieve a successful, albeit low yielding, glycosylation when using a protocol developed in Dr. Demchenko's laboratories at St. Louis University, as they realized that adding small, catalytic amounts of a strong acid (TMSOTf or TfOH) could dramatically increase the reaction rate of Koenigs-Knorr glycosylation, which is otherwise slow and sluggish (**Table 6**).^{216,217}

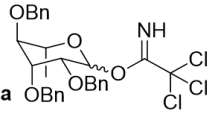
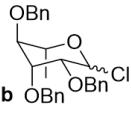
Donors	Entry	Donor (Eq)	Solvent (M)	Promoter (Eq)	Catalyst (Eq)	Temperature (°C)	Yield (%)	Selectivity (α:β)
 a	1	a (3)	DCM (0.05)	N/A	TMSOTf (0.5)	0	N/D	N/D
	2	a (3)	DCM (0.05)	N/A	TMSOTf (0.5)	-20	N/D	N/D
	3	a (3)	DCM (0.05)	N/A	TMSOTf (0.5)	-78	N/D	N/D
 b	4	b (2)	DCM (0.05)	N/A	FeCl ₃ (0.1)	-20	N/D	N/D
	5	b (2)	DCM (0.05)	N/A	FeCl ₃ (0.1)	-60	N/D	N/D
	6	b (1.25)	Tol (0.05)	Ag ₂ O (1)	TfOH (0.2)	0	20	4:1
	7	b (1.25)	Tol (0.05)	Ag ₂ O (1.5)	TfOH (0.3)	0	35	4:1
	8	b (1.25)	Tol (0.1)	Ag ₂ O (2)	TfOH (0.5)	0	60	4:1

Table 6 First attempts of glycosylation, comprising the modified Koenigs-Knorr Protocol

The low amount of acid involved in the reaction as well as the overall mildness of the protocol allowed us to obtain the desired compound FP20Rha, even though with a low yield (20%). This low yield is probably due to a mixture of substrate degradation, but also to electronic effects: previous studies showed that, in these conditions, electron-rich donors (e.g., benzylated) are less reactive than electron-poor ones (e.g., benzoylated). However, orthogonality considerations over protecting groups forced us to proceed with benzylated glycosyl donors, as deprotecting benzoyl groups would cleave the lipid chains on our substrate.

Notwithstanding the low yield, stimulated by this achievement, we optimized the reaction conditions for our peculiar situation, varying the amount of promoter (Ag₂O) and catalyst (TfOH), as well the concentration and the temperature, but maintaining the glycosyl donor (shown in table).

Due to this process, the yield was increased to 60%, a moderate, but nonetheless acceptable and satisfactory result. However, as soon as we applied the same optimized conditions to other glycosyl donors (such as glucose, galactose and mannose), the yield dropped significantly, reaching as low as 10%.

Bismuth Triflate Protocol

Due to the challenges we encountered with this reaction, we decided to change our approach and we started collaborating directly with Dr. Demchenko to find the best conditions to glycosylate FP20. As our starting point consisted in the modified Koenigs-Knorr protocol, we started trying various silver related conditions (resumed in **Table 7**). Furthermore, we tried switching one of the benzyls of the donor for an electron-withdrawing picoloyl group (pico), which be selectively cleaved by

treatment with $\text{Cu}(\text{OAc})_2$, in order to make the glycosyl donor more reactive under those specific conditions.

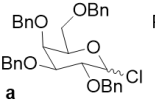
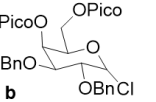
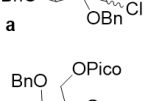
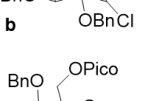
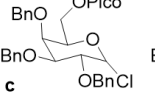
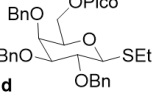
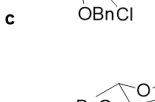
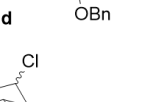
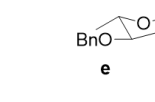
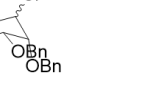


Donors		Entry	Donor (Eq)	Promoter (Eq)	Catalyst (Eq)	Solvent (M)	Time (h)	Yield (%)	Selectivity ($\alpha:\beta$)
		1	a (1.2)	Ag_2SO_4 (2.5)	TfOH (0.5)	Tol (0.05)	16	15%	>99:1
		2	a (1.2)	AgOTf (2.0)	N/A	Tol (0.05)	24	20%	N/D
		3	a (1.2)	AgOTf (2.0)	N/A	Tol (0.05)	7	30%	2:1
		4	b (1.2)	Ag_2SO_4 (2.5- \rightarrow 5)	TfOH (0.5- \rightarrow 2)	DCM (0.05)	48	10%	3:1
		5	c (1.2)	Ag_2SO_4 (2.5- \rightarrow 5)	TfOH (0.5- \rightarrow 2)	DCM (0.05)	48	40%	1:1.4
		6	d (1.2)	Ag_2SO_4 1.5 I_2 1.5	TfOH (0.2)	DCE (0.05)	5	40%	1:1.4
		7	d (1.2)	Ag_2SO_4 (2.5)	TfOH (2- \rightarrow 2.5)	DCM (0.05)	20	25%	1.6:1

Table 7 The first round of conditions tried during the collaboration with Dr. Demchenko.

However, silver failed to provide any improvements as a promoter, with yields ranging between 15% and 45%. Therefore, we decided to try $\text{Bi}(\text{OTf})_3$ as promoter while maintaining the chloride glycosyl donor, as it was proven in recent experiments to be a viable and milder substitute to silver salts.^{218,219}

After few optimization rounds, we found that 0.75 Eq of $\text{Bi}(\text{OTf})_3$ is the right amount of promoter, allowing us to achieve 84%-90% yields over 18h on different glycosyl donors bearing a pico group: both lower and higher equivalents of promoter resulted in lower yields, probably due to a disruptive interactions between bismuth and the amide on FP20 (**Table 8**).

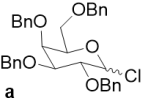
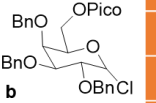
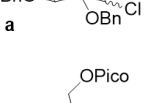
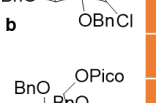
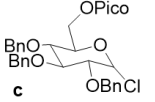
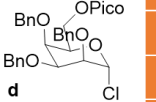
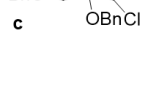
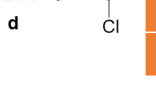






Donors		Entry	Donor (Eq)	Promoter (Eq)	Solvent (M)	Time (h)	Yield (%)	Selectivity ($\alpha:\beta$)
		1	a (1.2)	$\text{Bi}(\text{OTf})_3$ (0.35)	DCM (0.05)	72	45%	1.5:1
		2	b (1.2)	$\text{Bi}(\text{OTf})_3$ (0.35- \rightarrow 0.5)	DCM (0.05)	72	46%	1:1
		3	b (1.5- \rightarrow 2)	$\text{Bi}(\text{OTf})_3$ (0.5)	DCM (0.05)	20	60%	1:1
		4	b (2)	$\text{Bi}(\text{OTf})_3$ (0.75)	DCM (0.05)	18	84%	1:1.5
		5	c (2)	$\text{Bi}(\text{OTf})_3$ (0.75)	DCM (0.05)	16	84%	1:1.4
		6	b(2)	$\text{Bi}(\text{OTf})_3$ (0.9)	DCM (0.05)	18	80%	1:1
		7	d (2)	$\text{Bi}(\text{OTf})_3$ (0.75)	DCM (0.05)	18	94%	1.5:1

Table 8 The optimization process of the $\text{Bi}(\text{OTf})_3$ protocol.

Indeed, we observed this interaction when applying these conditions on non-pico donors resulted in drastically reduced yield (c.a. 40%) and in the formation of an unexpected byproduct. After characterizing of this byproduct by NMR (^1H , ^{13}C , COSY, HSQC, NOESY) and mass spectroscopy (ESI-TOF), we assigned the formula shown in **Figure 58**, where the FP20Rha lacks the amidic lipid chain and instead the nitrogen formed a covalent bond with the anomeric lipid chain. We later confirmed this effect by kinetic ^1H NMR studies on a mixture of FP20 and $\text{Bi}(\text{OTf})_3$, in which we observed a clear shift and disruption on the amide signal at 5.45 ppm.

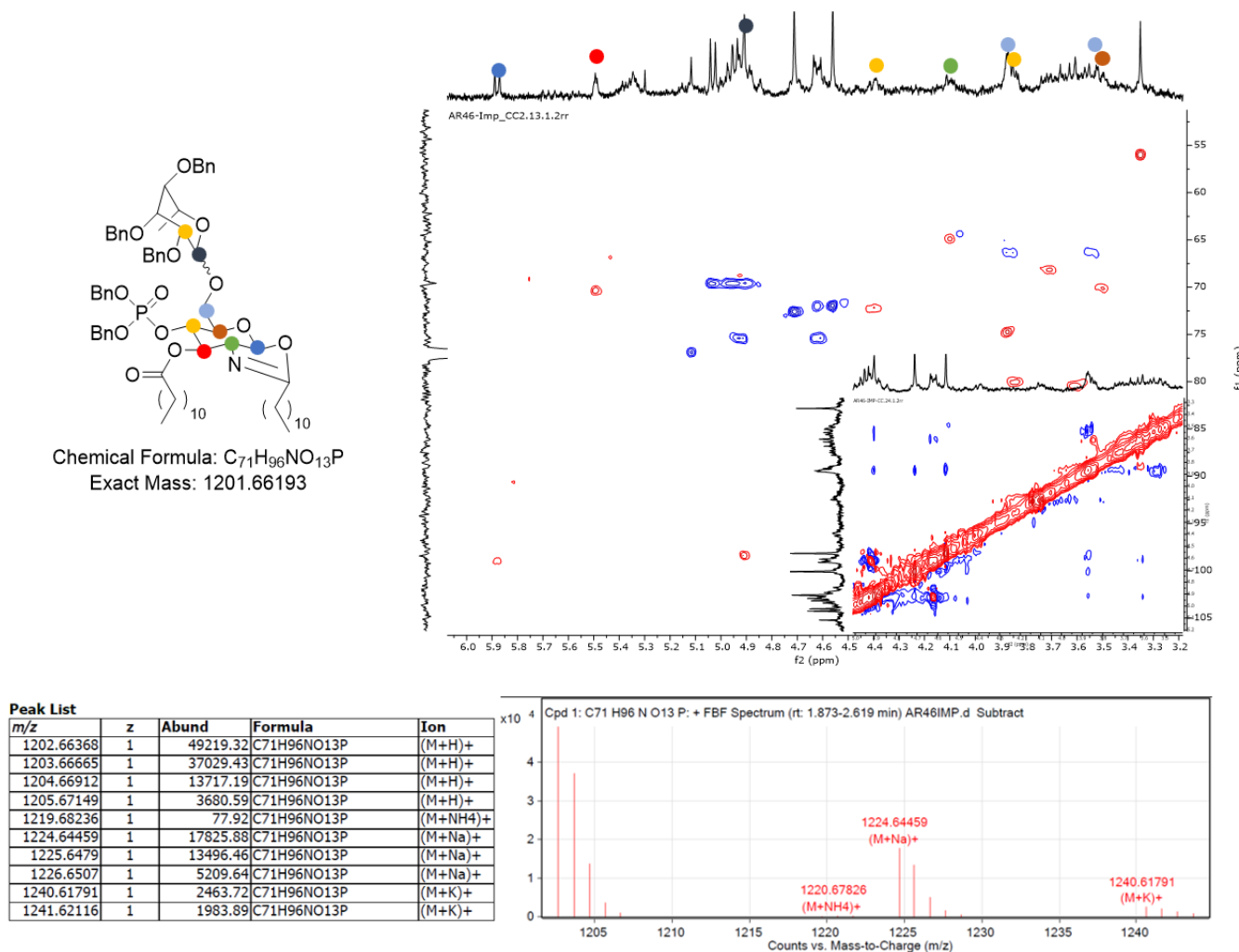


Figure 58 Characterization by NMR and mass spectroscopy of the byproduct obtained during $\text{Bi}(\text{OTf})_3$ glycosylation in absence of a picoloylated glycosyl donor. The most important NMR signals are highlighted and indicated by colored dots. The mass spectrum (ESI-TOF) confirms the molecular mass of the formula here hypothesized, while it is incompatible with a formula having a free amine and a normal acyl chain on 1-OH.

When a pico group is present, $\text{Bi}(\text{OTf})_3$ preferentially interacts with the pico nitrogen instead, thus avoiding substrate disruption: Indeed, we observed a significant interaction between Bismuth and the pico nitrogen when we mixed a picoloylated glycosyl donor with $\text{Bi}(\text{OTf})_3$ in an NMR tube and

checked it regularly at various timepoints, as proven by the shifts and broadening in ^1H NMR pico signals; the rest of the molecule remained instead largely unaffected, until degradation started to occur.

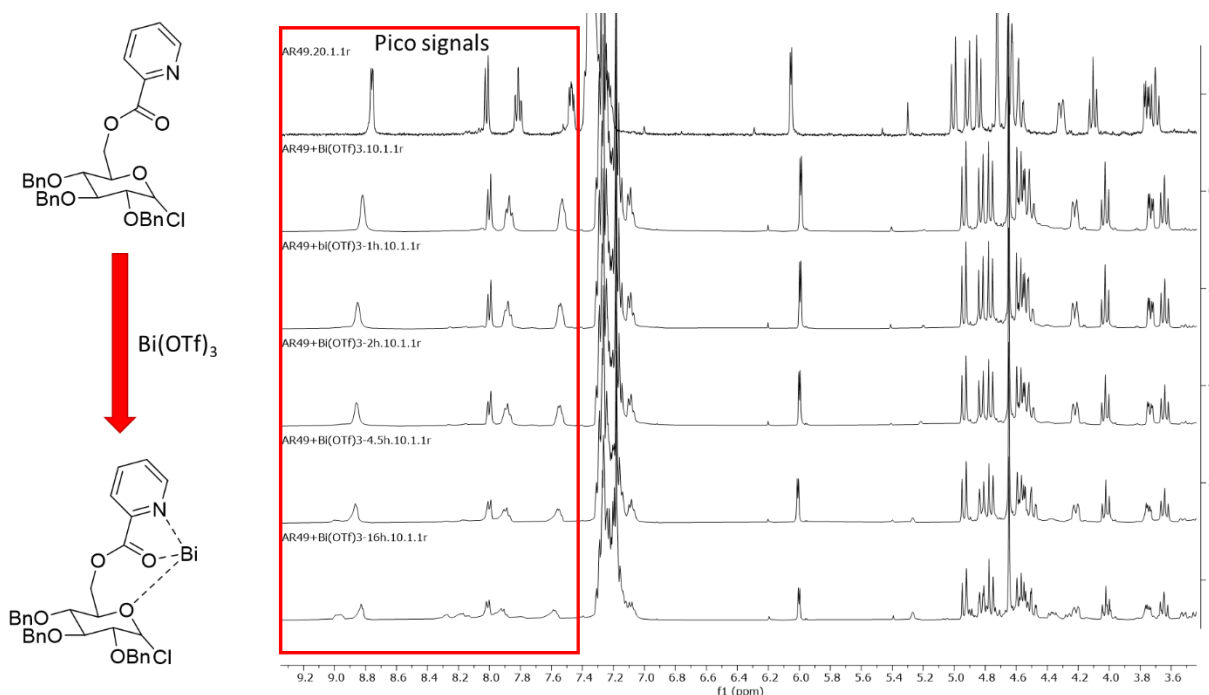


Figure 59 ^1H NMR of a picoloylated glycosyl donor in presence of $\text{Bi}(\text{OTf})_3$ at various timepoints. While most of the molecule remains largely unaffected, the signals of the pico group undergo a significant broadening.

We then concluded that, while affording high and consistent yields, this protocol can only be used in presence on picoloylated glycosyl donors, which can narrow the scope of the reaction. However, pico group can be easily and selectively removed, freeing a hydroxyl for further functionalization, which can be eventually iterated as it is to obtain a larger, more soluble and possibly more active oligosaccharide with moderate to high overall yields.

NIS and HOFox Protocol

After having achieved a first success in increasing the yield and expanding the scope of FP20 glycosylation using the $\text{Bi}(\text{OTf})_3$ protocol, we tried to obtain the same result on fully benzylated glycosyl donors, which would make the process obtaining singly glycosylated FP20 much smoother, as less deprotection steps would be required. However, we still had the limitations given by the nature of the substrate, which prevented us from using harsh conditions. Therefore, we applied a recently published protocol involving the use of SET Glycosyl donors, N-iodo-succinimide (NIS) as promoter and HOFox as catalyst.²²⁰

These conditions are exceptionally mild, as they don't involve the use of strong acid at all; furthermore, they can only activate thiols as leaving groups (through oxidation mediated by NIS), therefore, they can't possibly cleave the anomeric lipid chain of FP20.

Indeed, the reactants used proved to be perfectly orthogonal to all the groups present on our molecule and the protocols a whole worked extremely well practically without any optimization, affording high yields (around 90%) in few hours with all the sugars we tried (**Table 9**).

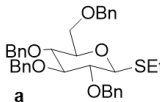
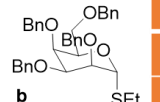
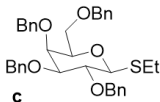
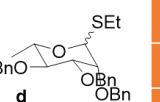
Donors		Entry	Donor (Eq)	Promoter (Eq)	Catalyst (Eq)	Solvent (M)	Time (h)	Yield (%)	Selectivity ($\alpha:\beta$)
		1	a (1.2)	NIS (1.2)	HOFox (0.5)	DCM (0.05)	3	84%	N/A
		2	a (2)	NIS (2)	HOFox (0.5)	DCM (0.05)	1.5	84%	1:1
		3	b (1.5)	NIS (2)	HOFox (0.5)	DCM (0.05)	4	90%	1:1
		4	c (2)	NIS (2)	HOFox (0.5)	DCM (0.05)	0.75	91%	1:1.5
		5	d(2)	NIS (2)	HOFox (0.5)	DCM (0.05)	1	86%	2:1

Table 9 Optimization process of the NIS/HOFox protocol.

Therefore, using the glycosylation protocols here described, we managed to rhamnosylate (FP20Rha), glucosylate (FP20Glc), galactosylate (FP20Gal), mannosylate (FP20Man) and lyxosylate (FP20Lyx) our substrate with high yields, even though with low to none diastereoselective. Indeed, all of our glycosylated compounds were obtained as diastereoisomeric mixture, and unfortunately, with exception of galactose, they were impossible to separate using standard laboratory techniques.

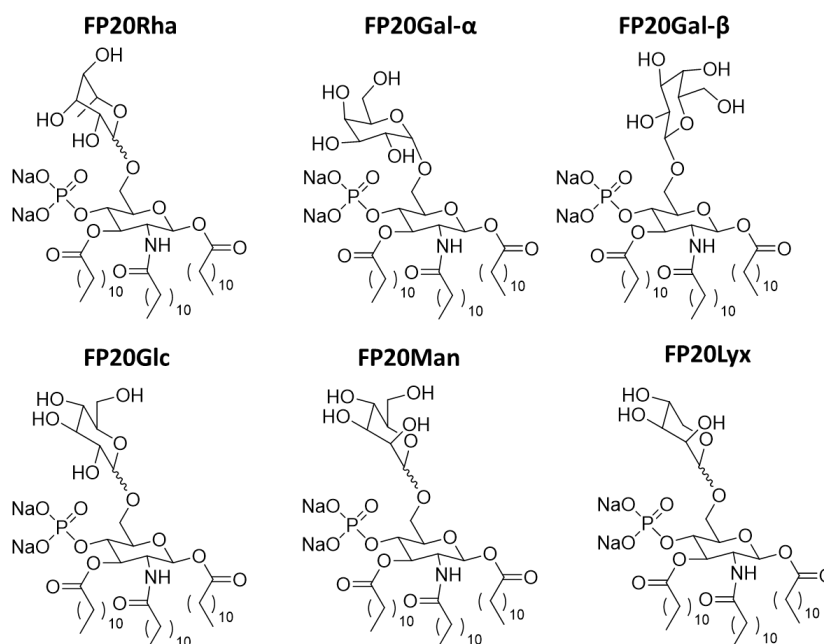


Figure 60 Our array of glycosylated FP20: FP20Rha, FP20Gal (α and β), FP20Glc, FP20Man and FP20Lyx.

FP20Rha and FP207 Biological Assessments

In Vitro Activity

Having achieved FP20 glycosylation and acylation, we tested the first two of the new compounds, FP20Rha and FP207, for their activity as a TLR4 agonist and as a vaccine adjuvant. The first activity assessment was performed on THP-1 X-Blue cells, an immortalized line of human monocytes differentiated into macrophages; these cells are modified to express the Secreted Embryonic Alkaline Phosphatase (SEAP) reporter gene under the control of NF- κ B, so that it is possible to check TLR4 activation through the SEAP colorimetric assay.

As we can see from the graph in **Figure 61**, FP207 and FP20Rha ability to elicit TLR4 activation is strikingly high, surpassing our initial expectation, to the point that the 25 μ M concentration elicit an equal or stronger response than the positive control and that the 1 μ M concentration shows a similar or better activation than MPLA in the same concentration range. Furthermore, both compounds maintain high levels of viability, except in the highest concentration (which is probably a consequence of being as immunogenic as LPS in that concentration range).

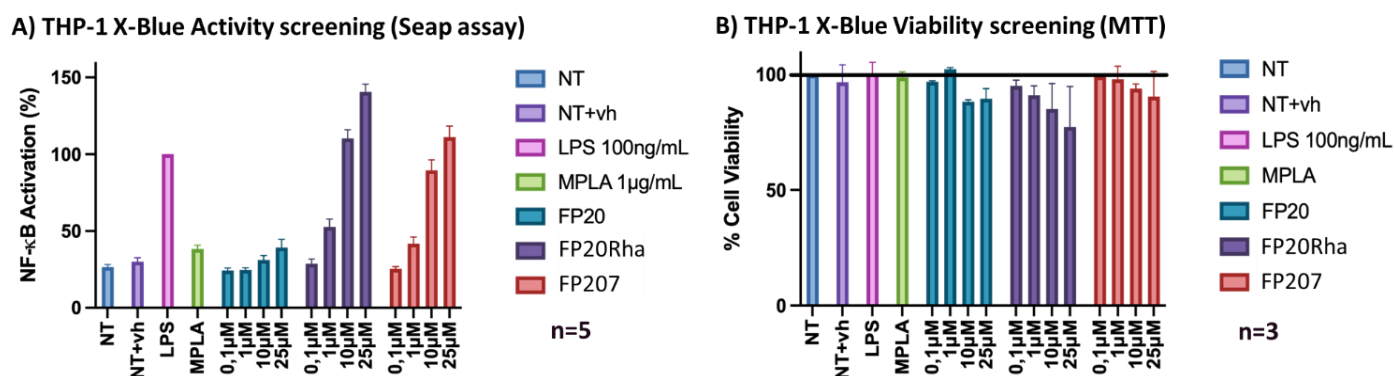


Figure 61 *In vitro* activity assessment. THP-1 X-Blue cells were treated with increasing concentrations (0.1-25 μ M) of FP20, FP207 and FP20Rha over 18 hours. Stimulation with smooth chemotype of LPS (S-LPS) and MPLA served as a positive control for the activation of the TLR4-mediated pathway. **A)** Activity screening through colorimetric SEAP assay. **B)** Viability screening through MTT assay.

Mechanism of Action Assessment

This high activation levels are explained by their mechanism of action, which appears to differ from the parent molecule FP20. We indeed observed different patterns when analyzing cells using Operetta[®] CLS[™], a high throughput microplate imager for high-content analysis (HCA). We tracked

the translocation into the nuclei of NF- κ B as a marker of TLR4 activation, following treatment with either LPS, MPLA, FP20, FP207 and FP20Rha. These data, which were obtained by Ana Rita Adelino Franco, will only be discussed briefly without being showed in here, as they will be an integral part of her PhD thesis.

THP-1-derived macrophages were treated with either LPS, MPLA, FP20, FP20Rha or FP207, and NF- κ B translocation into the nuclei was tracked through Operetta[®] CLS[™]. LPS treatment cause an almost complete NF- κ B enucleation, while both MPLA and FP18 treatments only lead to a partial intake; interestingly though, in FP20 case, only a small fraction on translocation takes place, suggesting a different mechanism of action than FP18 and MPLA. When cells are treated with a functionalized FP20, however, be it FP207 or FP20Rha, NF- κ B enucleation levels are restored, particularly in the case of FP20Rha in which they are 70% of LPS levels.

The differences we observed suggest that we have synthesized an array of compounds with small, but significant differences in their mechanism of action, which could cause them to preferentially activate either the MyD88 or the TRIF signaling pathway downstream of TLR4, or even to bypass TLR4 entirely to activate the non-canonical inflammasome mediated by NLRP3. This, in turn, is really advantageous, as in the future we could be able to have various vaccine adjuvants having diverse mechanisms, leading to better tailored vaccine adjusted toward either a type 1 or type 2 skewed immune response.

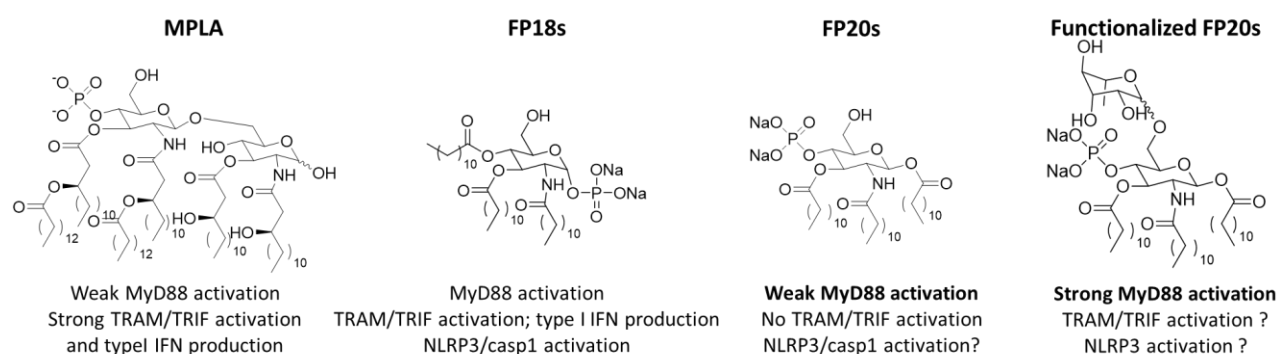


Figure 62 Our vaccine adjuvants (FP18, FP20 and functionalized FP20) and MPLA with their mechanistic differences. These could be exploited to produce better suited vaccines in the future.

In Vivo Studies

Finally, FP20Rha and FP207 were tested *in vivo* for their vaccine adjuvancy on C57BL/6 mice in collaboration with Dr. Anguita's group at CICBioGune in Bilbao. Mice were immunized on Day 0 and 21 with 10 μg of ovalbumin (OVA) as test antigen \pm 10 μg of adjuvant (MPL, FP20Rha, or FP207). Mice were sacrificed on day 42 and their sera analyzed to check the titers of ovalbumin specific antibodies produced.

The results demonstrate that both compounds are able to induce a marked production of IgG, on par with MPLA, which indicates an equal level of adjuvancy in mice. Furthermore, to assess compound toxicity *in vivo*, both weight and transaminases levels were monitored: collected data show that both FP20Rha and FP207 are nontoxic and perfectly viable. Indeed, even though in the first couple of days mice lost up to 2% of body weight, they swiftly recovered it without further damages, as also highlighted by the levels of transaminase: these levels are on par with the control group, and on day 20 they show how FP20Rha and FP207 are better tolerated than MPLA.

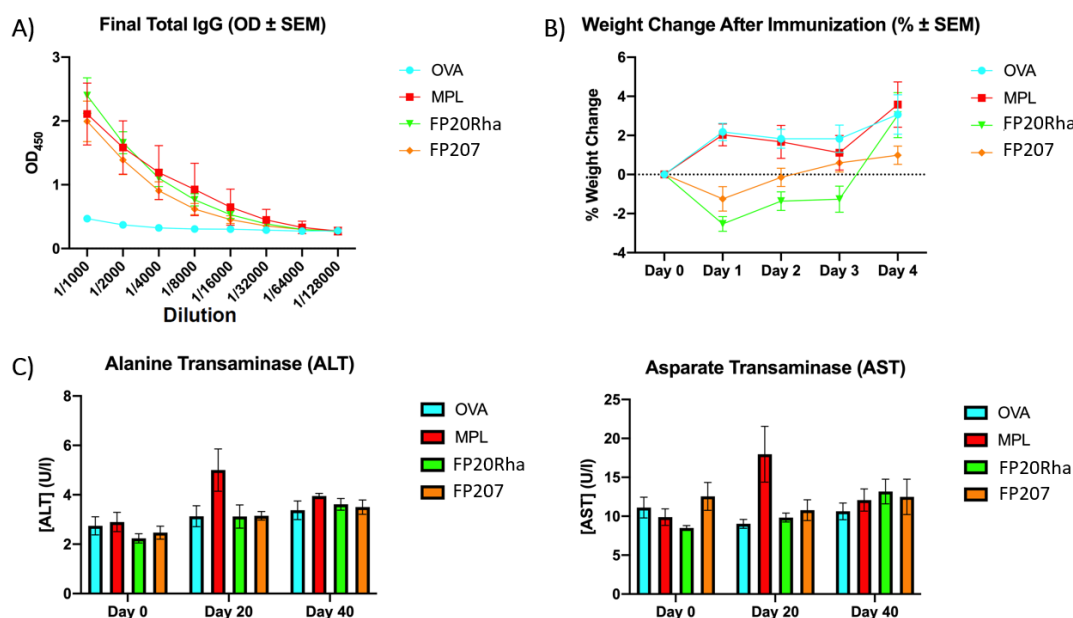


Figure 63 *In vivo* activity assessment of FP20Rha and FP207. C57BL/6 mice were treated with OVA and 10 μg of adjuvant at day 0 and day 21. **A)** Final total IgG titres, assessed by colorimetric assay. **B)** Weight changes in the first days after treatment. While initially FP20Rha and FP207 cause a small drop in weight, this is quickly recovered. **C)** Transaminases levels. FP20Rha and FP207 levels are in line with the control and lower than MPLA at day 20.

All these results suggest that our newest functionalized compounds are perfectly viable *in vivo*: even though the molecule formula is much simpler, they show results on par or even slightly better than MPLA in terms of adjuvancy and tolerability, but as their synthesis is easier, they would be much less expensive than MPLA itself.

CONCLUSION

Conclusion

Vaccines revolutionized healthcare, lowering morbidity and mortality of several diseases and increasing average life expectancy. Adjuvants have been pivotal in vaccine development, allowing for evolution toward subunit vaccines with retained efficacy, lower risks and requiring smaller dosage – an advantage important both for patient’s health and for vaccine cost and availability.^{1,2}

A prime candidate target for vaccine adjuvancy is TLR4, an immune receptor with a pivotal role in both innate and adaptive immunity, for its ability to shape the overall immune response.⁵⁴

Indeed, MPLA, a TLR4 targeted vaccine adjuvant, has been recently commercially approved either alone (MPL[®]) or in formulation (AS01, AS04) and it is currently in use in several human vaccines. Nonetheless, MPLA is commonly extracted and treated from bacterial sources (which lower safety profile) and, while a protocol for a totally synthetic MPLA exists, the synthesis is long, complex and expensive.^{29,109}

During the work exposed in this thesis, two new classes of easily available vaccine adjuvants were developed. In Chapter I, we shown FP18 class of compounds potential as vaccine adjuvants *in vitro* and *in vivo*. FP18 was rationally developed by changing the structure of our previously published TLR4 antagonist FP7, modifying its features according to previous studies showing TLR4 agonist activity in monosaccharide bearing three lipid chains and one negatively charged group, such as SDZ MRL 953 or ONO4007.

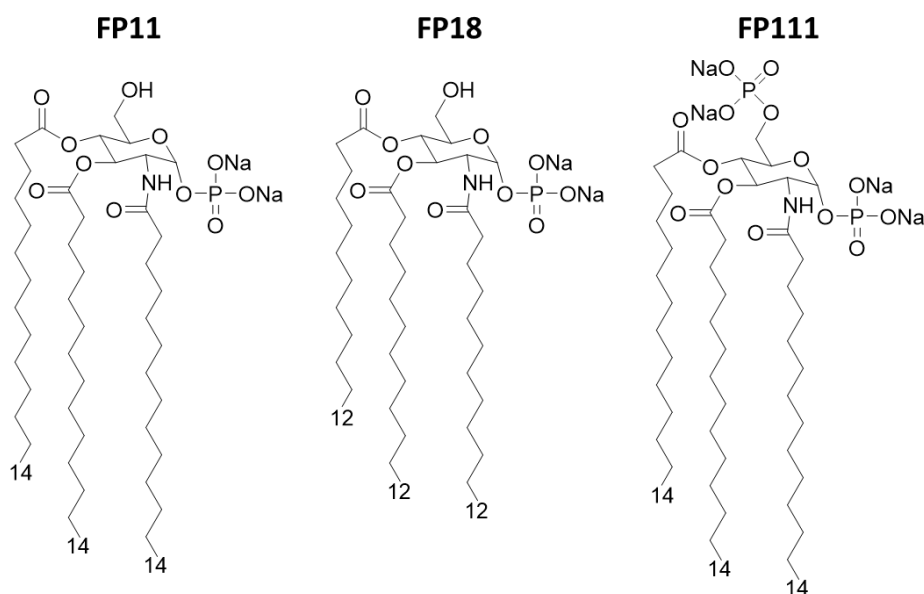


Figure 64 The molecules presented in Chapter I, FP11, FP18 and FP111, our first TLR4 agonists and vaccine adjuvants.

The original synthesis of FP18 was entirely modelled on FP7 synthesis with few changes, but eventually it was developed further as shown in chapter II. Both syntheses are however much more convenient than the one used to produce MPLA, making FP18 readily available and cheaper to prepare.

Even if the formula is simpler and the molecule is smaller, FP18 still maintains selectivity and immunogenicity levels comparable or even higher than those exhibited by MPLA, both *in vitro* and *in vivo*, while showing no meaningful toxicity. Indeed, FP18 was able to elicit a better OVA immunization than MPLA after the booster injection *in vivo* without any noticeable effect on body weight changes.

Interestingly, FP18 mechanism of action seems to differ from MPLA's: MPLA preferentially activates the TRIF-dependent pathway, while FP18 seems to activate both TRIF and MyD88 pathways, as well as the non-canonical NLRP3 inflammasome. Consequently, they also elicit different adaptive immune responses, which can be exploited for making better suited, tailored vaccines for different needs.

In chapter II, we shown two interesting advancements for monosaccharide TLR4 agonists. The first is the development of a new synthesis for FP18, which makes even more palatable for industrial scalability, as now it only requires 7 steps to be produced.

The second is the rational design of an even more promising class of vaccine adjuvants, FP20, which was designed to solve some issues arose with FP18, while having an even shorter synthesis (only composed by 6 reactions).

Indeed, FP18 suffered from limitations stemming from the position of its phosphate on the 1-OH, the anomeric position, which makes it a great leaving group (it is commonly used as such in many glycosylation protocols). This behaviour as leaving group lowered the stability of FP18, shortening its shelf life and hampering the possibility of functionalizing position 6-OH, which could be modified only with a second phosphate.

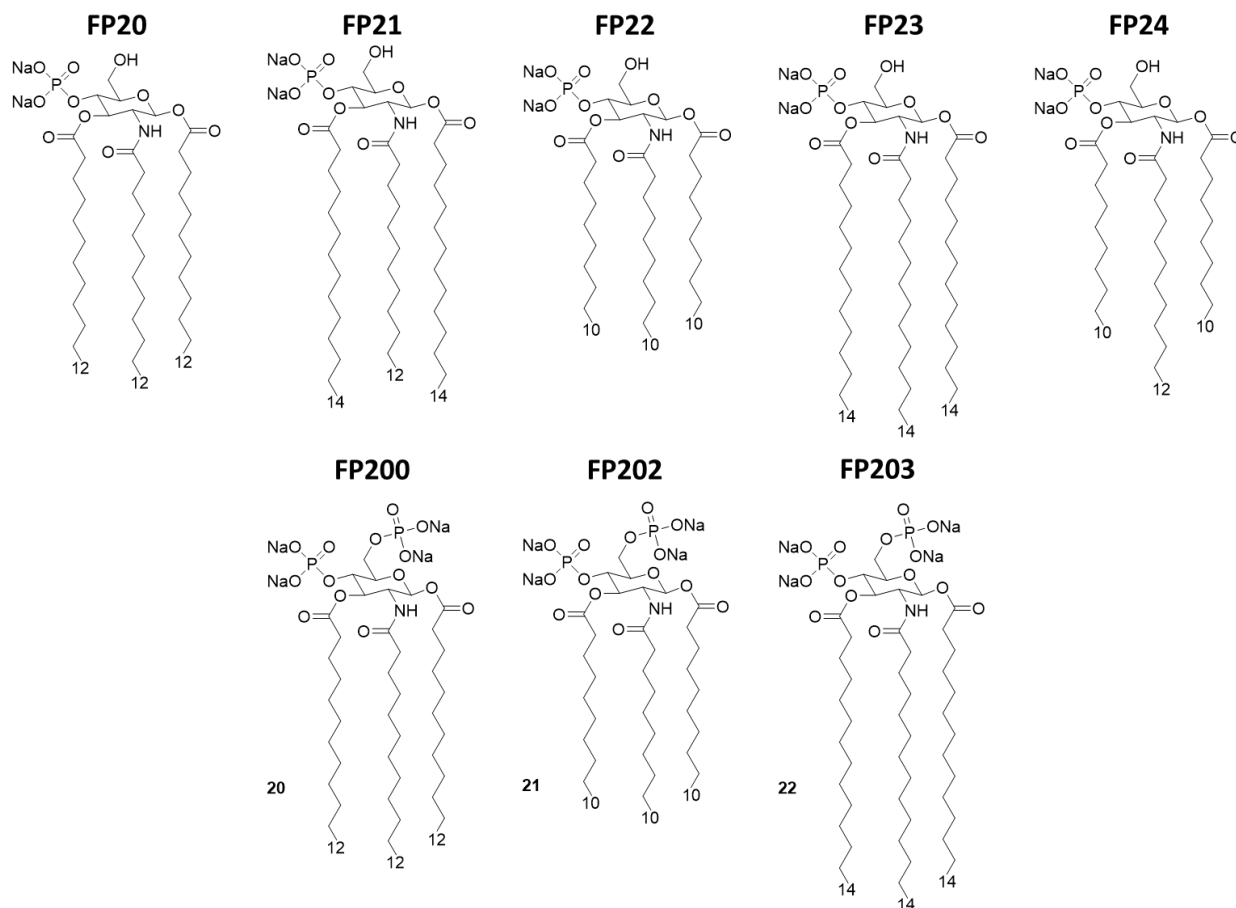


Figure 65 FP20 and its derivatives FP21, FP22, FP23 and FP24, together with their 6-OH phosphorylated counterparts, FP200, FP202 and FP203

These issues were elegantly solved simply by switching phosphate position from 1-OH to 4-OH, which made the molecule much more robust, while maintaining the same level of activity, selectivity and safety of FP18 *in vitro* but also *in vivo* (as outline in Chapter III). Furthermore, this switch opened the way to install various hydrophilic groups on the 6-OH to enhance pharmacologically relevant properties as solubility and bioavailability.

For one, this led to the interesting observation that while FP111, a diphosphate FP18 derivative, resulted completely inactive, FP200, the diphosphate version of FP20, still retained some level of activity: this helped us refine our SAR models and allowed to gather important insights on TLR4 mechanism and minimal requirements for activation.

On the other hand, compounds FP207 and FP20Rha, functionalized with neutral hydrophilic moieties, shown outstanding performance as TLR4 agonists, totally on a different scale than their parent unfunctionalized molecules.

Finally, in Chapter III we exposed more in detail the chemical efforts and biological results regarding these new functionalized compounds. While the synthesis of acylated compounds (such as FP207) was straightforward, as exposed in the patent in Chapter II, the chemical glycosylation to obtain e.g., FP20Rha was more challenging than expected, the main issue being the lability of the anomeric lipid chain. For this reason, the most common conditions didn't work due to their harshness, so that we needed to adopt milder protocols. The first one was a modified Koenigs-Knorr, which however afforded acceptable yields only with rhamnose; then, we applied milder conditions such as the $\text{Bi}(\text{OTf})_3$ and the NIS/HOFox protocols, which afforded high yields with all the glycosyl donors we tried, which allowed us to obtain several FP20 derivatives.

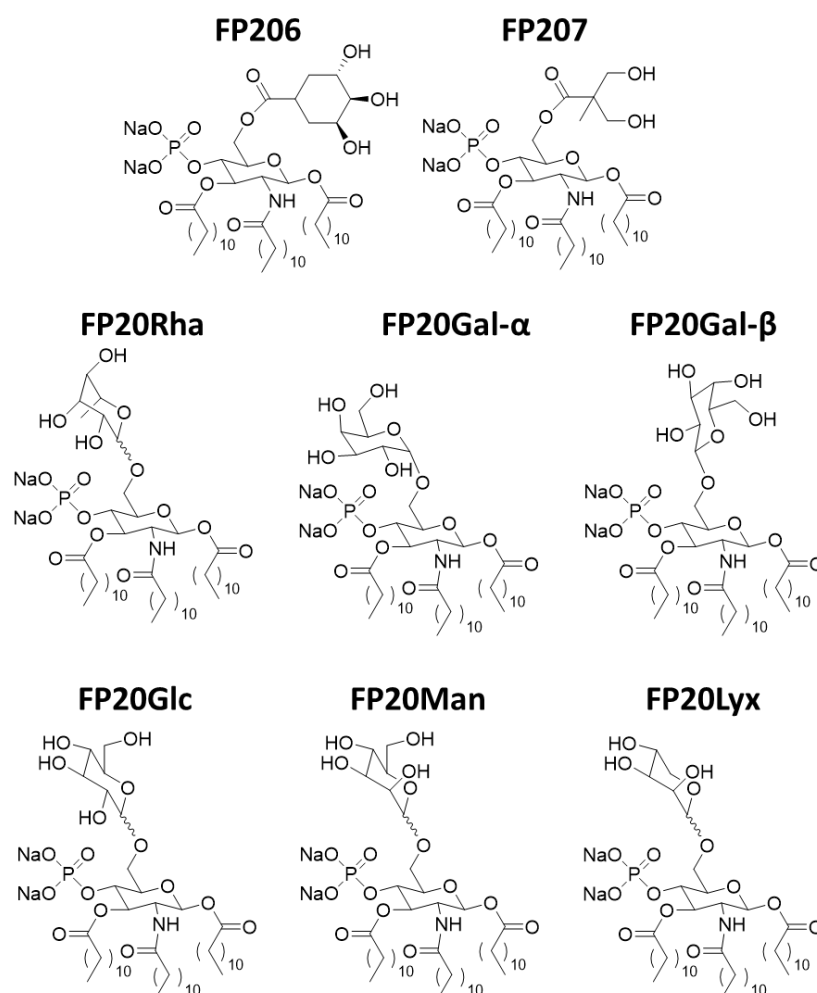


Figure 66 The molecules mainly treated in Chapter III, all derivatives of FP20 functionalized with neutral hydrophilic moieties: the acylated compounds FP206 and FP207 and the glycosylated compounds FP20Rha, FP20Gal- α , FP20Gal- β , FP20Glc, FP20man and FP20Lyx

The first two functionalized compounds we synthesized, FP207 and FP20Rha were chosen to be tested *in vitro* for their TLR4 agonism, which proved to be outstandingly high, to the point that they surpassed the positive control at 25 μ M and at 1 μ M scored the same agonism as MPLA at the same concentration range.

These results prompted us to study their mechanism of action, which shows differences from that of MPLA and from FP20 as well: while the latter only induce a low NF- κ B enucleation, probably caused by a weak MyD88 activation, both FP207 and FP20Rha cause high levels of NF- κ B translocation, indicating that they strongly engage the Myddosome.

Due to the mechanistic differences with their parent molecule, we were interested in assessing FP207 and FP20Rha adjuvancy *in vivo*. In collaboration with Dr. Anguita's group, we set an immunization experiment on C57BL/6 mice, which demonstrated how these compounds present the same levels of activity and toxicity of MPLA even though they're much simpler.

In conclusion, the compounds presented herein are promising candidates as novel vaccine adjuvants: they show the same level of activity and safety of MPLA, while being much easier and exponentially cheaper to produce, thanks to their simplicity, which makes them prime targets for industrial development. Nonetheless, the study on these compounds is still in the beginning, and some challenges are still present, such as the low solubility in water (partially solved by the addition of hydrophilic moieties on FP20). Furthermore, FP20 derivatives MOA it is still being studied and needs to be clarified before they can advance in development.

However, the work in this thesis lay the foundations for further advancements in the field of vaccine adjuvancy and therefore of vaccination itself, with the hope of impacting positively on human health.

AUTHOR'S CONTRIBUTION

Patents and Publications

- 1) Romerio, A.; Peri, F. Increasing the Chemical Variety of Modulators : An Overview. *Front. Immunol.* **2020**, *11* (July), 1–16.
- 2) Facchini, F. A.; Minotti, A.; Luraghi, A.; Romerio, A.; Gotri, N.; Matamoros-Recio, A.; Iannucci, A.; Palmer, C.; Wang, G.; Ingram, R.; Martin-Santamaria, S.; Pirianov, G.; De Andrea, M.; Valvano, M. A.; Peri, F. Synthetic Glycolipids as Molecular Vaccine Adjuvants: Mechanism of Action in Human Cells and In Vivo Activity. *J. Med. Chem.* **2021**, *64*, 12261–12272.
- 3) Romerio, A.; Peri, F. Italian patent application n. [102021000019544](#) of 22.07.2021 titled “New synthetic agonists of TLR4 receptor” and related PCT application n. PCT/IB2022/056615 of 19.07.2022
- 4) Luraghi, A.; Ferrandi, M.; Barassi, P.; Arici, M.; Hsu, S.; Torre, E.; Ronchi, C.; Romerio, A.; Chang, G.; Ferrari, P.; Bianchi, G.; Zaza, A.; Rocchetti, M.; Peri, F. Highly Selective SERCA2a Activators: Preclinical Development of a Congeneric Group of First-in-Class Drug Leads against Heart Failure. *J. Med. Chem.* **2022**, *65* (10), 7324–7333. **(Not included in this thesis)**

Communications

- 1) XIX CINMPIS Days in Pavia, February 20-21, 2020 – Oral Communication
- 2) BtBsDay 2020 (Virtual Event), December 15, 2020 – Poster Presentation
- 3) ACS Spring 2021 (Virtual Event), April 5-16, 2021 – Oral Communication
- 4) European Chemical Biology Symposium 2021 (Virtual Event), May 26-28, 2021 – Poster Presentation
- 5) XXVII Congresso Nazionale della Società Chimica Italiana (Virtual Event), September 14-23, 2021 – Oral Communication
- 6) BtBsDay 2021 in Milano, December 15, 2021– Oral Communication

ANNEXES

Computational Methods

Ligands 3D structure: construction, optimization and parameters derivation. The 3D structures of FP11, FP18 and FP111 were built with PyMOL molecular graphics and modeling package (www.pymol.org), using as a template the 6YA monosaccharide (GLYCAM database, www.glycam.org). The structures of the ligands were first refined at the AM1 level of theory, and then optimized at the Hartree-Fock level (HF/6-311G**) with Gaussian09.²²¹ The parameters needed for MD simulations were obtained using the standard Antechamber procedure in Amber14.²²² The partial charges were derived from the HF calculations, and formatted for AmberTools15 and Amber14 with Antechamber, assigning the general AMBER force field (GAFF) atom types, and GLYCAM force field atom types for the saccharide atoms.

Macromolecule preparation. 3D coordinates from the X-ray structure of the human (TLR4/MD-2/*E. coli* LPS)₂ ectodomain (PDB ID 3FXI) were retrieved from the Protein Data Bank (www.rcsb.org), and the chains A (TLR4) and C (MD-2) were extracted and considered as TLR4/MD-2 heterodimer in agonist conformation. Ligands and ions were removed. Hydrogen atoms were added to the X-ray structure using the pre-processing tool of the Protein Preparation Wizard of the Maestro package (www.schrodinger.com). The protein structure went through a restrained minimization under the OPLS3 force field with a convergence parameter to RMSD for heavy atoms kept default at 0.3 Å.

Docking calculations. AutoDockTools 1.5.6 program²²³ was used to assign the Gasteiger-Marsili empirical atomic partial charges to the atoms of both the ligands and the receptor. Nonpolar hydrogens were merged for the ligands. The structure of the receptor and the ligands were set rigid and flexible, respectively. Preliminary docked poses were obtained with AutoDock Vina 1.1.2.²²⁴ The box spacing was set to the default value of 1 Å; the size of the box was set to 33.00, 40.50, and 35.25 Å in the x, y, z-axes respectively, with the box center located equidistant to the mass center of residues Arg90 (MD-2), Lys122 (MD-2) and Arg264 (TLR4). The best-predicted docked poses from AutoDock Vina were redocked with AutoDock 4.2²²³ using the Lamarckian evolutionary algorithm; all parameters were kept default except that the number of genetic algorithm runs was set to 100 to enhance the sampling. Docking box spacing was set to 0.375 Å and box size was set to the same dimensions as for AutoDock Vina.

MD simulations. Selected docked complexes were submitted to all-atom MD simulations for 50 ns in the Amber14 suite using the force field ff14SB to describe the protein system. The simulation box was designed such that the edges were distant at least 10 Å of any atom. The system was solvated with the TIP3P water molecules model; Na⁺ ions were added to counterbalance the charges of the protein-ligand systems. All the simulations were performed with the same equilibration and production protocol. First, the system was submitted to 1000 steps of the steepest descent algorithm followed by 7000 steps of the conjugate gradient algorithm. A 100 kcal·mol⁻¹·Å⁻² harmonic potential constraint was applied to both the proteins and the ligand. In the subsequent steps, the harmonic potential was progressively lowered (respectively to 10, 5, and 2.5

kcal·mol⁻¹·Å⁻²) for 600 steps of the conjugate gradient algorithm each time, and then the whole system was minimized uniformly. Next, the system was heated from 0 to 100 K using the Langevin thermostat in the canonical ensemble (NVT) while applying a 20 kcal·mol⁻¹·Å⁻² harmonic potential restraint on the protein and the ligand. Finally, the system was heated from 100 to 300 K in the isothermal-isobaric ensemble (NPT) under the same restraint condition as in the previous step and followed by simulation for 100 ps with no harmonic restraint. At this point, the system was ready for the production run, which was performed using the Langevin thermostat under the NPT ensemble, at a 2 fs time step. All production runs were performed for 150 ns. The analysis was performed using the cpptraj module of AmberTools.²²⁵ Atomic coordinates of the TLR4 complexes (TLR4-FP11-01.pdb, TLR4-FP11-02.pdb, TLR4-FP18.pdb, TLR4-FP111-A.pdb and TLR4-FP111-B.pdb) after simulation are available.

Docking calculations of the binding of FP11, FP18, and FP111 to TLR4/MD-2

A deeper analysis of the docked binding poses revealed, in the case of FP18, a tendency for all poses to bury the three lipid acyl tails deep inside the hydrophobic cavity of MD-2, occupying the full pocket. In the case of FP11, different docked poses were obtained, most of them with all the FA chains allocated inside the MD-2 pocket, and other poses with one acyl chain located into the hydrophobic channel of MD-2, delimited by residues Arg90 and Phe126, and the other FA chains inside the MD-2 cavity (Fig. 1B, top). This second binding pose is similar to that observed for *E. coli* LPS in human and murine (TLR4/MD-2)₂ heterotetramers (PDB ID 3FXI¹⁹⁵ and 3VQ2²²⁶), where one FA chain is found occupying this channel. The presence of longer acyl chains in FP11 (C14 vs C12 in FP18) may favor the placement of one of them protruding into the MD-2 channel, whereas this phenomenon was not observed for FP18. Regarding FP111, in all AutoDock4 predicted poses, at least one FA tail was left outside the MD-2 pocket, without interacting either in the MD-2 Phe126 channel, and remaining exposed to the outer (Fig. 1B, bottom, left). These binding modes justify the unfavorable predicted binding energies.

The best docked clusters from each compound were visually inspected, with special attention to the ligand/receptor interactions, to establish a relationship between the chemical structure of the ligands and their effect on functional activity of TLR4 receptor. For FP11 and FP18, common features were observed. The polar head groups were placed at the entrance of MD-2 cavity, interacting with the polar residues present in that region, whereas the FA chains established contacts with many hydrophobic residues from the MD-2 pocket, specifically, Val24, Ile32, Ile46, Val48, Ile52, Leu54, Leu61, Ile63, Leu74, Phe76, Leu78, Ile80, Val82, Leu87, Ile94, Tyr102, Phe104, Ile117, Phe119, Phe121, Ile124, Phe126, Ser127, Tyr131, Val135, Phe147, Leu149, Phe151, and Ile153. The ligands phosphate groups were often placed at the rim of MD-2 where they are exposed to the solvent, in agreement with the reported X-ray crystallographic complexes of TLR4/MD-2

with glycolipids (for example, complex with Eritoran, PDB ID 2Z65,⁸⁴ or with lipid IVa, PDB ID 2E59²²⁷). Two different orientations have been reported for TLR4 binders, rotated 180° between them¹³³: type A (antagonist-like binding mode), similar to that found for lipid IVa in PDB ID 2E59,²²⁶ and type B (agonist-like binding mode), similar to that found for *E. coli* lipid A in PDB ID 3FXI.¹⁹⁵ These two different binding types lead to opposed biological activities.²²⁸ Remarkably, the obtained docked poses for FP11 and FP18 showed a type B like binding mode, in agreement with their reported *in vitro* agonist activity.

Most of the FP11 and FP18 poses presented the hydroxyl group of the saccharide moiety interacting with the Glu92 side chain from MD-2, and the amide CO group was often close to the Arg90 of MD-2, establishing hydrogen bonds and electrostatic interactions, while the ester oxygen of the 4-acyl chain interacted with the hydroxyl group of the MD-2 Ser120. The main difference observed between FP11 and FP18 ligands was related to the interactions established by the phosphate group; in FP11 poses, the phosphate interacted with the backbone of MD-2 Lys122, whereas in FP18 interacted with MD-2 Arg90 (Fig. 1B, top, right). The relevance of the interactions between the studied ligands and the above-mentioned MD-2 residues, which are key residues in the recognition of *E. coli* LPS by the TLR4/MD-2 complex according to the literature data must be highlighted.^{195,229}

As for FP111, although AutoDock Vina was able to produce plausible docked poses inside the TLR4/MD-2 system, AutoDock did not lead to poses with favorable predicted binding energies. It is well-known the better performance correlation between predicted binding free energy and experimental value for AutoDock *versus* AutoDock Vina, as well as better precision and success rates.²³⁰ Remarkably, FP111 poses showed the two above mentioned types of ligand poses, A and B, along the results generated by means of both docking programs (Fig. 1B, bottom, right). In any case, we also analysed the docking results for FP111 from AutoDock. FP111 poses were predicted to be anchored through one phosphate group to MD-2, and the second phosphate to positively charged residues present in TLR4; in the type A poses, the 6-phosphate group interacted with TLR4 residues, equivalent to the interaction of the 1-phosphate in the type B poses (Fig. 1B, bottom). The 6-phosphate should mimic the interaction of the hydroxyl group present in FP11 and FP18 but, given a bigger size and different electronic distribution, this interaction is not possible and tries to reach positive residues at TLR4. As a consequence of these contacts between FP111 and TLR4, the generated poses remained not as deep inside the MD-2 pocket as in the FP11 and FP18 cases, and more exposed to the solvent. These observations could explain the unfavorable predicted binding energy. We selected two of the best binding poses for further study, one type A (antagonist-like binding pose, Fig. 1B, bottom, right), and one type B (agonist-like binding pose, Fig. 1B, bottom, right). In the type A docked pose, rotated 180° with respect to FP11 and FP18 predicted poses, the 1-phosphate interacted with TLR4 Arg264, establishing two hydrogen bonds, and with MD-2 Tyr102 residue, whereas the 6-phosphate interacted with MD-2 residues Ser118 and Ser120. The 4-acyl chain was found outside MD-2, interacting with unexpected residues, such as

MD-2 Gly56, Ser57 and Lys58. These residues have not been reported before in the interaction between TLR4 modulators and the receptor complex. The other two FP111 acyl chains, buried inside MD-2, established contacts with Leu61, Phe76, Leu78, Ile94, Phe121, Lys122, Ile124, Phe126, Cys133, Val135 and Phe151. In the type B orientation, the 1-phosphate interacted with MD-2 Arg90 and Glu92 residues, establishing a hydrogen bond with the latter one, similar to the interaction previously described for the hydroxyl group of FP11 and FP18, and the 6-phosphate interacted with the Lys362 of TLR4. The disposition adopted by FP111 due to this last contact, forces to place the 4-acyl chain outside the MD-2 cavity, establishing a hydrogen bond between the ester CO group and the TLR4 Arg264 side chain. Additionally, other electrostatic and hydrophobic interactions were observed between this acyl tail and TLR4 residues, namely Asp101, Tyr292, Leu293, Tyr296, Ser317, Val318, Thr319, Asn339, Cys340 and Lys341, and between the remaining FA chains, located inside MD-2 protein, and MD-2 residues, such as Val24, Ile32, Ile46, Val48, Leu61, Ile63, Phe76, Leu78, Ile94, Tyr102, Phe104, Phe117, Phe119, Val135, Phe147 and Phe151. It is well known that the determining factors of the immunostimulatory activity of TLR4 modulators, are the number and the distribution of acyl chains and the phosphorylation pattern. As example, the orientation of the lipid IVa is rotated by 180° in the di-saccharide plan thus lipid IVa presents two different molecular patterns of interaction for human and mouse TLR4 receptors. These different binding modes of lipid IVa determine how the phosphate groups interact with the TLR4/MD-2 complex and are crucial for the observed different behaviour among both species.²²⁸ Interestingly, the distances between the two phosphates in all the FP111 docked solutions ranged from 5.4 to 8.2 Å, values lower to the distance between the two phosphates of the agonist *E. coli* lipid A at C1 and C4' positions (distance of 12.4 Å in PDB ID 3FXI¹⁹⁵). Specifically, the two phosphate groups were placed at a distance of 6.5 Å in the selected FP111 type A pose, and of 8 Å in the type B. Overall, we can conclude there is a different binding pattern for FP111 in comparison to FP11 and FP118, not including extensively reported and well-known TLR4/MD-2/ligand interactions,¹³³ as well as unfavorable predicted binding energies. This anomalous behaviour can be explained by the presence of two phosphate groups in 1, 6-positions simultaneously, that cannot allow a proper docking into the MD-2 rim and need to anchor to TLR4, unlike the mono (1-or 6-) phosphate pattern, accounting for the lack of activity observed for this compound.

MD simulations of (TLR4/MD-2)₂ complex with FP11 and FP18

Stability of the best FP11 and FP18 predicted binding modes was confirmed by molecular dynamics (MD) simulations. Starting from the docked TLR4/MD-2/ligand complexes, we constructed three (TLR4/MD-2/ligand)₂ heterodimer models (Fig. S1a) which were submitted to 50 ns MD simulations: the best pose from the FP18 docking calculations (Fig. S1b), and two from the FP11 results; one pose with all the ligand acyl chains inside the MD-2 pocket (FP11-01, Fig. S1b), and another one with one FA chain protruding towards

the MD-2 channel, and the other chains folded into the MD-2 cavity (FP11-02, Fig. S1c). After 50 ns simulation, the complexes remained stable, as shown by the RMSD analysis (Fig. S2).

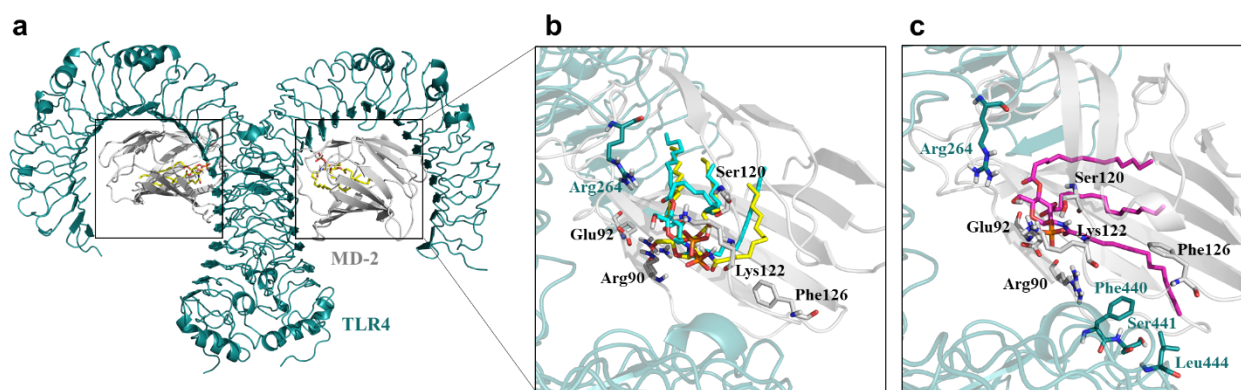


Fig. S1: MD simulations of ligands FP11 and FP18 selected binding modes.

a a general view of the simulated (TLR4/MD-2/FP18)₂ complex, as example. **b, c** Details of the averaged interactions between FP11 (blue and magenta sticks) and FP18 (yellow sticks) and TLR4/MD-2, over simulation time. During simulations, in the FP11 binding mode with the 2-acyl chain protruding within the MD-2 channel, this FA chain remained outside from the MD-2 pocket, pointing toward the partner TLR4, only in one of the (TLR4/MD-2/FP11)₂ subunits, interacting with residues Phe440, Ser441 and Leu444 from the partner TLR4 (**c**, FP11 as magenta sticks). Residue MD-2 Phe126 remained in agonist conformation throughout simulation time (t = 50 ns). TLR4 and MD-2 are respectively depicted in turquoise blue and grey cartoons. Residues that interacted with the ligands are in sticks with their corresponding individual labels.

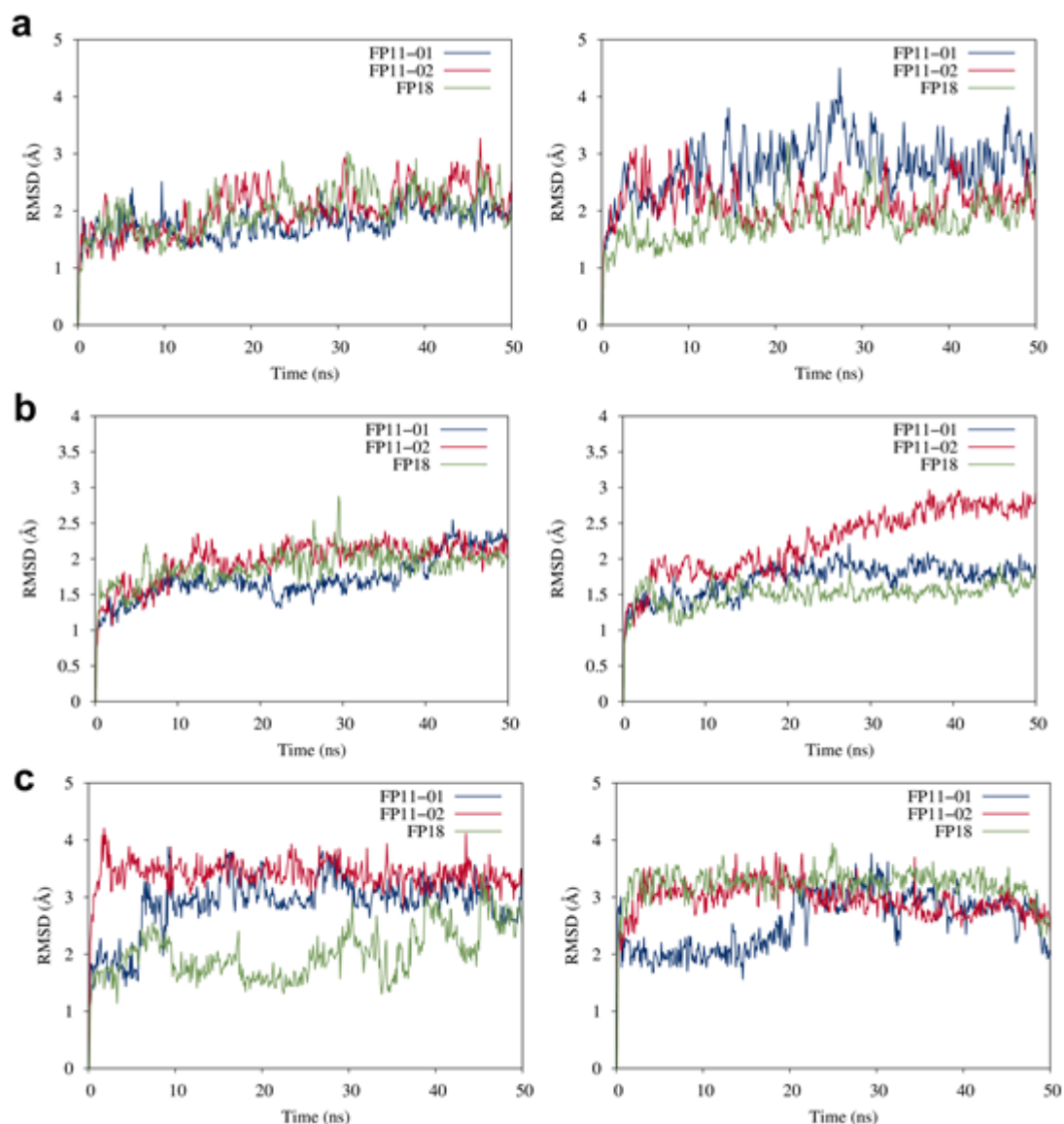


Fig. S2: Molecular dynamics simulations of the (TLR4/MD-2)₂ system in complex with ligands FP11 and FP18. a RMSD of the TLR4 chain A (on the left) and B (on the right) backbone over time. **b** RMSD of the MD-2 chain A (on the left) and B (on the right) backbone, over time. **c** RMSD for the heavy atoms of the ligands docked in TLR4/MD-2 chain A (on the left) and B (on the right), over time.

The relative orientation between the ligands and MD-2 was evaluated. We arbitrarily defined two vectors, one from the amide α -carbon atom to the ester α -carbon atom of the ligand, and another one from the α -carbon of residues Pro78 to Thr105 of MD-2 (Fig. S3a). The angle between these two vectors was plotted both over time, and it was observed that none of the ligands undergoes orientation flip during the 50 ns simulations, all remaining in the agonist type B orientation obtained from the docking calculations (Fig. S3b). Furthermore, the motion of the TLR4 molecular switch, MD-2 Phe126 chain was also evaluated (Fig. S4). FP11 and FP18 ligands were able to retain the agonist conformation for MD-2 Phe126 along simulation time.

Therefore, we suggest these complexes as plausible binding modes for FP11 and FP18 accounting for their agonist activity in the TLR4/MD-2 system.

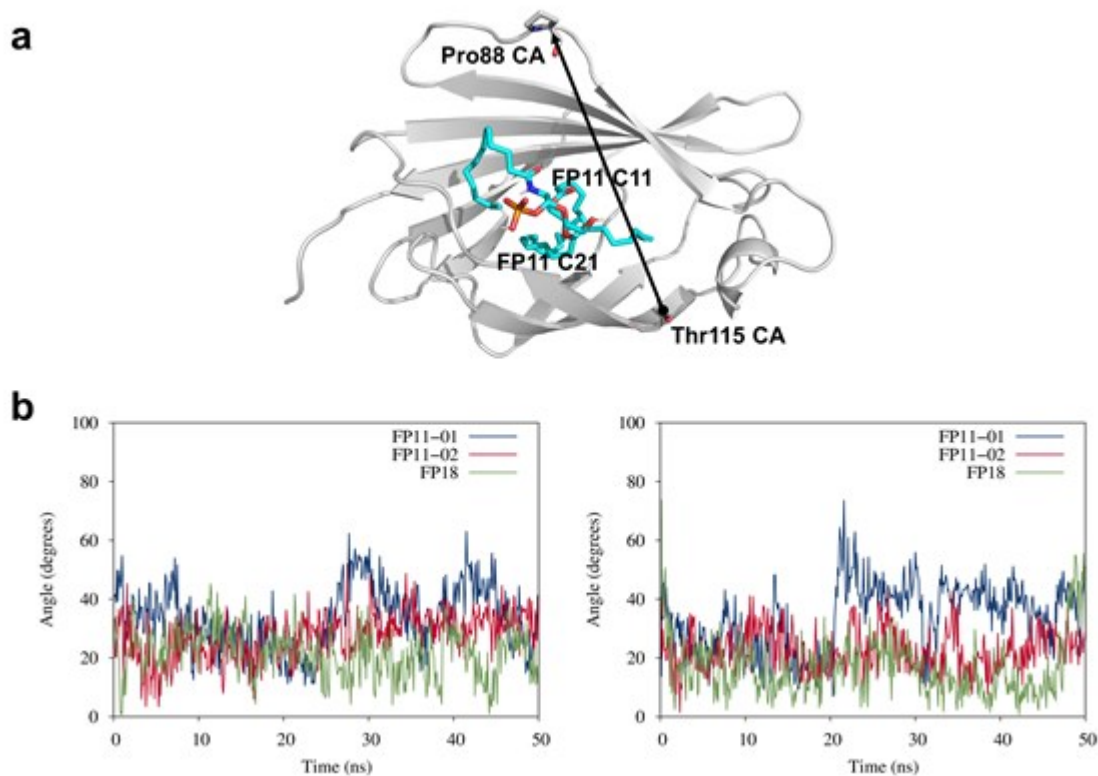


Fig. S3: Ligands orientation within the MD-2 pocket. **A)** Angle plotted over simulation time between two arbitrarily selected vectors starting from the α -carbon (CA) of Pro88 to the α -carbon of Thr115, and the vector from amide α -carbon atom (C11) and the ester α carbon atom (C21) of FP11, used to follow the orientation of the ligands along the MD simulations. Angle for MD-2 chain A, on the left and chain B, on the right. FP11 is used as an example; the same applies for the other ligands. **B)** Representation of the two selected vectors, within MD-2. Angle between 0 and 90 degrees is characteristic of the type B binding (agonist-like) as observed in the PDB ID 3FXI (TLR4/MD-2/*E. coli* LPS)₂ complex; angle between 90 and 180 degrees is characteristic of the type A binding mode (antagonist-like) as observed in the PDB ID 2E59 (MD-2/lipid-IVa) complex. MD-2 is represented as semi-transparent grey cartoon, and FP11 ligand as cyan sticks.

During the MD simulations, the similar interactions were observed for FP11 (FP11-01 and FP11-02) and FP18 compounds, in both TLR4/MD-2 units. The ligands suffered a slightly reorientation of the saccharide moiety, which allowed them to establish a new electrostatic contact with each corresponding TLR4 chain, concretely between the hydroxyl group of the ligands and the TLR4 Arg264 residue (Fig. S1b, c). Consequently, the interaction between the hydroxyl group of the compounds and MD-2 Glu92 was lost in all the cases, and this residue became to interact with both, the ester CO group or the oxygen of the ligands 2-acyl chain, depending on the case. Interestingly, in the MD simulation of the (TLR4/MD-2/FP18)₂ complex, the interaction between the phosphate group and MD-2 Arg90 was lost and two new contacts with MD-2

residues were established, a hydrogen bond with the backbone of Lys122, as observed in the FP11 docked poses, and a polar contact with Ser120. Regarding FP11 poses, a new polar contact was displayed between the ligand 1-phosphate group and MD-2 Ser120, as in FP18 simulation, additional to the initially present interaction with Lys122, predicted by docking programs, which was maintained along the simulations. The interaction between Arg90 and the amide CO group of the 2-acyl chain was maintained in all the ligands. Remarkably, when we constructed the full (TLR4/MD-2/ligand)₂ heterotetramer model of the FP11-02 pose for running the MD simulations, the FP11 lipid chain placed in the MD-2 channel, interacted with residues of the partner TLR4, concretely, Phe440 and Ser441. During the simulation of the (TLR4/MD-2/FP11-02)₂ complex, this chain remained outside from the MD-2 pocket, pointing toward the partner TLR4, only in one of the (TLR4/MD-2/FP11-02)₂ subunits. The interactions between this chain and the partner TLR4 residues Phe440 and Ser441, observed when we constructed the full (TLR4/MD-2/FP11-02)₂ complex, were maintained over time (Fig. S1c), and one more interaction was established between this FA chain and the counterpart TLR4 Leu444 residue. On the contrary, the same FP11-02 FA chain of the TLR4 counterpart, was folded into the MD-2 cavity during the simulation. The electrostatic and hydrophobic interactions with the rest of MD-2 residues, predicted by docking calculations, were maintained.

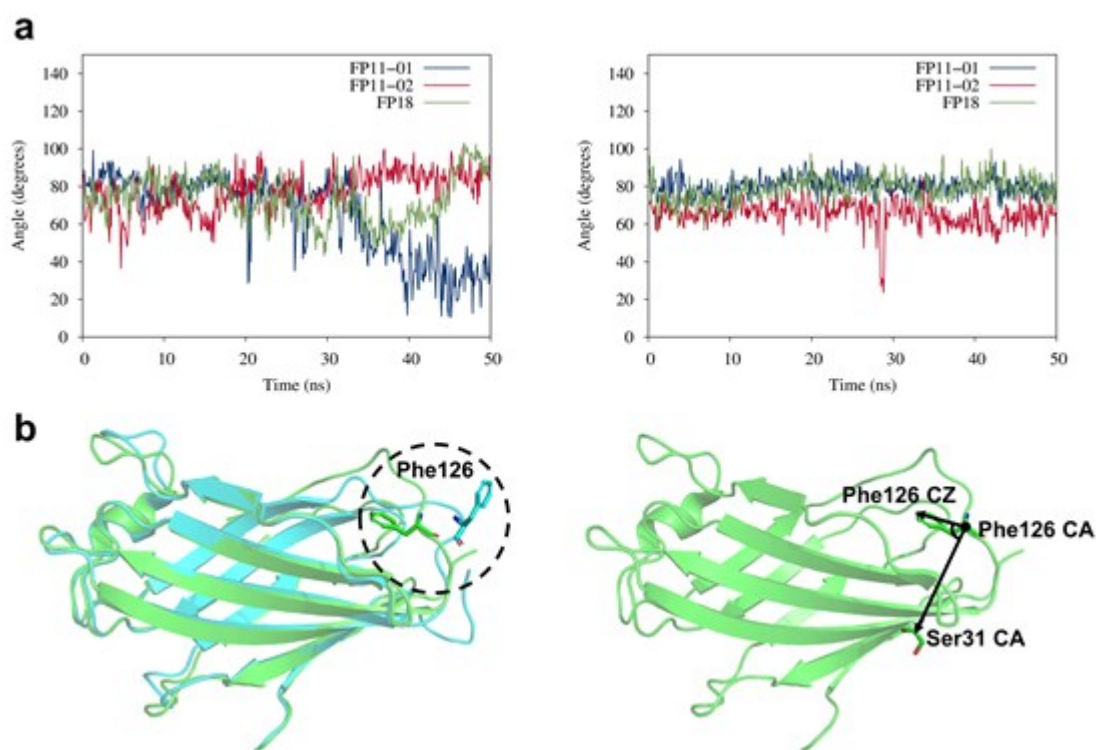


Fig. S4: Motion of the TLR4/MD-2 antagonist/agonist switch Phe126. A) Angle plotted over simulation time between two arbitrarily selected vectors starting both from the α -carbon (CA) of residue MD-2 Phe126 to, respectively, the zeta-carbon (CZ) of the same residue and the α -carbon (CA) of residue Ser31. Angle for MD-2 chain A, on the left and chain B, on the right. **B)** On the left: Superposition of the X-ray crystallographic structures of the agonist (green) and the antagonist (cyan) conformations of MD-2 from, respectively, PDB

ID 3FXI and 2E59. On the right: representation of the two selected vectors, within MD-2. Agonist MD-2 from PDB ID 3FXI and antagonist MD-2 from PDB ID 2E59 are represented in semi-transparent green and cyan cartoon, respectively. Bound ligands have been hidden for clarity (*E. coli* LPS in 3FXI; lipid IVA in 2E59). Conformational changes of the molecular switch Phe126 are marked. The angle plotted over time shows the stability of residue Phe126 during MD simulations associated with agonist activity of ligands. Angle between 0 and 100 degrees is characteristic of the agonist-like binding.

Chemical synthesis procedures

Compound 8

tert-butyldimethylsilyl-2-tetradecanamido-2-deoxy-3-O-tetradecanoyl-6-O-(4-methoxybenzyl)- β -D-glucopyranoside (8). Compound **6**¹³³ (320 mg, 0.38 mmol) was dissolved in dry THF (19 mL), 4Å molecular sieves (1.15 g) and NaCNBH₃ (157 mg, 18.38 mmol) were added. The reaction was stirred at r.t. for 1h, then TFA (581 mL, 7.6mmol) was added dropwise at 0°C. The resulting solution was left stirring for additional 45 min at r.t.. After neutralization with saturated NaHCO₃ solution, the mixture was extracted with DCM. Combined organic phases were with brine, dried over anhydrous Na₂SO₄, filtered and evaporated *in vacuo*. Crude was purified with flash chromatography (petroleum ether-EtOAc 8:2) to give compound **8** as a red oil (273 mg, 85%).

¹H NMR (400 MHz, CDCl₃, 25 °C, TMS) δ 7.23 (d, ³J_{H,H}=8.6 Hz, 2H; 2x H-*ortho* PMB), 6.85 (t, ³J_{H,H}=8.7 Hz, 2H: 2x H-*meta* PMB), 5.81 (d, ³J_{H,H}=9.3 Hz, 1H; NH), 5.04 (dd, ³J_{H,H}=10.7, 9.2 Hz, 1H; H-3), 4.67 (d, ³J_{H,H}=8.1 Hz, 1H, H-1), 4.54-4.42 (m, 2H; CH₂-Ph), 3.94 (m, 1H; H-2), 3.78 (s, 4H; OMe, H-5), 3.70 (dd, ³J_{H,H}=10.8, 5.3 Hz, 1H, H-6a), 3.54 (m, 2H, H-4, H-6b), 2.38-2.24 (t, ³J_{H,H}=7.8 Hz, 2H, CH₂ α -chain1), 2.15-1.98 (m, 2H, CH₂ α -chain2), 1.64-1.44 (m, 4H CH₂ β -chains1,2), 1.19 (m, 40H, 20x CH₂), 0.96-0.70 (m, 15H, 2xCH₃ chains1,2 ,tBu-Si), 0.03 (s, 3H; CH₃-Si), 0.00 (s, 3H; CH₃-Si).

¹³C NMR (101 MHz, CDCl₃, 25 °C, TMS) δ 174.88, 172.79, 159.29, 129.66, 129.30, 113.80, 96.53, 75.26, 73.71, 73.42, 71.25, 70.57, 55.46, 55.23, 36.98, 34.28, 31.93, 29.72, 29.68, 29.55, 29.47, 29.38, 29.36, 29.14, 25.57, 24.97, 22.69, 17.88, 14.13.

HRMS (ESI): m/z [M+Na⁺] calculated for C₄₈H₈₇NNaO₈Si⁺: 856.2972. Found: 856.2977.

Compound 9

tert-butyldimethylsilyl-2-dodecanamido-2-deoxy-3-O-dodecanoyl-6-O-(4-methoxybenzyl)- β -D-glucopyranoside (9). Compound **9** was synthesized starting from **7**¹³³ accordingly to the procedure presented for compound **8** in 83% yield.

¹H NMR (400 MHz, CDCl₃, 25 °C, TMS) δ 7.19 (d, ³J_{H,H}=8.3 Hz, 2H; 2x H-*ortho* PMB), 6.82 (t, ³J_{H,H}=8.5 Hz, 2H: 2x H-*meta* PMB), 6.29 (d, ³J_{H,H}=9.6 Hz, 1H; NH), 5.09 (t, ³J_{H,H}=9.9 Hz, 1H; H-3), 4.67 (d, ³J_{H,H}=8.0 Hz, 1H, H-1), 4.55-4.37 (m, 2H; CH₂-Ph), 3.94 (q, , ³J_{H,H}=9.6 Hz, 1H; H-2), 3.75 (s, 4H; OMe, H-5), 3.66 (dd, ³J_{H,H}=9.7, 7.2 Hz, 1H, H-

6a), 3.56 (m, 2H, H-4, H-6b), 2.36-2.20 (m, 2H, CH₂α-chain1), 2.16-2.01 (m, 2H, CH₂α-chain2), 1.64-1.44 (m, 4H CH₂β-chains1,2), 1.22 (m, 32H, 16x CH₂), 0.92-0.77 (m, 15H, 2xCH₃ chains1,2 ,tBu-Si), 0.05 (s, 3H; CH₃-Si), 0.02 (s, 3H; CH₃-Si).

¹³C NMR (101 MHz, CDCl₃, 25 °C, TMS) δ 175.13, 173.04, 159.53, 129.91, 129.55, 114.05, 96.78, 75.51, 73.96, 73.67, 71.49, 70.82, 55.71, 55.48, 37.23, 34.53, 32.18, 29.97, 29.93, 29.80, 29.72, 29.63, 29.60, 29.39, 25.82, 25.22, 22.94, 18.13, 14.38.

HRMS (ESI): m/z [M+Na⁺] calculated for C₄₄H₇₉NNaO₈Si⁺: 800.5467. Found: 800.5471.

Compound 10

10 *tert-butyldimethylsilyl-2-tetradecanamido-2-deoxy-3,4-di-O-tetradecanoyl-6-O-(4-methoxybenzyl)-β-D-glucopyranoside (10)*. To a 0°C cooled solution of compound **8** (263 mg, 0.32 mmol), DMAP (39 mg, 0.32 mmol), and TEA (87 μL ,0.63 mmol) in DCM (5 mL), myristoyl chloride (170 μL ,0.63 mmol) was added dropwise. The solution was stirred at r.t. for 1h. Solvents were evaporated *in vacuo* and crude product purified with flash chromatography (petroleum ether–EtOAc 9:1) to give compound **10** as a white solid (323 mg, 98%).

¹H NMR (400 MHz, CDCl₃, 25 °C, TMS) δ 7.23 (d, ³J_{H,H}=8.4 Hz, 2H, 2x H-ortho PMB), 6.85 (d, ³J_{H,H}=8.4 Hz, 2H, 2x H-meta PMB), 5.30 (d, 1H, NH), 5.15 (t, ³J_{H,H}=10.2 Hz, 1H, H-3), 5.03 (t, ³J_{H,H}=9.6 Hz, 1H, H-4), 4.77 (d, ³J_{H,H}=8.1 Hz, 1H, H-1), 4.45 (s, 2H, CH₂-Ph), 3.96-3.85 (m, 1H, H-2), 3.79 (s, 3H, OCH₃), 3.66-3.58 (m, 1H, H-5), 3.51 (m, 2H, H-6a, H-6b), 2.23 (t, ³J_{H,H}=7.8 Hz, 2H, CH₂α-chain1), 2.14 (t, ³J_{H,H}=7.6 Hz, 2H, CH₂α-chain2), 2.10-2.02 (m, 2H, CH₂α-chain3), 1.63-1.43 (m, 6H, CH₂β-chains1,2,3), 1.24 (m, 60H, 30xCH₂), 0.94-0.79 (m, 15H, 2xCH₃-chains1,2 ,tBu-Si), 0.12 (s, 3H; CH₃-Si), 0.08 (s, 3H; CH₃-Si).

¹³C NMR (101 MHz, CDCl₃, 25 °C, TMS) δ 173.89, 172.59, 172.26, 159.14, 129.98, 129.27, 113.67, 96.37, 73.50, 73.19, 72.31, 69.33, 69.27, 56.26, 55.23, 36.91, 34.18, 34.11, 32.78, 31.92, 29.67, 29.50, 29.36, 29.32, 29.14, 26.40, 25.58, 24.94, 24.79, 22.69, 17.88, 14.12, -4.02, -5.23.

HRMS (ESI): m/z [M+Na⁺] calculated for C₆₂H₁₁₃NNaO₉Si⁺: 1066.8077. Found: 1066.8081.

Compound 11

tert-butyldimethylsilyl-2-dodecanamido-2-deoxy-3,4-di-O-dodecanoyl-6-O-(4-methoxybenzyl)-β-D-glucopyranoside (11). Compound **11** was synthesized starting from **9** accordingly performing the acylation presented for compound **10** with lauroyl chloride. Compound was obtained in 97% yield.

¹H NMR (400 MHz, CDCl₃, 25 °C, TMS) δ 7.22 (d, ³J_{H,H}=8.6 Hz, 2H, 2x H-ortho PMB), 6.85 (d, ³J_{H,H} =8.6 Hz, 2H, 2x H-meta PMB), 5.34 (d, J =9.3 Hz, 1H, NH), 5.15 (t, ³J_{H,H}=9.9 Hz, 1H, H-3), 5.02 (t, ³J_{H,H}=9.6 Hz, 1H, H-4), 4.76 (d, ³J_{H,H}=8.0 Hz, 1H, H-1), 4.44 (s, 2H, CH₂-Ph), 3.91 (dt, ³J_{H,H} =10.8, 8.5 Hz, 1H, H-2), 3.79 (s, 3H, OCH₃), 3.64 (dt, ³J_{H,H} =9.6, 4.5 Hz, 1H, H-5), 3.54-3.48 (m, 2H, H-6a, H-6b), 2.22 (t, ³J_{H,H}=7.6 Hz, 2H, CH₂α-chain1), 2.14 (t,

$^3J_{H,H}=7.6$ Hz, 2H, CH₂α-chain2), 2.09-2.04 (m, 2H, CH₂α-chain3), 1.59-1.43 (m, 6H, CH₂β-chains1,2,3), 1.32-1.21 (m, 48H, 24xCH₂ chains), 0.91-0.83 (m, 15H, 2xCH₃-chains1,2 ,tBu-Si), 0.12 (s, 3H; CH₃-Si), 0.09 (s, 3H; CH₃-Si).
 ^{13}C NMR (101 MHz, CDCl₃, 25 °C, TMS) δ 173.98, 172.68, 172.34, 159.22, 130.06, 129.35, 113.75, 96.45, 73.58, 73.28, 72.39, 69.41, 69.35, 56.34, 55.31, 37.00, 34.26, 34.20, 32.87, 32.00, 29.76, 29.58, 29.45, 29.40, 29.22, 26.49, 25.67, 25.02, 24.88, 22.77, 17.97, 14.21, -3.94, -5.15.

HRMS (ESI): m/z [M+Na⁺] calculated for C₅₆H₁₀₁NNaO₉Si⁺: 982.7138. Found: 982.7143.

Compound 12

2-tetradecanamido-2-deoxy-3,4-di-O-tetradecanoyl-6-O-(4-methoxybenzyl)-β-D-glucopyranose (**12**).

Compound **10** (323 mg, 0.31 mmol) was dissolved in dry THF (15 mL) and cooled to -15 °C. A solution of TBAF (107 mg, 0.34 mmol) and AcOH (22 μL, 0.39 mmol) in THF (340 μL) was added. The reaction was stirred at -15 °C for 10 min, then allowed to warm at r.t. and stirred for additional 30 min. The solution was diluted with water and extracted with CH₂Cl₂. The combined organic layers were dried over anhydrous Na₂SO₄, filtered and evaporated *in vacuo*. The crude product was purified with flash chromatography (petroleum ether–EtOAc 7:3) to give afford **12** as a red oil (250 mg, 87%).

1H NMR (400 MHz, CDCl₃, 25 °C, TMS) δ 7.24 (d, $^3J_{H,H}=8.7$ Hz, 1H, 2x H-*ortho* PMB), 6.85 (d, $^3J_{H,H}=8.6$ Hz, 1H, 2x H-*meta* PMB), 5.71 (d, $^3J_{H,H}=9.5$ Hz, 1H, H-1), 5.34-5.23 (m, 2H, NH, H-3), 5.07 (t, $^3J_{H,H}=9.9$ Hz, 1H, H-4), 4.45 (s, 2H, CH₂-PMP), 4.32-4.24 (m, 1H, H-2), 4.19-4.11 (m, 1H, H-5), 3.79 (s, 3H, OCH₃), 3.55-3.38 (m, 1H, H-6a, H-6b), 3.02-2.84 (bs, 1H, OH), 2.22 (t, $^3J_{H,H}=7.6$ Hz, 2H, CH₂α-chain1), 2.18-2.05 (m, 4H, CH₂α-chain2,3), 1.68-1.41 (m, 6H, CH₂β-chains1,2,3), 1.24 (m, 60H, 30xCH₂), 0.88 (t, $^3J_{H,H}=6.7$ Hz, 9H, 3x CH₃-chains1,2,3).

^{13}C NMR (101 MHz, CDCl₃, 25 °C, TMS) δ 174.18, 173.02, 172.22, 159.29, 129.58, 113.73, 91.68, 73.18, 70.50, 68.85, 68.73, 55.22, 52.09, 36.73, 34.22, 34.11, 31.92, 29.68, 29.37, 29.28, 29.17, 25.59, 24.91, 22.69, 14.13.

HRMS (ESI): m/z [M+Na⁺] calculated for C₅₆H₉₉NNaO₉⁺: 952.7212. Found: 952.7217.

Compound 13

2-dodecanamido-2-deoxy-3,4-di-O-dodecanoyl-6-O-(4-methoxybenzyl)-β-D-glucopyranose (**13**). Compound **13** was synthesized starting from **11** accordingly to the procedure presented for compound **12** in 90% yield.

1H NMR (400 MHz, CDCl₃, 25 °C, TMS) δ 7.23 (d, $^3J_{H,H}=6.7$ Hz, 2H, 2x H-*ortho* PMB), 6.85 (d, $^3J_{H,H}=8.8$ Hz, 2H, 2x H-*meta* PMB), 5.27 (d, $^3J_{H,H}=9.9$ Hz, 1H, H-1), 5.26-5.23 (m, 1H, NH, H-3), 5.05 (t, $^3J_{H,H}=9.8$ Hz, 1H, H-4), 4.44 (s, 2H, CH₂-PMP), 4.31-4.22 (m, 1H, H-2), 4.19-4.10 (m, 1H, H-5), 3.79 (s, 3H, OCH₃), 3.52-3.41 (m, 2H, H-6a, H-6b), 2.36-2.02 (m, 6H, CH₂α-chain1,2,3), 1.57-1.45 (m, 6H, CH₂β-chains1,2,3), 1.25 (m, 48H, 24xCH₂ chains), 0.87 (s, 9H, 3x CH₃-chains1,2,3).

^{13}C NMR (101 MHz, CDCl₃, 25 °C, TMS) δ 173.61, 172.45, 171.65, 158.71, 129.01, 113.16, 91.11, 72.61, 69.93, 68.28, 68.16, 54.65, 51.51, 36.16, 33.65, 33.54, 31.35, 29.10, 28.80, 28.71, 28.59, 25.01, 24.34, 22.12, 13.56.

HRMS (ESI): m/z $[M+Na^+]$ calculated for $C_{50}H_{87}NNaO_9^+$: 868.6273. Found: 868.6278.

Compound 14

1-(dibenzyl)phospho-2-tetradecanamido-2-deoxy-3,4-di-O-tetradecanoyl-6-O-(4-methoxybenzyl)- α -D-glucopyranose (14). Compound **12** (100 mg, 0.11 mmol) was dissolved in dry CH_2Cl_2 (1.8 mL). Imidazolium triflate (83 mg, 0.32 mmol) and dibenzyl *N, N*-diisopropyl phosphoramidite (108 μ l, 0.32 mmol) were added, and the reaction was stirred for 30 min at r.t.. After cooling at $-20^\circ C$, *m*CPBA (93 mg, 0.54 mmol) was added, the reaction was then stirred overnight at r.t.. Mixture was diluted with CH_2Cl_2 , washed with a saturated solution of $NaHCO_3$ and brine. The organic layer was dried over anhydrous Na_2SO_4 , filtered and to dryness. The crude product was purified with flash chromatography (petroleum ether–EtOAc 8:2) affording compound **14** as a brown solid (70 mg, 55%).

1H NMR (400 MHz, $CDCl_3$, $25^\circ C$, TMS) δ : 7.42-7.27 (m, 10H, 2x BnO-P), 7.17 (d, $^3J_{H,H}=8.5$ Hz, 2H, 2x H-ortho PMB), 6.80 (d, $^3J_{H,H}=8.4$ Hz, 2H, 2x H-meta PMB), 5.71 (dd, $^3J_{H,P}=5.7$, $^3J_{H,H}=3.3$ Hz, 1H, H-1), 5.57 (d, $^3J_{H,H}=9.1$ Hz, 1H, NH), 5.24-5.14 (m, 2H, H-3, H-4), 5.11-4.95 (m, 4H, 2x $CH_2(Ph)$ -O-P), 4.45-4.23 (m, 3H; CH_2 -Ph PMB, H-2), 4.05 (m, 1H, H-5), 3.76 (s, 3H, OCH_3), 3.38 (d, $^3J_{H,H}=3.4$ Hz, 2H, H6a, H6b), 2.21 (t, $^3J_{H,H}=7.6$ Hz, 2H, $CH_2\alpha$ -chain1), 2.14 (t, $^3J_{H,H}=7.5$ Hz, 2H, $CH_2\alpha$ -chain2), 1.85 (m, 2H, $CH_2\alpha$ -chain3), 1.50 (m, 4H, $CH_2\beta$ -chains1,2), 1.46-1.36 (m, 2H, $CH_2\beta$ -chain3), 1.27 (m, 60H, 30x CH_2 chains), 0.88 (t, $^3J_{H,H}=6.6$ Hz, 9H, 3x CH_3 chains).

^{13}C NMR (101 MHz, $CDCl_3$, $25^\circ C$, TMS) δ 184.72, 174.06, 171.63, 139.76, 129.49, 128.71, 127.97, 113.65, 92.90, 75.02, 73.14, 71.00, 69.92, 69.78, 69.68, 69.29, 69.23, 67.79, 67.75, 55.18, 36.29, 34.14, 31.92, 29.67, 29.51, 29.16, 25.36, 24.84, 22.69, 14.13.

HRMS (ESI): m/z $[M+Na^+]$ calculated for $C_{70}H_{112}NNaO_{12}P^+$: 1212.7814. Found: 1212.7817.

Compound 15

1-(dibenzyl)phospho-2-dodecanamido-2-deoxy-3,4-di-O-dodecanoyl-6-O-(4-methoxybenzyl)- α -D-glucopyranose (15). Compound **15** was synthesized starting from **13** accordingly to the procedure presented for compound **14** in 55% yield.

1H NMR (400 MHz, $CDCl_3$, $25^\circ C$, TMS) δ : 7.36-7.31 (m, 10H, 2x BnO-P), 7.16 (d, $^3J_{H,H}=8.5$ Hz, 2H, 2x H-ortho PMB), 6.79 (d, $^3J_{H,H}=8.6$ Hz, 2H, 2x H-meta PMB), 5.70 (dd, $^3J_{H,P}=6.0$, $^3J_{H,H}=3.2$ Hz, 1H, H-1), 5.57 (d, $^3J_{H,H}=9.1$ Hz, 1H, NH), 5.21-5.15 (m, 2H, H-3, H-4), 5.11-4.91 (m, 4H, 2x $CH_2(Ph)$ -O-P), 4.70 (s, 3H; CH_2 -Ph PMB, H-2), 4.04 (s, 1H, H-5), 3.76 (s, 3H, OCH_3), 3.52-3.34 (m, 2H, H6a, H6b), 2.21 (t, $^3J_{H,H}=7.7$ Hz, 2H, $CH_2\alpha$ -chain1), 2.14 (t, $^3J_{H,H}=7.5$ Hz, 2H, $CH_2\alpha$ -chain2), 1.92-1.78 (m, 2H, $CH_2\alpha$ -chain3), 1.57-1.44 (m, 6H, $CH_2\beta$ -chains1,2,3), 1.26-1.23 (m, 48H, 24x CH_2 chains), 0.88 (t, $^3J_{H,H}=6.2$ Hz, 9H, 3x CH_3 chains).

^{13}C NMR (101 MHz, $CDCl_3$, $25^\circ C$, TMS) δ 174.05, 173.01, 171.85, 129.48, 128.71, 127.93, 113.65, 93.67, 75.01, 73.14, 70.99, 69.78, 67.76, 55.17, 31.93, 31.92, 29.67, 29.51, 29.37, 29.30, 29.23, 29.16, 25.36, 25.36, 24.84, 24.84, 22.70, 22.69, 22.69, 14.13, 14.13, 14.11.

HRMS (ESI): m/z [$M+Na^+$] calculated for $C_{64}H_{100}NNaO_{12}P^+$: 1128.6875. Found: 1128.6880.

FP11

1-phospho-2-tetradecanamido-2-deoxy-3,4-di-O-tetradecanoyl- α -D-glucopyranose (sodium salt) (FP11)

Compound **14** (25 mg, 0.021 mmol) was dissolved in degassed MeOH (1.3 mL), and 3 mg (10% weight) of 10% Pd-C was added under Ar atmosphere. The reaction mixture was stirred at r.t. under H_2 atmosphere overnight. Triethylamine (80 μ L) was added to the reaction mixture, and the suspension was filtered with a syringe filter and evaporated to dryness. The resulting solid was dissolved in CH_2Cl_2 /MeOH 1:2 (3 mL) and treated first with Amberlite IRA 120 H^+ exchange resin and then with IR 120 Na^+ , giving compound **FP11** as a white solid (16 mg, 82%).

1H NMR (400 MHz, CD_3OD , 25 $^\circ C$, TMS) δ : 5.47 (dd, $^3J_{H,P}=6.7$, $^3J_{H,H}=3.2$ Hz, 1H; H-1), 5.34 (t, $^3J_{H,H}=10.0$ Hz, 1H, H-3), 5.09 (t, $^3J_{H,H}=9.9$ Hz, 1H, H-4), 4.28 (dd, $^3J_{H,H}=10.8$, 2.5 Hz, 1H, H-2), 4.14-4.06 (m, 1H, H-5), 3.66 (m, 1H, H-6a), 3.56 (m, 1H, H-6b), 2.39-2.10 (m, 6H, 3x $CH_2\alpha$ -chains), 1.55 (s, 6H, 3x $CH_2\beta$ -chains), 1.29 (m, 60H, 30x CH_2 chains), 0.89 (t, $^3J_{H,H}=6.6$ Hz, 9H, 3x CH_3 -chains).

^{13}C NMR (101 MHz, $CDCl_3$, 25 $^\circ C$, TMS) δ 174.72, 172.78, 131.63, 109.99, 92.22, 73.52, 72.09, 66.78, 62.07, 59.75, 48.57, 38.68, 34.14, 33.96, 32.77, 31.96, 29.88, 29.80, 29.71, 29.67, 29.43, 29.29, 24.89, 22.72, 14.14, 1.03.

ESI-MS: $[M]^-$ m/z =888.6; found: m/z =888.7.

FP18

1-phospho-2-dodecanamido-2-deoxy 3,4-di-O-dodecanoyl- α -D-glucopyranose (sodium salt) (FP18). **FP18** was synthesized starting from **15** accordingly to the procedure presented for **FP11** in 80% yield.

1H NMR (400 MHz, CD_3OD , 25 $^\circ C$, TMS) δ : 5.57 (dd, $^3J_{H,P}=6.6$, $^3J_{H,H}=3.4$ Hz, 1H; H-1), 5.35 (dd, $^3J_{H,H}=10.8$ Hz, $^3J_{H,H}=9.4$ Hz, 1H, H-3), 5.16 (t, $^3J_{H,H}=9.8$ Hz, 1H, H-4), 4.34 (dt, $^3J_{H,H}=10.9$, 3.2 Hz, 1H, H-2), 4.12-4.05 (m, 1H, H-5), 3.69 (dd, $^3J_{H,H}=12.4$, $^3J_{H,H}=2.4$ Hz, 1H, H-6a), 3.58 (dd, $^3J_{H,H}=12.3$, $^3J_{H,H}=4.4$ Hz, 1H, H-6b), 2.41-2.17 (m, 6H, 3x $CH_2\alpha$ -chains), 1.57 (d, $J=8.3$ Hz, 6H, 3x $CH_2\beta$ -chains), 1.32 (s, 48H, 24x CH_2 chains), 0.92 (t, $^3J_{H,H}=6.5$ Hz, 9H, 3x CH_3 -chains)

^{13}C NMR (101 MHz, CD_3OD , 25 $^\circ C$, TMS) δ 175.08, 173.14, 172.51, 94.56, 71.23, 70.64, 68.48, 60.27, 51.72, 51.72, 51.64, 35.65, 33.73, 31.67, 29.36, 29.32, 29.28, 29.24, 29.21, 29.17, 29.14, 29.10, 28.83, 25.55, 24.52, 22.31, 13.01, 13.01.

ESI-MS: $[M]^-$ m/z =804.5396; found: m/z =804.5401.

Compound 16

2-tetradecanamido-2-deoxy-3,4-di-O-tetradecanoyl- α -D-glucopyranose (16). Compound **13** (120 mg, 0.129 mmol) was dissolved in degassed MeOH (8 mL), and 12 mg (10% weight) of 10% Pd-C was added under Ar

atmosphere. The reaction mixture was stirred at r.t. under H₂ atmosphere overnight. After Catalyst removal by filtration on Celite[®], solvent was evaporated *in vacuo* giving compound **16** as a white solid (100 mg, 95%).

¹H-NMR: (400 MHz, CDCl₃, 25 °C, TMS): δ 6.09 (d, ³J_{H,H}=9.1 Hz, 1H, H-1[⊖]), 5.34 (t, ³J_{H,H}=10.1 Hz, 1H, H-3), 5.02 (t, ³J_{H,H}=9.7 Hz, 1H, H-4), 4.21 (t, ³J_{H,H}=9.1 Hz, 1H, H-2), 4.04 (m, 1H, H-5), 3.67 (m, 1H, H-6a), 3.56 (m, 1H, H-6b), 2.25 (m, 4H, CH₂-chains_{1,2}), 2.11 (m, 4H, CH₂-chain₃), 1.52 (m, 6H, CH₂-chains_{1,2,3}), 1.23 (m, 60H, 30xCH₂), 0.86 (t, ³J_{H,H}=6.6 Hz, 9H, CH₃-chains_{1,2,3}).

¹³C NMR (101 MHz, CDCl₃, 25 °C, TMS): δ 174.15, 173.64, 173.17, 91.38, 70.30, 69.67, 68.57, 68.47, 61.17, 52.46, 36.71, 34.20, 34.15, 31.92, 31.88, 29.73, 29.71, 29.68, 29.56, 29.55, 29.49, 29.41, 29.38, 29.37, 29.30, 29.20, 29.17, 25.61, 24.97, 24.93, 22.70, 22.68, 14.12, 14.11.

HRMS (ESI): m/z [M+Na⁺] calculated for C₄₈H₉₁NNaO₈⁺: 832.6637. Found: 832.6639.

Compound 17

1,6-bis(dibenzyl)phospho-2-tetradecanamido-2-deoxy-3,4-di-O-tetradecanoyl-α-D-glucofuranose (**17**).

Compound **16** (50 mg, 0.062 mmol) was dissolved in dry CH₂Cl₂ (1.0 mL), then imidazolium triflate (72 mg, 0.28 mmol) and dibenzyl *N, N*-diisopropyl phosphoramidite (91 μL, 0.27 mmol) were added. The reaction was stirred at r.t. for 1.5 h. The solution was then cooled at 0°C and *m*CPBA (85 mg, 0.49 mmol) was added. After stirring at r.t. overnight, the mixture was diluted with CH₂Cl₂, washed with a saturated solution of NaHCO₃ and brine. The organic layer was dried over anhydrous Na₂SO₄, filtered and evaporated *in vacuo*. The crude product was purified with flash chromatography (petroleum ether–EtOAc 8:2) affording compound **17** as a brown solid (36 mg, 44%).

¹H-NMR: (400 MHz, CDCl₃, 25 °C, TMS): δ 7.44-7.21 (m, 20H, 4x Ar-H), 5.64 (dd, ³J_{H,H}=6.0, 3.3 Hz, 1H, H-1[⊖]), 5.61 (d, ³J_{H,H}=9.3 Hz, 1H, NH), 5.20-5.10 (m, 2H, H-3, H-5), 5.10-4.96 (m, 9H, 4x CH₂-Ph, H-4), 4.33 (t, ³J_{H,H}=9.8 Hz, 1H, H-2), 3.92 (m, 2H, H-6a, H-6b), 2.20 (m, 4H, CH₂-chains_{1,2}), 1.95-1.77 (m, 2H, CH₂-chain₃), 1.49 (m, 4H, CH₂-chains_{1,2}), 1.47-1.36 (m, 2H, CH₂-chain₃), 1.27 (m, 60H, 30xCH₂), 0.88 (t, ³J_{H,H}=6.6 Hz, 9H, CH₃-chains_{1,2,3}).

¹³C NMR (101 MHz, CDCl₃, 25 °C, TMS) δ 173.95, 171.72, 151.63, 128.86, 128.77, 128.73, 128.54, 128.53, 128.49, 128.47, 128.10, 128.03, 127.96, 127.89, 109.99, 96.23, 88.76, 88.44, 70.16, 69.88, 69.71, 69.44, 69.38, 66.67, 34.11, 31.92, 29.67, 29.51, 29.37, 29.31, 29.24, 29.16, 25.39, 24.85, 22.69, 14.13, 14.12.

HRMS (ESI): m/z [M+Na⁺] calculated for C₇₆H₁₁₇NNaO₁₄P₂⁺: 1352.7842. Found: 1352.7848.

FP111

1,6-bisphospho-2-tetradecanamido-2-deoxy-3,4-di-O-tetradecanoyl-α-D-glucofuranose (sodium salt)

(**FP111**) Compound **17** (33 mg, 0.028 mmol) was dissolved in degassed MeOH (1.3 mL), and 4 mg (10% weight) of 10% Pd-C was added under Ar atmosphere. The reaction mixture was stirred at r.t. under H₂ atmosphere overnight. Triethylamine (80 μL) was added to the reaction mixture, and the suspension was filtered with a

syringe filter and evaporated to dryness. The resulting solid was dissolved in CH₂Cl₂/MeOH 1:2 (3 mL) and treated first with Amberlite IRA 120 H⁺ exchange resin and then with IR 120 Na⁺, giving compound **FP111** as a white solid (20 mg, 68%).

¹H-NMR: (400 MHz, CD₃OD, 25 °C, TMS): 5.53 (dd, ³J_{H,H}=6.3, 3.2 Hz, 1H, H-1), 5.32 (t, ³J_{H,H}=10.8 Hz, 1H, H-3), 5.14 (t, ³J_{H,H}=9.8 Hz, 1H, H-4), 4.32 (dt, ³J_{H,H}=10.9, 3.1 Hz, 1H, H-2), 4.28-4.21 (m, 1H, H-5), 4.12-3.97 (m, 2H, H-6a, H-6b), 2.48-2.06 (m, 6H, CH₂-chains1,2,3), 1.71-1.47 (m, 6H, CH₂-chains1,2,3), 1.29 (s, 60H, 30xCH₂), 0.90 (t, ³J_{H,H}=6.6 Hz, 9H, CH₃-chains1,2,3).

¹³C NMR (101 MHz, CD₃OD, 25 °C, TMS) δ 210.68, 175.10, 172.94, 172.30, 127.68, 89.22, 85.74, 70.50, 69.44, 69.37, 68.31, 51.52, 48.20, 35.57, 33.65, 33.46, 31.71, 31.68, 29.47, 29.45, 29.28, 29.20, 29.12, 29.10, 29.02, 28.85, 28.80, 25.61, 24.50, 24.45, 22.35, 13.06, 13.05, -5.54.

ESI-MS: [M+H]⁺ m/z =968.6; found: m/z =968,7.

NMR spectra

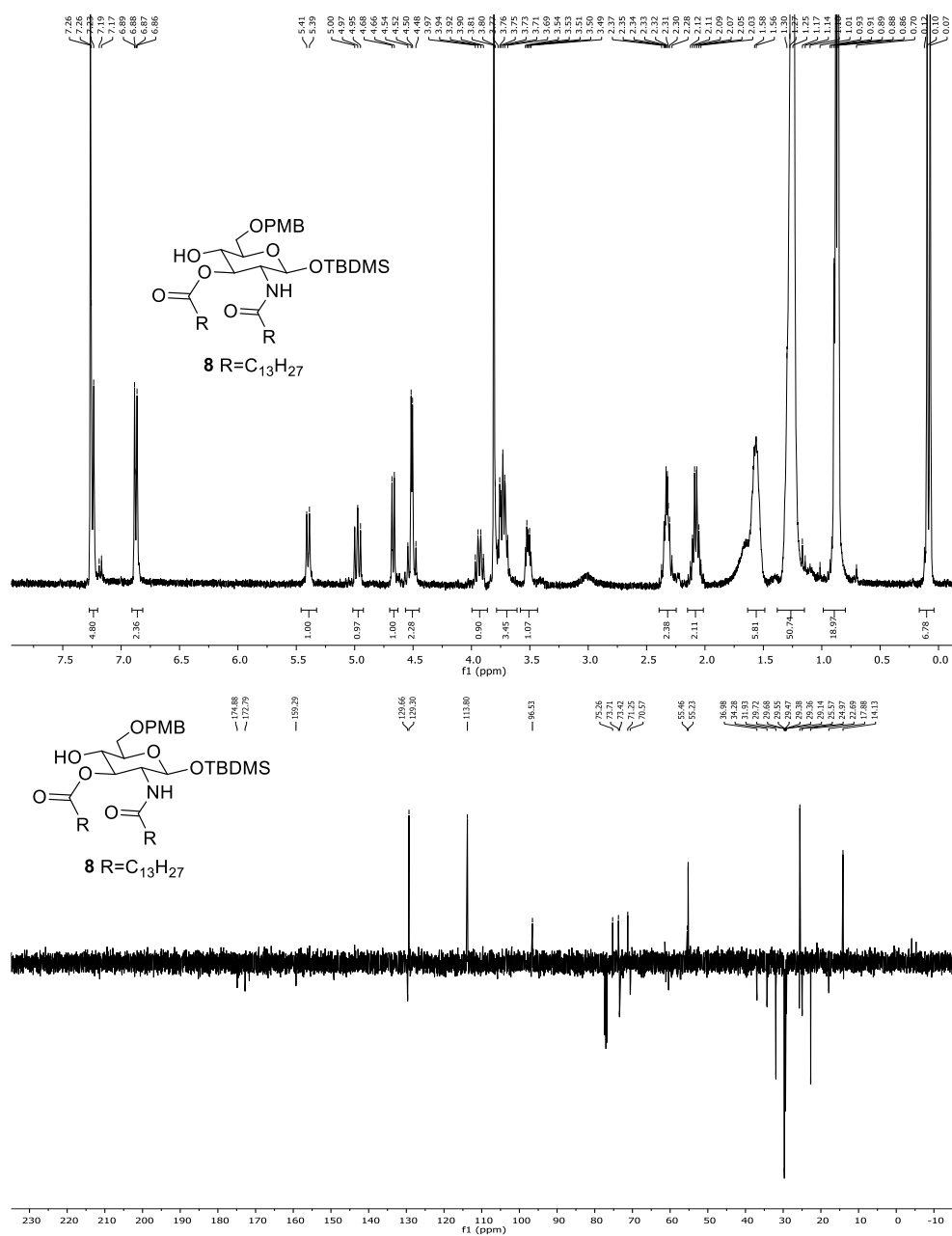
Fig. S5: Compound 8. ^1H NMR and ^{13}C APT NMR spectra in CDCl_3 

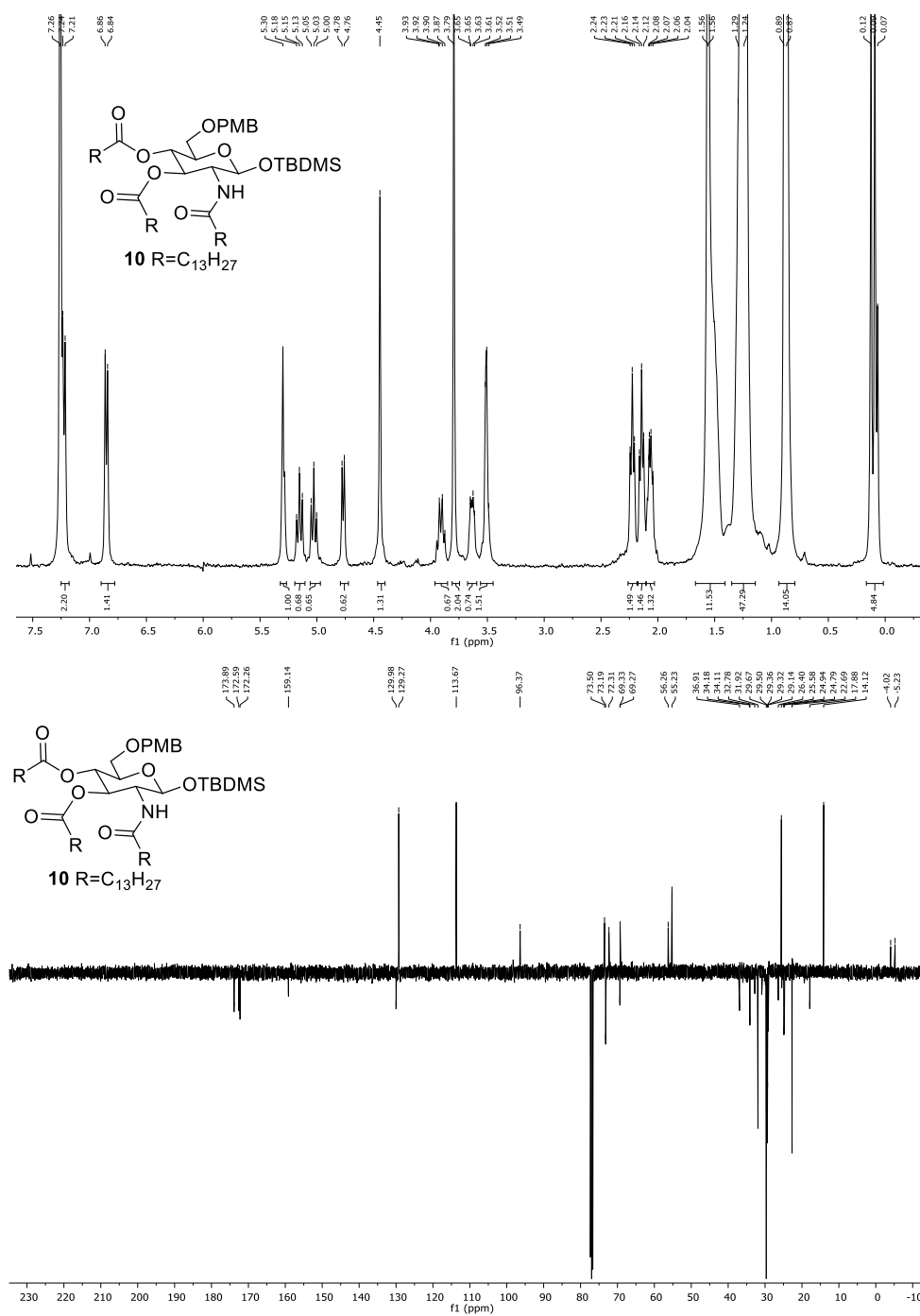
Fig. S6: Compound 10. ^1H NMR and ^{13}C APT NMR spectra in CDCl_3 

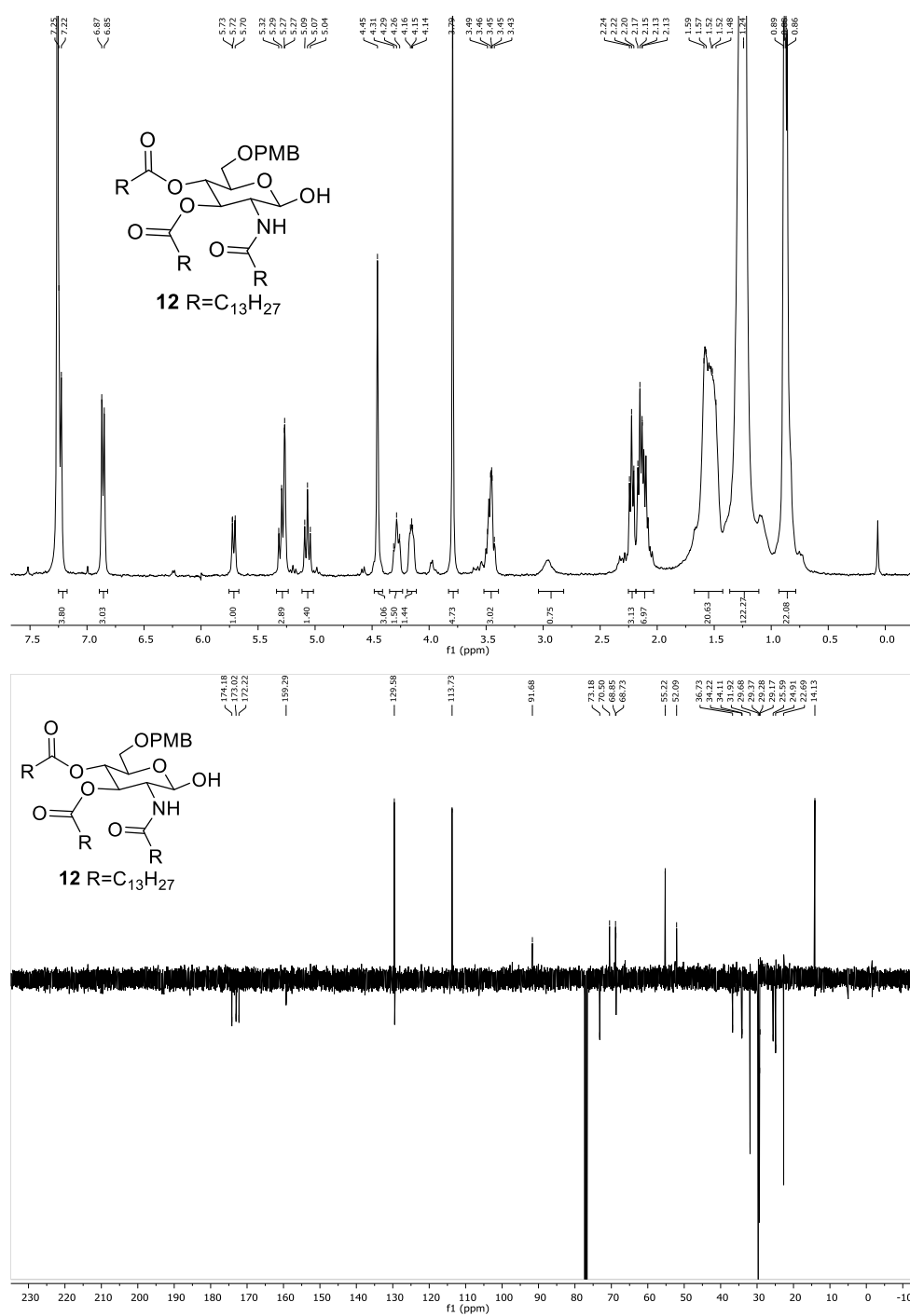
Fig. S7: Compound 12. ^1H NMR and ^{13}C APT NMR spectra in CDCl_3 

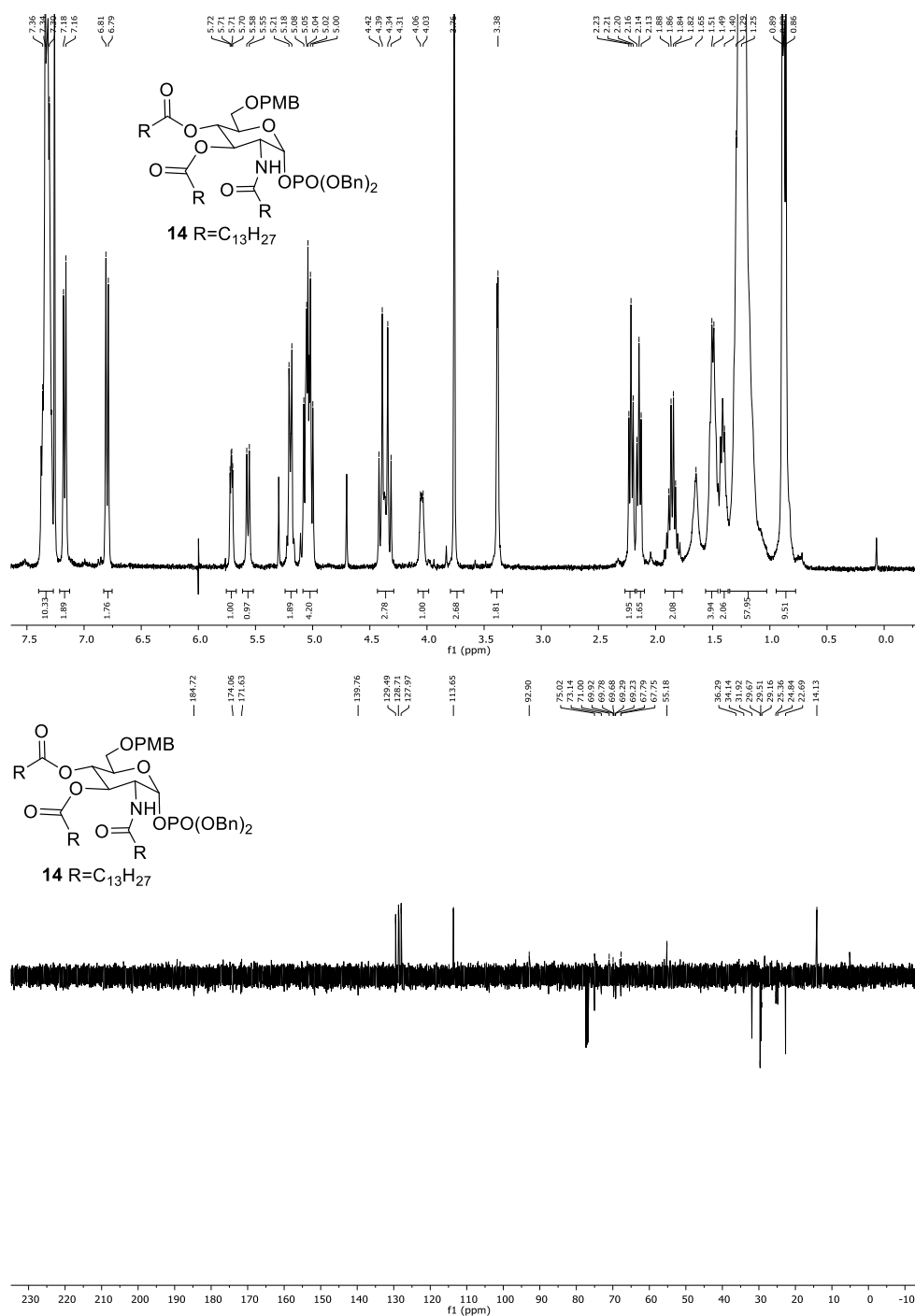
Fig. S8: Compound 14. ^1H NMR and ^{13}C APT NMR spectra in CDCl_3 

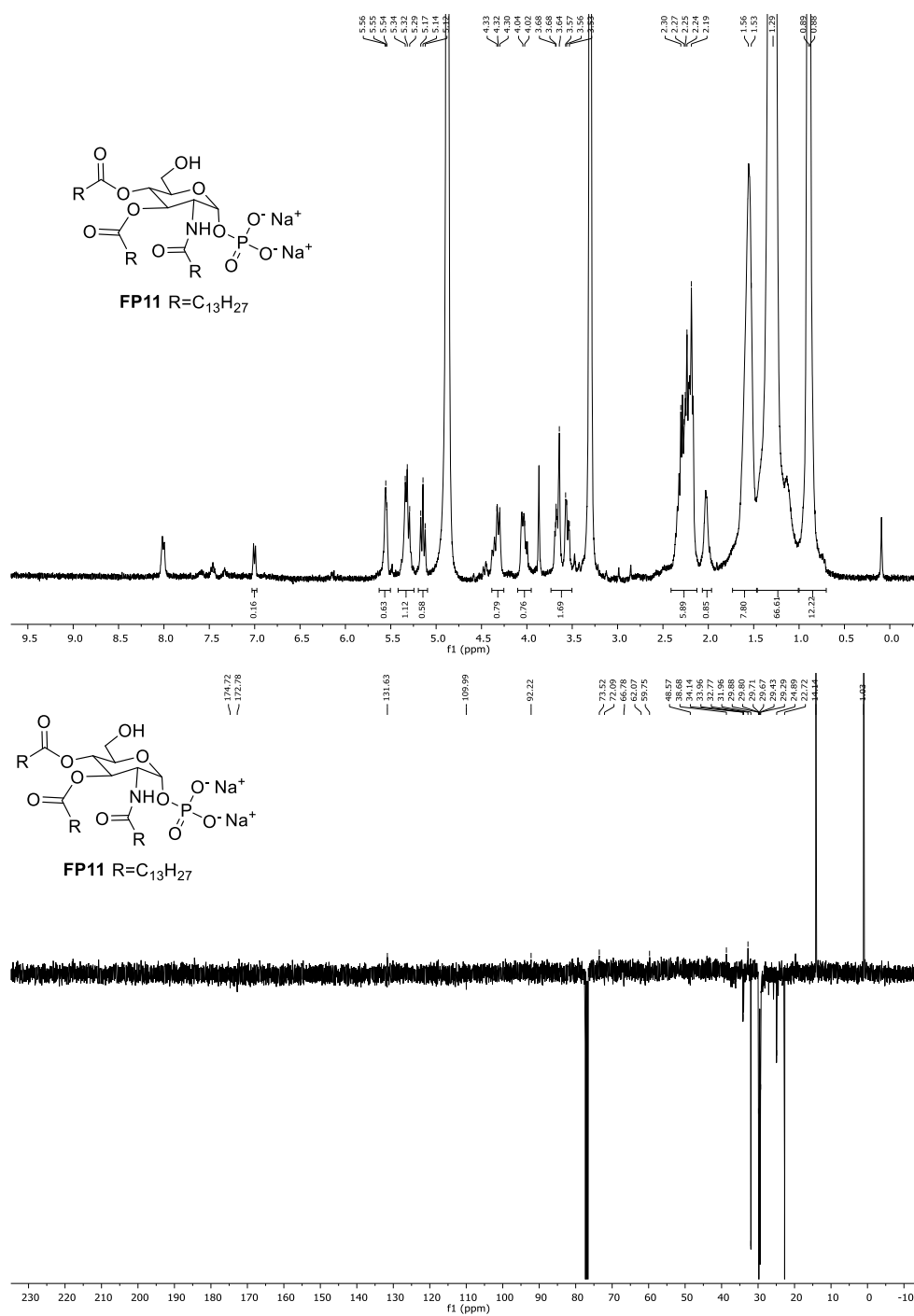
Fig. S9: Compound FP11. ^1H NMR and ^{13}C APT NMR spectra in CD_3OD 

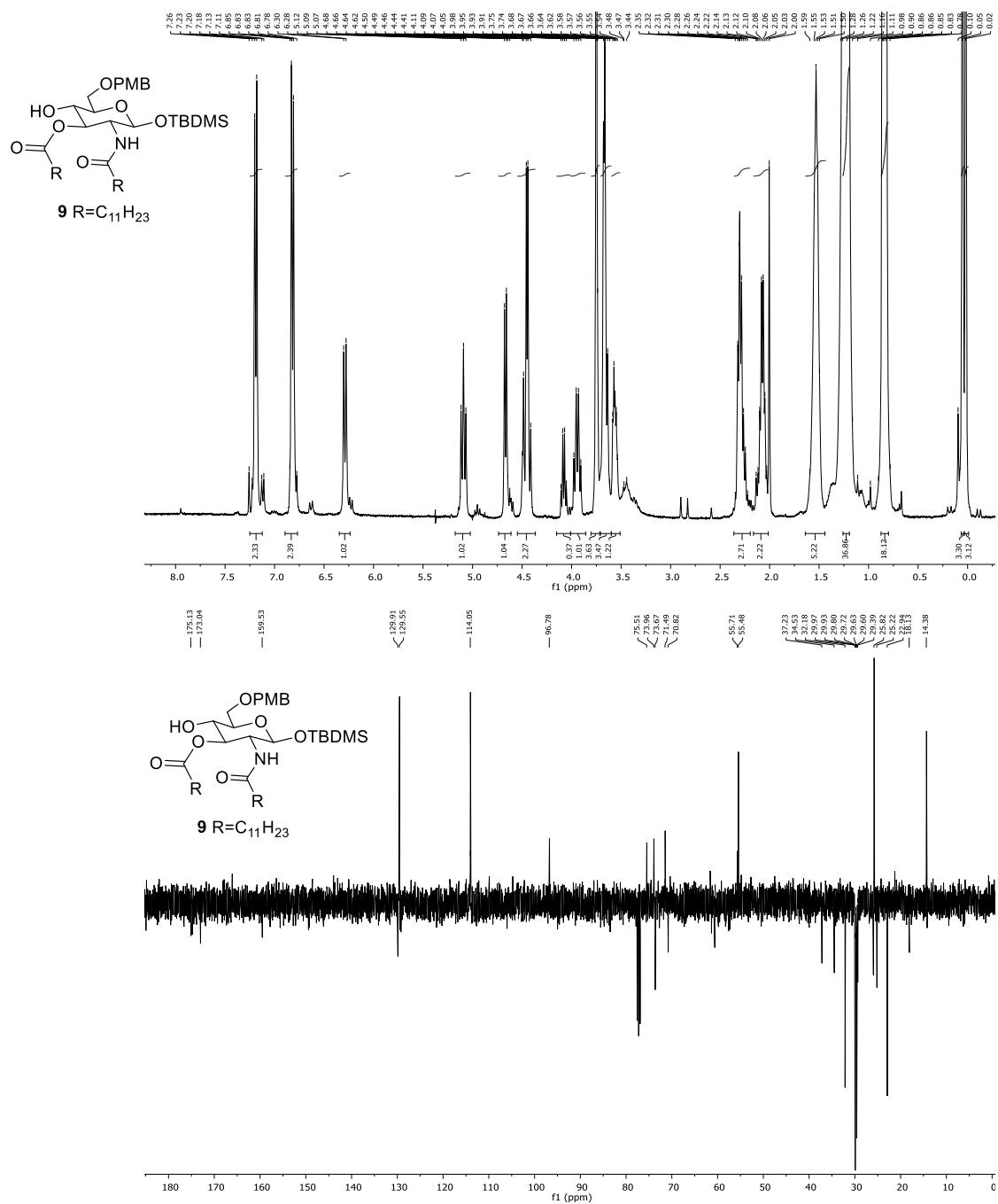
Fig. S10: Compound 9. ^1H NMR and ^{13}C APT NMR spectra in CDCl_3 

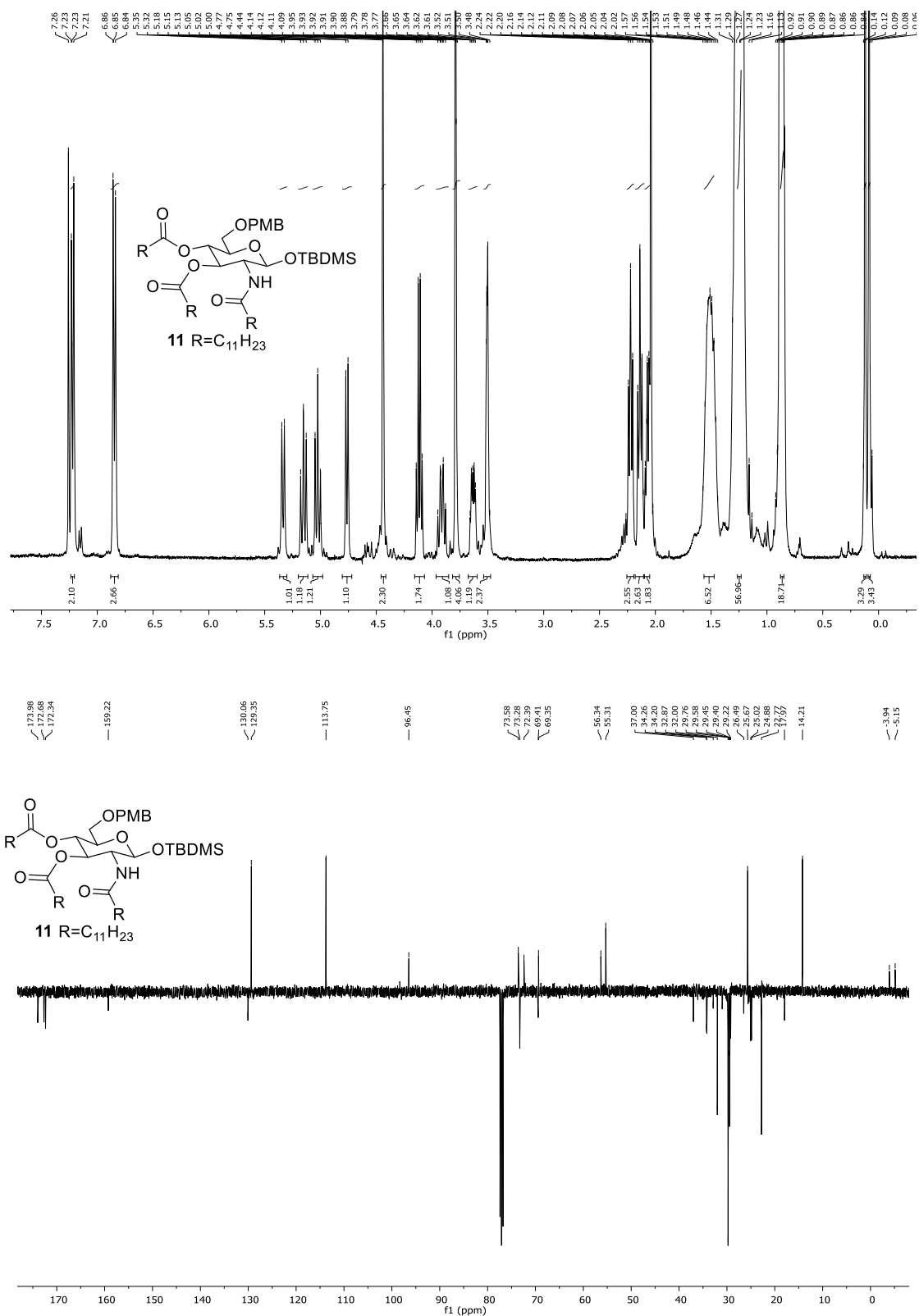
Fig. S11: Compound 11. ^1H NMR and ^{13}C APT NMR spectra in CDCl_3 

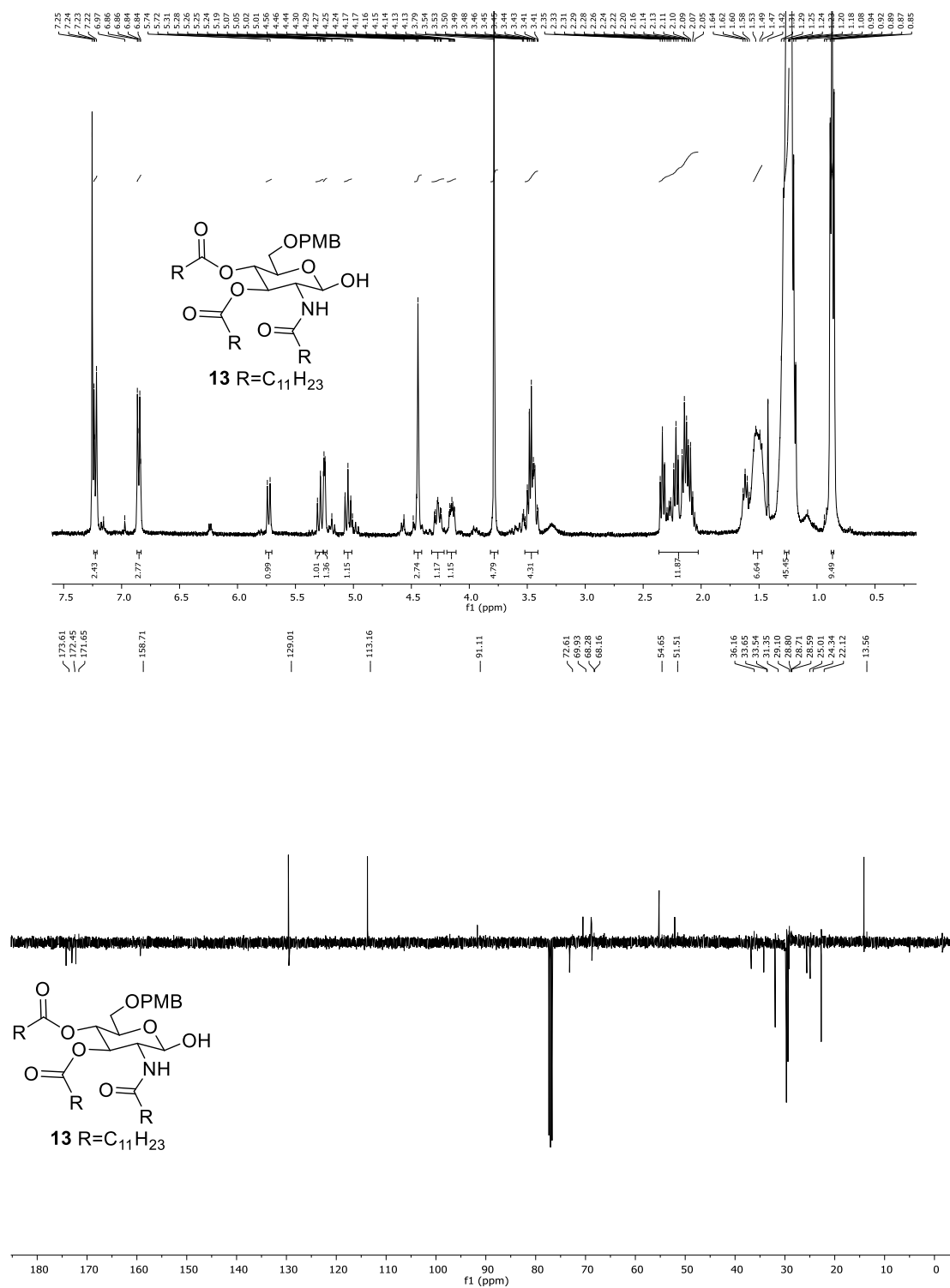
Fig. S12: Compound 13. ^1H NMR and ^{13}C APT NMR spectra in CDCl_3 

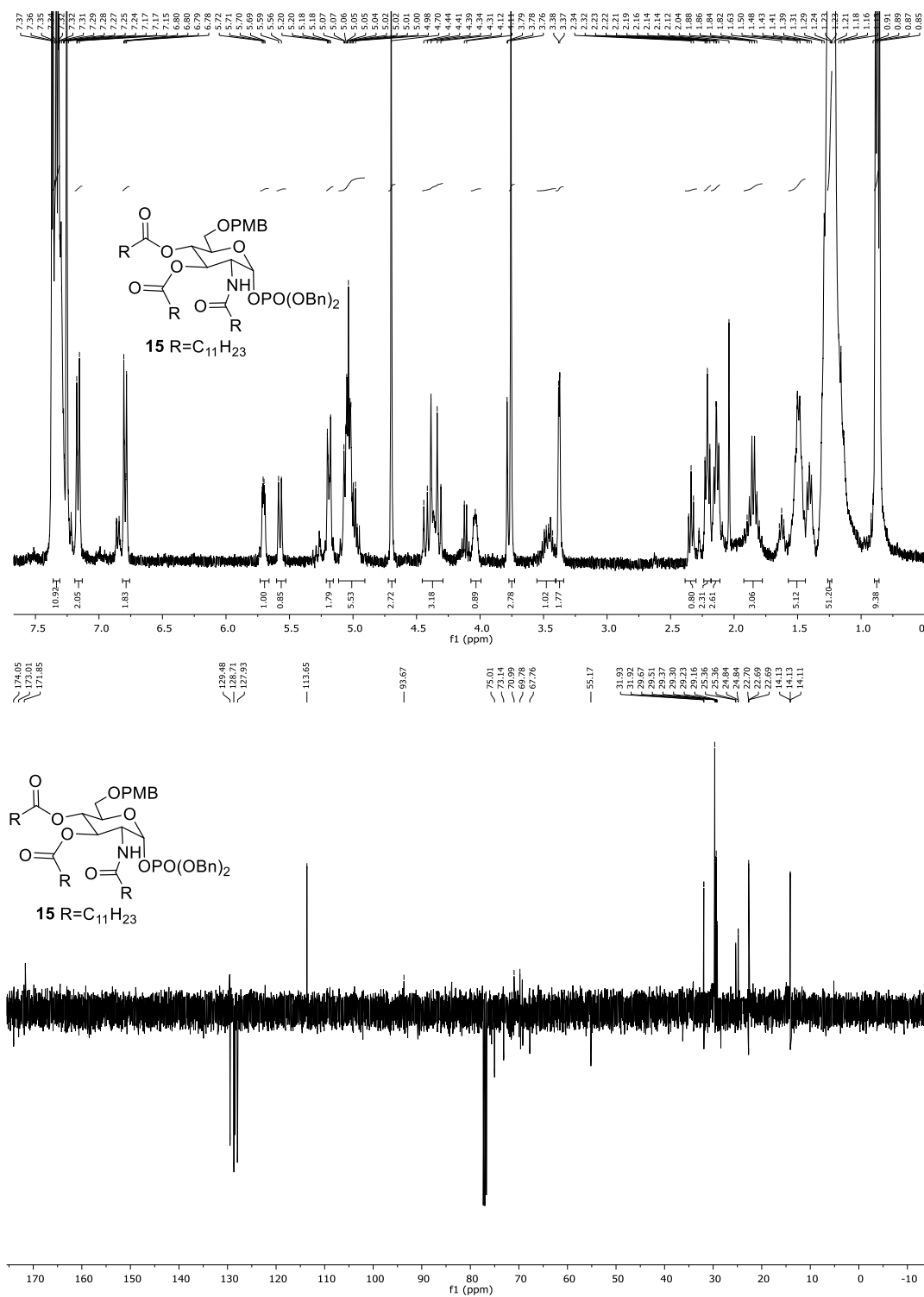
Fig. S13: Compound 15. ^1H NMR and ^{13}C APT NMR spectra in CDCl_3 

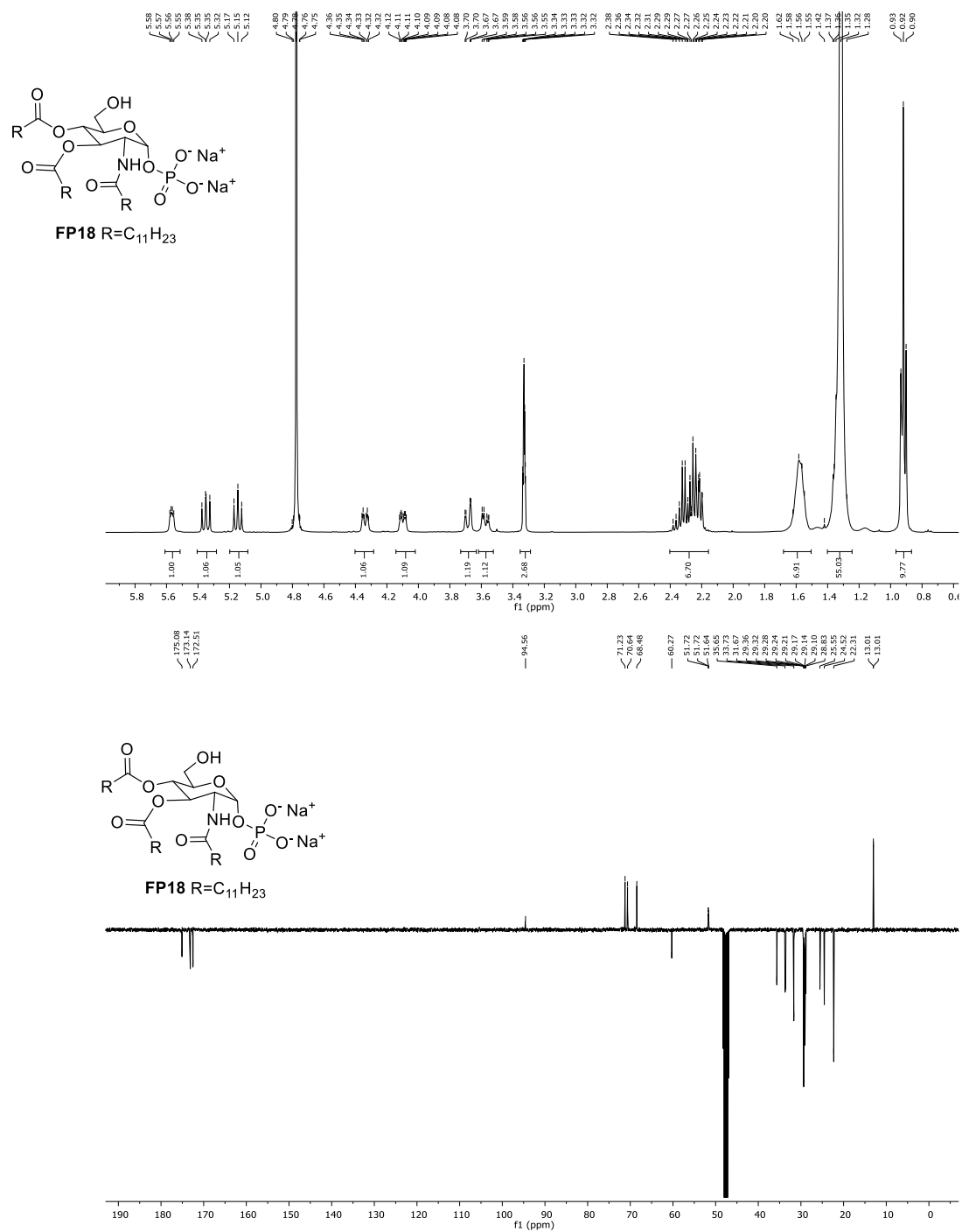
Fig. S14: Compound FP18. ^1H NMR and ^{13}C APT NMR spectra in CD_3OD 

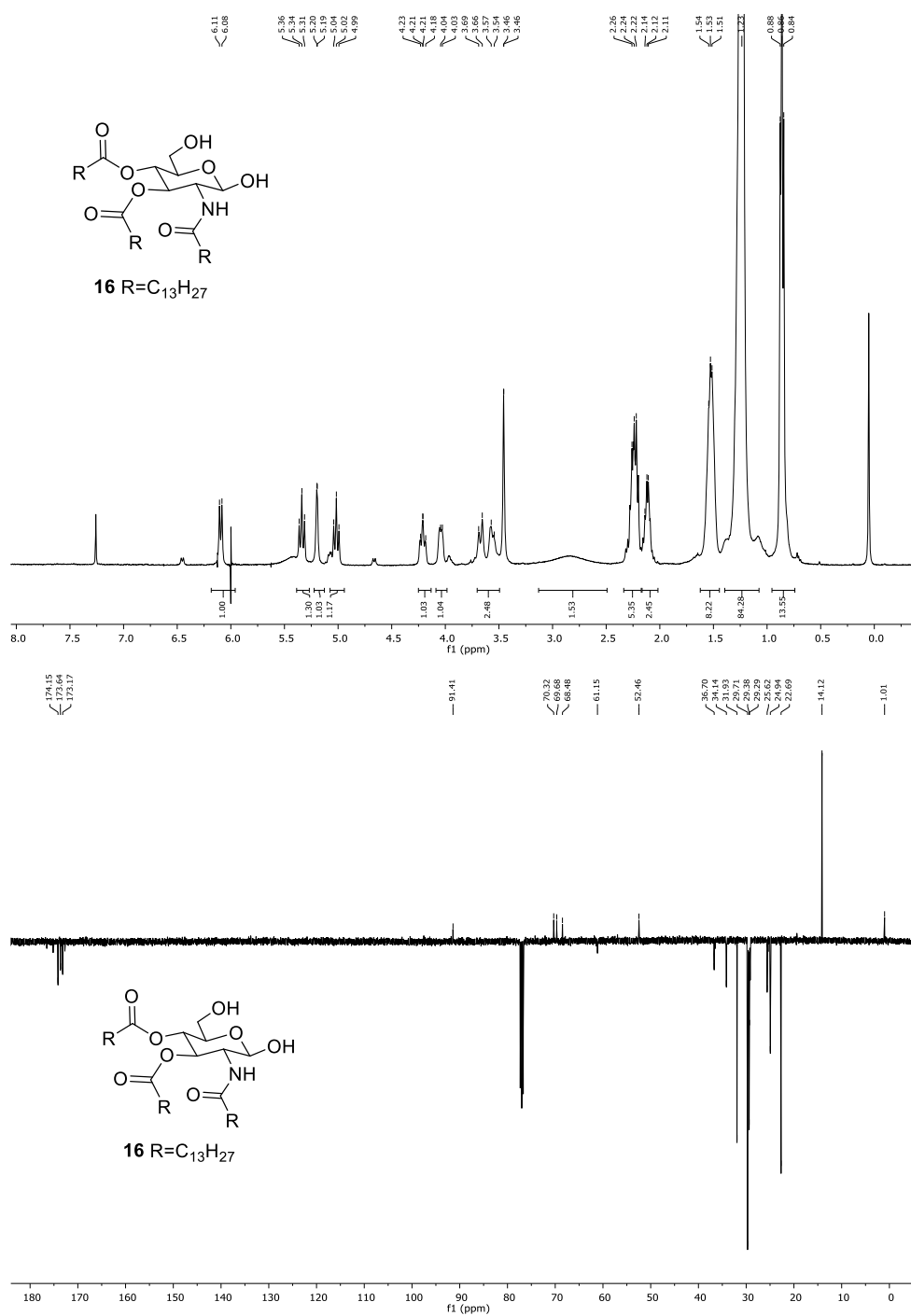
Fig. S15: Compound 16. ^1H NMR and ^{13}C APT NMR spectra in CDCl_3 

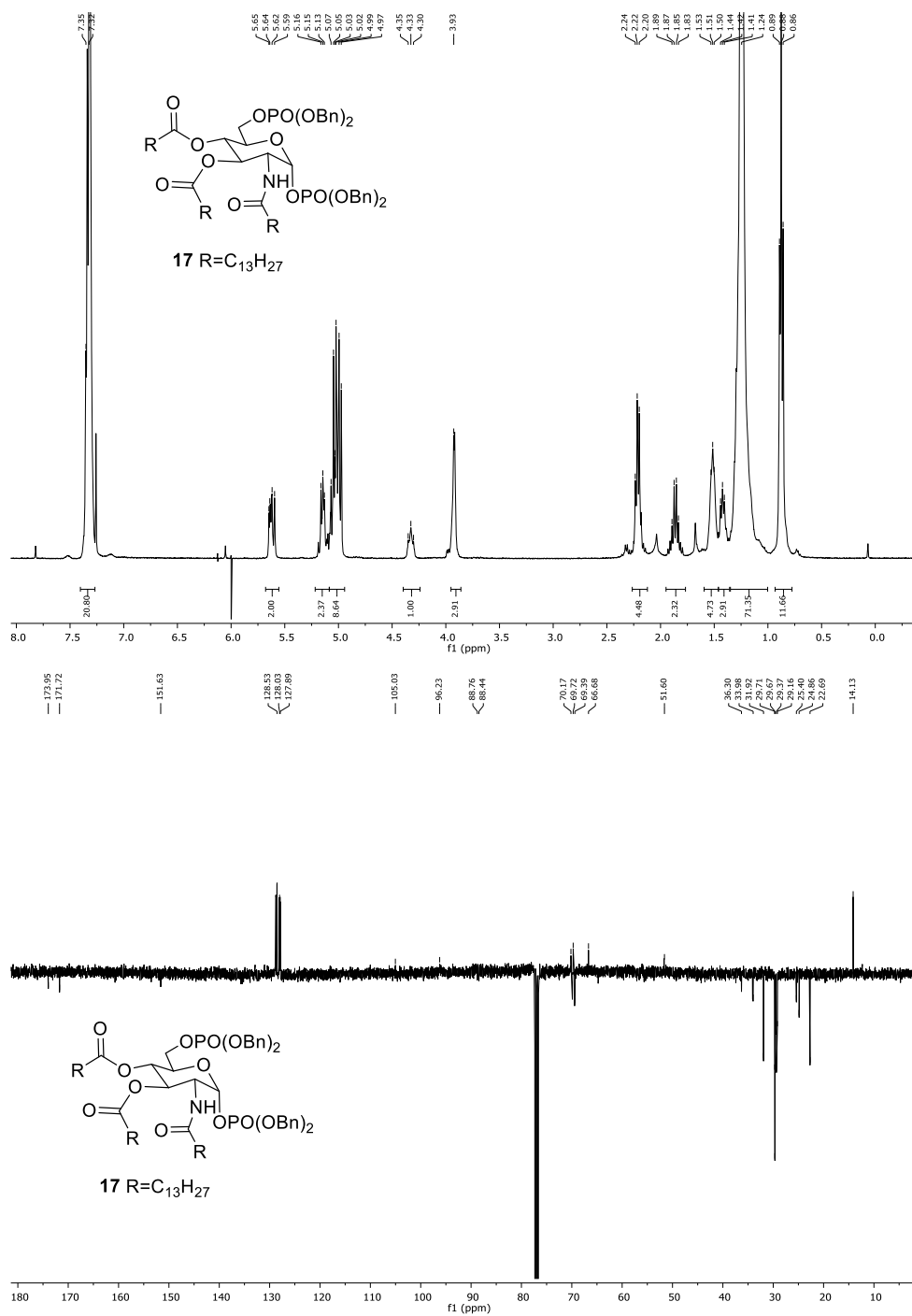
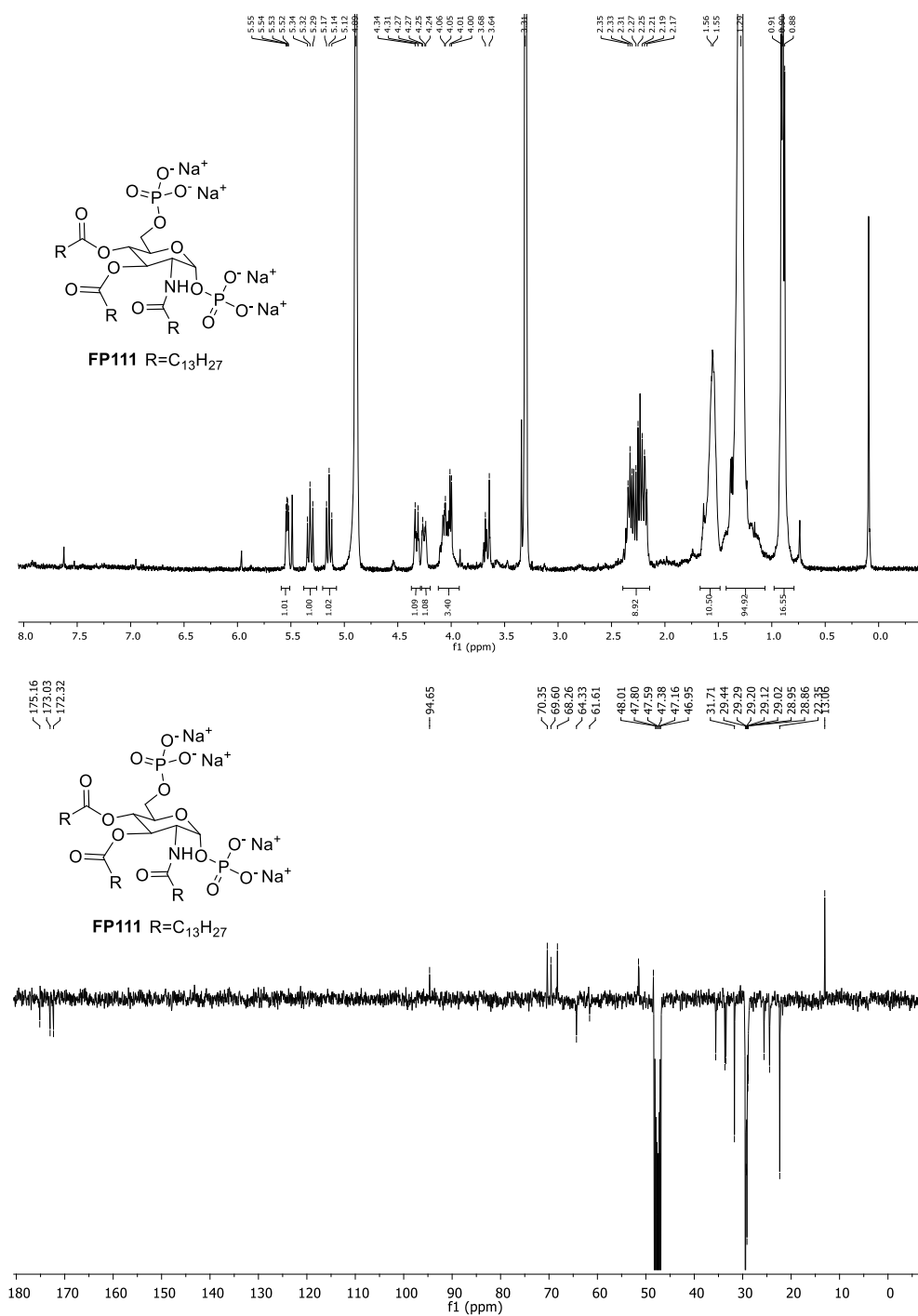
Fig. S16: Compound 17. ^1H NMR and ^{13}C APT NMR spectra in CDCl_3 

Fig. S17: Compound FP111. ^1H NMR and ^{13}C APT NMR spectra in CD_3OD 

In vitro evaluation of the cytotoxicity of compounds FP11 and FP18

THP1-derived macrophages were exposed to increasing concentration of compounds FP11 and FP18. FPs molecules do not affect THP-1 macrophage viability

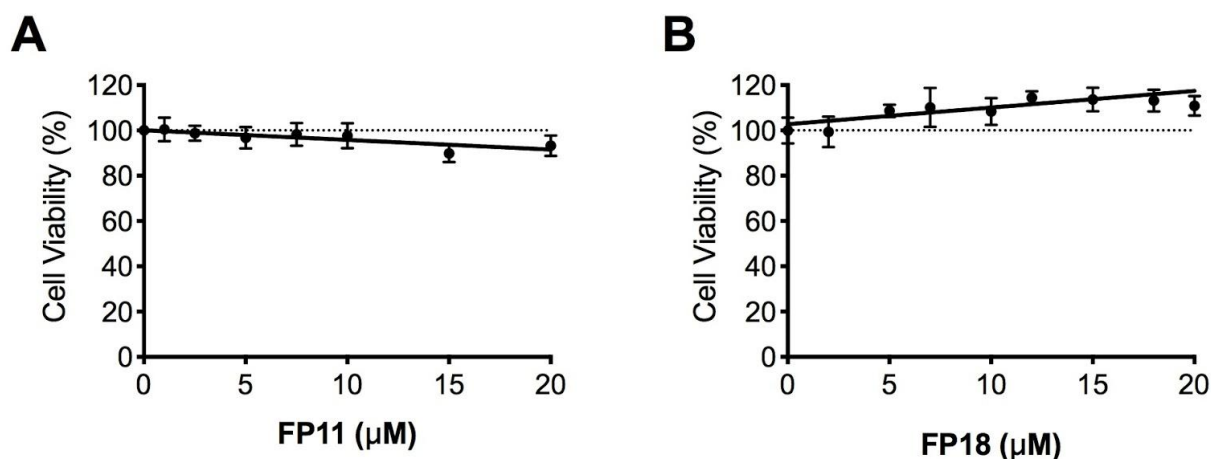


Fig. S18: THP1-derived macrophages were exposed to FP11 and FP18 (0-20 μM). Cell viability was measured via MTT assay. Results were normalised to untreated controls and shown as mean ±SD of 5 independent samples.

Table S1.

Cell Line	Resistance	Transfected gene	Cell/well
HEK-Blue hTLR4	HEK-Blue Selection 1x	TLR4/MD-2/CD14/SEAP	4×10^4
HEK-Blue hTLR2	HEK-Blue Selection 1x	TLR2/CD14/SEAP	4×10^4
HEK-Blue Null	Zeocin (200 μg/mL)	SEAP	4×10^4

Table S1: HEK reporter cell lines used. In the table are reported the reporter cell lines used, with the corresponding antibiotic resistance, genes expression and concentration used for the experiments.

Log P and log S calculations. The values of QPlogPo/w and QPlogS parameters were computationally calculated within the QikProp tool implemented in the Maestro package (www.schrodinger.com).

Table S2.

Compound	QPlogPo/w ^a	QPlogS ^b
FP11	10.260	-10.027
FP18	8.325	-8.765

^aPredicted octanol/water partition co-efficient log P.

^bPredicted aqueous solubility, log S. S in mol dm⁻³ is the concentration of the solute in a saturated solution that is in equilibrium with the crystalline solid.

Assessment of water solubility of FP11 and FP18 compounds as predicted by Qikprop. The highest log P value was obtained for FP11, indicating higher lipophilicity that might result in lower water solubility. This is in agreement with the lower log S value predicted for FP11, compared with FP18. In any case, this did not interfere with the performance of the cell assays.

BIBLIOGRAPHY

- (1) Kayser, V.; Ramzan, I. Vaccines and Vaccination: History and Emerging Issues. *Hum. Vaccines Immunother.* **2021**, *17* (12), 5255–5268.
- (2) Shah, R. R.; Hassett, K. J.; Brito, L. A. Overview of Vaccine Adjuvants: Introduction, History, and Current Status. In *Vaccine Adjuvants*; 2017; Vol. 1494, pp 1–13.
- (3) Stewart, A. J.; Devlin, P. M. The History of the Smallpox Vaccine. *J. Infect.* **2006**, *52* (5), 329–334.
- (4) Lawler, A. How a Public Health Crisis Nearly Derailed the American Revolution. *National Geographic*. 2020, pp 1–15.
- (5) Jenner, E. An Inquiry into the Causes and Effects of the Variolae Vaccinae: A Disease Discovered in Some of the Western Counties of England, Particularly Gloucestershire, and Known by the Name of the Cow Pox, 1798.
- (6) Delany, I.; Rappuoli, R.; Gregorio, E. De. Vaccines for the 21st Century. *Embo Mol. Med.* **2014**, *6* (6), 708–720.
- (7) Kean, S. 22 Orphans Gave Up Everything to Distribute the World’s First Vaccine. *The Atlantic*. 2021, pp 1–10.
- (8) Hilleman, M. R. Vaccines in Historic Evolution and Perspective: A Narrative of Vaccine Discoveries. *J. Hum. Virol.* **2000**, *3* (2), 63–76.
- (9) von Behring, E. Serum Therapy in Therapeutics and Medical Science Serum. *Nobel Prize Lecture*, 1901, 1–8.
- (10) Valent, P.; Groner, B.; Schumacher, U.; Superti-Furga, G.; Busslinger, M.; Kralovics, R.; Zielinski, C.; Penninger, J. M.; Kerjaschki, D.; Stingl, G.; Smolen, J. S.; Valenta, R.; Lassmann, H.; Kovar, H.; Jäger, U.; Kornek, G.; Müller, M.; Sörgel, F. Paul Ehrlich (1854-1915) and His Contributions to the Foundation and Birth of Translational Medicine. *J. Innate Immun.* **2016**, *8* (2), 111–120.
- (11) Vetter, V.; Denizer, G.; Friedland, L. R.; Krishnan, J.; Shapiro, M. Understanding Modern-Day Vaccines: What You Need to Know. *Ann. Med.* **2018**, *50* (2), 110–120.
- (12) Dattani, S.; Spooner, F.; Ochmann, S.; Roser, M. Polio <https://ourworldindata.org/polio>.
- (13) Polio Global Eradication Initiative. Polio Now <https://polioeradication.org/polio-today/polio-now/>.
- (14) World Health Organization. Polio Vaccines: WHO Position Paper – March, 2016. **2016**, 145–168.
- (15) Moloney, P. J. The Preparation and Testing of Diphtheria Toxoid (Anatoxine-Ramon). *Am. J.*

Public Health **1926**, 16 (12), 1208–1210.

- (16) World Health Organization. Diphtheria Vaccine: WHO Position Paper, August 2017 – Recommendations. *Vaccine* **2018**, 36 (2), 199–201.
- (17) World Health Organization. Tetanus Vaccines: WHO Position Paper, February 2017 – Recommendations. *Vaccine* **2018**, 36 (25), 3573–3575.
- (18) Pfizer. Understanding six types of vaccine technology
https://www.pfizer.com/news/articles/understanding_six_types_of_vaccine_technologies.
- (19) Michel, M. L.; Tiollais, P. Vaccins Anti-Hépatite B: Efficacité Protectrice et Outil Thérapeutique Potentiel. *Pathol. Biol.* **2010**, 58 (4), 288–295.
- (20) Roldão, A.; Mellado, M. C. M.; Castilho R, L.; Carrondo, M. J.; Alves, P. M. Virus-like Particles in Vaccine Development. *Expert Rev. Vaccines* **2010**, 9 (10), 1149–1176.
- (21) Nooraei, S.; Bahrulolum, H.; Hoseini, Z. S.; Katalani, C.; Hajizade, A.; Easton, A. J.; Ahmadian, G. Virus-like Particles: Preparation, Immunogenicity and Their Roles as Nanovaccines and Drug Nanocarriers. *J. Nanobiotechnology* **2021**, 19 (1), 1–27.
- (22) McKeage, K.; Romanowski, B. AS04-Adjuvanted Human Papillomavirus (HPV) Types 16 and 18 Vaccine (Cervarix®). *Drugs* **2011**, 71 (4), 465–488.
- (23) Heidelberger, M.; Avery, O. T. The Soluble Specific Substance of Pneumococcus. *J. Exp. Med.* **1924**, 40 (3), 301–316.
- (24) Francis, T.; Tillett, W. S. CUTANEOUS REACTIONS IN PNEUMONIA. THE DEVELOPMENT OF ANTIBODIES FOLLOWING THE INTRADERMAL INJECTION OF TYPE-SPECIFIC POLYSACCHARIDE. *J. Exp. Med.* **1930**, 52 (4), 573–585.
- (25) Hütter, J.; Lepenies, B. Carbohydrate-Based Vaccines: An Overview. In *Carbohydrate-Based Vaccines: Methods and Protocols*; 2015; Vol. 1331, pp 1–10.
- (26) Karikó, K.; Buckstein, M.; Ni, H.; Weissman, D. Suppression of RNA Recognition by Toll-like Receptors: The Impact of Nucleoside Modification and the Evolutionary Origin of RNA. *Immunity* **2005**, 23 (2), 165–175.
- (27) Jain, S.; Venkataraman, A.; Wechsler, M. E.; Peppas, N. A. Messenger RNA-Based Vaccines: Past, Present, and Future Directions in the Context of the COVID-19 Pandemic. *Adv. Drug Deliv. Rev.* **2020**, 179 (January).
- (28) Cui, Z. DNA Vaccine. *Adv. Genet.* **2005**, 54 (05), 257–289.
- (29) O’Hagan, D. T.; Lodaya, R. N.; Lofano, G. The Continued Advance of Vaccine Adjuvants – ‘We Can Work It Out.’ *Semin. Immunol.* **2020**, 50, 101426.

- (30) Lambrecht, B. N.; Kool, M.; Willart, M. A.; Hammad, H. Mechanism of Action of Clinically Approved Adjuvants. *Curr. Opin. Immunol.* **2009**, *21* (1), 23–29.
- (31) Raponi, A.; Brewer, J. M.; Garside, P.; Laera, D. Nanoalum Adjuvanted Vaccines: Small Details Make a Big Difference. *Semin. Immunol.* **2021**, *56* (November), 101544.
- (32) Freund, J.; Casals, J.; Hosmer, E. P. Sensitization and Antibody Formation after Injection of Tubercle Bacilli and Paraffin Oil. *Proc. Soc. Exp. Biol. Med.* **1937**, 509–513.
- (33) Chang, J. C. C.; Diveley, J. P.; Savary, J. R.; Jensen, F. C. Adjuvant Activity of Incomplete Freund's Adjuvant. *Adv. Drug Deliv. Rev.* **1998**, *32* (3), 173–186.
- (34) O'Hagan, D. T.; Ott, G. S.; De Gregorio, E.; Seubert, A. The Mechanism of Action of MF59 - An Innately Attractive Adjuvant Formulation. *Vaccine* **2012**, *30* (29), 4341–4348.
- (35) Tsai, T. F. Flud[®]-Mf59[®]-Adjuvanted Influenza Vaccine in Older Adults. *Infect. Chemother.* **2013**, *45* (2), 159–174.
- (36) Garçon, N.; Vaughn, D. W.; Didierlaurent, A. M. Development and Evaluation of AS03, an Adjuvant System Containing α -Tocopherol and Squalene in an Oil-in-Water Emulsion. *Expert Rev. Vaccines* **2012**, *11* (3), 349–366.
- (37) Pifferi, C.; Fuentes, R.; Fernández- Tejada, A. Carlo Pifferi , Roberto Fuentes and Alberto Fernández- Tejada. *Nat. Rev. Chem.* **2021**, *5* (March), 197–216.
- (38) Medzhitov, R. Toll-Like Receptors and Innate Immunity. *Nat. Rev. Immunol.* **2001**, *1* (1), 135–145.
- (39) Bode, C. CpG DNA as a Vaccine Adjuvant. *Expert Rev. Vaccines* **2011**, *10* (4), 499–511.
- (40) Casella, C. R.; Mitchell, T. C. Putting Endotoxin to Work for Us: Monophosphoryl Lipid a as a Safe and Effective Vaccine Adjuvant. *Cell. Mol. Life Sci.* **2008**, *65* (20), 3231–3240.
- (41) Rosewich, M.; Lee, D.; Zielen, S. Pollinex Quattro: An Innovative Four Injections Immunotherapy in Allergic Rhinitis. *Hum. Vaccines Immunother.* **2013**, *9* (7), 1523–1531.
- (42) Carter, D.; Fox, C. B.; Day, T. A.; Guderian, J. A.; Liang, H.; Rolf, T.; Vergara, J.; Sagawa, Z. K.; Ireton, G.; Orr, M. T.; Dsbien, A.; Duthie, M. S.; Coler, R. N.; Reed, S. G. A Structure-function Approach to Optimizing TLR4 Ligands for Human Vaccines. *Clin. Transl. Immunol.* **2016**, *5*.
- (43) Iribarren, K.; Bloy, N.; Buqué, A.; Cremer, I.; Eggermont, A.; Fridman, W. H.; Fucikova, J.; Galon, J.; Špišek, R.; Zitvogel, L.; Kroemer, G.; Galluzzi, L. Trial Watch: Immunostimulation with Toll-like Receptor Agonists in Cancer Therapy. *Oncoimmunology* **2016**, *5* (3).
- (44) Anwar, M. A.; Shah, M.; Kim, J.; Choi, S. Recent Clinical Trends in Toll-like Receptor Targeting Therapeutics. *Med. Res. Rev.* **2019**, *39*, 1053–1090.

- (45) Bonam, S. R.; Partidos, C. D.; Halmuthur, S. K. M.; Muller, S. An Overview of Novel Adjuvants Designed for Improving Vaccine Efficacy. *Trends Pharmacol. Sci.* **2017**, *38* (9), 771–793.
- (46) Medzhitov, R.; Janeway, C. A. J. Innate Immunity : Impact on the Adaptive Immune Response. *Curr. Opin. Immunol.* **1997**, *9* (1), 4–9.
- (47) Hernandez, C.; Huebener, P.; Schwabe, R. F. Damage-Associated Molecular Patterns in Cancer: A Double-Edged Sword. *Oncogene* **2016**, *35* (46), 5931–5941.
- (48) Akira, S.; Uematsu, S.; Takeuchi, O. Pathogen Recognition and Innate Immunity. *Cell* **2006**, *124* (4), 783–801.
- (49) Mogensen, T. H. Pathogen Recognition and Inflammatory Signaling in Innate Immune Defenses. *Clin. Microbiol. Rev.* **2009**, *22* (2), 240–273.
- (50) Mohan, C.; Zhu, J. Toll-like Receptor Signaling Pathways - Therapeutic Opportunities. *Mediators Inflamm.* **2010**, *2010*.
- (51) Hoebe, K.; Janssen, E.; Beutler, B. The Interface between Innate and Adaptive Immunity. *Nat. Immunol.* **2004**, *5* (10), 971–974.
- (52) NATIONAL INSTITUTES OF HEALTH. *Understanding the Immune System How It Works*; 2003.
- (53) Netea, M. G.; Schlitzer, A.; Placek, K.; Joosten, L. A. B.; Schultze, J. L. Innate and Adaptive Immune Memory: An Evolutionary Continuum in the Host's Response to Pathogens. *Cell Host Microbe* **2019**, *25* (1), 13–26.
- (54) Iwasaki, A.; Medzhitov, R. Control of Adaptive Immunity by the Innate Immune System. *Nat. Immunol.* **2015**, *16* (4), 343–353.
- (55) Triantafilou, M.; Miyake, K.; Golenbock, D. T.; Triantafilou, K. Mediators of Innate Immune Recognition of Bacteria Concentrate in Lipid Rafts and Facilitate Lipopolysaccharide-Induced Cell Activation. *J. Cell Sci.* **2002**, *115* (12), 2603–2611.
- (56) Gabius, H. J.; Siebert, H. C.; André, S.; Jiménez-Barbero, J.; Rüdiger, H. Chemical Biology of the Sugar Code. *ChemBioChem* **2004**, *5* (6), 740–764.
- (57) Duan, T.; Du, Y.; Xing, C.; Wang, H. Y.; Wang, R. F. Toll-Like Receptor Signaling and Its Role in Cell-Mediated Immunity. *Front. Immunol.* **2022**, *13* (March), 1–22.
- (58) Jahanban-Esfahlan, R.; Seidi, K.; Majidinia, M.; Karimian, A.; Yousefi, B.; Nabavi, S. M.; Astani, A.; Berindan-Neagoe, I.; Gulei, D.; Fallarino, F.; Gargaro, M.; Manni, G.; Pirro, M.; Xu, S.; Sadeghi, M.; Nabavi, S. F.; Shirooie, S. Toll-like Receptors as Novel Therapeutic Targets for Herpes Simplex Virus Infection. *Rev. Med. Virol.* **2019**, *29* (4), 1–14.
- (59) Iannucci, A.; Caneparo, V.; Raviola, S.; Debernardi, I.; Colangelo, D.; Miggiano, R.; Griffante,

- G.; Landolfo, S.; Gariglio, M.; De Andrea, M. Submitted_Toll-like Receptor 4-Mediated Inflammation Triggered by Extracellular IFI16 Is Enhanced by Lipopolysaccharide Binding.
- (60) Perrin-Cocon, L.; Aublin-Gex, A.; Sestito, S. E.; Shirey, K. A.; Patel, M. C.; André, P.; Blanco, J. C.; Vogel, S. N.; Peri, F.; Lotteau, V. TLR4 Antagonist FP7 Inhibits LPS-Induced Cytokine Production and Glycolytic Reprogramming in Dendritic Cells, and Protects Mice from Lethal Influenza Infection. *Sci. Rep.* **2017**, *7* (January), 1–13.
- (61) Cochet, F.; Peri, F. The Role of Carbohydrates in the Lipopolysaccharide (LPS)/Toll-like Receptor 4 (TLR4) Signaling. *Int. J. Mol. Sci.* **2017**, *18* (11).
- (62) Beamer, L. J.; Carroll, S. F.; Eisenberg, D. The BPI/LBP Family of Proteins: A Structural Analysis of Conserved Regions. *Protein Sci.* **1998**, *7* (4), 906–914.
- (63) Lamping, N.; Hoess, A.; Yu, B.; Park, T. C.; Kirschning, C. J.; Pfeil, D.; Reuter, D.; Wright, S. D.; Herrmann, F.; Schumann, R. R. Effects of Site-Directed Mutagenesis of Basic Residues (Arg 94, Lys 95, Lys 99) of Lipopolysaccharide (LPS)-Binding Protein on Binding and Transfer of LPS and Subsequent Immune Cell Activation. *J. Immunol.* **1996**, *157* (10), 4648–4656.
- (64) Wright, S. D.; Ramos, R. A.; Tobias, P. S.; Ulevitch, R. J.; Mathison, J. C. CD14, a Receptor for Complexes of Lipopolysaccharide (LPS) and LPS Binding Protein. *Science (80-.)*. **1990**, *249* (4975), 1431–1433.
- (65) Ryu, J. K.; Kim, S. J.; Rah, S. H.; Kang, J. I.; Jung, H. E.; Lee, D.; Lee, H. K.; Lee, J. O.; Park, B. S.; Yoon, T. Y.; Kim, H. M. Reconstruction of LPS Transfer Cascade Reveals Structural Determinants within LBP, CD14, and TLR4-MD2 for Efficient LPS Recognition and Transfer. *Immunity* **2017**, *46* (1), 38–50.
- (66) Huber, R. G.; Berglund, N. A.; Kargas, V.; Marzinek, J. K.; Holdbrook, D. A.; Khalid, S.; Piggot, T. J.; Schmidtchen, A.; Bond, P. J. A Thermodynamic Funnel Drives Bacterial Lipopolysaccharide Transfer in the TLR4 Pathway. *Structure* **2018**, *26* (8), 1151-1161.e4.
- (67) Triantafilou, M.; Triantafilou, K.; Fernandez, N. Rough and Smooth Forms of Fluorescein-labelled Bacterial Endotoxin. *Eur. J. Biochem.* **2000**, *267*, 2218–2226.
- (68) Kagan, J. C.; Medzhitov, R. Phosphoinositide-Mediated Adaptor Recruitment Controls Toll-like Receptor Signaling. *Cell* **2006**, *125* (5), 943–955.
- (69) Billod, J. M.; Lacetera, A.; Guzmán-Caldentey, J.; Martín-Santamaría, S. Computational Approaches to Toll-Like Receptor 4 Modulation. *Molecules* **2016**, *21* (8), 1–24.
- (70) Visintin, A.; Mazzoni, A.; Spitzer, J. A.; Segal, D. M. Secreted MD-2 Is a Large Polymeric Protein That Efficiently Confers Lipopolysaccharide Sensitivity to Toll-like Receptor 4. *Proc.*

Natl. Acad. Sci. U. S. A. **2001**, *98* (21), 12156–12161.

- (71) Park, B. S.; Song, D. H.; Kim, H. M.; Choi, B. S.; Lee, H.; Lee, J. O. The Structural Basis of Lipopolysaccharide Recognition by the TLR4-MD-2 Complex. *Nature* **2009**, *458* (7242), 1191–1195.
- (72) Shimazu, R.; Akashi, S.; Ogata, H.; Nagai, Y.; Fukudome, K.; Miyake, K.; Kimoto, M. MD-2, a Molecule That Confers Lipopolysaccharide Responsiveness on Toll- like Receptor 4. *J. Exp. Med.* **1999**, *189* (11), 1777–1782.
- (73) Janeway, C. A.; Medzhitov, R. Innate Immune Recognition. *Annu. Rev. Immunol.* **2002**, *20* (2), 197–216.
- (74) Kobe, B.; Kajava, A. V. The Leucine-Rich Repeat as a Protein Recognition Motif. *Curr. Opin. Struct. Biol.* **2001**, *11* (6), 725–732.
- (75) Funami, K.; Matsumoto, M.; Oshiumi, H.; Inagaki, F.; Seya, T. Functional Interfaces between TICAM-2/TRAM and TICAM-1/TRIF in TLR4 Signaling. *Biochem. Soc. Trans.* **2017**, *45* (4), 929–935.
- (76) Brade, L.; Brandenburg, K.; Kuhn, H. M.; Kusumoto, S.; Macher, I.; Rietschel, E. T.; Brade, H. The Immunogenicity and Antigenicity of Lipid A Are Influenced by Its Physicochemical State and Environment. *Infect. Immun.* **1987**, *55* (11), 2636–2644.
- (77) Alexander, C.; Rietschel, E. T. Bacterial Lipopolysaccharides and Innate Immunity. *J. Endotoxin Res.* **2001**, *7* (3), 167–202.
- (78) Molinaro, A.; Holst, O.; Lorenzo, F. Di; Callaghan, M.; Nurisso, A.; D’Errico, G.; Zamyatina, A.; Peri, F.; Berisio, R.; Jerala, R.; Jiménez-Barbero, J.; Silipo, A.; Martín-Santamarí, S. Chemistry of Lipid a: At the Heart of Innate Immunity. *Chem. - A Eur. J.* **2015**, *21* (2), 500–519.
- (79) Kawahara, K.; Tsukano, H.; Watanabe, H.; Lindner, B.; Matsuura, M. Modification of the Structure and Activity of Lipid A in Yersinia Pestis Lipopolysaccharide by Growth Temperature. *Infect. Immun.* **2002**, *70* (8), 4092–4098.
- (80) Calabrese, V.; Cighetti, R.; Peri, F. Molecular Simplification of Lipid A Structure: TLR4-Modulating Cationic and Anionic Amphiphiles. *Mol. Immunol.* **2015**, *63* (2), 153–161.
- (81) Vanaja, S. K.; Russo, A. J.; Behl, B.; Banerjee, I.; Yankova, M.; Deshmukh, S. D.; Rathinam, V. A. K. Bacterial Outer Membrane Vesicles Mediate Cytosolic Localization of LPS and Caspase-11 Activation. *Cell* **2016**, *165* (5), 1106–1119.
- (82) Mueller, M.; Lindner, B.; Kusumoto, S.; Fukase, K.; Schromm, A. B.; Seydel, U. Aggregates Are the Biologically Active Units of Endotoxin. *J. Biol. Chem.* **2004**, *279* (25), 26307–26313.

- (83) Brandenburg, K.; Wiese, A. Endotoxins : Relationships between Structure , Function , and Activity. *Curr. Top. Med. Chem.* **2004**, No. 4, 1127–1146.
- (84) Kim, H. M.; Park, B. S.; Kim, J. I.; Kim, S. E.; Lee, J. J. O.; Oh, S. C.; Enkhbayar, P.; Matsushima, N.; Lee, H.; Yoo, O. J.; Lee, J. J. O. Crystal Structure of the TLR4-MD-2 Complex with Bound Endotoxin Antagonist Eritoran. *Cell* **2007**, *130* (5), 906–917.
- (85) Tanimura, N.; Saitoh, S. I.; Ohto, U.; Akashi-Takamura, S.; Fujimoto, Y.; Fukase, K.; Shimizu, T.; Miyake, K. The Attenuated Inflammation of MPL Is Due to the Lack of CD14-Dependent Tight Dimerization of the TLR4/MD2 Complex at the Plasma Membrane. *Int. Immunol.* **2014**, *26* (6), 307–314.
- (86) Artner, D.; Oblak, A.; Ittig, S.; Garate, J. A.; Horvat, S.; Arrieumerlou, C.; Hofinger, A.; Oostenbrink, C.; Jerala, R.; Kosma, P.; Zamyatina, A. Conformationally Constrained Lipid a Mimetics for Exploration of Structural Basis of TLR4/MD-2 Activation by Lipopolysaccharide. *ACS Chem. Biol.* **2013**, *8* (11), 2423–2432.
- (87) Teghanemt, A.; Zhang, D.; Levis, E. N.; Weiss, J. P.; Gioannini, T. L. Molecular Basis of Reduced Potency of Underacylated Endotoxins. *J. Immunol.* **2005**, *175* (7), 4669–4676.
- (88) Beveridge, T. J. Structures of Gram-Negative Cell Walls and Their Derived Membrane Vesicles. *J. Bacteriol.* **1999**, *181* (16), 4725–4733.
- (89) Youn, J. H.; Oh, Y. J.; Kim, E. S.; Choi, J. E.; Shin, J.-S. High Mobility Group Box 1 Protein Binding to Lipopolysaccharide Facilitates Transfer of Lipopolysaccharide to CD14 and Enhances Lipopolysaccharide-Mediated TNF- α Production in Human Monocytes. *J. Immunol.* **2008**, *180* (7), 5067–5074.
- (90) Powers, K. A.; Szász, K.; Khadaroo, R. G.; Tawadros, P. S.; Marshall, J. C.; Kapus, A.; Rotstein, O. D. Oxidative Stress Generated by Hemorrhagic Shock Recruits Toll-like Receptor 4 to the Plasma Membrane in Macrophages. *J. Cell Biol.* **2006**, *174* (3), 1951–1961.
- (91) Cribbs, S. K.; Martin, G. S. Expanding the Global Epidemiology of Sepsis. *Crit. Care Med.* **2007**, *35* (11), 2646–2648.
- (92) Mackay, I. R.; Rosen, F. S. Autoimmune Diseases. *N. Engl. J. Med.* **2001**, *345* (5), 340–350.
- (93) Awasthi, S. Toll-like Receptor-4 Modulation for Cancer Immunotherapy. *Front. Immunol.* **2014**, *5* (JUL), 1–5.
- (94) Andreakos, E.; Sacre, S.; Foxwell, B. M.; Feldmann, M. The Toll-like Receptor-Nuclear Factor KB Pathway in Rheumatoid Arthritis. *Front. Biosci.* **2005**, *10*, 2478–2488.
- (95) Tobias, P.; Curtiss, L. K. Paying the Price for Pathogen Protection: Toll Receptors in

- Atherogenesis. *J. Lipid Res.* **2005**, *46* (3), 404–411.
- (96) Rice, T. W.; Wheeler, A. P.; Bernard, G. R.; Vincent, J.-L.; Angus, D. C.; Aikawa, N.; Demeyer, I.; Sainati, S.; Amlot, N.; Cao, C.; Li, M.; Matsuda, H.; Mouri, K.; Cohen, J. A Randomized, Double-Blind, Placebo-Controlled Trial of TAK-242 for the Treatment of Severe Sepsis*. *Crit. Care Med.* **2010**, *38* (8).
- (97) Zaffaroni, L.; Peri, F. Recent Advances on Toll-like Receptor 4 Modulation: New Therapeutic Perspectives. *Future Med. Chem.* **2018**, *10* (4), 461–476.
- (98) Manček-Keber, M.; Jerala, R. Postulates for Validating TLR4 Agonists. *Eur. J. Immunol.* **2015**, *45* (2), 356–370.
- (99) Gregg, K. A.; Harberts, E.; Gardner, F. M.; Pelletier, M. R.; Cayatte, C.; Yu, L.; McCarthy, M. P.; Marshall, J. D.; Ernst, R. K. Rationally Designed TLR4 Ligands for Vaccine Adjuvant Discovery. *MBio* **2017**, *8* (3), 1–14.
- (100) Zamyatina, A. Aminosugar-Based Immunomodulator Lipid A: Synthetic Approaches. *Beilstein J. Org. Chem.* **2017**, *14*, 25–53.
- (101) Przetak, M.; Chow, J.; Cheng, H.; Rose, J.; Hawkins, L. D.; Ishizaka, S. T. Novel Synthetic LPS Receptor Agonists Boost Systemic and Mucosal Antibody Responses in Mice. *Vaccine* **2003**, *21* (9–10), 961–970.
- (102) Goff, P. H.; Hayashi, T.; He, W.; Yao, S.; Cottam, H. B.; Tan, G. S.; Crain, B.; Krammer, F.; Messer, K.; Pu, M.; Carson, D. A.; Palese, P.; Corr, M. Synthetic Toll-like Receptor 4 (TLR4) and TLR7 Ligands Work Additively via MyD88 to Induce Protective Antiviral Immunity in Mice. *J. Virol.* **2017**, *91* (19), 1–12.
- (103) Honegr, J.; Malinak, D.; Dolezal, R.; Soukup, O.; Benkova, M.; Hroch, L.; Benek, O.; Janockova, J.; Kuca, K.; Prymula, R. Rational Design of Novel TLR4 Ligands by in Silico Screening and Their Functional and Structural Characterization in Vitro. *Eur. J. Med. Chem.* **2018**, *146*, 38–46.
- (104) Qureshi, N.; Takayama, K.; Ribi, E. Purification and Structural Determination of Nontoxic Lipid A Obtained from the Lipopolysaccharide of Salmonella Typhimurium. *J. Biol. Chem.* **1982**, *257* (19), 11808–11815.
- (105) Mata-Haro, V.; Cekic, C.; Martin, M.; Chilton, P. M.; Casella, C. R.; Mitchell, T. C. The Vaccine Adjuvant Monophosphoryl Lipid A as a TRIF-Biased Agonist of TLR4. *Science (80-.)*. **2007**, *316* (August), 1628–1633.
- (106) Guo, J.; Chen, Y.; Lei, X.; Xu, Y.; Liu, Z.; Cai, J.; Gao, F.; Yang, Y. Monophosphoryl Lipid a

Attenuates Radiation Injury through TLR4 Activation. *Oncotarget* **2017**, *8* (49), 86031–86042.

- (107) Needham, B. D.; Carroll, S. M.; Giles, D. K.; Georgiou, G.; Whiteley, M.; Trent, M. S. Modulating the Innate Immune Response by Combinatorial Engineering of Endotoxin. *Proc. Natl. Acad. Sci. U. S. A.* **2013**, *110* (4), 1464–1469.
- (108) Gregg, K. A.; Harberts, E.; Gardner, F. M.; Pelletier, M. R.; Cayatte, C.; Yu, L.; McCarthy, M. P.; Marshall, J. D.; Ernst, R. K. A Lipid A-Based TLR4 Mimetic Effectively Adjuvants a Yersinia Pestis RF-V1 Subunit Vaccine in a Murine Challenge Model. *Vaccine* **2018**, *36* (28), 4023–4031.
- (109) Coler, R. N.; Bertholet, S.; Moutaftsi, M.; Guderian, J. A.; Windish, H. P.; Baldwin, S. L.; Laughlin, E. M.; Duthie, M. S.; Fox, C. B.; Carter, D.; Friede, M.; Vedvick, T. S.; Reed, S. G. Development and Characterization of Synthetic Glucopyranosyl Lipid Adjuvant System as a Vaccine Adjuvant. *PLoS One* **2011**, *6* (1), 1–12.
- (110) Anderson, R. C.; Fox, C. B.; Dutil, T. S.; Shaverdian, N.; Evers, T. L.; Poshusta, G. R.; Chesko, J.; Coler, R. N.; Friede, M.; Reed, S. G.; Vedvick, T. S. Physicochemical Characterization and Biological Activity of Synthetic TLR4 Agonist Formulations. *Colloids Surfaces B Biointerfaces* **2010**, *75* (1), 123–132.
- (111) Arias, M. A.; van Roey, G. A.; Tregoning, J. S.; Moutaftsi, M.; Coler, R. N.; Windish, H. P.; Reed, S. G.; Carter, D.; Shattock, R. J. Glucopyranosyl Lipid Adjuvant (Gla), a Synthetic Tlr4 Agonist, Promotes Potent Systemic and Mucosal Responses to Intranasal Immunization with Hivgp140. *PLoS One* **2012**, *7* (7), 1–8.
- (112) McKay, P. F.; Cope, A. V.; Mann, J. F. S.; Joseph, S.; Esteban, M.; Tatoud, R.; Carter, D.; Reed, S. G.; Weber, J.; Shattock, R. J. Glucopyranosyl Lipid a Adjuvant Significantly Enhances HIV Specific T and B Cell Responses Elicited by a DNA-MVA-Protein Vaccine Regimen. *PLoS One* **2014**, *9* (1).
- (113) Anderson, J.; Olafsdottir, T. A.; Kratochvil, S.; McKay, P. F.; östensson, M.; Persson, J.; Shattock, R. J.; Harandi, A. M. Molecular Signatures of a TLR4 Agonist-Adjuvanted HIV-1 Vaccine Candidate in Humans. *Front. Immunol.* **2018**, *9* (FEB), 1–11.
- (114) Aznar, M. A.; Tinari, N.; Rullán, A. J.; Sánchez-Paulete, A. R.; Rodriguez-Ruiz, M. E.; Melero, I. Intratumoral Delivery of Immunotherapy—Act Locally, Think Globally. *J. Immunol.* **2017**, *198* (1), 31–39.
- (115) Sagiv-Barfi, I.; Lu, H.; Hewitt, J.; Hsu, F. J.; Meulen, J. ter; Levy, R. Intratumoral Injection of

TLR4 Agonist (G100) Leads to Tumor Regression of A20 Lymphoma and Induces Abscopal Responses. *Blood* **2015**, *126* (23), 820.

- (116) Bhatia, S.; Miller, N. J.; Lu, H.; Longino, N. V.; Ibrani, D.; Shinohara, M. M.; Byrd, D. R.; Parvathaneni, U.; Kulikauskas, R.; ter Meulen, J.; Hsu, F. J.; Koelle, D. M.; Nghiem, P. Intratumoral G100, a TLR4 Agonist, Induces Antitumor Immune Responses and Tumor Regression in Patients with Merkel Cell Carcinoma. *Clin. Cancer Res.* **2019**, *25* (4), 1185–1195.
- (117) Liang, H.; Poncet, D.; Seydoux, E.; Rintala, N. D.; Maciel, M.; Ruiz, S.; Orr, M. T. The TLR4 Agonist Adjuvant SLA-SE Promotes Functional Mucosal Antibodies against a Parenterally Delivered ETEC Vaccine. *npj Vaccines* **2019**, *4* (1), 8–15.
- (118) Hagar, J. A.; Powell, D. A.; Aachoui, Y.; Ernst, R. K.; Miao, E. A. Cytoplasmic LPS Activates Caspase-11: Implications in TLR4-Independent Endotoxic Shock. *Science* (80-.). **2013**, *341* (6151), 1250–1253.
- (119) Adanitsch, F.; Shi, J.; Shao, F.; Beyaert, R.; Heine, H.; Zamyatina, A. Synthetic Glycan-Based TLR4 Agonists Targeting Caspase-4/11 for the Development of Adjuvants and Immunotherapeutics. *Chem. Sci.* **2018**, *9* (16), 3957–3963.
- (120) Borio, A.; Holgado, A.; Garate, J. A.; Beyaert, R.; Heine, H.; Zamyatina, A. Disaccharide-Based Anionic Amphiphiles as Potent Inhibitors of Lipopolysaccharide-Induced Inflammation. *ChemMedChem* **2018**, *13* (21), 2317–2331.
- (121) Lam, C.; Hildebrandt, J.; Schutze, E.; Rosenwirth, B.; Proctor, R. A.; Liehl, E.; Stutz, P. Immunostimulatory, but Not Antiendotoxin, Activity of Lipid X Is Due to Small Amounts of Contaminating N,O-Acylated Disaccharide-1-Phosphate: In Vitro and in Vivo Reevaluation of the Biological Activity of Synthetic Lipid X. *Infect. Immun.* **1991**, *59* (7), 2351–2358.
- (122) Flad, H. D.; Loppnow, H.; Rietschel, E. T.; Ulmer, A. J. Agonists and Antagonists for Lipopolysaccharide-Induced Cytokines. *Immunobiology* **1993**, *187* (3–5), 303–316.
- (123) Funatogawa, K.; Matsuura, M.; Nakano, M.; Kiso, M.; Hasegawa, A. Relationship of Structure and Biological Activity of Monosaccharide Lipid A Analogues to Induction of Nitric Oxide Production by Murine Macrophage RAW264.7 Cells. *Infect. Immun.* **1998**, *66* (12), 5792–5798.
- (124) Matsuura, M.; Kiso, M.; Hasegawa, A. Activity of Monosaccharide Lipid A Analogues in Human Monocytic Cells as Agonists or Antagonists of Bacterial Lipopolysaccharide. *Infect. Immun.* **1999**, *67* (12), 6286–6292.

- (125) Cighetti, R.; Ciaramelli, C.; Sestito, S. E.; Zanoni, I.; Kubik, Ł.; Ardá-Freire, A.; Calabrese, V.; Granucci, F.; Jerala, R.; Martín-Santamaría, S.; Jiménez-Barbero, J.; Peri, F. Modulation of CD14 and TLR4×MD-2 Activities by a Synthetic Lipid A Mimetic. *ChemBioChem* **2014**, *15* (2), 250–258.
- (126) De Paola, M.; Sestito, S. E.; Mariani, A.; Memo, C.; Fanelli, R.; Freschi, M.; Bendotti, C.; Calabrese, V.; Peri, F. Synthetic and Natural Small Molecule TLR4 Antagonists Inhibit Motoneuron Death in Cultures from ALS Mouse Model. *Pharmacol. Res.* **2016**, *103*, 180–187.
- (127) Shirey, K. A.; Lai, W.; Scott, A. J.; Lipsky, M.; Mistry, P.; Pletneva, L. M.; Karp, C. L.; McAlees, J.; Gioannini, T. L.; Weiss, J.; Chen, W. H.; Ernst, R. K.; Rossignol, D. P.; Gusovsky, F.; Blanco, J. C. G.; Vogel, S. N. The TLR4 Antagonist Eritoran Protects Mice from Lethal Influenza Infection. *Nature* **2013**, *497* (7450), 498–502.
- (128) Michelsen, K. S.; Wong, M. H.; Shah, P. K.; Zhang, W.; Yano, J.; Doherty, T. M.; Akira, S.; Rajavashisth, T. B.; Arditi, M. Lack of Toll-like Receptor 4 or Myeloid Differentiation Factor 88 Reduces Atherosclerosis and Alters Plaque Phenotype in Mice Deficient in Apolipoprotein E. *Proc. Natl. Acad. Sci. U. S. A.* **2004**, *101* (29), 10679–10684.
- (129) Palmer, C.; Peri, F.; Neumann, F.; Ahmad, F.; Leake, D. S.; Pirianov, G. The Synthetic Glycolipid-Based TLR4 Antagonist FP7 Negatively Regulates in Vitro and in Vivo Haematopoietic and Non-Haematopoietic Vascular TLR4 Signaling. *Innate Immun.* **2018**, *24* (7), 411–421.
- (130) Facchini, F. A.; Coelho, H.; Sestito, S. E.; Delgado, S.; Minotti, A.; Andreu, D.; Jiménez-Barbero, J.; Peri, F. Co-Administration of Antimicrobial Peptides Enhances Toll-like Receptor 4 Antagonist Activity of a Synthetic Glycolipid. *ChemMedChem* **2018**, *13* (3), 280–287.
- (131) Cooperstock, M. S. Inactivation of Endotoxin by Polymyxin B. *Antimicrob. Agents Chemother.* **1974**, *6* (4), 422–425.
- (132) Rosenfeld, Y.; Papo, N.; Shai, Y. Endotoxin (Lipopolysaccharide) Neutralization by Innate Immunity Host-Defense Peptides: Peptide Properties and Plausible Modes of Action. *J. Biol. Chem.* **2006**, *281* (3), 1636–1643.
- (133) Facchini, F. A.; Zaffaroni, L.; Minotti, A.; Rapisarda, S.; Rapisarda, V.; Forcella, M.; Fusi, P.; Airoldi, C.; Ciaramelli, C.; Billod, J. M.; Schromm, A. B.; Braun, H.; Palmer, C.; Beyaert, R.; Lapenta, F.; Jerala, R.; Pirianov, G.; Martín-Santamaría, S.; Peri, F. Structure-Activity Relationship in Monosaccharide-Based Toll-like Receptor 4 (TLR4) Antagonists. *J. Med.*

Chem. **2018**, *61* (7), 2895–2909.

- (134) Cochet, F.; Facchini, F. A.; Zaffaroni, L.; Billod, J. M.; Coelho, H.; Holgado, A.; Braun, H.; Beyaert, R.; Jerala, R.; Jimenez-Barbero, J.; Martin-Santamaria, S.; Peri, F. Novel Carboxylate-Based Glycolipids: TLR4 Antagonism, MD-2 Binding and Self-Assembly Properties. *Sci. Rep.* **2019**, *9* (1), 1–13.
- (135) Piazza, M.; Rossini, C.; Fiorentina, S. D.; Pozzi, C.; Comelli, F.; Bettoni, I.; Fusi, P.; Costa, B.; Peri, F. Glycolipids and Benzylammonium Lipids as Novel Antisepsis Agents: Synthesis and Biological Characterization. *J. Med. Chem.* **2009**, *52* (4), 1209–1213.
- (136) Lonez, C.; Vandenbranden, M.; Ruyschaert, J. M. Cationic Lipids Activate Intracellular Signaling Pathways. *Adv. Drug Deliv. Rev.* **2012**, *64* (15), 1749–1758.
- (137) Piazza, M.; Calabrese, V.; Baruffa, C.; Gioannini, T.; Weiss, J.; Peri, F. The Cationic Amphiphile 3,4-Bis(Tetradecyloxy)Benzylamine Inhibits LPS Signaling by Competing with Endotoxin for CD14 Binding. *Biochem. Pharmacol.* **2010**, *80* (12), 2050–2056.
- (138) Ciaramelli, C.; Calabrese, V.; Sestito, S. E.; Pérez-Regidor, L.; Klett, J.; Oblak, A.; Jerala, R.; Piazza, M.; Martín-Santamaría, S.; Peri, F. Glycolipid-Based TLR4 Modulators and Fluorescent Probes: Rational Design, Synthesis, and Biological Properties. *Chem. Biol. Drug Des.* **2016**, *88* (2), 217–229.
- (139) Barboza, R.; Lima, F. A.; Reis, A. S.; Murillo, O. J.; Peixoto, E. P. M.; Bandeira, C. L.; Fotoran, W. L.; Sardinha, L. R.; Wunderlich, G.; Bevilacqua, E.; Lima, M. R. D. I.; Alvarez, J. M.; Costa, F. T. M.; Gonçalves, L. A.; Epiphanyo, S.; Marinho, C. R. F. TLR4-Mediated Placental Pathology and Pregnancy Outcome in Experimental Malaria. *Sci. Rep.* **2017**, *7* (1), 1–12.
- (140) Okada, T.; Kawakita, F.; Nishikawa, H.; Nakano, F.; Liu, L.; Suzuki, H. Selective Toll-Like Receptor 4 Antagonists Prevent Acute Blood-Brain Barrier Disruption After Subarachnoid Hemorrhage in Mice. *Mol. Neurobiol.* **2019**, *56* (2), 976–985.
- (141) Hawkins, L. D.; Ishizaka, S. T.; Lewis, M.; McGuinness, P.; Nault, A.; Rose, J.; Rossignol, D. P. (12) United States Patent, 2001.
- (142) Morefield, G. L.; Hawkins, L. D.; Ishizaka, S. T.; Kissner, T. L.; Ulrich, R. G. Synthetic Toll-like Receptor 4 Agonist Enhances Vaccine Efficacy in an Experimental Model of Toxic Shock Syndrome. *Clin. Vaccine Immunol.* **2007**, *14* (11), 1499–1504.
- (143) Church, J. S.; Milich, L. M.; Lerch, J. K.; Popovich, P. G.; McTigue, D. M. E6020, a Synthetic TLR4 Agonist, Accelerates Myelin Debris Clearance, Schwann Cell Infiltration, and Remyelination in the Rat Spinal Cord. *Glia* **2017**, *65* (6), 883–899.

- (144) Chan, M.; Hayashi, T.; Mathewson, R. D.; Nour, A.; Hayashi, Y.; Yao, S.; Tawatao, R. I.; Crain, B.; Tsigelny, I. F.; Kouznetsova, V. L.; Messer, K.; Pu, M.; Corr, M.; Carson, D. A.; Cottam, H. B. Identification of Substituted Pyrimido[5,4-b]Indoles as Selective TollLike Receptor 4 Ligands. *J. Med. Chem.* **2013**, *56*, 4206–4223.
- (145) Goff, P. H.; Hayashi, T.; Martínez-Gil, L.; Corr, M.; Crain, B.; Yao, S.; Cottam, H. B.; Chan, M.; Ramos, I.; Eggink, D.; Heshmati, M.; Krammer, F.; Messer, K.; Pu, M.; Fernandez-Sesma, A.; Palese, P.; Carson, D. A. Synthetic Toll-Like Receptor 4 (TLR4) and TLR7 Ligands as Influenza Virus Vaccine Adjuvants Induce Rapid, Sustained, and Broadly Protective Responses. *J. Virol.* **2015**, *89* (6), 3221–3235.
- (146) Michaeli, A.; Mezan, S.; Kühbacher, A.; Finkelmeier, D.; Elias, M.; Zatsopin, M.; Reed, S. G.; Duthie, M. S.; Rupp, S.; Lerner, I.; Burger-Kentscher, A. Computationally Designed Bispecific MD2/CD14 Binding Peptides Show TLR4 Agonist Activity. *J. Immunol.* **2018**, *201* (11), 3383–3391.
- (147) Honegr, J.; Dolezal, R.; Malinak, D.; Benkova, M.; Soukup, O.; De Almeida, J. S. F. D.; Franca, T. C. C.; Kuca, K.; Prymula, R. Rational Design of a New Class of Toll-like Receptor 4 (Tlr4) Tryptamine Related Agonists by Means of the Structure- and Ligand-Based Virtual Screening for Vaccine Adjuvant Discovery. *Molecules* **2018**, *23* (1).
- (148) Ii, M.; Matsunaga, N.; Hazeki, K.; Nakamura, K.; Takashima, K.; Seya, T.; Hazeki, O.; Kitazaki, T.; Iizawa, Y. A Novel Cyclohexene Derivative, Ethyl (6R)-6-[N-(2-Chloro-4-Fluorophenyl)Sulfamoyl]Cyclohex-1-ene-1-Carboxylate (TAK- 242), Selectively Inhibits Toll-Like Receptor 4-Mediated Cytokine Production through Suppression of Intracellular Signaling. *Mol. Pharmacol.* **2006**, *69* (4), 1288–1295.
- (149) Takashima, K.; Matsunaga, N.; Yoshimatsu, M.; Hazeki, K.; Kaisho, T.; Uekata, M.; Hazeki, O.; Akira, S.; Iizawa, Y.; Ii, M. Analysis of Binding Site for the Novel Small-Molecule TLR4 Signal Transduction Inhibitor TAK-242 and Its Therapeutic Effect on Mouse Sepsis Model. *Br. J. Pharmacol.* **2009**, *157* (7), 1250–1262.
- (150) Matsunaga, N.; Tsuchimori, N.; Matsumoto, T.; Ii, M. TAK-242 (Resatorvid), a Small-Molecule Inhibitor of Toll-like Receptor (TLR) 4 Signaling, Binds Selectively to TLR4 and Interferes with Interactions between TLR4 and Its Adaptor Molecules. *Mol. Pharmacol.* **2011**, *79* (1), 34–41.
- (151) Miller, Y. I. Toll-like Receptors and Atherosclerosis: Oxidized LDL as an Endogenous Toll-like Receptor Ligand. *Future Cardiol.* **2005**, *1* (6), 785–792.

- (152) Wang, X. T.; Lu, Y. X.; Sun, Y. H.; He, W. K.; Liang, J. B.; Li, L. TAK-242 Protects against Apoptosis in Coronary Microembolization-Induced Myocardial Injury in Rats by Suppressing TLR4/NF-KB Signaling Pathway. *Cell. Physiol. Biochem.* **2017**, *41* (4), 1675–1683.
- (153) Gutsche, C. D. Calixarenes. *Acc. Chem. Res.* **1983**, *16* (5), 161–170.
- (154) Shinkai, S.; Arimura, T.; Araki, K.; Kawabata, H.; Satoh, H.; Tsubaki, T.; Manabe, O.; Sunamoto, J. Syntheses and Aggregation Properties of New Water-Soluble Calixarenes. *J. Chem. Soc. Perkin Trans. 1* **1989**, No. 11, 2039–2045.
- (155) Nimse, S. B.; Kim, T. Biological Applications of Functionalized Calixarenes. *Chem. Soc. Rev.* **2013**, *42* (1), 366–386.
- (156) Saluja, V.; Sekhon, B. S. Calixarenes and Cucurbiturils: Pharmaceutial and Biomedical Applications. *J. Pharm. Educ. Res.* **2013**, *4* (1), 16–25.
- (157) Sestito, S. E.; Facchini, F. A.; Morbioli, I.; Billod, J. M.; Martin-Santamaria, S.; Casnati, A.; Sansone, F.; Peri, F. Amphiphilic Guanidinocalixarenes Inhibit Lipopolysaccharide (LPS)-and Lectin-Stimulated Toll-like Receptor 4 (TLR4) Signaling. *J. Med. Chem.* **2017**, *60* (12), 4882–4892.
- (158) Chen, X.; Dings, R. P. M.; Nesmelova, I.; Debbert, S.; Haseman, J. R.; Maxwell, J.; Hoye, T. R.; Mayo, K. H. Topomimetics of Amphipathic β -Sheet and Helix-Forming Bactericidal Peptides Neutralize Lipopolysaccharide Endotoxins. *J. Med. Chem.* **2006**, *49* (26), 7754–7765.
- (159) Wang, X.; Zhang, Y.; Peng, Y.; Hutchinson, M. R.; Rice, K. C.; Yin, H.; Watkins, L. R. Pharmacological Characterization of the Opioid Inactive Isomers (+)-Naltrexone and (+)-Naloxone as Antagonists of Toll-like Receptor 4. *Br. J. Pharmacol.* **2016**, *173* (5), 856–869.
- (160) Zhang, X.; Cui, F.; Chen, H.; Zhang, T.; Yang, K.; Wang, Y.; Jiang, Z.; Rice, K. C.; Watkins, L. R.; Hutchinson, M. R.; Li, Y.; Peng, Y.; Wang, X. Dissecting the Innate Immune Recognition of Opioid Inactive Isomer (+)-Naltrexone Derived Toll-like Receptor 4 (TLR4) Antagonists. *J. Chem. Inf. Model.* **2018**, *58* (4), 816–825.
- (161) Achek, A.; Shah, M.; Seo, J. Y.; Kwon, H.-K.; Gui, X.; Shin, H.-J.; Cho, E.-Y.; Lee, B. S.; Kim, D.-J.; Lee, S. H.; Yoo, T. H.; Kim, M. S.; Choi, S. Linear and Rationally Designed Stapled Peptides Abrogate TLR4 Pathway and Relieve Inflammatory Symptoms in Rheumatoid Arthritis Rat Model. *J. Med. Chem.* **2019**, *62*Achek, A (14), 6495–6511.
- (162) Oemer, G.; Lackner, K.; Muigg, K.; Krumschnabel, G.; Watschinger, K.; Sailer, S.; Lindner, H.; Gnaiger, E.; Wortmann, S. B.; Werner, E. R.; Zschocke, J.; Keller, M. A. Molecular Structural Diversity of Mitochondrial Cardiolipins. *Proc. Natl. Acad. Sci. U. S. A.* **2018**, *115* (16), 4158–

4163.

- (163) Mueller, M.; Brandenburg, K.; Dedrick, R.; Schromm, A. B.; Seydel, U. Phospholipids Inhibit Lipopolysaccharide (LPS)-Induced Cell Activation: A Role for LPS-Binding Protein. *J. Immunol.* **2005**, *174* (2), 1091–1096.
- (164) Balasubramanian, K.; Maeda, A.; Lee, J. S.; Mohammadyani, D.; Dar, H. H.; Jiang, J. F.; Croix, C. M. S.; Watkins, S.; Tyurin, V. A.; Tyurina, Y. Y.; Klöditz, K.; Polimova, A.; Kapralova, V. I.; Xiong, Z.; Ray, P.; Klein-Seetharaman, J.; Mallampalli, R. K.; Bayir, H.; Fadeel, B.; Kagan, V. E. Dichotomous Roles for Externalized Cardiolipin in Extracellular Signaling: Promotion of Phagocytosis and Attenuation of Innate Immunity. *Sci. Signal.* **2015**, *8* (395).
- (165) Pizzuto, M.; Lonez, C.; Baroja-Mazo, A.; Martínez-Banaclocha, H.; Tourlomousis, P.; Gangloff, M.; Pelegrin, P.; Ruyschaert, J. M.; Gay, N. J.; Bryant, C. E. Saturation of Acyl Chains Converts Cardiolipin from an Antagonist to an Activator of Toll-like Receptor-4. *Cell. Mol. Life Sci.* **2019**, 3667–3678.
- (166) Walsh, C.; Gangloff, M.; Monie, T.; Smyth, T.; Wei, B.; McKinley, T. J.; Maskell, D.; Gay, N.; Bryant, C. Elucidation of the MD-2/TLR4 Interface Required for Signaling by Lipid IVa. *J. Immunol.* **2008**, *181* (2), 1245–1254.
- (167) Huo, M.; Chen, N.; Chi, G.; Yuan, X.; Guan, S.; Li, H.; Zhong, W.; Guo, W.; Soromou, L. W.; Gao, R.; Ouyang, H.; Deng, X.; Feng, H. Traditional Medicine Alpinetin Inhibits the Inflammatory Response in Raw 264.7 Cells and Mouse Models. *Int. Immunopharmacol.* **2012**, *12* (1), 241–248.
- (168) Hu, K.; Yang, Y.; Tu, Q.; Luo, Y.; Ma, R. Alpinetin Inhibits LPS-Induced Inflammatory Mediator Response by Activating PPAR- γ in THP-1-Derived Macrophages. *Eur. J. Pharmacol.* **2013**, *721* (1–3), 96–102.
- (169) Liang, Y.; Shen, T.; Ming, Q.; Han, G.; Zhang, Y.; Liang, J.; Zhu, D. Alpinetin Ameliorates Inflammatory Response in LPS-Induced Endometritis in Mice. *Int. Immunopharmacol.* **2018**, *62* (July), 309–312.
- (170) Liu, T. gang; Sha, K. hui; Zhang, L. guo; Liu, X. xian; Yang, F.; Cheng, J. ying. Protective Effects of Alpinetin on Lipopolysaccharide/D-Galactosamine-Induced Liver Injury through Inhibiting Inflammatory and Oxidative Responses. *Microb. Pathog.* **2019**, *126* (May 2018), 239–244.
- (171) Lampiasi, N.; Montana, G. The Molecular Events behind Ferulic Acid Mediated Modulation of IL-6 Expression in LPS-Activated Raw 264.7 Cells. *Immunobiology* **2016**, *221* (3), 486–493.
- (172) Mir, S. M.; Ravuri, H. G.; Pradhan, R. K.; Narra, S.; Kumar, J. M.; Kuncha, M.; Kanjilal, S.;

- Sistla, R. Ferulic Acid Protects Lipopolysaccharide-Induced Acute Kidney Injury by Suppressing Inflammatory Events and Upregulating Antioxidant Defenses in Balb/c Mice. *Biomed. Pharmacother.* **2018**, *100* (November 2017), 304–315.
- (173) Yin, P.; Zhang, Z.; Li, J.; Shi, Y.; Jin, N.; Zou, W.; Gao, Q.; Wang, W.; Liu, F. Ferulic Acid Inhibits Bovine Endometrial Epithelial Cells against LPS-Induced Inflammation via Suppressing NK-KB and MAPK Pathway. *Res. Vet. Sci.* **2019**, *126* (August), 164–169.
- (174) Rehman, S. U.; Ali, T.; Alam, S. I.; Ullah, R.; Zeb, A.; Lee, K. W.; Rutten, B. P. F.; Kim, M. O. Ferulic Acid Rescues LPS-Induced Neurotoxicity via Modulation of the TLR4 Receptor in the Mouse Hippocampus. *Mol. Neurobiol.* **2019**, *56* (4), 2774–2790.
- (175) Azam, S.; Jakaria, M.; Kim, I. S.; Kim, J.; Ezazul Haque, M.; Choi, D. K. Regulation of Toll-like Receptor (TLR) Signaling Pathway by Polyphenols in the Treatment of Age-Linked Neurodegenerative Diseases: Focus on TLR4 Signaling. *Front. Immunol.* **2019**, *10* (MAY).
- (176) Offit, P. A.; Quarles, J.; Gerber, M. A.; Hackett, C. J.; Marcuse, E. K.; Kollman, T. R.; Gellin, B. G.; Landry, S. Addressing Parents' Concerns: Do Multiple Vaccines Overwhelm or Weaken the Infant's Immune System? *Pediatrics* **2002**, *109* (1), 124–129.
- (177) Shaw, W. A.; Burgess, S. W.; Li, S.; Hickman, D. T.; Lopez-Deber, M. P. DISACCHARIDE SYNTHETIC LIPID COMPOUNDS AND USES THEREOF, 2016.
- (178) 699800P Avanti MPLA (PHAD®)
<https://www.sigmaaldrich.com/IT/it/product/avanti/699800p>.
- (179) KISO, M.; HASEGAWA, A. Synthetic Studies on the Lipid A Component of Bacterial Lipopolysaccharide. **1983**, 277–300.
- (180) Tamai, R.; Asai, Y.; Hashimoto, M.; Fukase, K.; Kusumoto, S.; Ishida, H.; Kiso, M.; Ogawa, T. Cell Activation by Monosaccharide Lipid A Analogues Utilizing Toll-like Receptor 4. *Immunology* **2003**, *110* (1), 66–72.
- (181) Johnson, D. A.; Sowell, C. G.; Johnson, C. L.; Livesay, M. T.; Keegan, D. S.; Rhodes, M. J.; Ulrich, J. T.; Ward, J. R.; Cantrell, J. L.; Brookshire, V. G. Synthesis and Biological Evaluation of a New Class of Vaccine Adjuvants: Aminoalkyl Glucosaminide 4-Phosphates (AGPs). *Bioorganic Med. Chem. Lett.* **1999**, *9* (15), 2273–2278.
- (182) Johnson, D. A. TLR4 Agonists as Vaccine Adjuvants: A Chemist's Perspective. *Expert Rev. Vaccines* **2013**, *12* (7), 711–713.
- (183) Lam, C.; Schutze, E.; Hildebrandt, J.; Aschauer, H.; Liehl, E.; Macher, I.; Stutz, P. SDZ MRL 953, a Novel Immunostimulatory Monosaccharidic Lipid A Analog with an Improved

Therapeutic Window in Experimental Sepsis. *Antimicrob. Agents Chemother.* **1991**, *35* (3), 500–505.

- (184) Kiani, A.; Tschiersch, A.; Gaboriau, E.; Otto, F.; Seiz, A.; Knopf, H. P.; Stütz, P.; Färber, L.; Haus, U.; Galanos, C.; Mertelsmann, R.; Engelhardt, R. Downregulation of the Proinflammatory Cytokine Response to Endotoxin by Pretreatment with the Nontoxic Lipid a Analog SDZ MRL 953 in Cancer Patients. *Blood* **1997**, *90* (4), 1673–1683.
- (185) Reed, S. G.; Orr, M. T.; Fox, C. B. Key Roles of Adjuvants in Modern Vaccines. *Nat. Med.* **2013**, *19* (12), 1597–1608.
- (186) Brubaker, S. W.; Bonham, K. S.; Zanoni, I.; Kagan, J. C. Innate Immune Pattern Recognition: A Cell Biological Perspective. *Annu. Rev. Immunol.* **2015**, *33* (1), 257–290.
- (187) Kawai, T.; Akira, S. The Role of Pattern-Recognition Receptors in Innate Immunity: Update on Toll-like Receptors. *Nat. Immunol.* **2010**, *11* (5), 373–384.
- (188) van Dinther, D.; Stolk, D. A.; van de Ven, R.; van Kooyk, Y.; de Gruijl, T. D.; den Haan, J. M. M. Targeting C-Type Lectin Receptors: A High-Carbohydrate Diet for Dendritic Cells to Improve Cancer Vaccines. *J. Leukoc. Biol.* **2017**, *102* (4), 1017–1034.
- (189) Garaude, J.; Kent, A.; van Rooijen, N.; Blander, J. M. Simultaneous Targeting of Toll- and Nod-Like Receptors Induces Effective Tumor-Specific Immune Responses. *Sci. Transl. Med.* **2012**, *4* (120), 120ra16-120ra16.
- (190) Johnson, D. A.; Baldrige, J. R. TLR4 Agonists as Vaccine Adjuvants. In *Vaccine Adjuvants and Delivery Systems*; John Wiley & Sons, Inc.: Hoboken, NJ, USA, 2007; pp 131–156.
- (191) Reed, S. G.; Hsu, F.-C.; Carter, D.; Orr, M. T. The Science of Vaccine Adjuvants: Advances in TLR4 Ligand Adjuvants. *Curr. Opin. Immunol.* **2016**, *41*, 85–90.
- (192) Johnson, D. Synthetic TLR4-Active Glycolipids as Vaccine Adjuvants and Stand-Alone Immunotherapeutics. *Curr. Top. Med. Chem.* **2008**, *8* (2), 64–79.
- (193) Fox, C. B.; Friede, M.; Reed, S. G.; Ireton, G. C. Synthetic and Natural TLR4 Agonists as Safe and Effective Vaccine Adjuvants. In *Subcellular Biochemistry*; 2010; pp 303–321.
- (194) Shetab Boushehri, M. A.; Lamprecht, A. TLR4-Based Immunotherapeutics in Cancer: A Review of the Achievements and Shortcomings. *Mol. Pharm.* **2018**, *15* (11), 4777–4800.
- (195) Park, B. S.; Song, D. H.; Kim, H. M.; Choi, B.-S.; Lee, H.; Lee, J.-O. The Structural Basis of Lipopolysaccharide Recognition by the TLR4–MD-2 Complex. *Nature* **2009**, *458* (7242), 1191–1195.
- (196) Hoebe, K.; Du, X.; Georgel, P.; Janssen, E.; Tabet, K.; Kim, S. O.; Goode, J.; Lin, P.; Mann, N.;

- Mudd, S.; Crozat, K.; Sovath, S.; Han, J.; Beutler, B. Identification of Lps2 as a Key Transducer of MyD88-Independent TIR Signaling. *Nature* **2003**, *424* (6950), 743–748.
- (197) Gandhapudi, S. K.; Chilton, P. M.; Mitchell, T. C. TRIF Is Required for TLR4 Mediated Adjuvant Effects on T Cell Clonal Expansion. *PLoS One* **2013**, *8* (2), e56855.
- (198) Sharp, F. A.; Ruane, D.; Claass, B.; Creagh, E.; Harris, J.; Malyala, P.; Singh, M.; O'Hagan, D. T.; Pétrilli, V.; Tschopp, J.; O'Neill, L. A. J.; Lavelle, E. C. Uptake of Particulate Vaccine Adjuvants by Dendritic Cells Activates the NALP3 Inflammasome. *Proc. Natl. Acad. Sci.* **2009**, *106* (3), 870–875.
- (199) Li, H.; Willingham, S. B.; Ting, J. P.-Y.; Re, F. Cutting Edge: Inflammasome Activation by Alum and Alum's Adjuvant Effect Are Mediated by NLRP3. *J. Immunol.* **2008**, *181* (1), 17–21.
- (200) Dinarello, C. A. Blocking IL-1 in Systemic Inflammation. *J. Exp. Med.* **2005**, *201* (9), 1355–1359.
- (201) Sutton, C.; Brereton, C.; Keogh, B.; Mills, K. H. G.; Lavelle, E. C. A Crucial Role for Interleukin (IL)-1 in the Induction of IL-17–Producing T Cells That Mediate Autoimmune Encephalomyelitis. *J. Exp. Med.* **2006**, *203* (7), 1685–1691.
- (202) Romerio, A.; Peri, F. Increasing the Chemical Variety of Modulators : An Overview. *Front. Immunol.* **2020**, *11* (July), 1–16.
- (203) Cekic, C.; Casella, C. R.; Eaves, C. A.; Matsuzawa, A.; Ichijo, H.; Mitchell, T. C. Selective Activation of the P38 MAPK Pathway by Synthetic Monophosphoryl Lipid A. *J. Biol. Chem.* **2009**, *284* (46), 31982–31991.
- (204) Reed, S. G.; Carter, D. SYNTHETIC GLUCOPYRANOSYL LIPID ADJUVANTS ADJUVANTS, 2014.
- (205) De Yang; Satoh, M.; Ueda, H.; Tsukagoshi, S.; Yamazaki, M. Activation of Tumor-Infiltrating Macrophages by a Synthetic Lipid A Analog (ONO-4007) and Its Implication in Antitumor Effects. *Cancer Immunol. Immunother.* **1994**, *38* (5), 287–293.
- (206) Satoh, Kazusa Tsurumaki, Hideaki Ka, M. Induction of Intratumoral Tumor Necrosis Factor by a Synthetic Lipid A Analog, ONO-4007, with Less Tolerance in Repeated Administration and Its Implication in Potent Antitumor Effects with Low Toxicity. *Cancer Immunol. Immunother.* **2002**, *50* (12), 653–662.
- (207) Cighetti, R.; Ciaramelli, C.; Sestito, S. E.; Zanoni, I.; Kubik, Ł.; Ardá-Freire, A.; Calabrese, V.; Granucci, F.; Jerala, R.; Martín-Santamaría, S.; Jiménez-Barbero, J.; Peri, F. Modulation of CD14 and TLR4·MD-2 Activities by a Synthetic Lipid A Mimetic. *ChemBioChem* **2014**, *15* (2), 250–258.

- (208) Facchini, F. A.; Zaffaroni, L.; Minotti, A.; Rapisarda, S.; Rapisarda, V.; Forcella, M.; Fusi, P.; Airoldi, C.; Ciaramelli, C.; Billod, J.-M.; Schromm, A. B.; Braun, H.; Palmer, C.; Beyaert, R.; Lapenta, F.; Jerala, R.; Pirianov, G.; Martin-Santamaria, S.; Peri, F. Structure-Activity Relationship in Monosaccharide-Based Toll-like Receptor 4 (TLR4) Antagonists. *J. Med. Chem.* **2018**, *61* (7).
- (209) Facchini, F. A.; Di Fusco, D.; Barresi, S.; Luraghi, A.; Minotti, A.; Granucci, F.; Monteleone, G.; Peri, F.; Monteleone, I. Effect of Chemical Modulation of Toll-like Receptor 4 in an Animal Model of Ulcerative Colitis. *Eur. J. Clin. Pharmacol.* **2020**, *76* (3).
- (210) Moncrieffe, M. C.; Bollschweiler, D.; Li, B.; Penczek, P. A.; Hopkins, L.; Bryant, C. E.; Klenerman, D.; Gay, N. J. MyD88 Death-Domain Oligomerization Determines Myddosome Architecture: Implications for Toll-like Receptor Signaling. *Structure* **2020**, *28* (3), 281-289.e3.
- (211) Marty-Roix, R.; Vladimer, G. I.; Pouliot, K.; Weng, D.; Buglione-Corbett, R.; West, K.; MacMicking, J. D.; Chee, J. D.; Wang, S.; Lu, S.; Lien, E. Identification of QS-21 as an Inflammasome-Activating Molecular Component of Saponin Adjuvants. *J. Biol. Chem.* **2016**, *291* (3), 1123–1136.
- (212) Vono, M.; Taccone, M.; Caccin, P.; Gallotta, M.; Donvito, G.; Falzoni, S.; Palmieri, E.; Pallaoro, M.; Rappuoli, R.; Di Virgilio, F.; De Gregorio, E.; Montecucco, C.; Seubert, A. The Adjuvant MF59 Induces ATP Release from Muscle That Potentiates Response to Vaccination. *Proc. Natl. Acad. Sci.* **2013**, *110* (52), 21095–21100.
- (213) Rietschel, E. T.; Kirikae, T.; Schade, F. U.; Mamat, U.; Schmidt, G.; Loppnow, H.; Ulmer, A. J.; Zähringer, U.; Seydel, U.; Di Padova, F.; Schreier, M.; Brade, H. Bacterial Endotoxin: Molecular Relationships of Structure to Activity and Function. *FASEB J.* **1994**, *8* (2), 217–225.
- (214) Jakobs, C.; Bartok, E.; Kubarenko, A.; Bauernfeind, F.; Hornung, V. Immunoblotting for Active Caspase-1; 2013; pp 103–115.
- (215) Oliva, C.; Turnbough, C. L.; Kearney, J. F. CD14-Mac-1 Interactions in Bacillus Anthracis Spore Internalization by Macrophages. *Proc. Natl. Acad. Sci. U. S. A.* **2009**, *106* (33), 13957–13962.
- (216) Singh, Y.; Demchenko, A. V. Koenigs–Knorr Glycosylation Reaction Catalyzed by Trimethylsilyl Trifluoromethanesulfonate. *Chem. - A Eur. J.* **2019**, *25* (6), 1461–1465.
- (217) Shadrack, M.; Singh, Y.; Demchenko, A. V. Stereocontrolled A-Galactosylation under Cooperative Catalysis. *J. Org. Chem.* **2020**, *85*, 15936–15944.
- (218) Shadrack, M.; Stine, K. J.; Demchenko, A. V. Expanding the Scope of Stereoselective α -

Galactosylation Using Glycosyl Chlorides. *Bioorganic Med. Chem. Lett.* **2022**, *73*.

- (219) Steber, H. B.; Singh, Y.; Demchenko, A. V. Bismuth(III) Triflate as a Novel and Efficient Activator for Glycosyl Halides. *Org. Biomol. Chem.* **2021**, *19* (14), 3220–3233.
- (220) Escopy, S.; Singh, Y.; Stine, K. J.; Demchenko, A. V. A Streamlined Regenerative Glycosylation Reaction: Direct, Acid-Free Activation of Thioglycosides. *Chem. - A Eur. J.* **2021**, *27* (1), 354–361.
- (221) M. J. Frisch, G. W. Trucks, H. B. Schlegel, G. E. Scuseria, M. A. Robb, J. R. Cheeseman, G. Scalmani, V. Barone, B. Mennucci, G. A. Petersson, H. Nakatsuji, M. Caricato, X. Li, H. P. Hratchian, A. F. Izmaylov, J. Bloino, G. Zheng, J. L. Sonnenberg, M. Had, W. C. *Gaussian 09, Revision A.1*; 2009.
- (222) Case, D. A.; Babin, V.; Berryman, J.; Betz, R. M.; Cai, Q.; Cerutti, D. S.; Cheatham, T. E., III; Darden, T. A.; Duke, R. E.; Gohlke, H.; Goetz, A. W.; Gusarov, S.; Homeyer, N.; Janowski, P.; Kaus, J.; Kolossváry, I.; Kovalenko, A.; Lee, T. S.; LeGrand, S, X. . K. *P. A. Amber 14*; 2014.
- (223) Morris, G. M.; Huey, R.; Lindstrom, W.; Sanner, M. F.; Belew, R. K.; Goodsell, D. S.; Olson, A. J. AutoDock4 and AutoDockTools4: Automated Docking with Selective Receptor Flexibility. *J. Comput. Chem.* **2009**, *30* (16), 2785–2791.
- (224) Trott, O.; Olson, A. J. AutoDock Vina: Improving the Speed and Accuracy of Docking with a New Scoring Function, Efficient Optimization, and Multithreading. *J. Comput. Chem.* **2009**, NA-NA.
- (225) Roe, D. R.; Cheatham, T. E. PTRAJ and CPPTRAJ: Software for Processing and Analysis of Molecular Dynamics Trajectory Data. *J. Chem. Theory Comput.* **2013**, *9* (7), 3084–3095.
- (226) Ohto, U.; Fukase, K.; Miyake, K.; Shimizu, T. Structural Basis of Species-Specific Endotoxin Sensing by Innate Immune Receptor TLR4/MD-2. *Proc. Natl. Acad. Sci.* **2012**, *109* (19), 7421–7426.
- (227) Ohto, U.; Fukase, K.; Miyake, K.; Satow, Y. Crystal Structures of Human MD-2 and Its Complex with Antiendotoxic Lipid IVa. *Science (80-.)*. **2007**, *316* (5831), 1632–1634.
- (228) Scior, T.; Lozano-Aponte, J.; Figueroa-Vazquez, V.; Yunes-Rojas, J. A.; Zähringer, U.; Alexander, C. THREE-DIMENSIONAL MAPPING OF DIFFERENTIAL AMINO ACIDS OF HUMAN, MURINE, CANINE AND EQUINE TLR4/MD-2 RECEPTOR COMPLEXES CONFERRING ENDOTOXIC ACTIVATION BY LIPID A, ANTAGONISM BY ERITORAN AND SPECIES-DEPENDENT ACTIVITIES OF LIPID IVA IN THE MAMMALIAN LPS SE. *Comput. Struct. Biotechnol. J.* **2013**, *7* (9), e201305003.

- (229) Paramo, T.; Piggot, T. J.; Bryant, C. E.; Bond, P. J. The Structural Basis for Endotoxin-Induced Allosteric Regulation of the Toll-like Receptor 4 (TLR4) Innate Immune Receptor. *J. Biol. Chem.* **2013**, *288* (51), 36215–36225.
- (230) Nguyen, N. T.; Nguyen, T. H.; Pham, T. N. H.; Huy, N. T.; Bay, M. Van; Pham, M. Q.; Nam, P. C.; Vu, V. V.; Ngo, S. T. Autodock Vina Adopts More Accurate Binding Poses but Autodock4 Forms Better Binding Affinity. *J. Chem. Inf. Model.* **2020**, *60* (1), 204–211.